TECHNICAL REPORT STANDARD TITLE PAGE

1. Report No.	2. Government Accession No.	3. Recipient's Catalog No.

4. Title and Subtitle	5. Report Date
"The Effect of Diaphragms in Prestressed Concrete Girder and Slab Bridges"	October 1973
	6. Performing Organization Code
7. Author(s)	8. Performing Organization Report No.
S. Sengupta and J. E. Breen	Research Report 158-1F
9. Performing Organization Name and Address	10. Work Unit No.
Center for Highway Research The University of Texas at Austin Austin, Texas 78712	11. Contract or Grant No. Research Study 3-5-71-158
	13. Type of Report and Period Covered
12. Sponsoring Agency Name and Address Texas Highway Department Planning & Research Division P. O. Box 5051 Austin, Texas 78763	Final Sept. 1970 - August 1973
	14. Sponsoring Agency Code

15. Supplementary Notes
Work done in cooperation with Federal Highway Administration, Department of Transportation
Research Study Title: "Diaphragm Requirements for Prestressed Concrete Bridges"

16. Abstract

Four scale microconcrete model bridges were tested. Experimental variables included span, skew angle, stiffness, location and number of diaphragms. Service load level behavior was studied under static, cyclic and impact loads with successive removal of diaphragms. Behavior at overload and ultimate load conditions was documented from ultimate static and impact load tests. Characteristics studied were load distribution under static service loads and overloads, ultimate load capacities and failure modes of girders, cracking and ultimate load capacities of slabs, dynamic amplification, bridge damping, fundamental modes of vibration and natural frequencies, response to lateral impacts, and stresses in diaphragms. A computer program was verified with experimental results and used to generalize findings. The only significant role of interior diaphragms found is to distribute the load more evenly. In no case was an appreciable reduction in the governing design moment found. A cost analysis showed it would be more economical to provide increased girder strength than to rely on improved distribution of load decreasing the girder design moment due to provision of diaphragms. Design live loads for girders determined from the distribution factors of the 1969 AASHO specifications were found to be conservative even without diaphragms. Provision of interior diaphragms made the girders more vulnerable to damages from lateral impacts. It was recommended that interior diaphragms not be provided in simply supported prestressed concrete girder and slab bridges. Provision of exterior diaphragms or some alternate method of supporting or strengthening the free edge of the transverse slab was considered necessary for reliable serviceability.

17. Key Words	18. Distribution Statement
microconcrete, model, span, skew angle, stiffness, static, cyclic, impact, computer	

19. Security Classif. (of this report)	20. Security Classif. (of this page)	21. No. of Pages	22. Price
Unclassified	Unclassified	256	

Form DOT F 1700.7 (8-69)

THE EFFECT OF DIAPHRAGMS IN PRESTRESSED CONCRETE GIRDER AND SLAB BRIDGES

by

S. Sengupta
and
J. E. Breen

Research Report Number 158-1F

Research Project Number 3-5-71-158
Diaphragm Requirements for Prestressed Concrete Bridges

Conducted for

The Texas Highway Department
In Cooperation with the
U. S. Department of Transportation
Federal Highway Administration

by

CENTER FOR HIGHWAY RESEARCH
THE UNIVERSITY OF TEXAS AT AUSTIN

October 1973

The contents of this report reflect the views of the authors, who are responsible for the facts and the accuracy of the data presented herein. The contents do not necessarily reflect the official views or policies of the Federal Highway Administration. This report does not constitute a standard, specification, or regulation.

P R E F A C E

This report summarizes a detailed investigation of the role of exterior and interior diaphragms in typical prestressed concrete girder and slab bridges. The report presents comparative data concerning the behavior of such bridges with and without diaphragms as determined from tests of highly accurate model structures.

Very detailed information and data tabulations from the physical tests and detailed information concerning the spectral analysis procedures used in the study have been presented in a Ph.D. dissertation which is referenced in this report. In addition, a copy of this dissertation has been deposited with The University of Texas Center for Highway Research and the Texas Highway Department Bridge Division for use by readers seeking more details on physical tests and comparisons. The dissertation which has been put on file is: Sengupta, S., "The Effect of Diaphragms in Prestressed Concrete Girder and Slab Bridges," Ph.D. Dissertation, University of Texas at Austin, August, 1973.

This work is a part of Research Study 3-5-71-158 entitled "Diaphragm Requirements for Prestressed Concrete Bridges." The studies described herein were conducted as a part of the overall research program of The University of Texas at Austin, Center for Highway Research, under the administrative direction of Dr. Clyde E. Lee. The work was sponsored jointly by the Texas Highway Department and the U.S. Department of Transportation, Federal Highway Administration, under an agreement between The University of Texas at Austin and the Texas Highway Department.

Liaison with the sponsoring agencies was maintained through the contact representatives, Mr. Vernon C. Harris of the Texas Highway Department, and Mr. J. W. Bowman of the Federal Highway Administration. Valuable assistance in the direction of the program was provided by Mr. Robert L. Reed of the Bridge Division of the Texas Highway Department.

This study was directed by John E. Breen, Professor of Civil Engineering, at the Civil Engineering Structures Research Laboratory of the University's Balcones Research Center. The overall testing and analysis program was supervised by S. Sengupta, Research Engineer, Center for Highway Research. Valuable assistance in the use of spectral analysis procedures for data interpretation was provided by Donald E. Smith, Research Engineer, working under the direction of Dr. Edward J. Powers, Associate Professor of Electrical Engineering. The technical assistance of Mr. Jerry Crane, Technical Staff Assistant, Center for Highway Research, was invaluable in utilization of the complex instrumentation.

A B S T R A C T

Four highly accurate 1/5.5 scale microconcrete model bridges were tested in order to document the effects of diaphragms in prestressed concrete girder and slab bridges. Experimental variables included: span, skew angle, stiffness, location and number of diaphragms. Service load level behavior was studied under static, cyclic and impact loads with successive removal of diaphragms. Behavior at overload and ultimate load conditions was documented from various ultimate static load and impact load tests.

The bridge characteristics studied were: load distribution under static service loads and overloads, ultimate load capacities and failure modes of girders, cracking and ultimate load capacities of slabs, dynamic load distribution and dynamic amplification, bridge damping, fundamental modes of vibration and natural frequencies, response to lateral impacts, and stresses in diaphragms.

A computer program for analysis of the bridge was verified by comparison with the experimental results and then was employed to generalize some of the findings.

It was found that the only significant role of interior diaphragms is to distribute the load more evenly across the bridge. However, in no case was an appreciable reduction in the governing design moment found. For typical prestressed concrete girder and slab bridges a cost analysis showed that it would be more economical to provide increased girder strength than to rely on improved distribution of load decreasing the girder design moment due to provision of diaphragms. Design live loads for girders as determined from the distribution factors of the 1969 AASHO specifications were found to be conservative even without diaphragms. Provision of interior diaphragms actually made the girders more vulnerable to damages from lateral impacts. Based on the results it was recommended that interior diaphragms should not be provided in simply supported prestressed concrete

girder and slab bridges. Provision of exterior diaphragms or some alternate method of supporting or strengthening the free edge of the transverse slab was considered necessary for reliable serviceability.

S U M M A R Y

This report presents a detailed study of the role of exterior and interior diaphragms in typical prestressed concrete girder and slab bridges. Using accurate reduced scale models the role of diaphragms at service and ultimate load levels was studied under static, cyclic, and impact loads.

Examination of the test results indicated no significant contribution of the interior diaphragms to dynamic load distribution or bridge damping. No change was noted in fundamental modes of vibration or in natural frequencies with or without diaphragms. A slight improvement in load distribution under static loads was noted for some load cases when interior diaphragms were present. However, in no case was an appreciable reduction in the governing design moment found. Based on the results it was recommended that interior diaphragms should not be provided in this type bridge. Provision of exterior diaphragms or some alternate method of supporting or strengthening the free edge of the transverse slab was considered necessary for serviceability.

I M P L E M E N T A T I O N

This study indicates that the only significant beneficial role of the interior diaphragms is to distribute the live load more evenly. Within the practical range of bridge excitation, the diaphragms become less important under dynamic loads. Since the presence or absence of diaphragms has no effect on the distribution of dead load moment, the reduction in total design moment for a girder due to the provision of interior diaphragms was found to be a maximum of 6 percent. This reduction in design moment could only be realized if a detailed analysis was carried out. Under the typical design procedures using distribution factors as given in the AASHO specifications, adequate conservatism is already built in so that the 6 percent can be neglected. Even if such an analysis was carried out and the reduction in design moment taken advantage of, an economic study is given to show that with realistic costs extra capacity could be provided in the girder far cheaper than the cost of provision of interior diaphragms.

Consideration of typical cost figures for this type of bridge system indicates that elimination of the interior diaphragms can save about 3.5 percent of the superstructure cost in addition to the possibility of significant reduction in the superstructure construction time and increased convenience in scheduling of deck operations. Relatively simple bracing systems have been and can be used to provide temporary supports for the girders during construction steps.

The study indicated that if the interior diaphragms are provided they make the girders more susceptible to damage from lateral impacts similar to an over-height vehicle striking the bottom flange of a girder. Thus, whether the design is based on a detailed analysis or on AASHO formulas, interior diaphragms should not be provided in simply supported prestressed concrete girder and slab bridges where the slab is continuous over the girders and where full composite action is assured.

The study also indicated that the only significant role of end diaphragms is to act as a supporting member for the free end of the slab at the approach span. The tests indicate an adequate ultimate load capacity when the diaphragms are omitted. However, the susceptibility of the slab to cracking at service load levels makes the slab edge without diaphragms of questionable serviceability. These diaphragms may be omitted if the slab is thickened or provided with additional reinforcement sufficient to significantly improve the cracking load capacity. Unless a suitable criterion for serviceability is determined and a reliable method to design an alternative end slab detail is developed, it is recommended that end diaphragms be provided.

TABLE OF CONTENTS

L I S T O F F I G U R E S

L I S T O F T A B L E S

N O T A T I O N

A	= Area of the noncomposite girder section
A, A_1, A_2	= Amplitudes
a	= Acceleration
a, b, c	= Coordinate axes for discrete element model
B_{12}	= Cross-power amplitude spectrum
C	= Coefficient of damping
C_{cr}	= Critical damping coefficient
C.V.	= Coefficient of variation
D	= Distance
D.C.	= Distribution coefficient
D.C.(M)	= Moment distribution coefficient = $M/\Sigma M$ at a given span
D.C.(δ)	= Deflection distribution coefficient = $\delta/\Sigma\delta$ at a given span
DF	= Distribution factor (see Sec. 5.2.3 for definition)
DF(M)	= Moment distribution factor
DF(δ)	= Deflection distribution factor
d	= Longer side of a rectangular section
E	= Modulus of elasticity
E_c	= Modulus of elasticity of concrete
EI_D	= Diaphragm flexural stiffness
EI_G	= Composite girder flexural stiffness
EI_S	= Slab flexural stiffness per unit width
e	= Shorter side of a rectangular section
F	= Force
$F_{i,j}$	= Force at any point i,j
f	= Frequency
f'_c	= Compressive strength of concrete
$f_{aliasing}$	= Cut-off frequency of the "aliasing" filter
f_B	= Frequency of beating due to mixing of two signals having slightly different frequencies

f_L = Natural frequency of the longitudinal mode of bridge vibration

f_{max} = Maximum desired frequency in a spectrum

f_s = Period of X(f) in frequency domain

$f_{sampling}$ = Sampling frequency

f_T = Natural frequency of the torsional mode of bridge vibration

G = Shear modulus

g = Acceleration due to gravity

h_a, h_b, h_c = Spacings of elastic joints in a, b, and c directions in a discrete element model

I = Moment of inertia

j = $\sqrt{-1}$

K = Torsional rigidity

K_1 = St. Venant's part of the torsional rigidity

K_2 = Torsional rigidity due to composite action

K_{12}, $K_{12}(f)$ = Squared coherency of two data signals

k = An integer number or variable

L = Span of the bridge

ℓ = Length

M = Moment

M_{max} = Maximum girder moment at a given transverse section of the bridge

m = Mass per unit length; number of frequency band widths on which spectral estimates are averaged

N = Total number of samples for a data length

N_a, N_c = Number of increments in a and c directions in a discrete element model

n = An integer number or variable; number of some quantity

P_{11} = Auto-power spectrum of a data signal $x_1(t)$

P_{12} = Cross-power spectrum of two data signals

P_{22} = Auto-power spectrum of a data signal $x_2(t)$

Q = Area to calculate torsional rigidity due to composite action

$R_{m,n}$ = Functions of geometric and elastic properties at joint m,n of a discrete element model

S = Spacing of girders

s = Scale factor

s_i = Scale factor for any quantity i

T	= Time window (i.e., time length) for sampling
TA, TB, TC	= Standard truck loads (see Figs. 2.25, 2.26)
T_p	= Time period
T1, T2, T3	= Standard truck loads for ultimate test on Bridge 4 (see Fig. 2.27)
t	= Time
X, $X(f)$	= Fourier transform of some time function $x(t)$
X, Y	= Truck load multipliers
$X_r(i)$	= Refined Fourier transform of i^{th} harmonic
X_1, X_2	= Fourier transforms of data 1 and data 2
x	= Variable distance
$x(t)$, $x_1(t)$ $x_2(t)$	= Data signals
Z	= Section modulus
α	= Skew angle of the bridge; angle between axes a and c of a discrete element model
β	= A coefficient to determine torsional rigidity of the girder
Δf	= Elementary frequency band width
Δt	= Sample interval
δ	= Deflection
δ_f	= Frequency band width or frequency resolution in a spectrum
$\delta_{k,\ell}$	= Deflection at any point k,ℓ in a discrete element model
δ_{max}	= Maximum girder deflection at any transverse section of the bridge
ϵ	= Strain
θ, θ_1, θ_2	= Phase angles
μ	= Mass
ν_c	= Poisson's ratio of concrete
ρ	= Specific mass
Σ	= Summation
ΣM	= Sum of all the girder moments across any transverse section of the bridge
$\Sigma\delta$	= Sum of all the girder deflections across any transverse section of the bridge
σ	= Stress; standard deviation
ω	= Some angle; diameter of reinforcement bars or wires
ω_{12}	= Cross-power phase spectrum

CHAPTER 1

INTRODUCTION

1.1 General

In the construction of prestressed concrete girder and slab bridges one of the most time-consuming and vexing details has been the provision of diaphragms at the girder ends and at intermediate points along the span. The primary function of the end diaphragms is to provide support for the free end of the slab. It is generally assumed that the interior diaphragms substantially improve the transverse load distribution and stiffen the entire structure with respect to vibration. Supposedly, diaphragms also act as stiffeners for edge girders subjected to unforeseen lateral loads, such as when struck by an over-height vehicle passing under the bridge. Lastly, in the case of very slender girders, diaphragms may stiffen the girders against wind and water forces and against lateral buckling. This slenderness problem is typical of steel girder bridges and is not generally significant for commonly used prestressed concrete girders.

The exact extent of diaphragm effectiveness has been a matter of dispute. Potential savings in girder costs due to improved load distribution may actually be more than offset by the cost of diaphragms and their related time delay. The large number of bridges of this type built annually makes this a problem of significance.

A number of basic questions need to be answered:

(1) What roles do diaphragms play in prestressed concrete girder and slab bridges?

(2) How can diaphragms be used most effectively?

(3) What are the relative costs of providing diaphragms and savings from their provision?

(4) What are the proper design criteria for diaphragms?

1.2 Previous Investigations

1.2.1 Effect of Diaphragms under Static Loads

1.2.1.1 Diaphragm Effects in I-beam Bridges in General

While discussing the role of diaphragms in I-beam bridges in 1949, Newmark commented:

> Since the slab acts as a very effective diaphragm, it is unnecessary to provide additional diaphragms, except for construction purposes, if the slab can perform its function of distributing loads to the beams at the same time that it provides roadway for wheels to roll over. Where it is expedient or desirable to make the slab thin, therefore flexible, some additional transverse bridging is desirable. In general, however, such bridging is not particularly effective except for loads at or close to the section where the transverse frames are located.[30*]

This statement was sharply criticized by Balog, who emphasized that properly designed diaphragms are efficient in distributing the loads and in addition they facilitate the application of new methods of slab construction.[6]

Tests and analysis of steel girder bridges[43,23,52] indicate that when slender girders are used the provision of diaphragms is a critical factor in economic design. Speaking of slender steel girder bridges, Lount[23] said:

> Addition of diaphragms to bridge structures provides better transverse distribution, stiffens the bridge, reduces vibration and deflection effects, increases the real safety of the structure, reduces hazards from fatigue loading and permits crossing of very heavy individual loadings in emergencies.

Diaphragm effectiveness seems substantially less in prestressed girder bridges. Based on tests of a half-scale model of a 66 ft. span, precast prestressed concrete continuous bridge, Mattock and Kaar[27] found that the AASHO design girder load distribution was realized without interior diaphragms. They indicated that effective diaphragms must be

---

*Superscript numbers refer to the Bibliography.

continuous across the bridge and are economic only if a more precise lateral load distribution analysis is used in the design of the longitudinal girders.

From plexiglas model tests and theoretical analyses of similar stressed concrete girder bridges, Carpenter and Magura[15] found the most effective diaphragm location to be at midspan. Further addition of diaphragms did not appreciably change the maximum moment. They concluded:

> Test results indicate that bridges of this type will be adequate without interior diaphragms in the span if the girders are proportioned for moment according to AASHO specifications; indeed, interior girders may be significantly overdesigned. Moreover, addition of interior diaphragms tends to further decrease the load taken by the interior girders while increasing the load taken by exterior girders above design values.

Similar conclusions were reached by Self[38] from a theoretical and experimental study on prestressed concrete girder and slab bridges.

1.2.1.2 Diaphragm Effectiveness under Different Loadings

Using finite element techniques, Gustafson and Wright[16] studied the effect of diaphragms at quarter points of the span in an 80 ft. span steel girder bridge, applying concentrated loads at various points across the midspan. They found that the diaphragms had little effect on the exterior girder moments, but had a pronounced effect in reducing maximum moments in interior girders.

Theoretical studies on simply supported straight I-beam bridges by Wei[50] and simply supported straight prestressed concrete girder and slab bridges by Sithichaikasem and Gamble[40] indicate that under single truck loads the effect of diaphragms is less significant than under point loads. However, under AASHO[1] design truck loads an increase in the maximum moment was noted for the exterior girders.

1.2.1.3 Effect of Bridge Parameters and Diaphragm Stiffness

For steel I-beam bridges in the span range of 50 to 80 ft., Wei[50] found that the diaphragm effectiveness in distributing loads increases with increasing girder spacing. For bridges having girder stiffness to slab stiffness ratio $EI_G/(EI_S \cdot L)$ in the range of 5 to 20, Wei found that a

diaphragm with a stiffness 40 percent of the main girder is as good as an infinitely stiff diaphragm and that a diaphragm stiffness of 5 to 10 percent of the girder is most practical. The studies of Sithichaikasem and Gamble[40] indicate that for prestressed concrete girder and slab bridges diaphragms are more effective for larger girder spacing to span ratio (S/L) and larger values of $EI_G/(EI_S \cdot L)$. However, they indicated that beyond the span range of 60 to 70 ft. diaphragms either produce no reduction or increase the girder design moment. They also emphasized that the diaphragms should be of proper stiffness. Otherwise, the diaphragms may actually increase the girder design moment.

1.2.1.4 Effective Diaphragm Location

Many authors[12,15,40,50] indicated that the most effective diaphragm location is at midspan. Ramesh and others[33] conducted model studies to determine an efficient arrangement of cross girders (i.e., diaphragms) in skew bridges. It was inferred that arrangements in which the diaphragms are normal to the longitudinals (Fig. 1.1a) are more rigid than when the diaphragms are parallel to the support (Fig. 1.1b).

Makowski[25] indicated that a single diaphragm at midspan is as effective as two such diaphragms at one-third points of the span. Further, three diaphragms at one-fourth, one-half, and three-fourths span are equivalent to four such diaphragms located at one-fifth, two-fifths, three-fifths and four-fifths span.

Hendry and Jaeger[18] presented a formula to evaluate the approximate effective stiffness of diaphragms. This formula implies that for a given diaphragm stiffness a single diaphragm at midspan is as effective in distributing loads as two such diaphragms at one-third points of the span.

Kumar[21] stressed that the number and size of diaphragms play a very important role in optimizing lateral load distribution in reinforced concrete T-beam and slab bridges. He concluded that a diaphragm at midspan is most effective for lateral load distribution and that any further increase in the number of diaphragms decreases the load distribution.

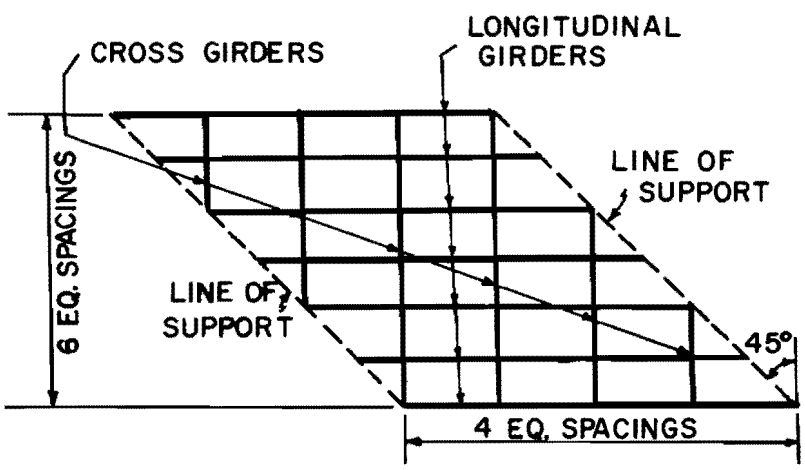

(a) CROSS GIRDERS NORMAL TO LONGITUDINAL GIRDERS

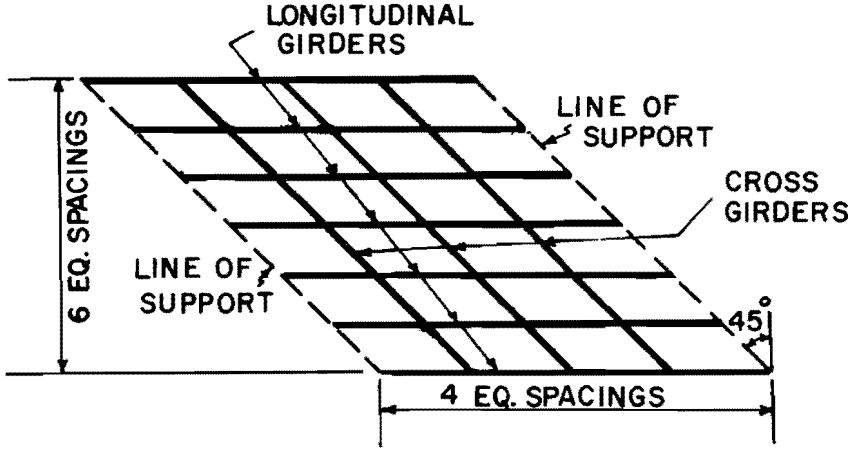

(b) CROSS GIRDERS PARALLEL TO LINE OF SUPPORT

Fig. 1.1 Arrangement of cross girders. (Ref. 33.)

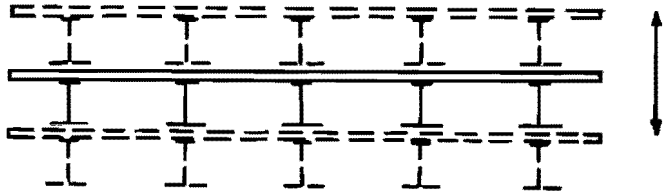

(a) VERTICAL VIBRATION (LONGITUDINAL MODE)

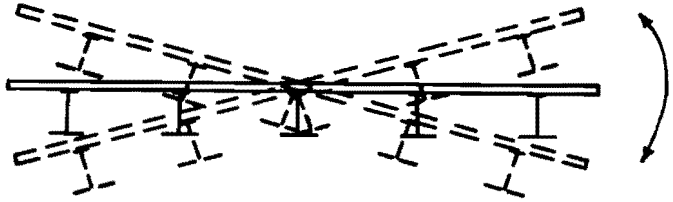

(b) TORSIONAL VIBRATION

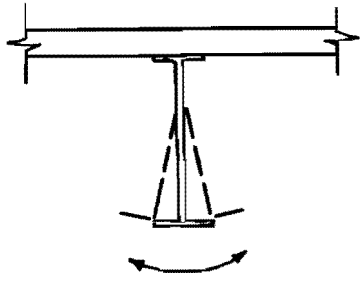

(c) LATERAL OSCILLATION OF THE BOTTOM BEAM FLANGE

Fig. 1.2 Different modes of bridge vibration.

1.2.1.4 Summary

The preceding discussions suggest that diaphragms are more effective for bridges with large S/L and large $EI_G/EI_S \cdot L$ values. Continuity, stiffness and location of the diaphragms are important factors. As the diaphragms are located farther away from midspan their effectiveness decreases. This implies that the diaphragms at the end of the span are least effective in distributing loads.

Wong and Gamble[53] examined the effect of diaphragms in prestressed concrete girder and slab bridges under static loads. Consideration of the cost of diaphragms and the cost of increasing the girder strength led to the conclusion that diaphragms should not be provided in straight prestressed concrete girder and slab bridges unless necessary for construction purposes.

1.2.2 Diaphragm Effectiveness under Dynamic Loads

While discussing the results from an experimental study on dynamic behavior of prestressed concrete model bridges, Self[38] indicated the possibility of three types of significant bridge vibrations (as shown in Fig. 1.2a, b and c). Only the third type (as in Fig. 1.2c) is effectively eliminated by diaphragms. However, he mentioned that even without diaphragms this mode is of secondary importance. He also found that the diaphragms had little influence on impact factors.

Self's work is the only study directly related to diaphragm effectiveness under dynamic loads. Model studies of the dynamic response of a multiple girder bridge by Walker[48] showed that instantaneous transverse distribution of dynamic effects is more uniform than distribution of static effects. For the model tested, contribution of the torsional mode of vibration was found to be negligible. Since the torsional rigidities of the model beams were very much higher than those of the prototype, the reliability of the second part of the findings seems questionable. From truck load tests on an actual bridge, Kinnier[20] indicated that at higher speeds loads were more evenly distributed. However, deflections and stresses in the stringers increased. Because of more even distribution of dynamic effects, these reports of Walker and Kinnier tend to indicate a reduction in the effectiveness of diaphragms under dynamic loads.

1.2.3 Human Response to Bridge Vibration

Apart from the strength requirements in some cases it may be considered important that a bridge should not vibrate so much as to make a pedestrian uncomfortable. Wright and Walker[54] commented,

> pedestrians and occupants of moving vehicles appear to respond primarily to the accelerations in the dynamic component of bridge motion. . . . Human response to acceleration, like that to sound, varies with the logarithm of amplitude [of acceleration].

They indicated that under transient vibrations tolerance limits for acceleration amplitude are much greater than for the case of sustained vibration. Since acceleration is proportional to deflection times the square of frequency and transient vibration relates directly to the damping characteristics, it appears that flexibility, natural frequency, and damping of the bridge are relevant bridge parameters affecting human response to bridge vibration.

1.3 Code Provisions and Current Practice

Depending on the type of slab and girder bridge, AASHO[1] specifies the following requirements: In concrete T-beam bridges, for spans more than 40 ft., diaphragms or spreaders should be provided between the beams at the middle or at third points. The same provisions also apply to prestressed concrete girders.

For unsupported slab edges, that is

> . . . at the end of the bridge or at points where the continuity of the slab is broken, diaphragms or other suitable means are required to support these edges. These diaphragms shall be designed to resist the full moment and shear produced by the wheel loads which can come on them.[1]

AASHO does not provide any design recommendations for the diaphragms, except those mentioned above. Neither does it give any consideration to the effect of diaphragms on load distribution, which is related only to the spacing of the girders. It appears that AASHO requirements for interior diaphragms are mainly for the purpose of construction (as a beam spacer) and for girder stability (to prevent buckling of the girder webs).

Current prestressed concrete girder bridge standards for the Texas Highway Department indicate provision of diaphragms at midpoints for spans 50 ft. or less, at 1/3 points for spans 50 ft. through 90 ft., and at 1/4 points for spans over 90 ft. The drawings show two types of interior diaphragms (see Fig. 2.7) of greatly different stiffnesses and strengths. The choice is optional. This seems to indicate that the interior diaphragms are not intended to function as specific structural members. End diaphragms are required in all cases.

1.4 Objective and Scope of Study

Though opinions vary, the foregoing discussion tends to question the oft-cited reasons for providing diaphragms. However, it is apparent that no conclusive decision which will justify the provision or removal of diaphragms can be reached without a more detailed investigation. This investigation should include the study of the following bridge characteristics:

(1) Load distribution under static service loads
(2) Load distribution under static overloads
(3) Ultimate load capacity and failure modes
(4) Cracking and ultimate load capacities of the unsupported slab edges due to wheel loads
(5) Dynamic load distribution
(6) Dynamic amplification
(7) Fundamental modes of vibration and their frequencies
(8) Bridge damping
(9) Response to lateral impacts
(10) Stresses in diaphragms
(11) Wind, water, and lateral buckling effects in slender girders.

The objective of this study is to investigate the diaphragm effects on these bridge characteristics in order to develop more rational rules for the provision of diaphragms. The scope of this study excludes problems associated with slender beams or construction problems, and includes experiments on physical models under static and dynamic loads along with theoretical investigations to extend the results through possible generalizations. Although investigations are carried out on simply supported prestressed

concrete I-beam and slab bridges only, many of the findings are expected to be applicable to reinforced concrete T-beam and continuous bridges also.

The basis for the experimental test programs and the methods used to reduce and interpret the data are presented in Chapters 2 and 3, respectively. The theory of the analytical computer program used to study the effects of parameters is discussed briefly in Chapter 4, which also includes the guide lines used to evaluate the input parameters and shows program verification by comparison with experimental results. Test results are interpreted and discussed in Chapter 5. Based on the experimental and analytical findings, an implementation procedure is presented in Chapter 6. Chapter 7 gives the final conclusions and recommendations. Notations and symbols used are defined wherever they first appear; however, for convenience of reference they are grouped together under the heading "Notation" at the beginning of the text.

CHAPTER 2

EXPERIMENTAL TEST PROGRAM

2.1 General

Structural models are widely used in research and are not uncommon in design, particularly for complicated structures. Analytical techniques are available (discussed in Chapter 4) for predicting the behavior of slab and girder bridges under static loads and within elastic ranges. General performance of these techniques has been compared[3,15] with experimental results with very good correlation. No analytical method is yet available to handle dynamic loads, impact loads, or even static loads beyond the elastic range, with sufficient accuracy so as to be able to distinguish between the bridge performances with and without diaphragms. Thus, it was felt necessary to determine experimentally (using accurate structural models) those aspects which cannot otherwise be reliably determined, and to verify the accuracy of the computer program developed earlier[47] and used to predict the effect of diaphragms.

2.2 Scale Factor

The selection of scale factor is crucial in several ways. The basic criterion is to minimize cost of the investigation without sacrificing significant accuracy. Previous cost vs. model scale studies[22] indicate that for concrete structures the total fabrication and loading cost reduces drastically as the scale factor decreases from 1 to about 1/5, that between 1/5 to 1/10 there is an almost flat minimum cost zone, and that beyond the 1/10 scale cost again rises slowly. Because of the availability of properly sized prestressing wires for the model, a scale factor of 1/5.5 (the largest possible in the minimum cost zone), was chosen. An added reason in choosing this scale factor was the availability of formwork and prestressing bed used previously[5] in a virtually identical 1/5.5 scale bridge.

2.3 Similitude Requirements

Similitude requirements are the "laws" of modeling and are used to establish the design of a reduced scale model of a prototype so as to determine the response characteristics of the prototype from those of the model. General discussions of these requirements can be found elsewhere.[51,55] The model-prototype relationship for this experiment was set by:

(1) All significant variables were listed and their fundamental dimensions determined (see Cols. 1 & 3 of Table 2.1).

(2) The fundamental dimensions of the study were determined as those of specific mass, time, and distance.

(3) Distance, mass/unit length, and modulus of elasticity were chosen as dimensionally independent variables in accordance with the following rules:

   (a) Their number should be equal to the number of fundamental variables.

   (b) They must contain among themselves all the fundamental dimensions.

   (c) All of them must have different dimensions.

   (d) None of these variables should be dimensionless.

(4) The fundamental dimensions were then expressed in terms of symbols (Col. 2, Table 2.1) of these dimensionally independent variables, e.g.

$$\ell \doteq D$$

$$\rho \doteq mD^{-2}$$

$$t \doteq m^{1/2} E^{-1/2}$$

Where D, m and E are the symbols for distance, mass/unit length and modulus of elasticity, respectively, and ℓ, ρ and t are the fundamental dimensions. Using the previously mentioned relationships, all dimensions in Col. 3 were expressed in terms of D, m, and E.

(5) Model-prototype relations for D, m and E were chosen arbitrarily as given in the first three rows of Col. 4, where subscripts m and p refer to model and prototype variables; s is the scale factor and s_i refers to the corresponding variable. As all the dimensions were expressed in terms of D, m, and E, by simple substitution all the scale factors were expressed in terms of

TABLE 2.1. SIMILITUDE REQUIREMENTS

(1) Variable	(2) Symbol	(3) Dimension	(4) General Similitude Law	(5) Scale Factors for this Study
Distance	D	ℓ	$D_m = s_D \cdot D_p$	1/5.5
Mass per Unit Length	m	$\rho \cdot \ell^2$	$m_m = s_m \cdot m_p$	1/5.5
Modulus of Elasticity	E	$\rho \cdot \ell^2 \cdot t^{-2}$	$E_m = s_E \cdot E_p$	1
Angle	ϕ	--	$\phi_m = \phi_p$	1
Moment of Inertia	I	ℓ^4	$I_m = s_D^4 \cdot I_p$	$1/(5.5)^4$
Section Modulus	Z	ℓ^3	$Z_m = s_D^3 \cdot Z_p$	$1/(5.5)^3$
Force	F	$\rho \cdot \ell^4 \cdot t^{-2}$	$F_m = s_D^2 \cdot s_E \cdot F_p$	$1/(5.5)^2$

TABLE 2.1 (Continued)

(1) Variable	(2) Symbol	(3) Dimension	(4) General Similitude Law	(5) Scale Factors for this Study
Moment	M	$\rho \cdot \ell^5 \cdot t^{-2}$	$M_m = s_E \cdot s_D^3 \cdot M_p$	$1/(5.5)^3$
Time	t	t	$t_m = s_m^{1/2} \cdot s_E^{-1/2} \cdot t_p$	$1/\sqrt{5.5}$
Mass	μ	$\rho \cdot \ell^3$	$\mu_m = s_m \cdot s_D \cdot \mu_p$	$1/(5.5)^2$
Specific Mass	ρ	ρ	$\rho_m = s_m \cdot s_D^{-2} \cdot \rho_p$	5.5
Stress	σ	$\rho \cdot \ell^2 \cdot t^{-2}$	$\sigma_m = s_E \cdot \sigma_p$	1
Strain	ε	--	$\varepsilon_m = \varepsilon_p$	1
Deflection	δ	ℓ	$\delta_m = s_D \cdot \delta_p$	1/5.5
Acceleration	a	$\ell \cdot t^{-2}$	$a_m = s_D \cdot s_m^{-1} \cdot s_E \cdot a_p$	1
Dead Weight	F_d	$\rho \cdot \ell^3 \cdot g^*$	$F_{dm} = s_m \cdot s_D \cdot F_{dp}$	$1/(5.5)^2$
Frequency	f	t^{-1}	$f_m = s_m^{-1/2} \cdot s_E^{-1/2} \cdot f_p$	$\sqrt{5.5}$

* g = acceleration due to gravity.

s_D, s_m and s_E, as shown in Col. 4. These are the general similitude laws for the model.

(6) Choosing $s_D = 1/5.5$, $s_m = 1/5.5$ and $s_E = 1$, the numerical values of all the scale factors for this model were obtained. These are shown in Col. 5. The choice of s_D was made on the basis of the cost analysis as mentioned in Sec. 2.2. s_m and s_E values were chosen such that the similitude requirements can be conveniently realized in the physical model.

Column 5 of Table 2.1 indicates that the specific mass of the model material should be 5.5 times that of the prototype. This requirement could not be satisfied and had to be compensated for. With proper compensation this should not affect the static test results and should affect the dynamic test results only to the extent that the inertia forces act on the surface instead of acting at every point of the structure. The magnitudes of these forces conform with the similitude requirements.

2.4 Materials

Model materials cannot be obtained by rigorously scaling down the different components according to similitude requirements. Scaling down is impossible at a molecular level. However, this does not impose any practical limitation on selection of model materials. As long as the Poisson's ratio, the stress-strain characteristics and the failure criterion of the model materials conform to those of the prototype materials at all levels of stress and strain, it is not required that all constituents be scaled.[29,55]

These requirements have been closely satisfied by using micro-concrete, annealed steel wire for non-prestressed reinforcement, and 3/32 in. nominal diameter, 7 wire stainless steel aircraft control cable strands for prestressing steel. These materials were successfully used in previous investigations.[5,7,22] Figure 2.1 shows typical characteristics of the annealed steel wires and the microconcrete. Figure 2.2 shows load-strain relationships for the prestressing strands. The microconcrete mix design is given in Table 2.2.[5,7] Average concrete strengths for different elements of all the bridges are given in Table 2.3. The scatter in concrete strengths about the average values which are shown in Table 2.3 was small. The only exception was in the case of Bridge 2 where the average cylinder strength for Girder 1 was found to be 4200 psi, much less than the average strength

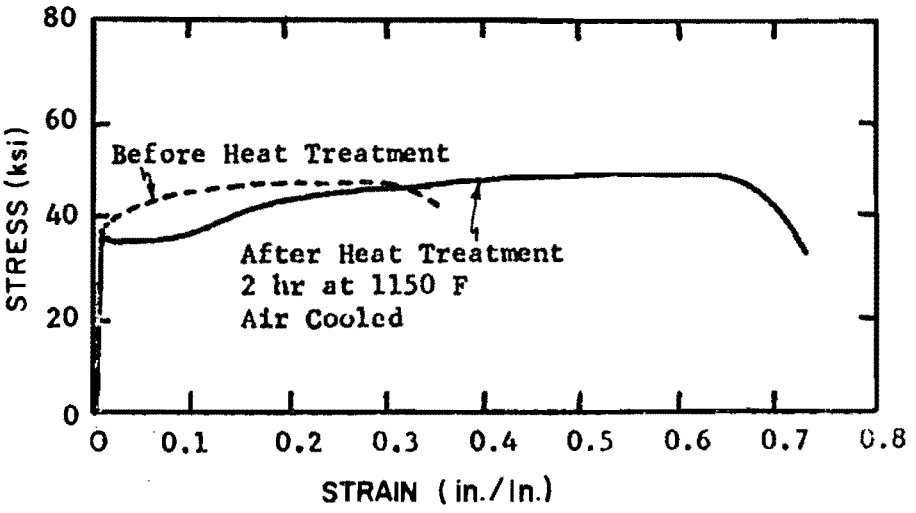

(a) Model reinforcement wire

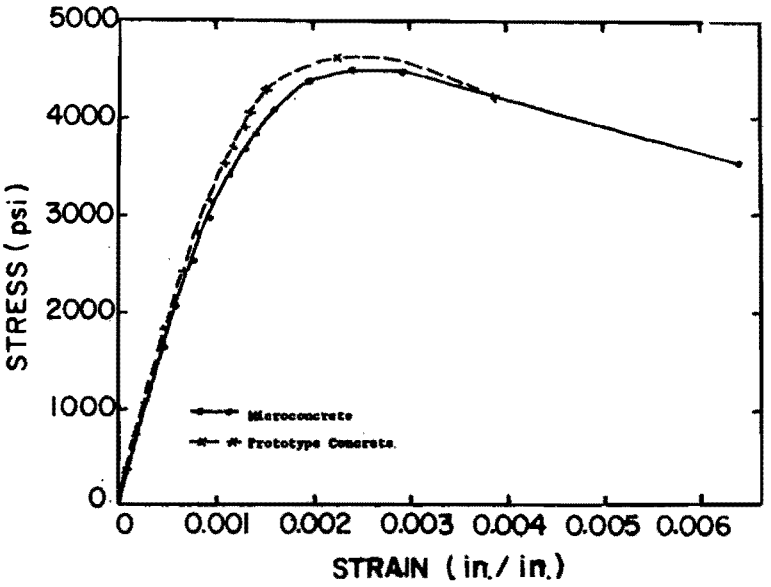

(b) Microconcrete and prototype concrete

Fig. 2.1 Stress-strain relationships of reinforcement and concrete (taken from Ref. 22).

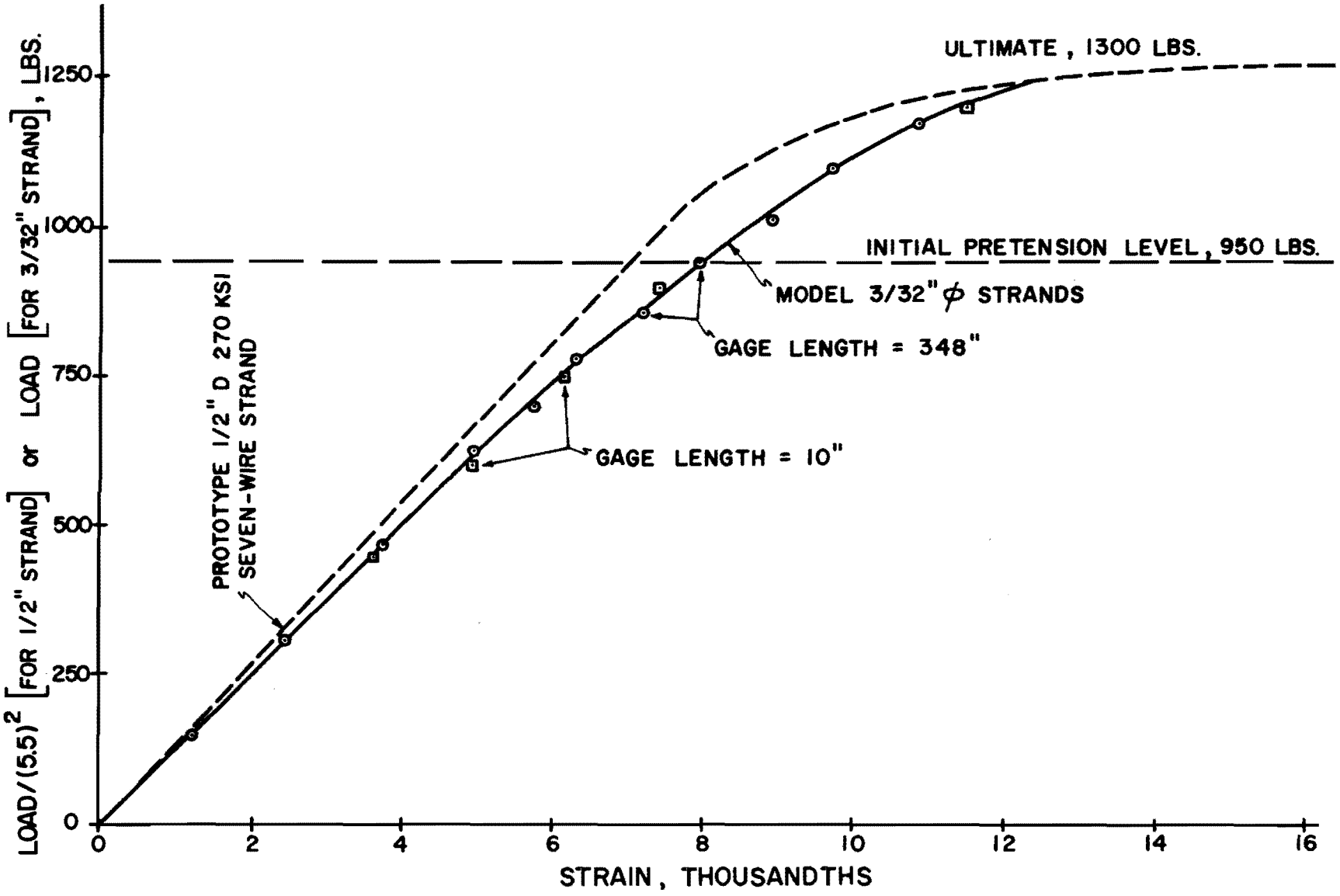

Fig. 2.2 Load versus strain relationship for 1/2 in. and 3/32 in. seven wire strands. (Ref. 7.)

TABLE 2.2. CONCRETE MIX PROPORTIONS FOR ONE CU. FT.

	Mix #1 (Precast Girders)	Mix #2 (Diaphragms, Bent Caps, and Slab)
Cement	30 lbs.	17.9 lbs.
Water	15.5 lbs.	13.4 lbs.
Airsene L (water reducing admixture)	36.0 cc	27.0 cc
Aggregate:		
TCM 1/8	27.6 lbs.	31.0 lbs.
Ottawa Sand	32.0 lbs.	35.7 lbs.
Blast Sand #1	29.4 lbs.	33.2 lbs.
Blast Sand #2	8.5 lbs.	9.6 lbs.
Colorado River Sand	8.5 lbs.	9.6 lbs.

TABLE 2.3 MODEL CONCRETE STRENGTH, PSI

Bridge No.	Girder	Slab	Interior Diaphragms	Exterior Diaphragms
1	5220	3230	3000	3750
2	6750	3730	3920	3400
3	6975	3860	3500	3500
4	7500	4960	2900	2900

of the other five girders (6750 psi). The girder concrete strengths for this bridge were checked by elastic rebound hammer tests. The strengths obtained were 5200 psi for Girder 1 and 6740 psi (average) for the other five girders. This discrepancy in Girder 1 strength was probably due to some gross mistake in proportioning the concrete mix. This girder strength was neglected in calculating the average girder concrete strength shown in Table 2.3.

2.5 Specimens

Four standard Texas Highway Department simple span bridges, each having 6 prestressed concrete girders, were chosen for this study. Prototype plans and girder details for the bridges are given in Appendix A. General model plans, locations, and types of diaphragms and a sectional view of the composite girder used are shown in Figs. 2.3 through 2.9. Model slab thickness should be 1-3/8 in. Due to some formwork errors, actual slab thickness in Bridges 1 and 2 was 1-1/2 in. In Figs. 2.7 and 2.8, Type D4 diaphragms are standard exterior diaphragms for the Texas Highway Department bridges. Type D3 diaphragms are interior diaphragms used in standard concrete bridges by the Bureau of Public Roads. Figure 2.10 shows the modifications used in Bridges 3 and 4 as an alternative to standard end diaphragms. Important characteristics of the model bridges are summarized in Table 2.4. In this table, flange width and E values were calculated using Sec. 8.7.2 and 8.3 of the ACI 318-71 Building Code.[2] Moments of inertia were calculated for gross sections neglecting the steel except in the case of composite girders where the flange steel and prestressing steel were taken into account.

2.6 Specimen Preparation

Formwork, fabrication, prestressing and casting operations for identical models have been described earlier in detail by Barboza[7] and by Bakir.[5] A description of necessary modifications and a summary of procedures are given below.

2.6.1 Formwork

The formwork for all the precast elements (girders, bent caps and Type D1 diaphragms) was made of plexiglas and for the cast-in-place elements (slabs and other diaphragms) was made of plywood with laquer finished surfaces.

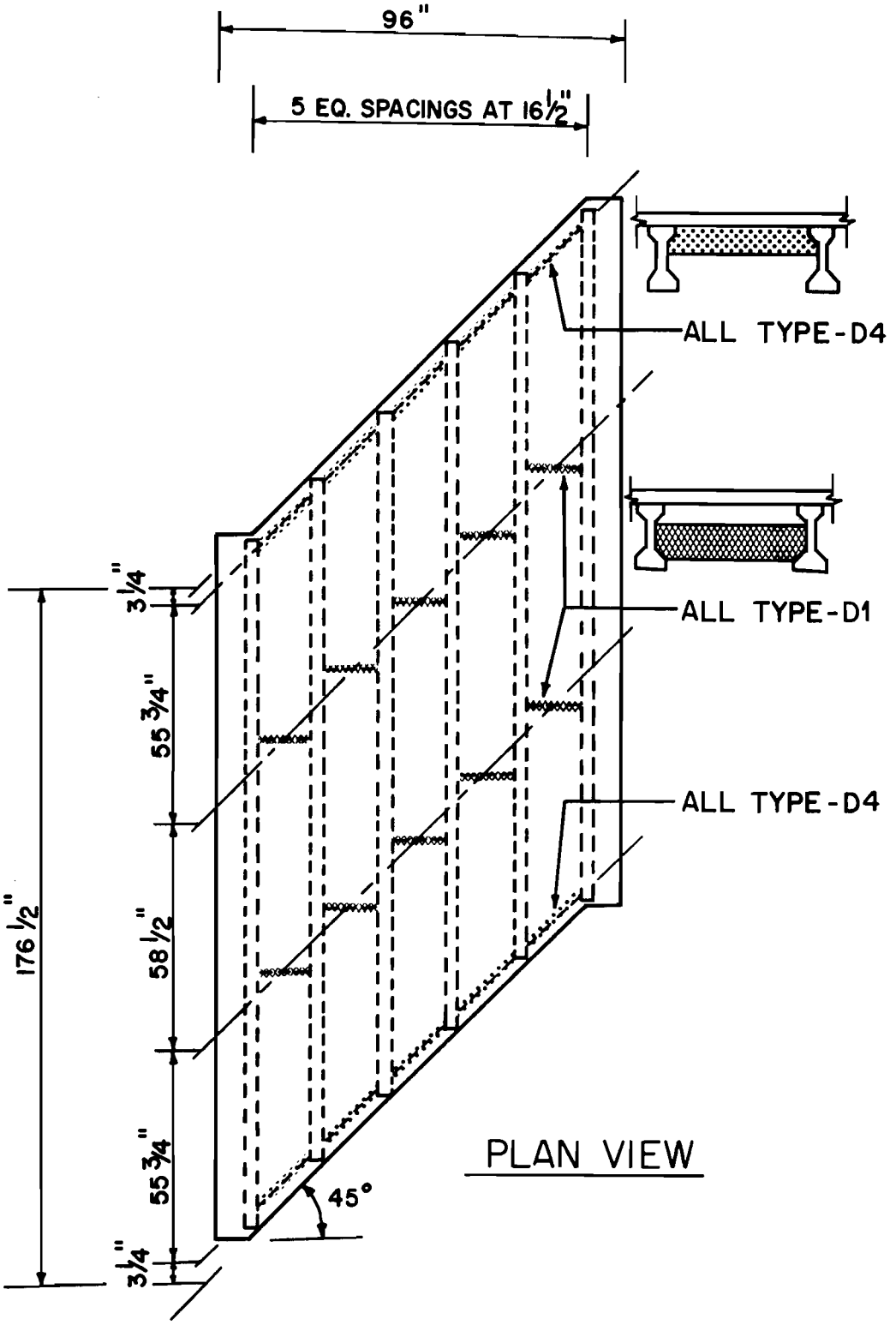

Fig. 2.3 Bridge 1, general plan, diaphragm types and locations.

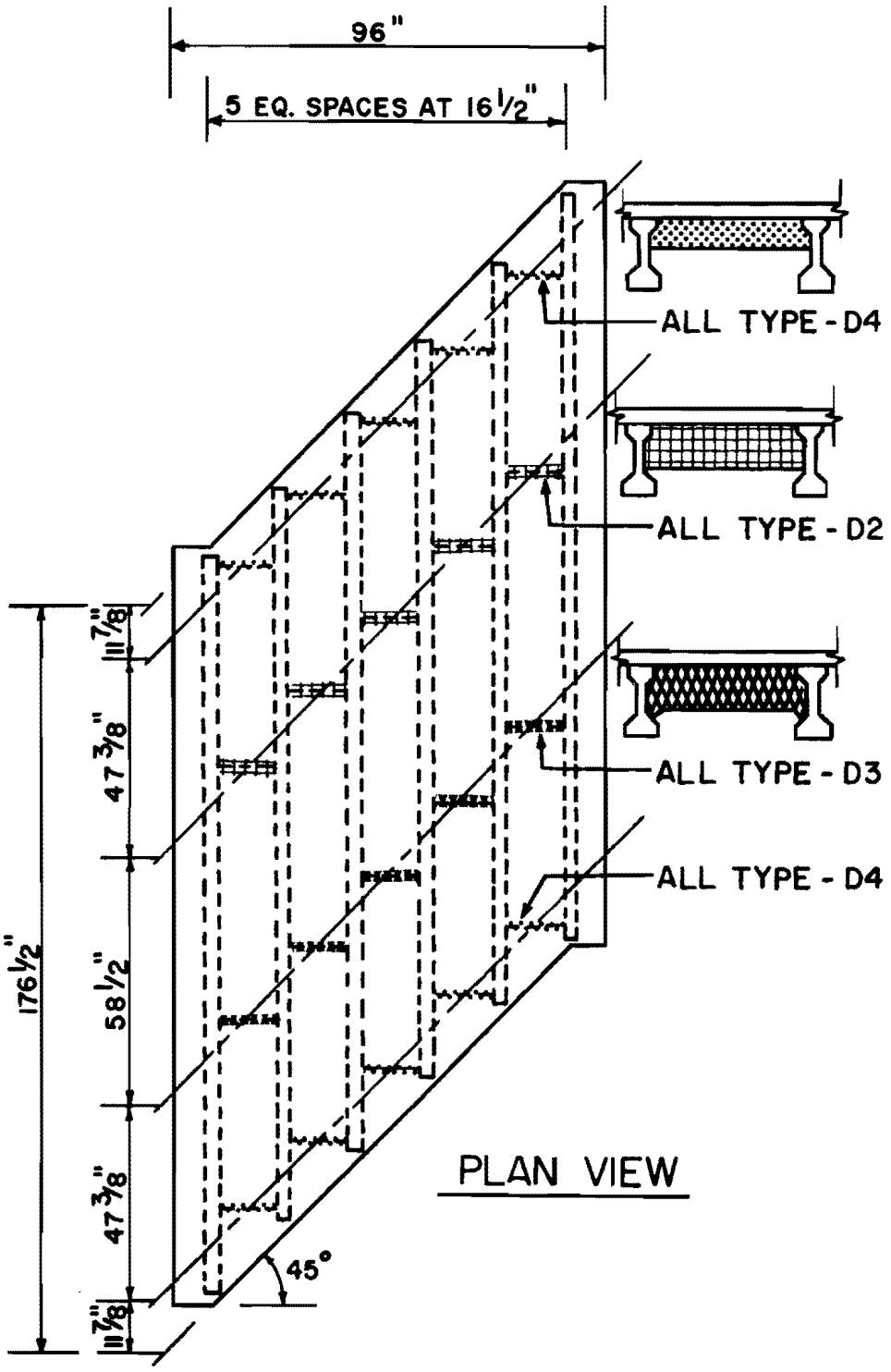

Fig. 2.4 Bridge 2, general plan, diaphragm types and locations.

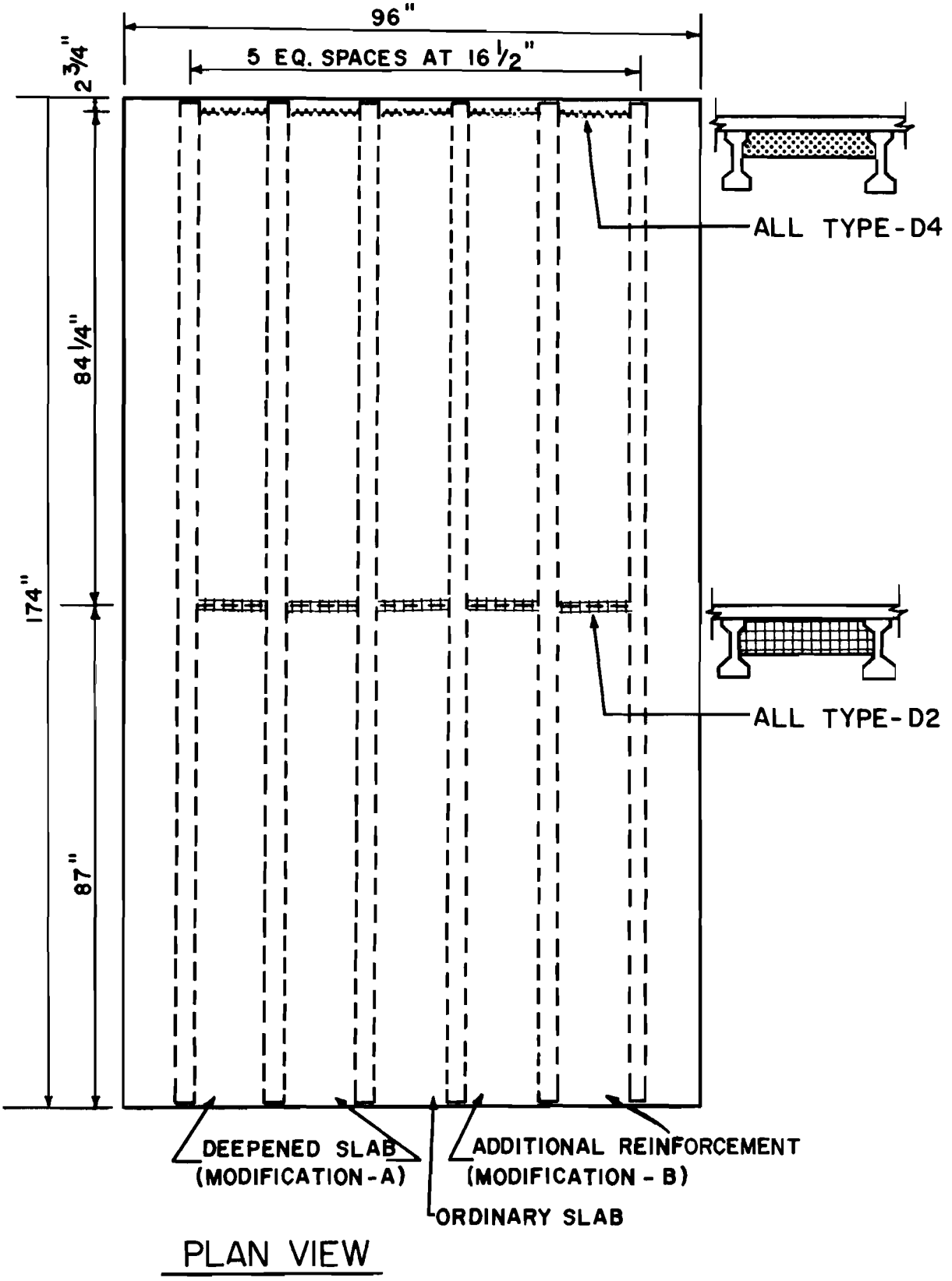

Fig. 2.5 Bridge 3, general plan, diaphragm types and locations.

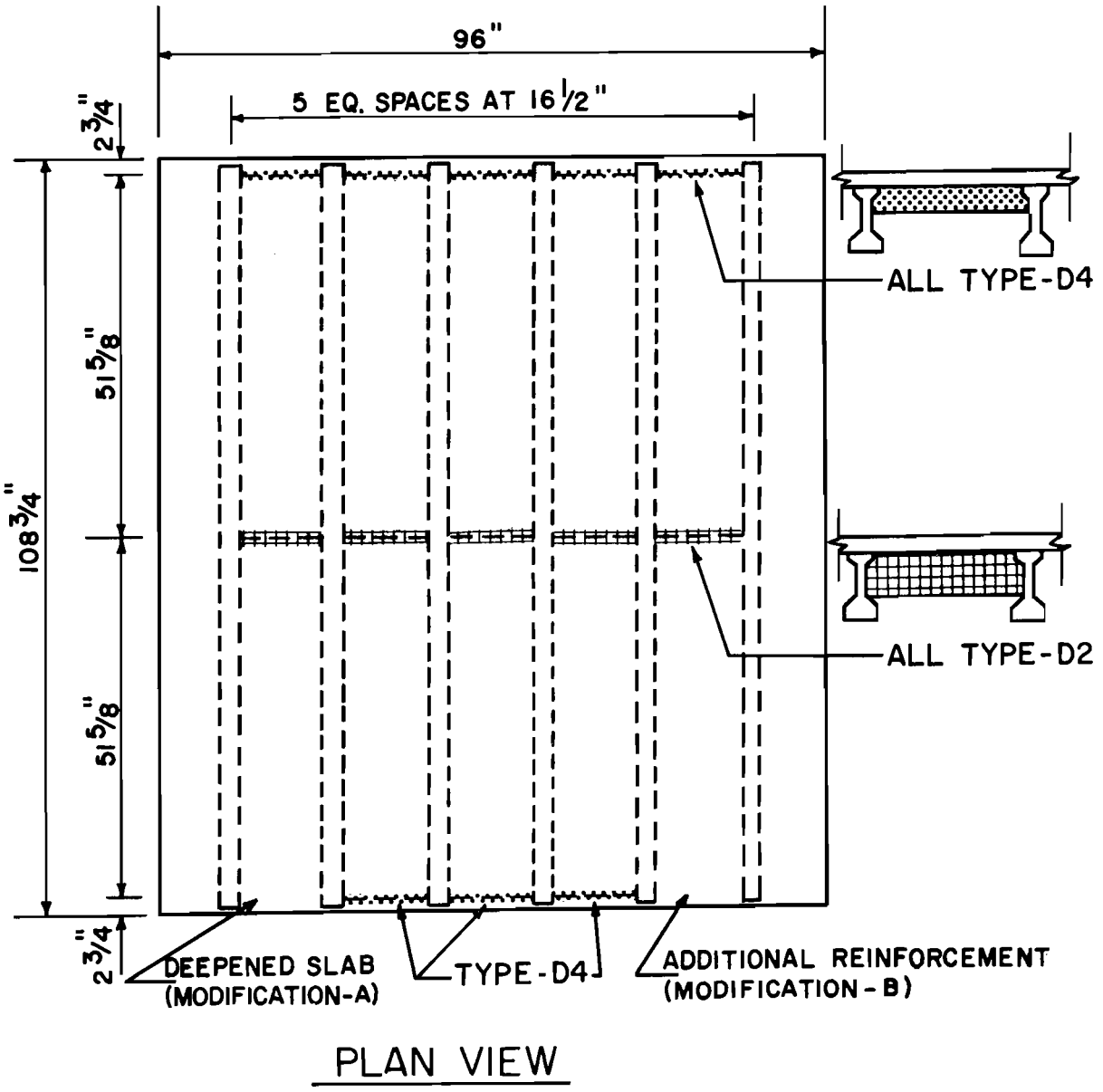

Fig. 2.6 Bridge 4, general plan, diaphragm types and locations.

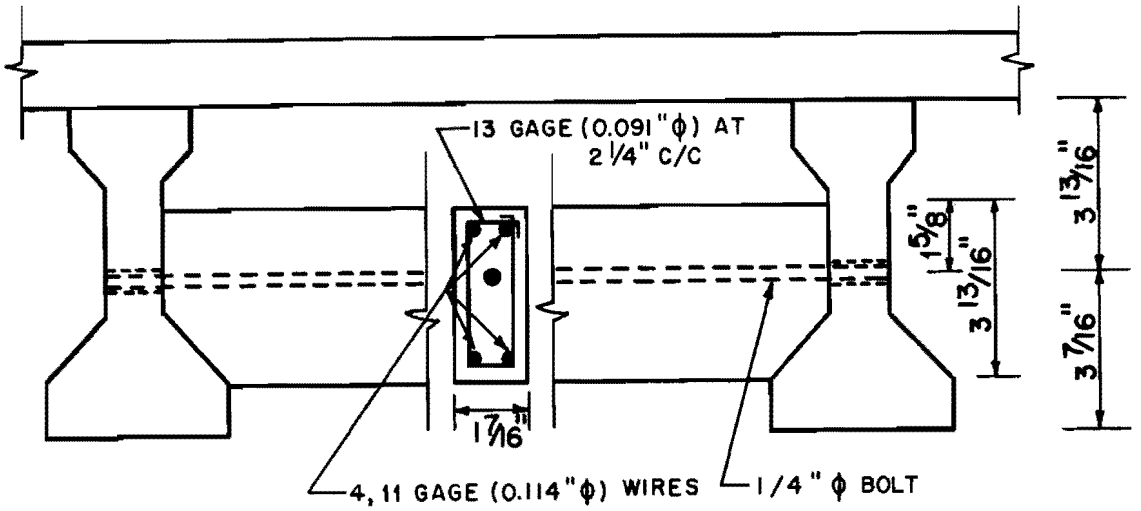

INTERIOR DIAPHRAGM, TYPE-D1

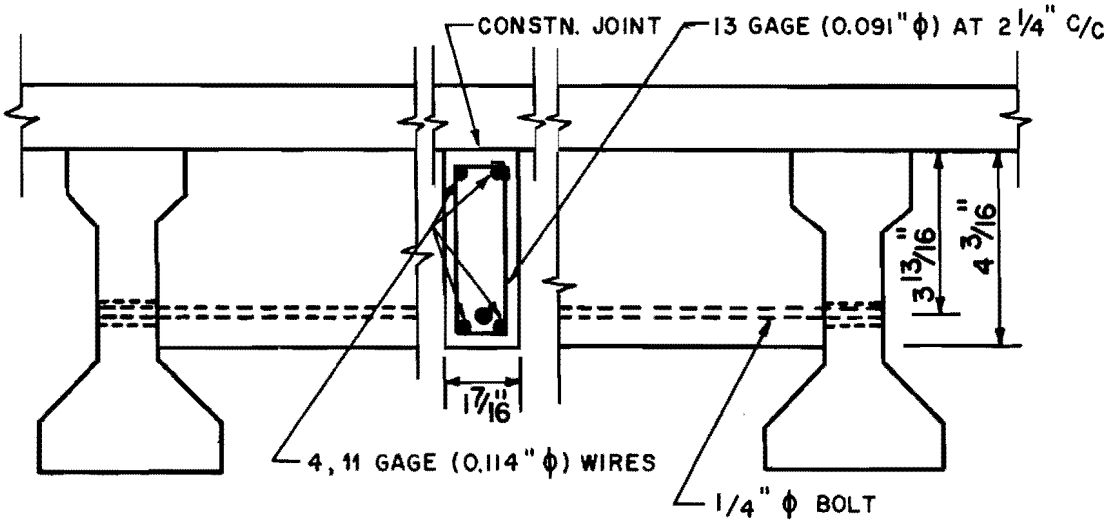

INTERIOR DIAPHRAGM, TYPE-D2

Fig. 2.7 Diaphragm details.

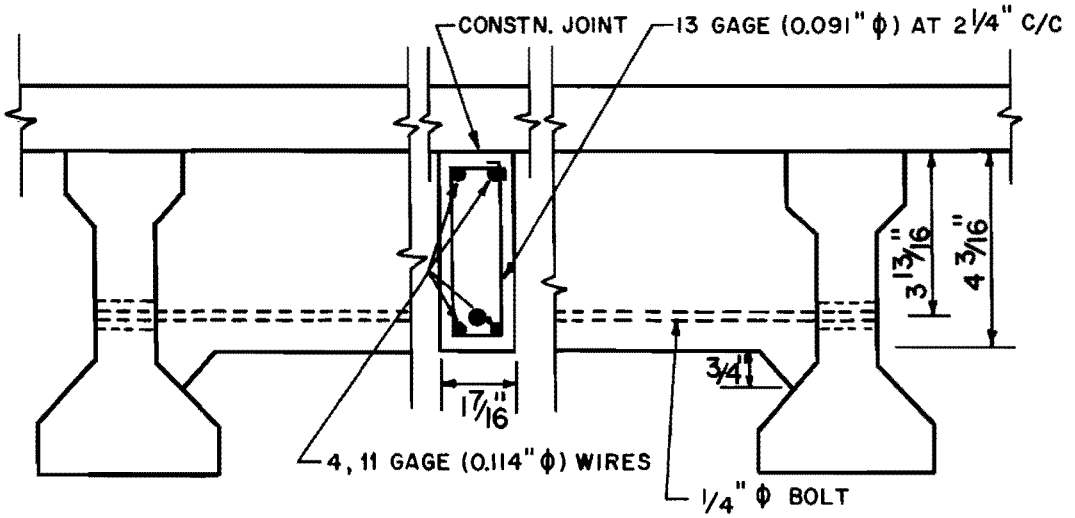

INTERIOR DIAPHRAGM, TYPE-D3

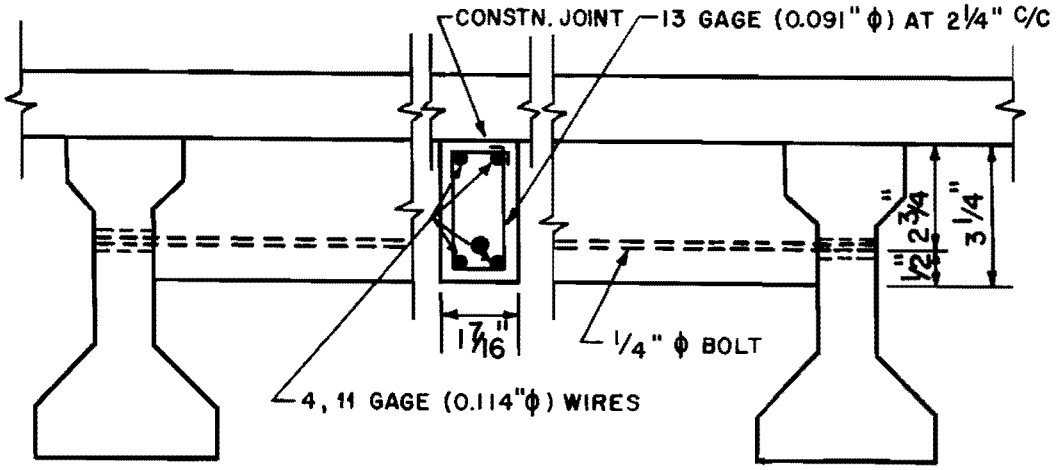

END DIAPHRAGM, TYPE-D4

Fig. 2.8 Diaphragm details.

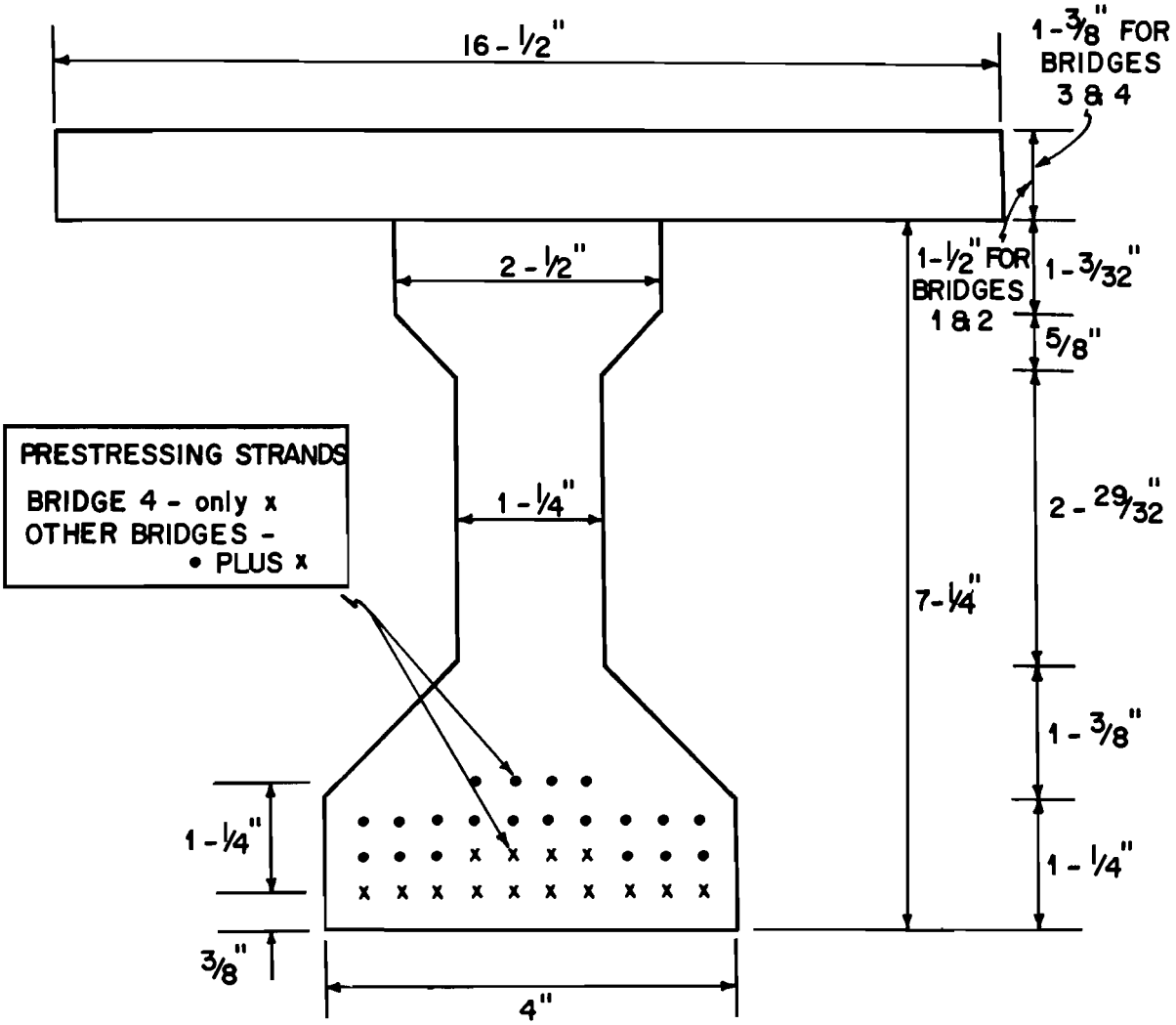

Fig. 2.9 Section of composite girder at midspan.

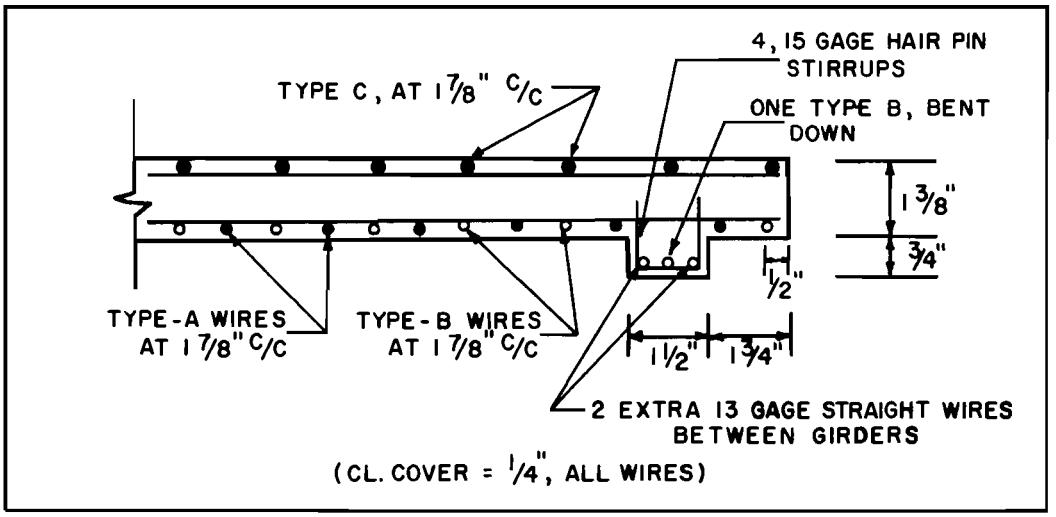

(A) DEEPENED SLAB - MODIFICATION A

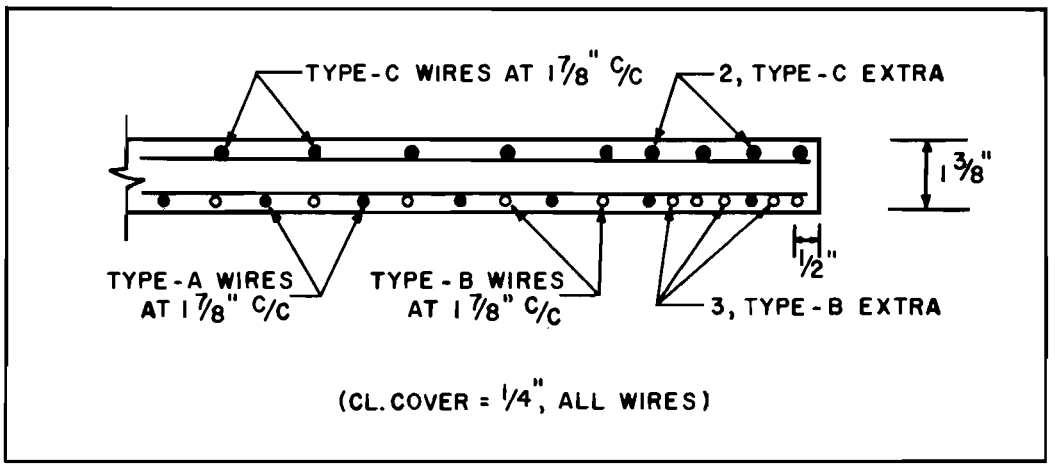

(B) EXTRA REINF. - MODIFICATION B

WIRE TYPE	GAGE #	DIAMETER	SHAPE
A	11	0.121"	
B	13	0.092"	
C	11	0.121"	

Fig. 2.10 Longitudinal section of slab along and between the girders showing modifications at end span zone.

TABLE 2.4. IMPORTANT MODEL BRIDGE CHARACTERISTICS

Bridge No.	1	2	3	4
Span (L), in.	172	172	172	107
Distance between girders (S), in.	16.5	16.5	16.5	16.5
Skew Angle (α), Degrees	45	45	0	0
Location and Stiffness (EI_D) of Interior Diaphragms, lbs. in.^{2}	Staggered at 1/3 points. 2.20×10^7	Staggered at 1/3 points. 1.26×10^8	Continuous at midspan. 1.16×10^8	Continuous at midspan. 1.13×10^8
Location and Stiffness (EI_D) of Exterior Diaphragms, lbs. in.^{2}	Continuous at endspan. 7.00×10^7	Staggered at endspan. 7.03×10^7	Continuous at endspan. 6.80×10^7	Continuous at endspan. 6.50×10^7
Slab Stiffness (EI_S) per inch width, lbs. in.^{2}/in.	9.10×10^5	9.80×10^5	7.80×10^5	8.50×10^5
Composite Girder Stiffness (EI_G), lbs. in.^{2}	1.40×10^9	1.48×10^9	1.49×10^9	1.53×10^9

2.6.2 Non-Prestressed Reinforcement

The precise diameter wires required by similitude laws were not available for the non-prestressed reinforcement. Nearest available gage nondeformed wires were used. Table 2.5 shows the required and actual wire sizes. The discrepancies were minor.

TABLE 2.5. REINFORCEMENT

Prototype Bar	Model Diameter	
	Required	Actual
#4	0.091 in.	0.092 in.
#5	0.114 in.	0.121 in.
#6	0.136 in.	0.135 in.

Reinforcement spacings were in accordance with the maximum allowable in design drawings.

2.6.3 Prestressing

Pretensioning was accomplished by several stages of stressing. In each stage the force was measured by a load cell, and was checked by a pressure gage and also by elongation of the strands. Allowances were made for draped tendons so that after draping all tendons were equally stressed to the level shown in Fig. 2.2.

2.6.4 Instrumentation

One-fourth in. strain gages were mounted on 1/8 in. diameter annealed wires by using Eastman 910 cement, insulated by a coating of rubber compound and finally covered by Furane Plastic for mechanical protection. These wires were tied accurately in position to serve as strain sensors. Usually the gage locations in girders were at 1/4, mid and 3/4 spans, although additional gages were also mounted at other points of interest. Several diaphragms in each bridge were instrumented with upper and lower gages at midspan of the diaphragms. In addition, gages were mounted at several points

in the slab. Some 1 in. long surface gages were mounted on slabs to study surface strains. Figure 2.11 shows typical gage locations in girder and diaphragm sections.

2.6.5 Casting and Curing

Microconcrete materials were mixed in a 2 cu. ft. mixer. The quantity of water was adjusted to keep the desired mix consistency. The specimen was covered with wet cloth for two days. The forms were stripped on the fifth day after casting. Five 3 in. x 6 in. concrete cylinders were cast for each girder, eight cylinders for each slab, and at least three cylinders for each set of diaphragms.

2.6.6 Support Conditions

Three-sixteenth in. thick rubber pads were used instead of neoprene pads. Graphite powder was spread on these pads to assure smooth movement of supported girder ends. As specified in the 1971 Texas Highway Department bridge drawings, bent cap pins for the intermediate girders were eliminated for Bridge 3 and Bridge 4. To simulate an interior span, dummy exterior slabs with one end supported on each bent cap, at either side of the bridge span, were used. They were loaded to produce accurate dead load reactions on the bent caps (see Fig. 2.12).

2.6.7 Dead Load Compensation

To satisfy the similitude requirements for dead load of the bridge, it was necessary to provide compensatory dead load blocks. These loads could not be hung loosely as done previously[5,7] in static load studies, but had to be installed so as to move in unison with the vibrating bridge to simulate the inertia forces. Dynamic tests on a single model girder were made (see next section) to find an efficient method for dead load compensation. Figure 2.13 shows how the dead loads were hung in the test bridges. The chains used to hang the blocks from girders were prestretched using about 500 lbs. force to ensure that no plastic deformation of the chains would occur during bridge vibration and to make the chains fit centrally with the top flange of the girders. The distribution of dead loads was governed by the following criteria:

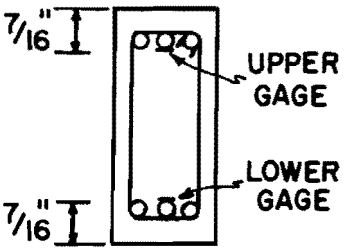

(a) Diaphragms - Type D1 gages are at diaphragm midspan

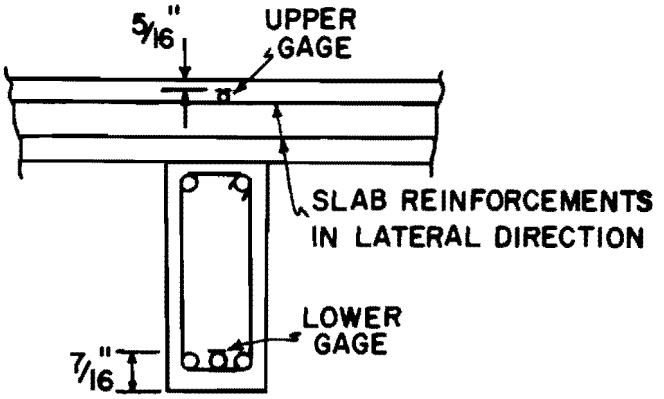

(b) Diaphragms - other types, gages are at diaphragm midspan

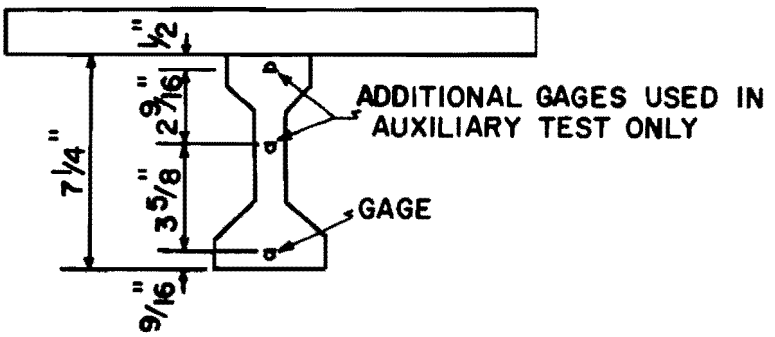

(c) Girders

Fig. 2.11 Typical strain gage locations in diaphragm and girder sections.

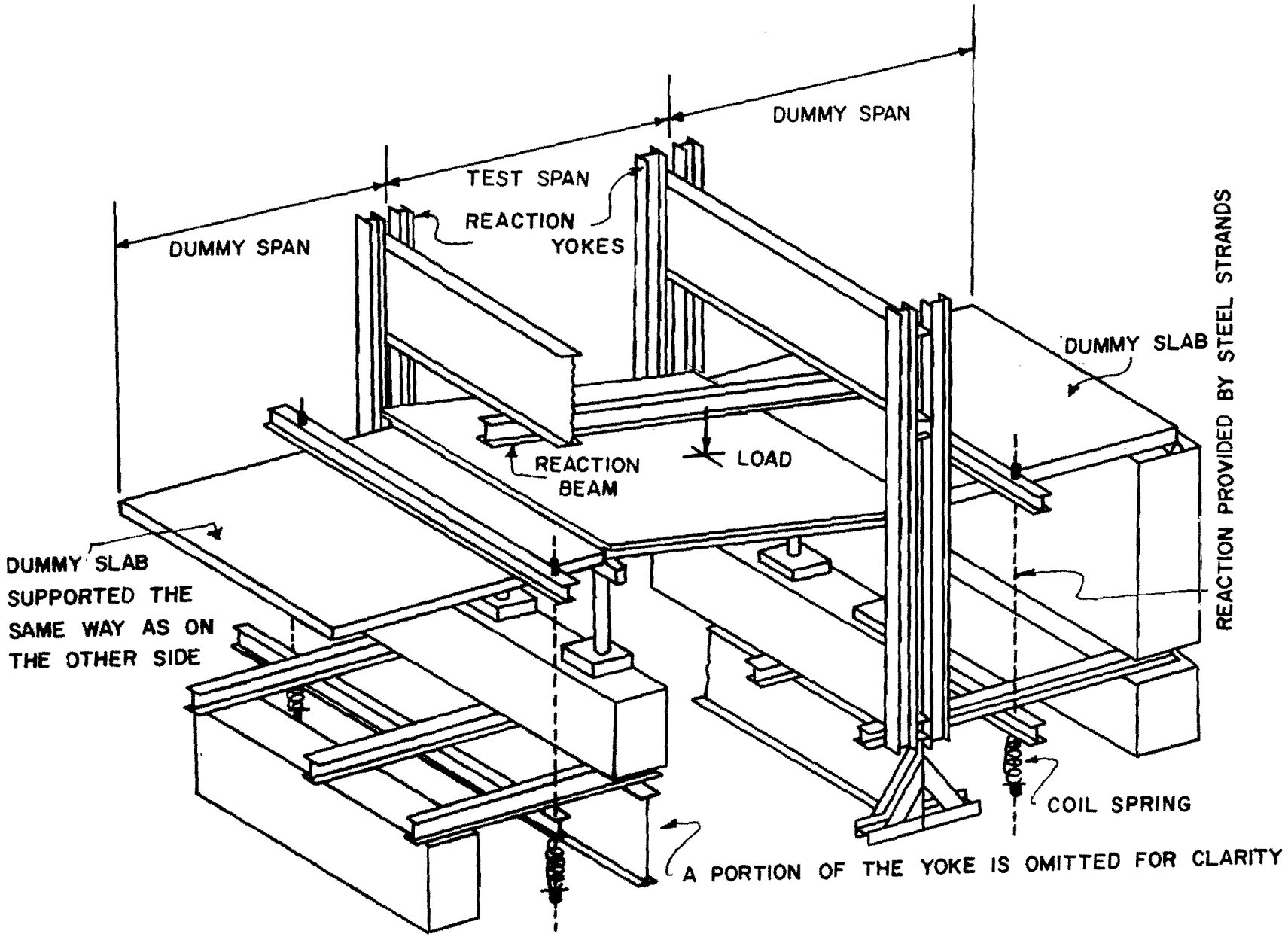

Fig. 2.12 Static load setup and dummy slabs.

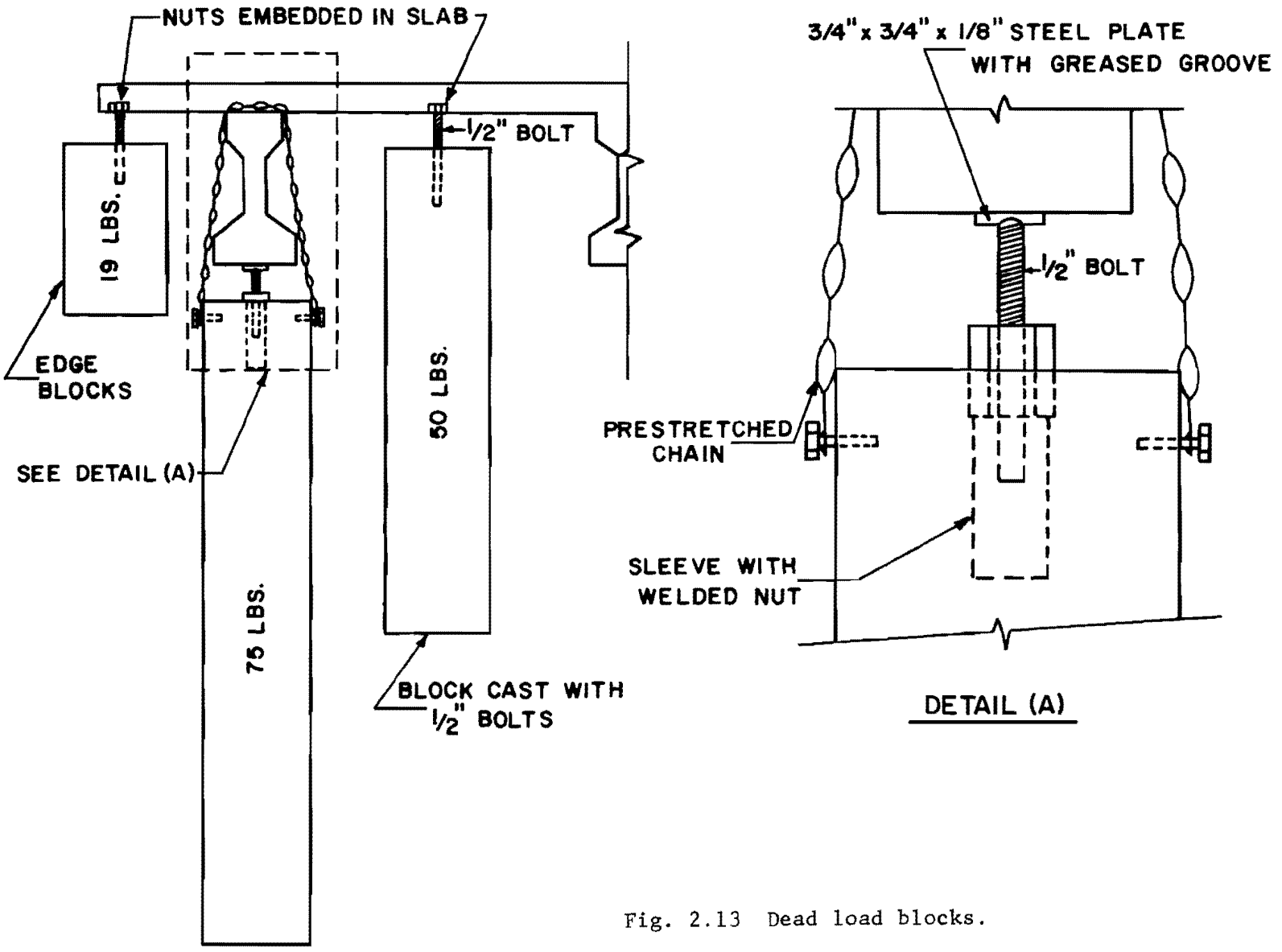

Fig. 2.13 Dead load blocks.

(a) They should be close enough to represent uniform load distribution along the girders.

(b) There should be enough working room to put the blocks in position and to adjust them whenever necessary.

(c) The maximum transverse moment in the slab due to the load hung from the slab should be the same as required for dead load similitude.

(d) Total load per unit length on the girders should conform with similitude requirements.

Usual spacing of the blocks was about 8 in. c/c, with some adjustment whenever it was necessary to keep the blocks clear of diaphragms and loading devices.

2.7 Auxiliary Tests

A series of auxiliary tests was necessary to verify dead load compensation, to obtain moment-strain diagrams and flexural stiffnesses of the girders, and to check the performance of the cyclic loading, dynamic instrumentation and recording devices. A single composite girder with flange width equal to the center line distance between the girders was tested. The girder was simply supported and was instrumented with strain gages at end, quarter and midspans. These gages were located at exactly the same height from the bottom flange as those used later to instrument the bridge girders. Additional gages were mounted at approximately the center height and near the top of the girder to study sectional behavior (Fig. 2.11c).

2.7.1 Static Tests

Point loads were applied at the third points of the span. The magnitude of the maximum load was approximately 60 percent of the cracking load obtained from a previous test.[7] Strains at mid, quarter and end spans and deflections at mid and quarter spans were measured. The beam was loaded and unloaded several times and readings were taken again at the fifth cycle of loading. The following observations were made:

(1) Moment-strain relationships were identical for mid and quarter spans and they were almost linear within the loading range. Differences in observed strains in successive loading cycles were small. The average relationship is shown as a curve in Fig. 2.14. The maximum deviation of measured

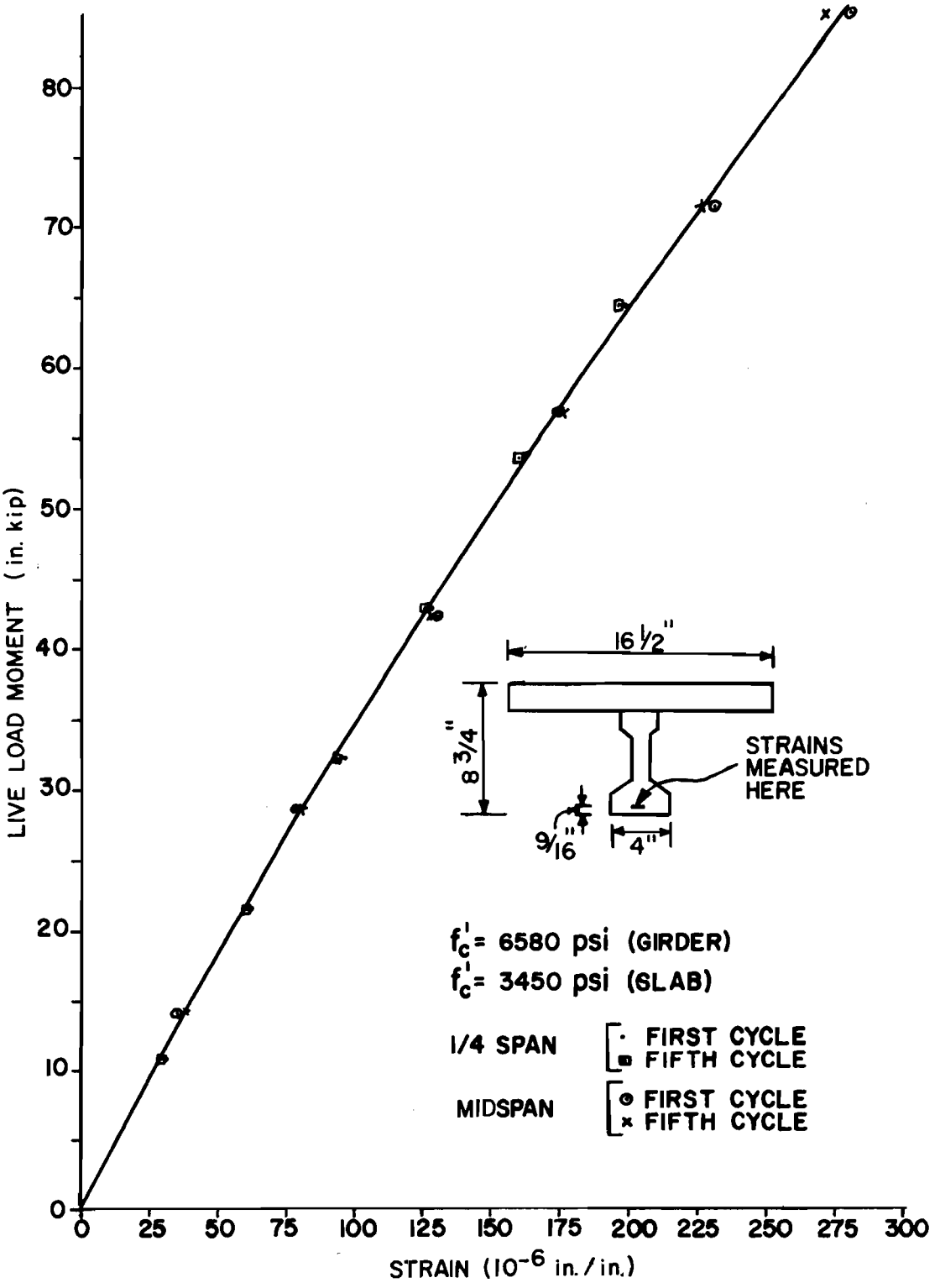

Fig. 2.14 Auxiliary test, girder moment-strain relationship.

moments was 1.5 in. kip and the standard deviation of the measured moments was 0.82 in. kip.

(2) The girder stiffnesses obtained from midspan deflections were 1.73×10^9 lb. in.^{2} and 1.68×10^9 lb. in.^{2} for the first and fifth cycle, respectively.

(3) Measured strains at different heights of the girder section verified that plane sections remain plane. The calculated position of the neutral axis matched that obtained from the experiment.

2.7.2 Dynamic Tests

Cyclic loads were applied at midspan over a frequency range of 4 to 15 Hz. Deflections at supports, quarter span, midspan and at the bottom of one dead load block at midspan of the girder were measured by LVDT's (Linear Variable Differential Transformers) with the signals recorded on magnetic tape. Also recorded were the strains at mid and quarter spans.

Types of dead load blocks used in the auxiliary dynamic experiments are shown in Fig. 2.15. Type-A blocks were found to be completely unsatisfactory because of yielding of the hooks and subsequent loss of support for the blocks as the test continued. Therefore, this type was abandoned. Type-B blocks were satisfactory at lower frequencies, but at higher frequencies (beyond 8 Hz) the steel straps loosened. The general performance of this system was checked with a theoretical analysis.[10] The usual range of variation of the coefficient of damping is from 0.5 to 6 percent of critical damping in conventional bridges. The actual value depends on the type of bridge and support conditions.[49] An approximate average value of 3 percent of critical damping was used in this theoretical analysis. Later in this research program, experimental results indicated 1 percent would have been more appropriate.

Typical results are shown in Figs. 2.16 through 2.18. The quarter span responses were essentially similar with those at midspan and are shown for one case only. It can be seen from Fig. 2.18 that at high frequencies damping is very high. This is because some of the dead load blocks lost contact with the girder, and, also the steel straps tieing the blocks together loosened. Until this occurred, the blocks

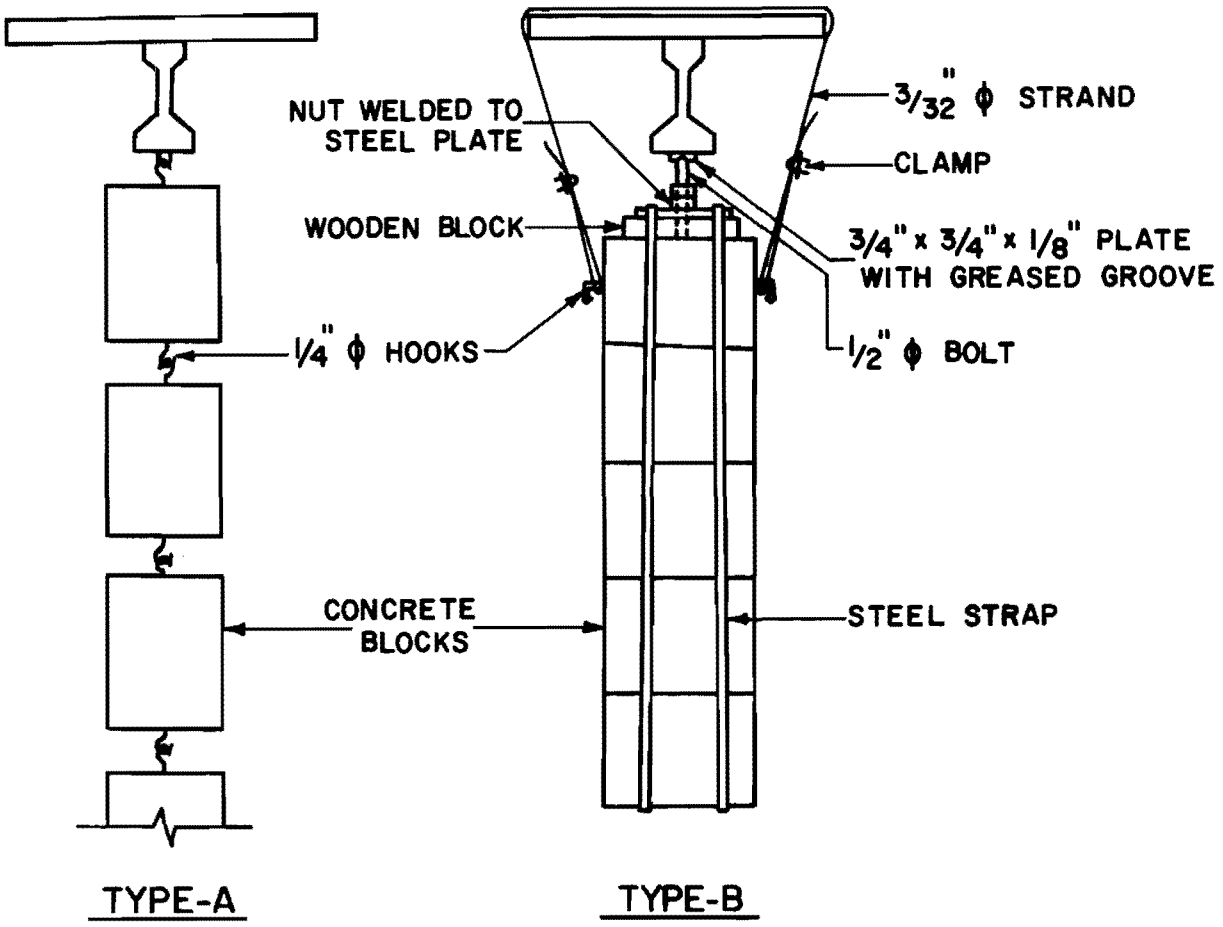

Fig. 2.15 Auxiliary test of dead load blocks.

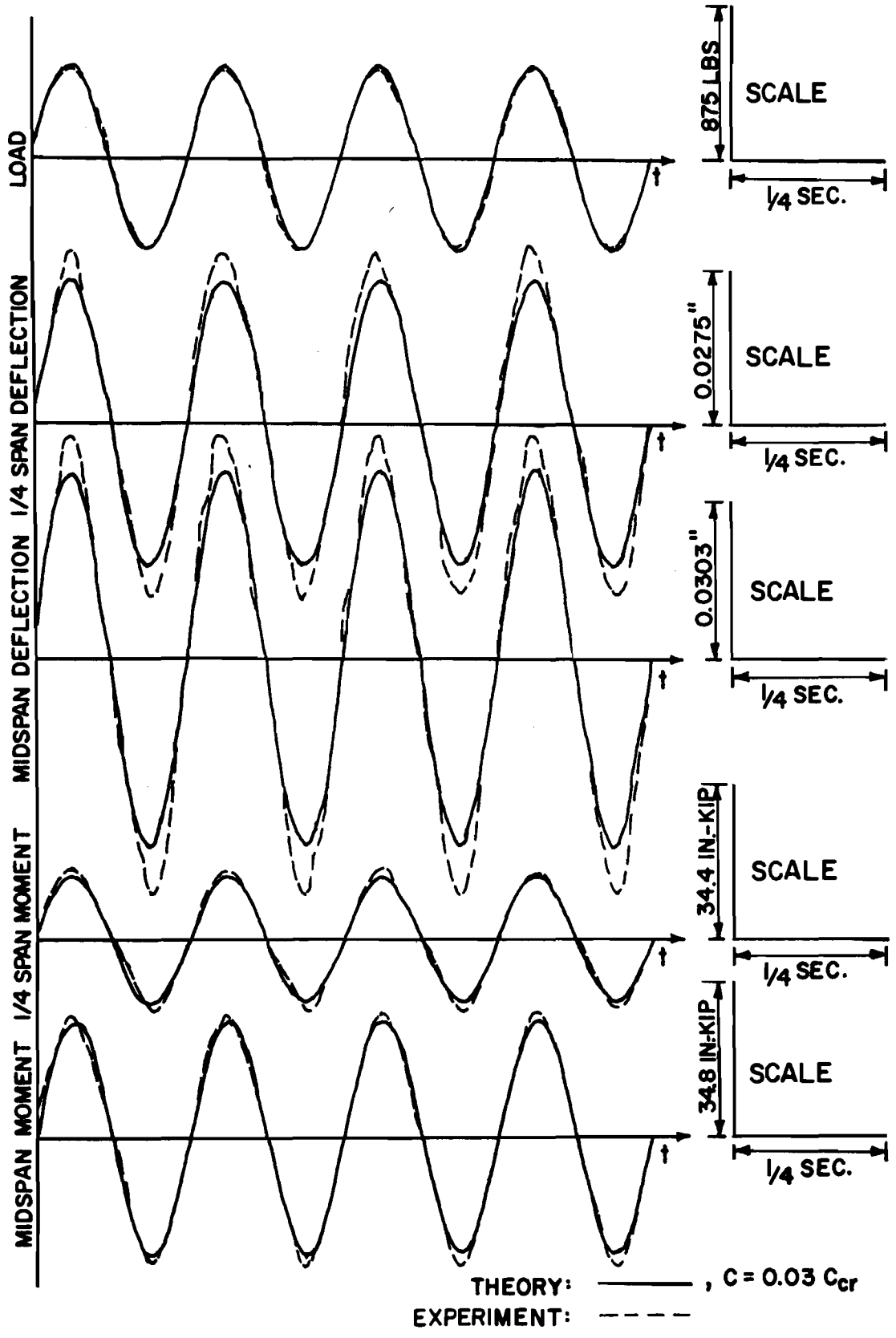

Fig. 2.16 Auxiliary test, beam response at 4 Hz.

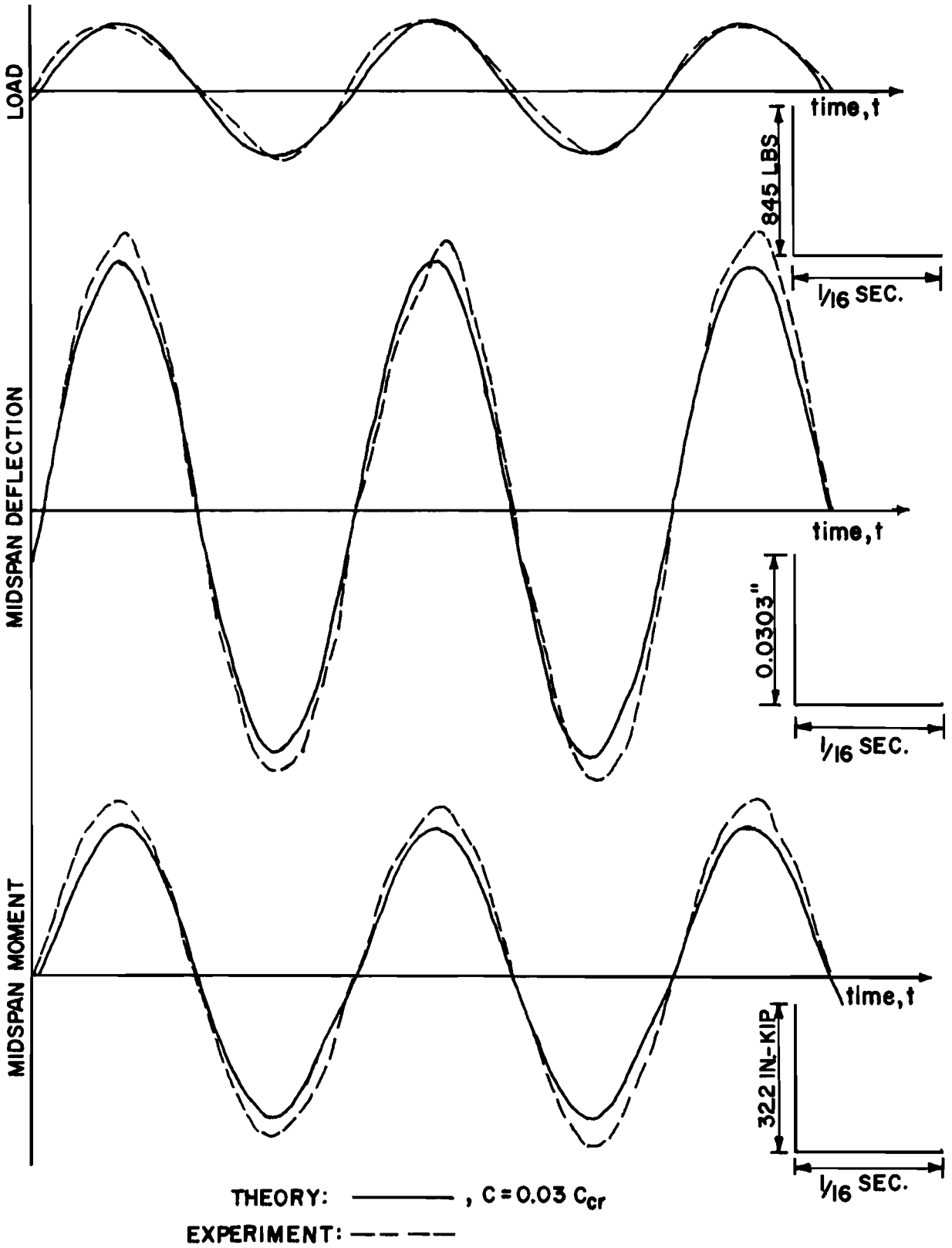

Fig. 2.17 Auxiliary test, beam response at 7.6 Hz.

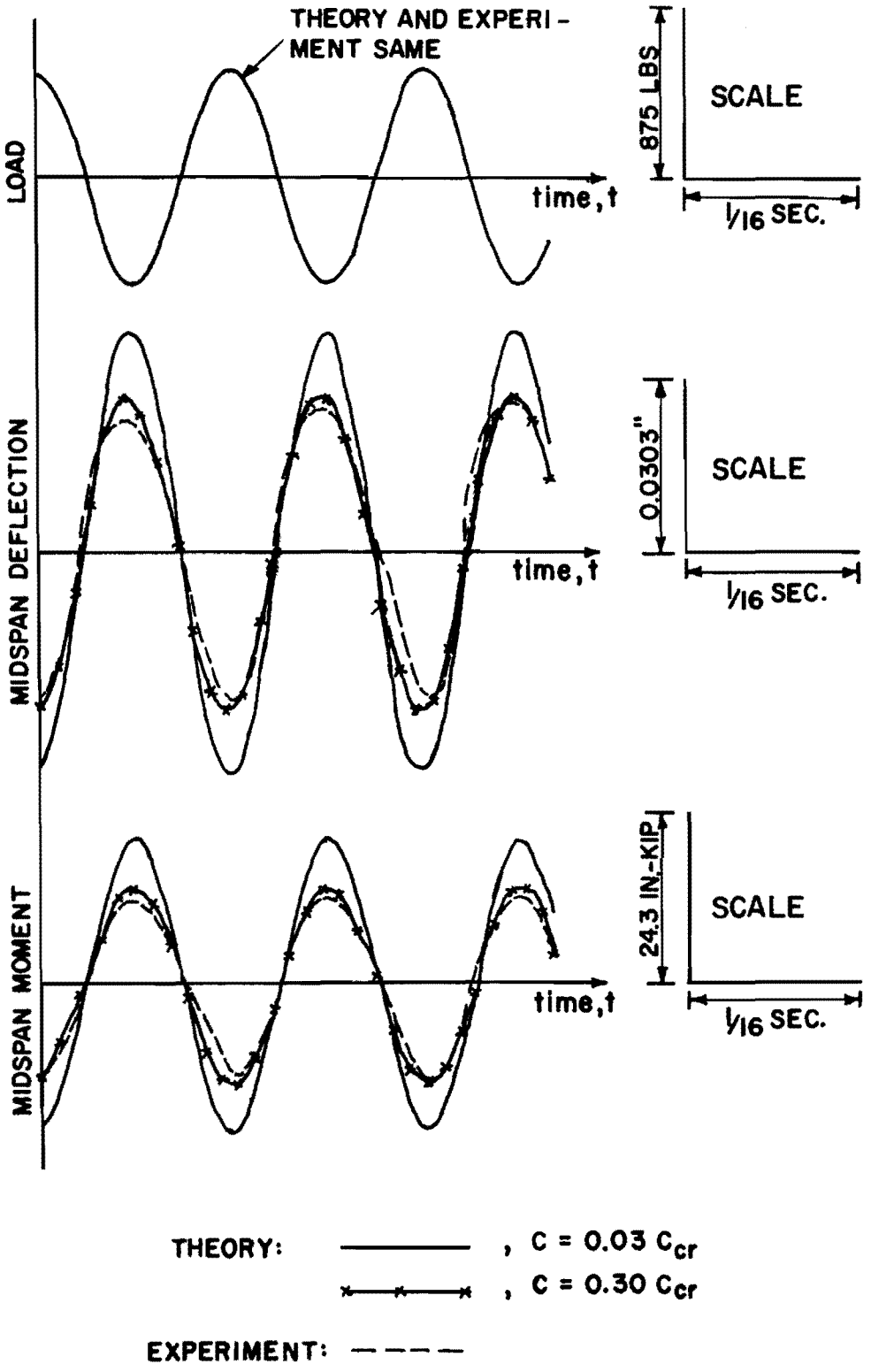

Fig. 2.18 Auxiliary test, beam response at 14.2 Hz.

and the girder vibrated in unison as shown in Fig. 2.19 and agreement of the girder response with theory was good as shown in Fig. 2.17. The situation was improved significantly when a singly cast monolithic block was used to replace the multiple blocks at a single point. This block maintained contact with the girder even when the test was run at 9 Hz, very close to the calculated resonant frequency of 10.3 Hz, for about half an hour. Finally, for ease of erection and also to reduce elastic deformation of the beam dead load block connection, prestretched steel chains were used to hang the blocks from the girder (Fig. 2.13).

2.8 Test Setup - Loading and Measurement Systems

Static loads were applied as shown schematically in Fig. 2.12. Loads were applied by hydraulic rams, measured and checked by highly sensitive load cells and pressure gages. All point loads were applied through the loading blocks shown in Fig. 2.20a, corresponding to typical design truck tires at 80 psi. Axle and truck loads include a 25 percent impact factor and were applied as shown in Fig. 2.20b and c.

The cyclic loading setup is shown in Fig. 2.21. The static part of the load, dynamic amplitude, and frequency were controlled by adjusting the initial deflection, cam eccentricity, and motor speed. To get a wider frequency range, the pulley ratio can be changed. Frequencies were measured and checked by an electronic counter and a tachometer.

The setup for vertical impact is shown in Fig. 2.22. The height of fall was roughly adjusted by the movable plate. The impacting load was lifted up and the open end of the string was hooked into the V-notch in the movable plate. The height of fall was finally adjusted by the turnbuckle. By pulling the free end of the string out of the notch the impacting load was released to fall freely on the slab.

The setup for lateral impact is shown in Fig. 2.23. The load was pulled up to the desired height which could be read directly from a height-of-fall dial and then let fall like a pendulum to impact laterally.

Dynamic load, deflection, and strain signals were picked up by load cells, LVDT's, and strain gages. The measurement operation is shown

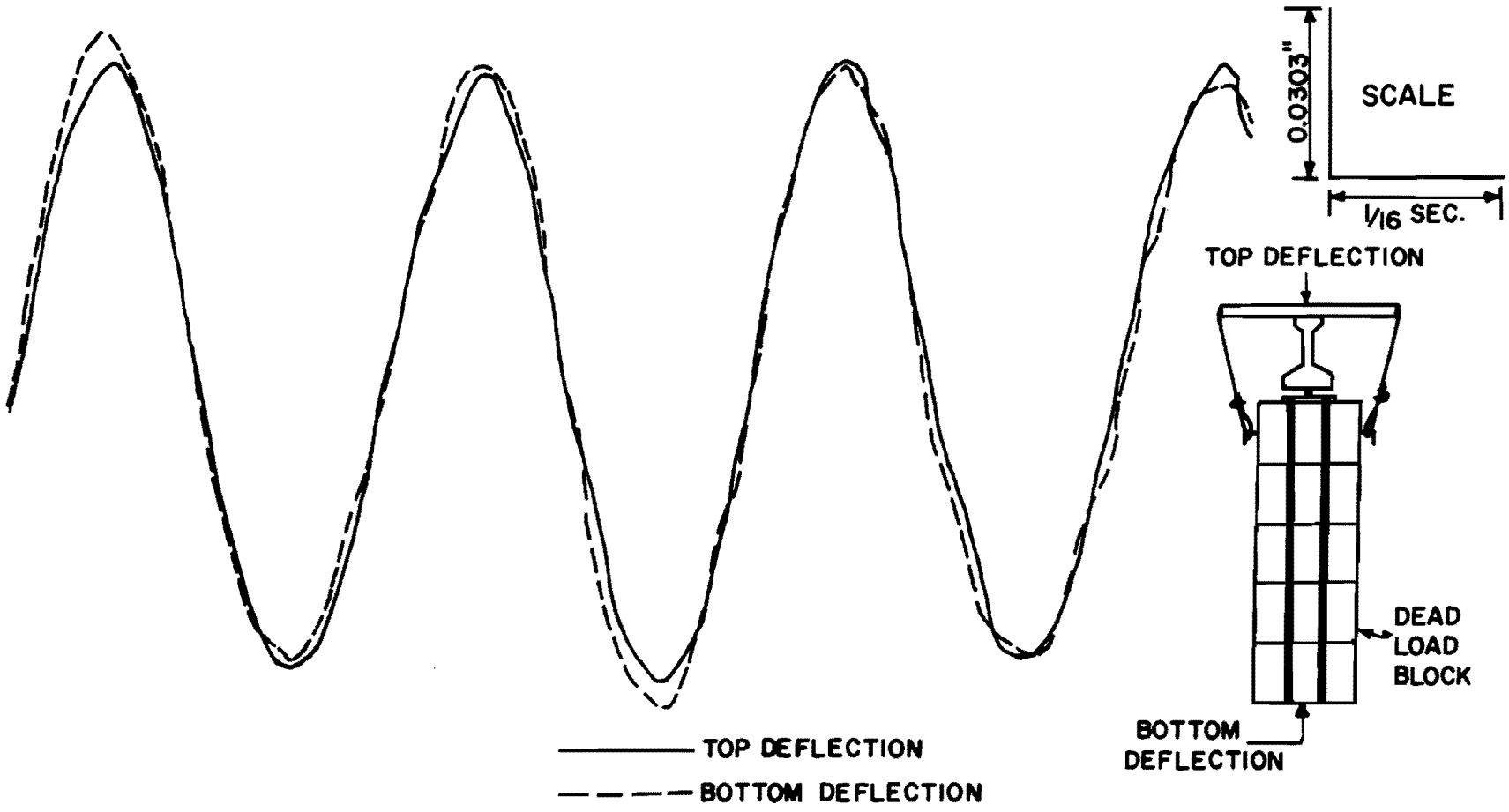

Fig. 2.19 Auxiliary test, beam top and dead load block bottom deflections at midspan; driving frequency = 7.6 Hz.

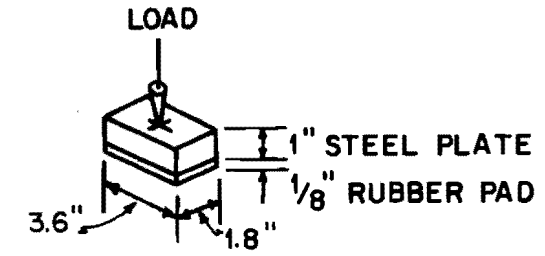

(a) POINT LOAD

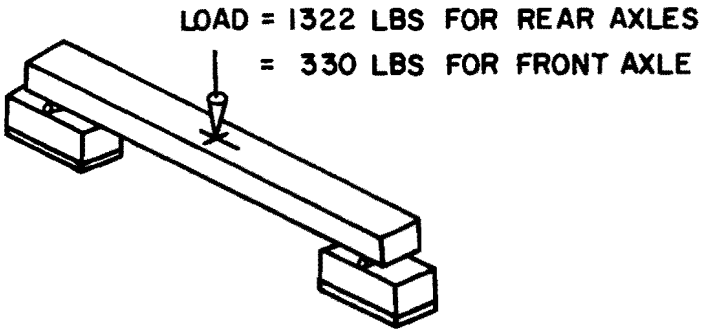

(b) MODEL AXLE LOAD

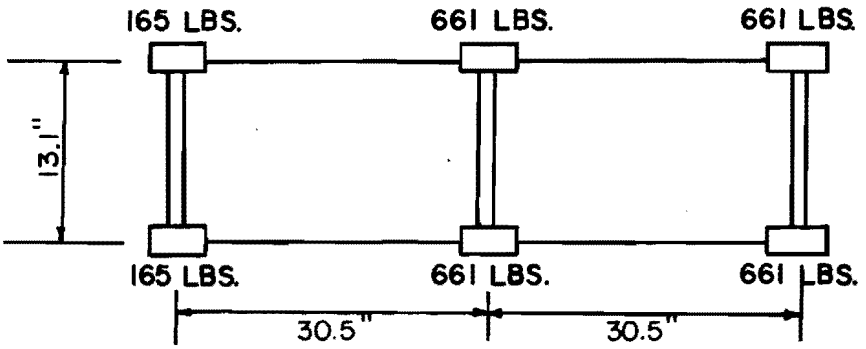

(c) MODEL HS20-44 TRUCK LOAD (INCLUDES 25% IMPACT FACTOR)

Fig. 2.20 Loading block and model loads.

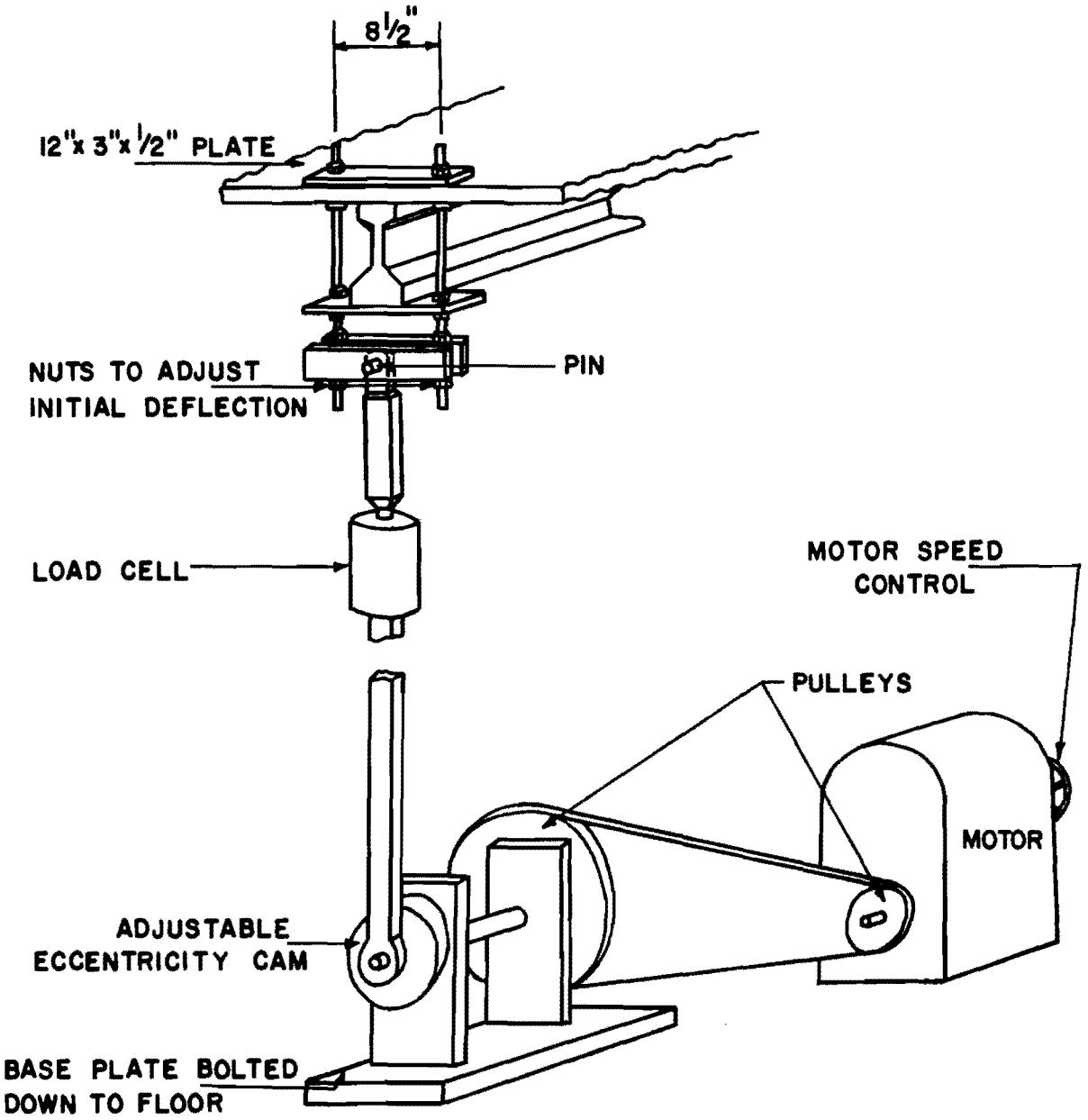

Fig. 2.21 Cyclic load setup.

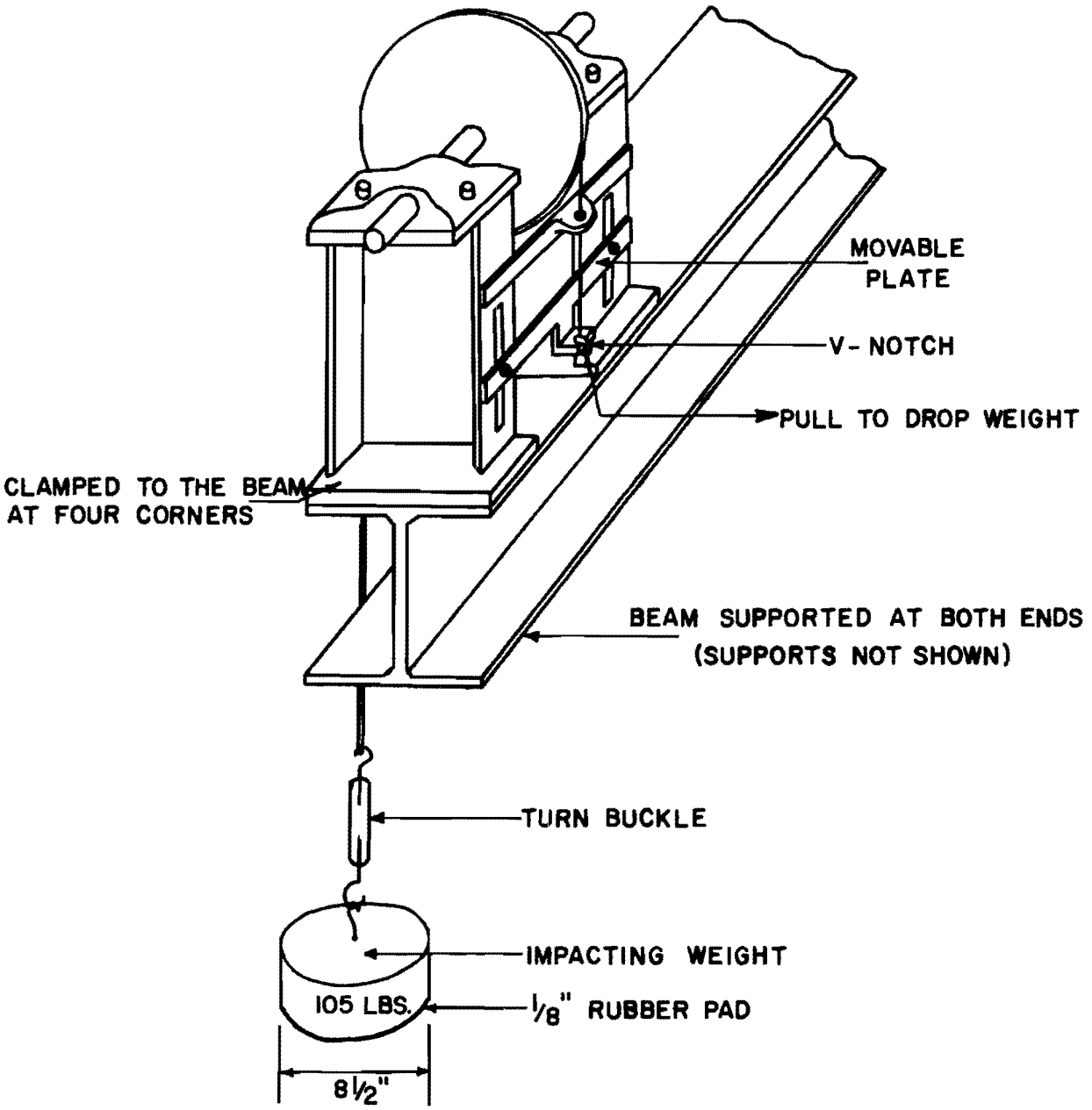

Fig. 2.22 Vertical impact setup.

Fig. 2.23 Lateral impact setup.

schematically in Fig. 2.24. The exciting voltage was selected to get as high a signal as possible without damaging the transducer. The signals picked up by the transducers were passed through the signal conditioner to the differential amplifier where the common mode voltages (i.e. noise picked up in wiring and instrumentation) were attenuated and the signals amplified to the desired level. These amplified signals were passed through a low pass filter, built in with the amplifier, to further attenuate the high frequency noises before they were finally recorded in an eight track magnetic tape recorder. During or just after recording, the signals were checked by displaying them on an oscilloscope or on an oscillograph.

2.9 Testing

A very wide range of different kinds of tests was conducted on all four bridges. For convenience of description they are grouped here under the headings service load and ultimate load tests.

2.9.1 Service Load Tests

To study the effect of diaphragms on elastic behavior of bridges, these tests were performed in three different stages; namely, with all the diaphragms in position (as in Figs. 2.3 through 2.6), with interior diaphragms removed, and with all the diaphragms removed. These stages of tests will hereafter be called Series-A, Series-B, and Series-C, respectively. All three series of tests were conducted on Bridges 1, 2, and 4. Analysis of Bridge 1 and Bridge 2 data showed that exterior diaphragms have little effect on load distribution. Computer analysis (discussed in Chapter 4) of Bridge 3 showed negligible effects of exterior diaphragms on the load distribution. So for Bridge 3 it was decided to eliminate test Series-C and instead run some ultimate wheel load tests in the end span zones with standard end diaphragms and also with different modified end slab sections (see Figs. 2.8 and 2.10).

The different kinds of service load tests performed were:

(1) Static point and truck loads: To study the load distribution characteristics and also to determine stress magnitudes in diaphragms, point loads of 1 kip magnitude were applied at several points at mid and 3/4 spans and also right over the diaphragms. Standard truck loads (Fig. 2.20c) were

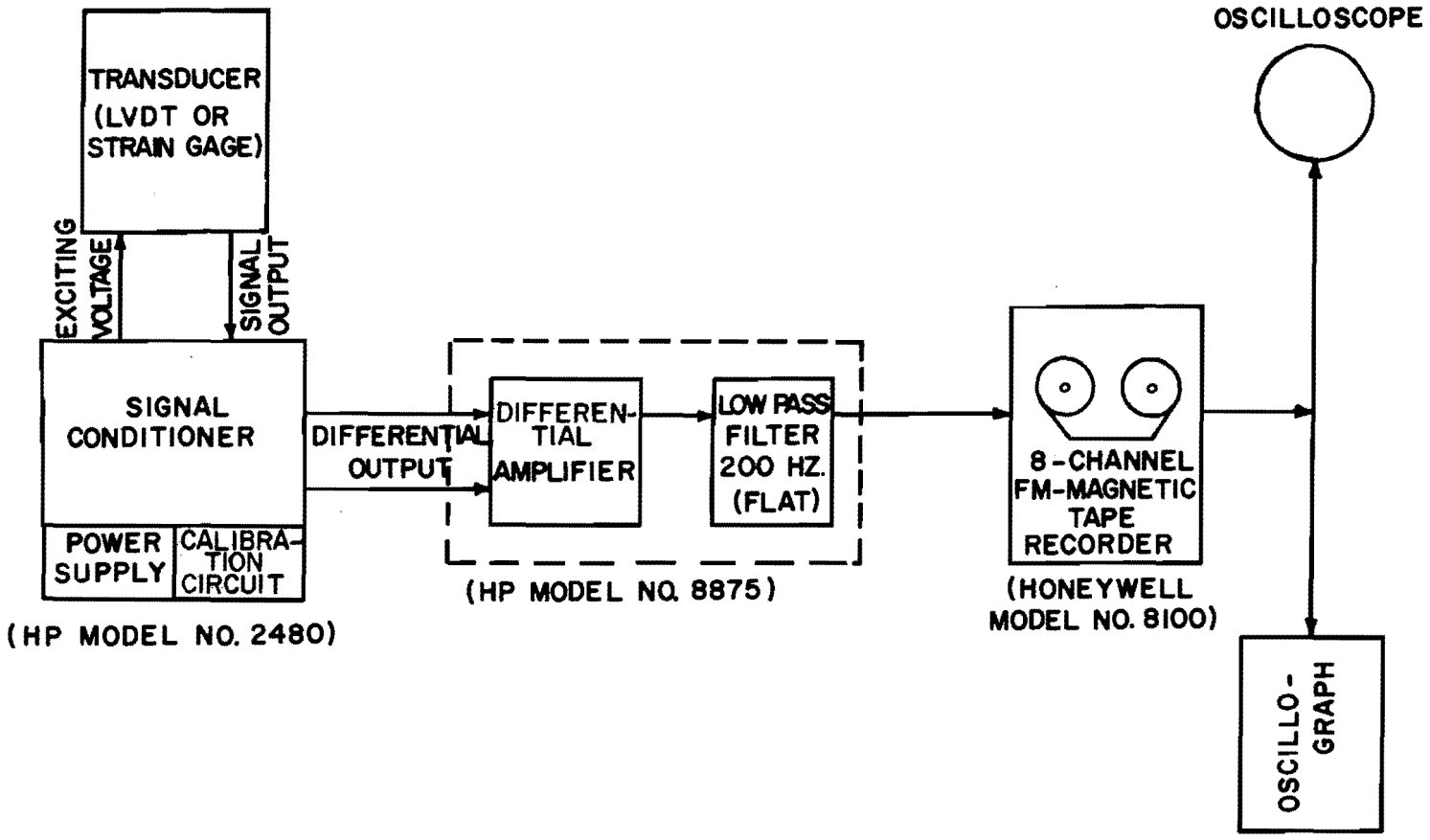

Fig. 2.24 Measurement of dynamic data.

applied in side and center lanes (Figs. 2.25 and 2.26). Deflections at supports and strains and deflections at 1/4, mid, 3/4 and other spans of interest, of all girders were measured. In addition, top and bottom strains in a large number of diaphragms were recorded.

(2) Cyclic loads: To find out dynamic amplification and dynamic load distribution characteristics, cyclic loads were applied at midspans of Girders 1 and 3. Midspan girder strains and deflections were measured. For a few cases dynamic strains in interior diaphragms were also measured. The frequency range for each bridge was selected from the following criteria.

(a) Load frequencies to which actual bridges are normally subjected--based on previous studies[11,49] this range for the model was found to be about 3 to 7 Hz, with heavier loads in the lower ranges.

(b) Natural frequencies of the bridges--dynamic amplifications are maximum where the load frequency is the same as the natural frequency of the structure. As the load frequency approached the natural frequency, the bridge vibration started to pick up very fast. Lest some damage occur to the bridge, it was decided to limit the load frequency to 75 percent of the lowest natural frequency of the bridge. This set the upper limit of load frequency for Bridges 1, 2, and 3 at about 7.5 Hz and for Bridge 4 at about 16 Hz.

(c) The capacity of the loading device--the frequency range of the device was 4 to 13 Hz for bridge loading.

Based on the above criteria, Bridges 1 and 2 were tested at 4 and 7 Hz, Bridge 3 at 4, 6, and 7.5 Hz, and Bridge 4 at 6, 9, and 13 Hz. The general testing procedure was as follows:

(a) The static and dynamic portions of the loading were adjusted so that the maximum load on the girder was approximately equal to the design load and the minimum load was near zero, but never less than zero.

(b) The transducers (LVDT's or strain gages) were hooked up.

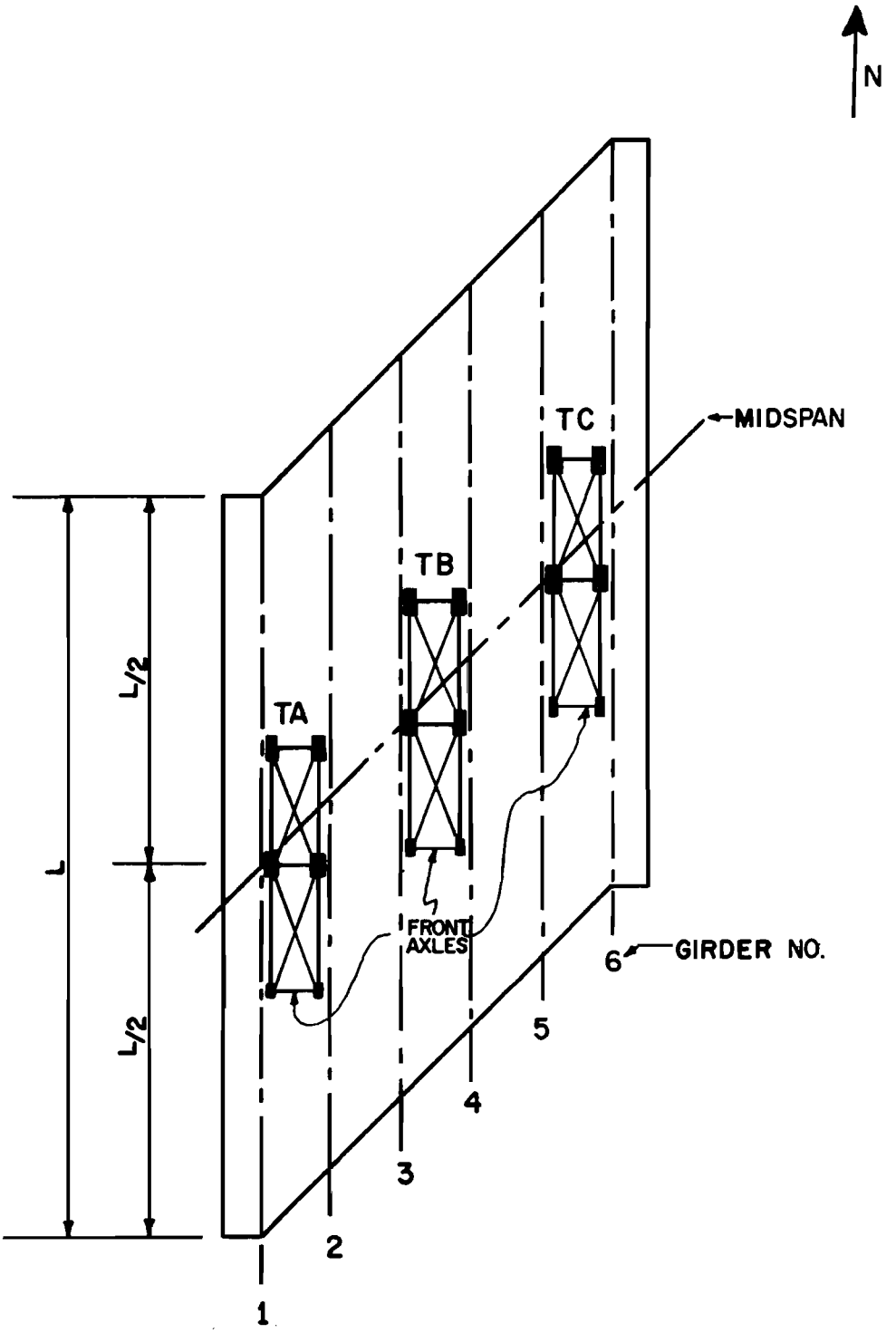

Fig. 2.25 Truck load locations, Bridge 1 and Bridge 2.

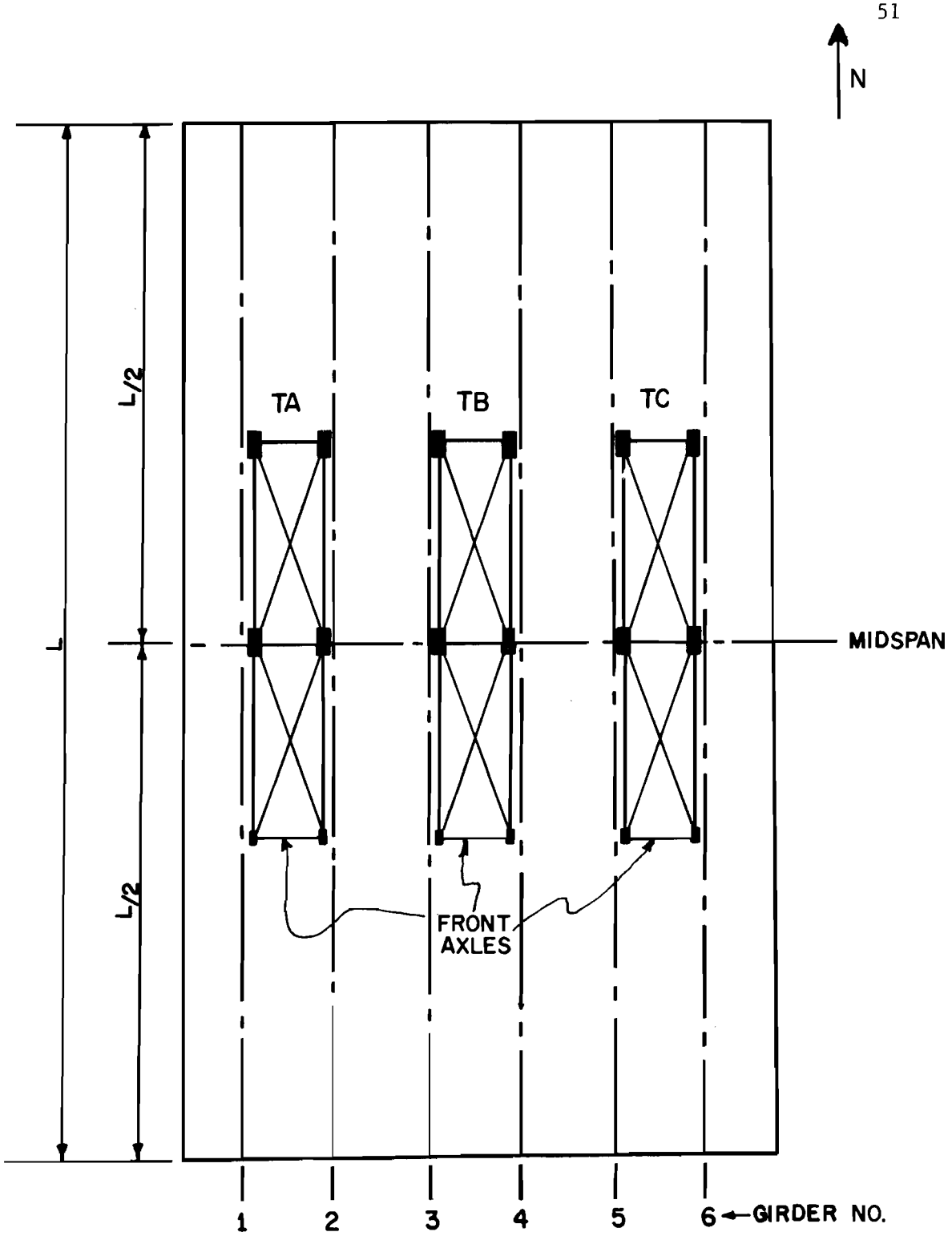

Fig. 2.26 Truck load locations, Bridge 3 and Bridge 4.

(c) The exciting voltage was set (usually between 6 and 8 volts for strain gages and LVDT's, and 10 volts for load cells) and recorded.

(d) Amplifications for all channels were adjusted to the desired level (3 for LVDT's and 3,000 for strains) and the filters were set for 200 Hz.

(e) After turning the cam to the null position each channel was calibrated. The calibrations were recorded on magnetic tape and played back on the oscilloscope display to verify the recording techniques.

(f) For deflection measurements, one end of the LVDT was glued down to the slab using a fast setting glue.

(g) The motor was started, the frequency adjusted, and then the signals were recorded.

(h) As a check the signals were played back on the scope for visual observation.

(3) Vertical impacts: To determine the natural frequencies and damping of the bridges, impact tests were conducted by dropping a 105 lb. weight on several points across midspan of the bridge. The heights of fall were selected so that no damage would be caused to the bridge although signals large enough to record would be obtained. Midspan strain and deflection signals were recorded on magnetic tape.

2.9.2 Ultimate Tests

After the service load tests were completed, the following ultimate tests were performed:

(1) Ultimate flexural tests: To find out the ultimate load capacities and the distribution characteristics at overloads, ultimate tests were performed on Bridges 1 and 4. On Bridge 1 the truck loads TA, TB, and TC (see Fig. 2.25) were all increased to 3 times standard truck loads (as in Fig. 2.20c). Then the side truck load TA was increased until failure while TB and TC were maintained constant at 3 times design load. On Bridge 4,

standard model truck loads as shown in Fig. 2.20c were applied in all three lanes in accordance with Sec. 1.2.6 of AASHO,[1] such as to cause maximum moment in Girder 3 (Fig. 2.27). Keeping the outer truck loads at the service load level, the central truck was then increased until the bridge failed. Girder strains and deflections were recorded.

(2) Lateral impacts: The purpose of this loading was to compare the extent of damage caused to the exterior girder by laterally impacting loads (such as when struck by an over-height vehicle passing under the bridge) when the diaphragms were present and when the diaphragms were removed. In Bridge 2, diaphragms of Type D1 were cast at the end spans and precast diaphragms of the same kind were placed at one-third spans between Girders 1 and 4. In Bridge 3, end diaphragms of Type D1 were cast under the deepened slab zone (see Fig. 2.5), and precast diaphragms of Type D1 were placed at one-third spans between Girders 1 and 4. End joints were carefully grouted with epoxy mortar where precast diaphragms were used. Diaphragm locations for the lateral impact tests are shown in Fig. 2.28.

The point of lateral impact in all cases was at midspan and on the bottom flange of the girder (see Fig. 2.23). After Girders 1 and 6 of Bridge 2 were tested, they were sawed off (see Fig. 2.28a) and tests were conducted on Girders 2 and 5. This was done because of a large discrepancy in concrete strengths between Girders 1 and 6. In Bridge 2 only the impacting force was measured. In Bridge 3 both the impacting forces and the lateral deflections of the bottom flanges of the girders were measured by load cells and LVDT's, respectively, and recorded on magnetic tape. The different tests conducted are summarized in Table 2.6.

After the lateral impact tests, Girders 2 and 5 of Bridge 2, and Girders 1 and 6 of Bridge 3 were tested with midspan vertical point loads applied simultaneously on both the exterior girders to determine the load-deflection characteristics of these damaged girders. In Bridge 2 these loads were increased to near failure. In Bridge 3 these loads were increased to only a few kips. Midspan deflections were recorded. After the simultaneous loading tests on Bridge 2, the loads were removed and applied again on one girder at a time until failure.

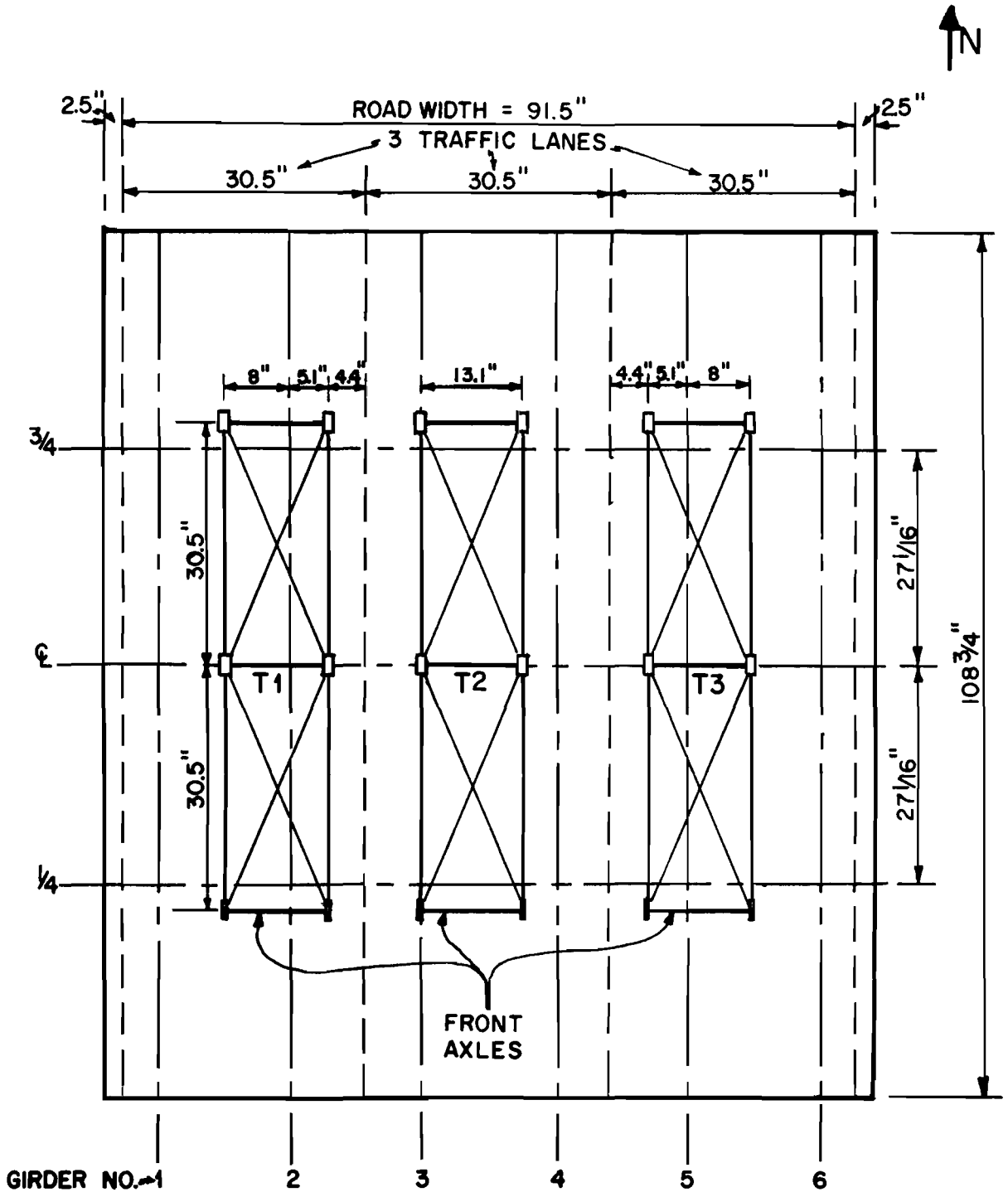

Fig. 2.27 Location of truck loads for Bridge 4 ultimate test.

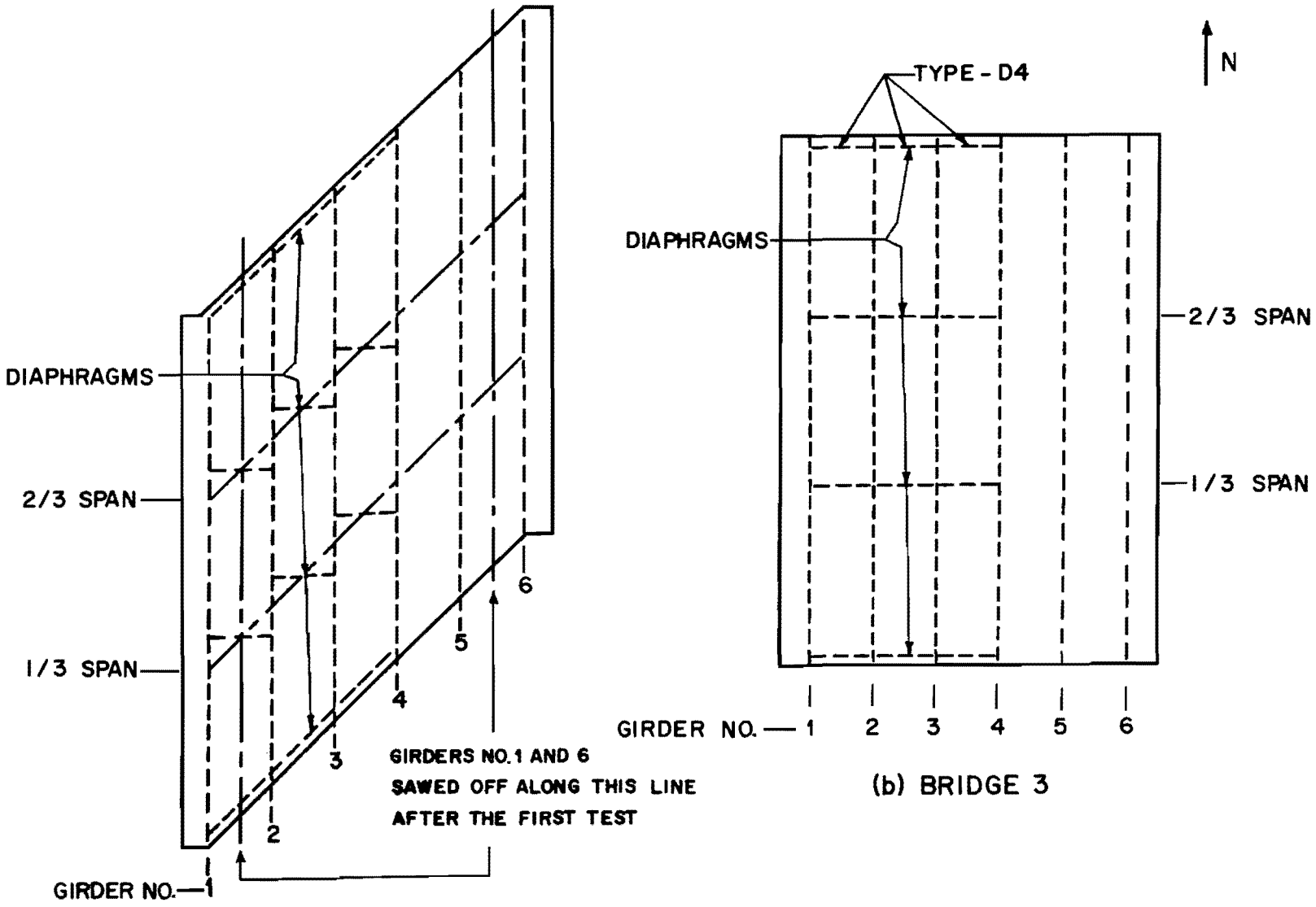

Fig. 2.28 Diaphragm locations during lateral impact tests (all diaphragms are of Type D1 except as shown otherwise).

TABLE 2.6. LATERAL IMPACT TESTS

Bridge No.	Girder No.	Case	Point of Impact	Impacting Weight (lbs.)	Height of Fall (in.)	Number of Tests
2	1	With Diaphragms	Midspan Bottom Flange	110 110 200	2 26 28	1 2 2
2	6	Without Diaphragms	Midspan Bottom Flange	110 110 200	2 26 28	1 2 3
2	2	With Diaphragms	Midspan Bottom Flange	110 110 200	2 26 30	2 2 2
2	5	Without Diaphragms	Midspan Bottom Flange	110 110 200	2 26 30	2 2 2
3	1	With Diaphragms	Midspan Bottom Flange	200	4, 6, 8, 10, 12, 14, 16, 18, 22, 29	One test for each height of fall
3	6	Without Diaphragms	Midspan Bottom Flange	200	4, 6, 8, 10, 12, 14, 16, 18, 22, 29, 32, 36, 40, 44	One test for each height of fall

(3) Other tests: To determine the load-carrying capacity of the slab at the end spans, with or without exterior diaphragms, and also with different modified sections (Fig. 2.10) several ultimate wheel load tests were conducted. Strains at the top and bottom of the loaded sections were recorded to get an estimate of the cracking load. In addition, some punching tests on the slab and flexural tests on the longitudinal edge of the slab were made to determine ultimate wheel load capacities under such loads. Figures 2.29a and 2.29b show typical ultimate wheel load tests.

2.10 Tests on Full Scale Model

Strain gages were mounted at the top and bottom reinforcement levels of exterior and interior diaphragms of a full scale prestressed concrete girder and slab bridge.[13] Plan and section of the bridge, test load location, and diaphragm locations are shown in Fig. 2.30. The diaphragm details are as per Texas Highway Department drawings as given in Appendix A. Top and bottom strains in diaphragms at mid and south end spans between Girders 2 and 4 were measured under a static load F = 48 kips (see Fig. 2.30) and a dynamic axle load of an amplitude of 20 kips and a frequency of 3.3 Hz. Measured strains were very small. Maximum recorded strain was under the dynamic load in an interior diaphragm and its peak-to-peak value (i.e. double amplitude) was found to be less than 10 micro in./in., which would correspond to about 45 psi stress.

(a) Punching test on slab

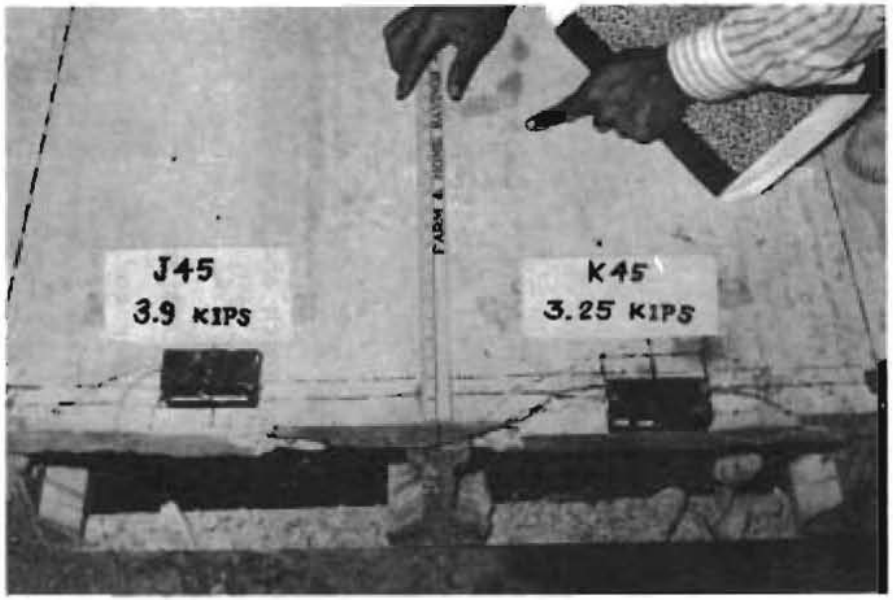

(b) End zone slab after failure

Fig. 2.29 Ultimate wheel load tests.

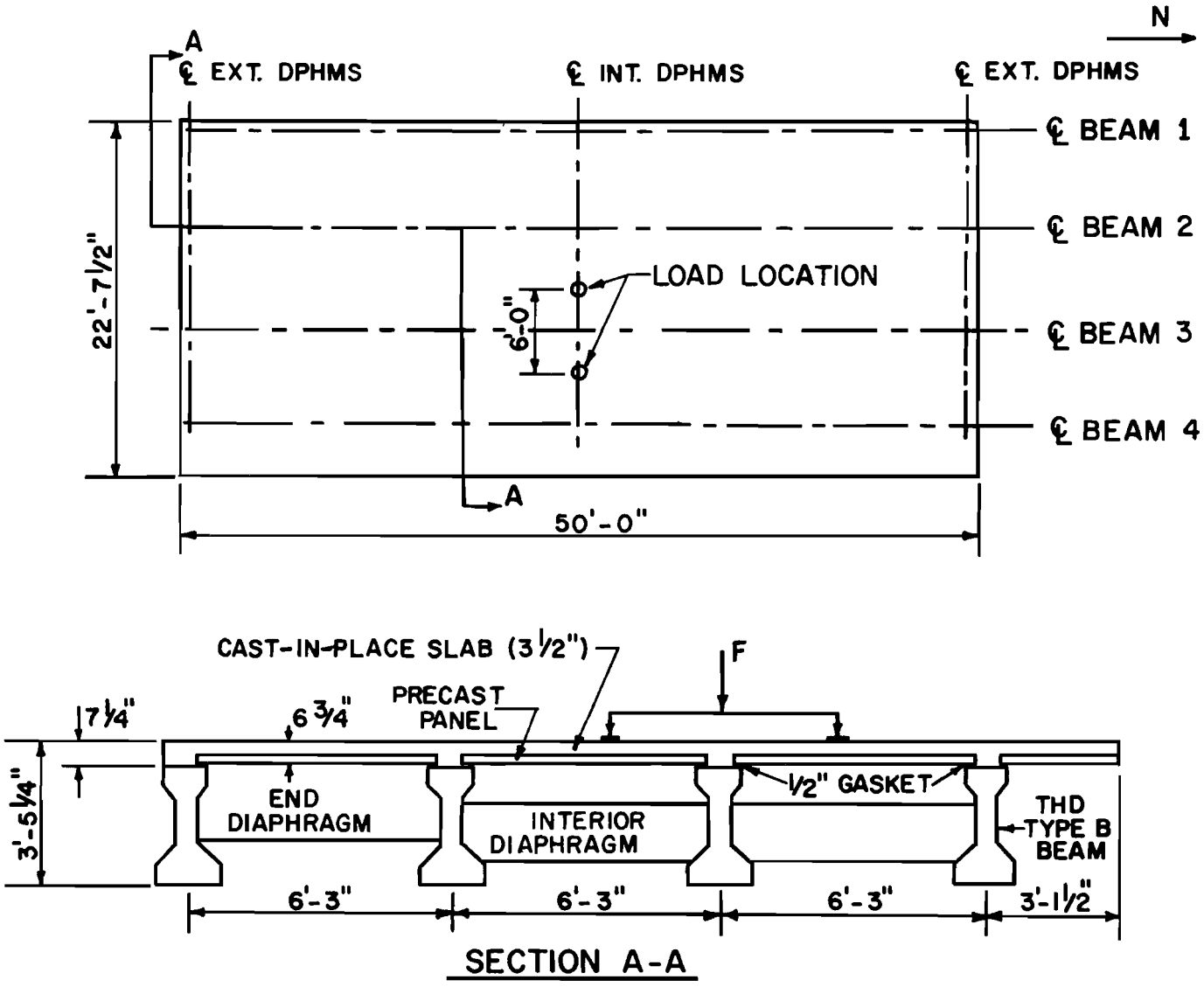

Fig. 2.30 Full scale model of prestressed concrete panel type bridge (taken from reference 13).

CHAPTER 3

METHODS OF DATA ANALYSIS

3.1 General

This chapter presents the methods used to reduce the experimental raw data to useful quantities to determine the effectiveness of diaphragms in bridges. Ultimate load capacities, failure modes, and extent of damage due to lateral impacts were directly recorded or observed during experimentation. The methods used to reduce the other data are described in the following sections.

3.2 Reduction of Static Data

3.2.1 Girder Moments and Deflections

In calculating strain and deflection values under service load, the zero readings before and after loading were averaged to reduce the effects of temperature drift and dial backlash error. For Bridges 1 and 2, girder moments were computed from the measured strains using the girder moment-strain relationship of Fig. 2.14. In Bridges 3 and 4 a girder moment-strain relationship was obtained for each girder by tests on the model itself [39] and was used to reduce the test data for Bridge 3 and Bridge 4. The interpreted moments were normalized by dividing each girder moment at a particular bridge cross section by the summation of all the girder moments across that section. The deflection readings were corrected by deducting girder support deflections and then normalized in the same manner. For overloads the strains were not reduced to moments because of unreliable moment-strain relationships.

3.2.2 Diaphragm Stresses

Extreme fiber stresses in diaphragms were obtained by linearly extrapolating implanted strain gage readings to the extreme top and bottom

fibers of the diaphragms and then by multiplying those values by the corresponding modulus of elasticity calculated on the basis of Sec. 8.3 of ACI 318-71.[2]

3.2.3 Cracking Loads in the End Span Slab

End slab tensile strains were plotted against corresponding loads. A typical case is shown in Fig. 3.1 where strains were measured from implanted bottom gages. A sudden change in the slope of the curve indicated the cracking load. Cracking strains were obtained by linearly extrapolating the top and bottom strains just below cracking load to the extreme tensile fiber.

3.3 Reduction of Dynamic Data

Dynamic data reduction was carried out by two methods, as described in the following sections. The first method, termed direct analysis, is simpler but cannot be applied to all data cases. It cannot be used to determine fundamental mode shapes or to determine a meaningful response from data signals which are not truly sinusoidal. In such cases, the second method, an advanced technique, termed spectral analysis, can be used.

3.3.1 Direct Analysis

Information about natural frequencies was obtained by playing back on an oscillograph the recorded free vibration deflection and strain signals produced by application of vertical impacts. It was indicated in Chapter 1 that the fundamental modes of bridge vibrations are longitudinal and torsional. For impacts near the midspan center line of the bridge, torsional mode excitation of interior girders will be negligible. Under such an impact, the interior girders vibrate only in the longitudinal mode. From the trace of such a response, the longitudinal mode frequency f_L and corresponding coefficient of damping can easily be calculated. For instance, from Fig. 3.2a,

time t = 5.16 sec. for 50 cycles;

so

$$f_L = 50/5.16 = 9.69 \text{ Hz}$$

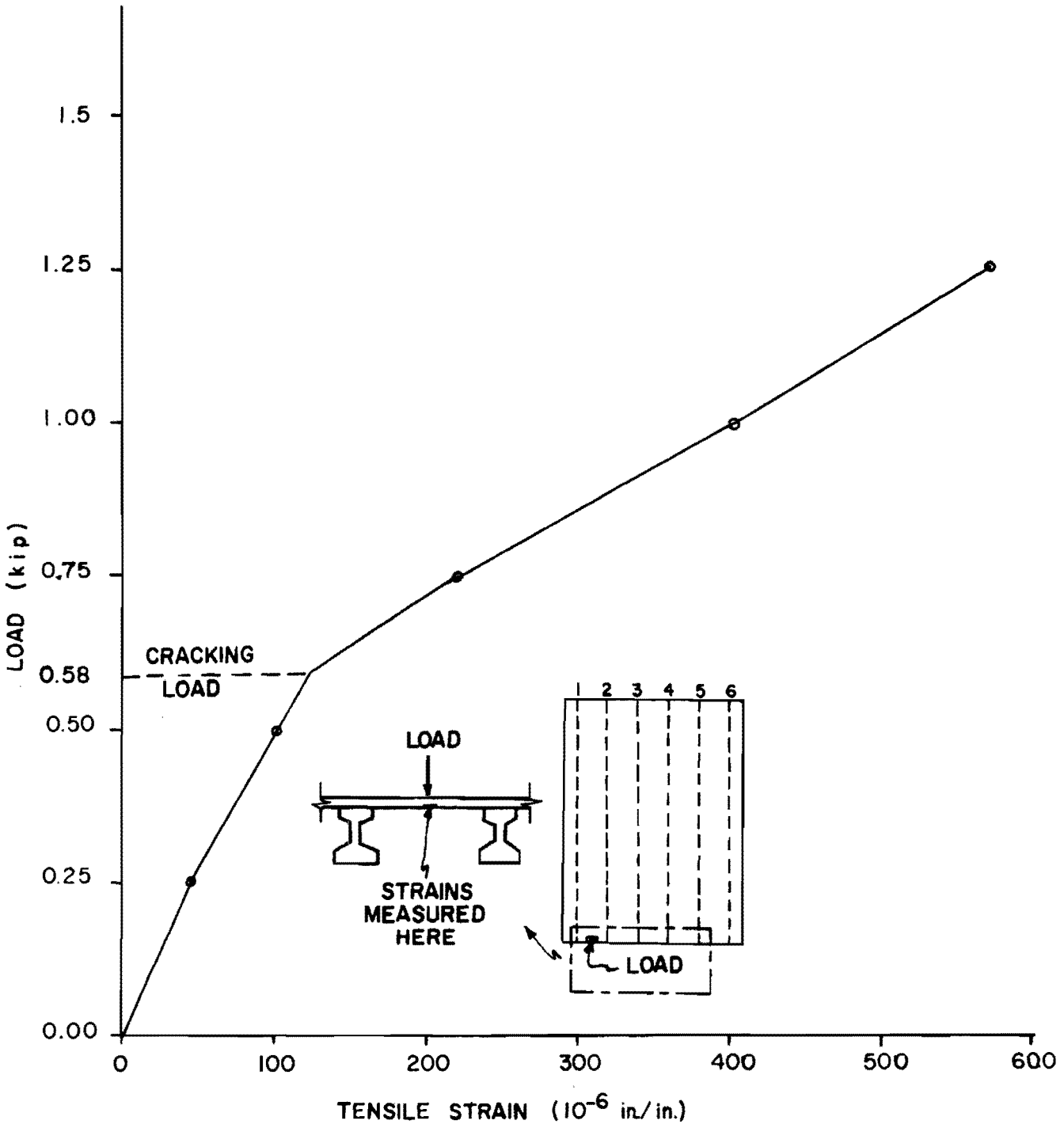

Fig. 3.1 Estimation of cracking load of slab when subjected to a wheel load at the free edge.

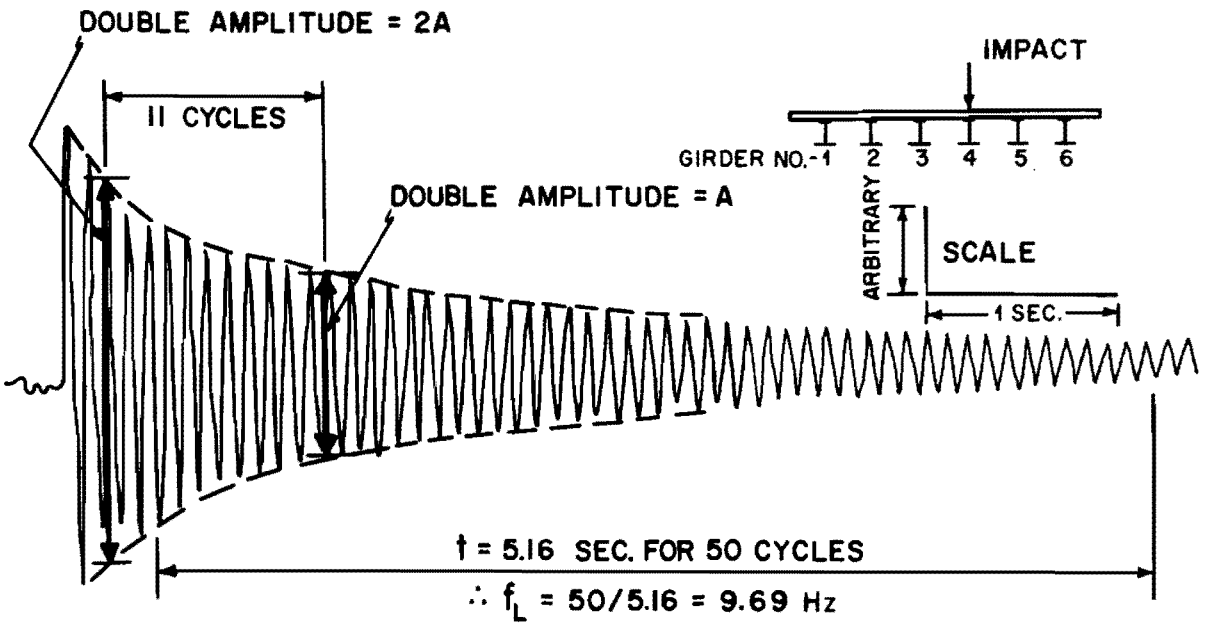

(a) Girder 4 midspan deflection due to impact at midspan on Girder 4.

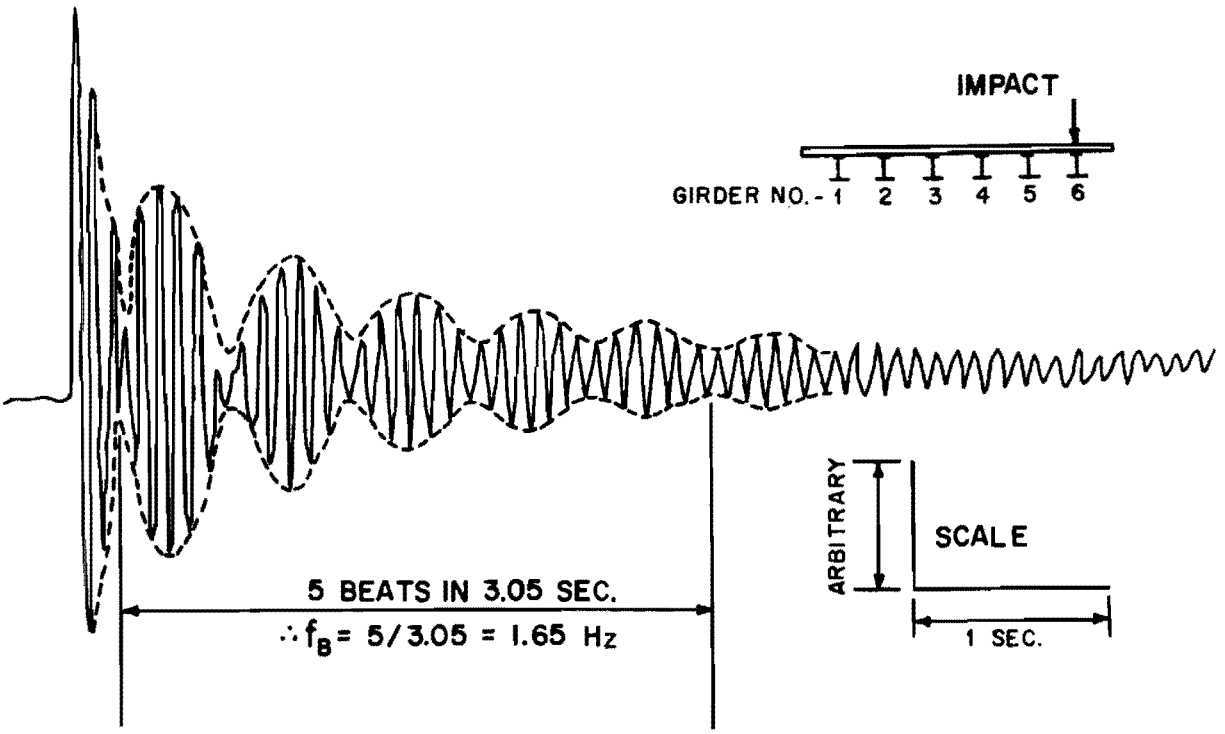

(b) Girder 6 midspan deflection due to impact at midspan on Girder 6.

Fig. 3.2 Oscillographic traces of free vibration deflection - Bridge 3, Series-A.

For small damping (up to about 20 percent of the critical), the coefficient of damping C can be expressed[44] in terms of critical damping C_{cr} by

$$C = \left[\frac{1}{2\pi n} \ln\left(\frac{A_1}{A_2}\right)\right] C_{cr} \tag{3.1}$$

where A_1 and A_2 are amplitudes measured at any time t and at n cycles later. For $A_1/A_2 = 2$, Eq. 3.1 reduces to

$$C = \frac{0.11}{n} C_{cr} \tag{3.2}$$

In the particular case shown in Fig. 3.2a, n = 11

$$\therefore C = 0.01\, C_{cr} = 1\% \text{ of critical damping.}$$

Damping coefficients were calculated by using Eq. 3.2 where n was measured after the first three cycles of vibrations. This was done to avoid disturbances observed in most of the cases at the initial part of the signal due to imperfect impact. In some cases where initial disturbances were small, these coefficients were calculated at various points of the signal to find out the variation of damping with decreasing amplitude (see Sec. 5.3.1).

When the bridge was impacted vertically at midspan of an exterior girder, both the longitudinal and torsional modes were excited. Resulting deflections and strains contain both longitudinal and torsional fundamental frequencies. This mixture caused some beating effect as shown in Fig. 3.2b. If f_L, f_T and f_B are the frequencies of longitudinal mode, torsional mode and beating, respectively, then[44]

$$f_B = |(f_L - f_T)|$$

or

$$f_T = f_L \pm f_B \tag{3.3}$$

In the case of torsional vibrations, the beams deflect vertically as in the longitudinal mode in addition to twisting. Because of the additional twisting effect it is assumed that the frequency for the torsional mode of vibration will be higher than that for the longitudinal mode. Thus,

$$f_T = f_L + f_B \tag{3.4}$$

The calculation of f_L has been described earlier. Values of f_B were obtained from exterior girder strain and deflection responses due to impacts on exterior girder midspans. A typical case for deflection response is shown in Fig. 3.2b. In this particular case f_L = 9.69 Hz, f_B = 1.65 Hz. Therefore, f_T = 9.69 + 1.65 = 11.34 Hz.

To reduce the sinusoidal cyclical load data, oscillographic traces of loads, deflections, and strains, along with the corresponding calibrations, were obtained by playing back the taped signals. Using the calibrating steps, data were transformed to loads, strains and deflections. Girder strains and deflections were then divided by the corresponding load, to get strain and deflection amplitudes for loads of unit amplitude. Only Bridge 4 data were sinusoidal enough to be analyzed by this method. Typical load and bridge response signals from Bridge 4 are shown in Figs. 3.3a and 3.3b. In the other bridges, in many cases the data showed presence of a considerable amount of higher harmonic signals (see Fig. 3.4). Cyclic data for these bridges had to be reduced by spectral analysis technique.

3.3.2 Spectral Analysis[8,19,41,42]

In Fig. 3.4 some mixing of higher harmonics may be observed. Because of this, direct analysis could not be effectively used. However, if this signal can be decomposed into its constituent harmonics, then meaningful bridge response at different frequencies (i.e. at the frequencies of the constituent harmonics) can be determined. The essential purpose of the spectral analysis is to resolve the signal into its constituent harmonics. In Ref. 39, the principle of this analysis and its application in the data reduction are discussed in some deatil. A brief summary is given in the following sections.

3.3.2.1 Principle of Analysis

An oversimplification of the spectral analysis procedure is that a function x(t) may be transformed using Fourier integral expressions so that it can be expressed as a sum of a set of sinusoids of frequency f, amplitude A(f) and phase angle φ(f). Integration of the transformation provides a

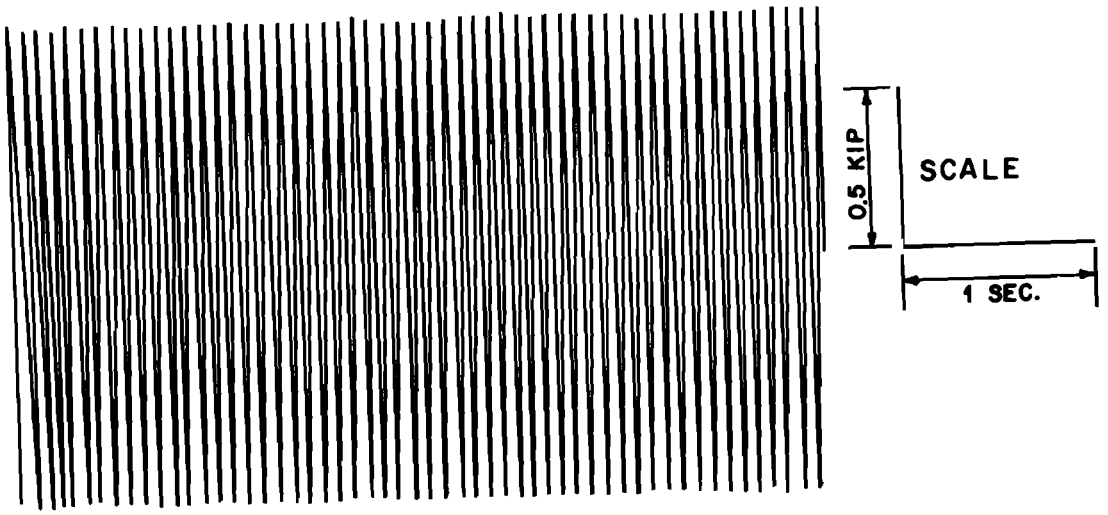

(a) Load at Girder 1 midspan, 12.7 Hz

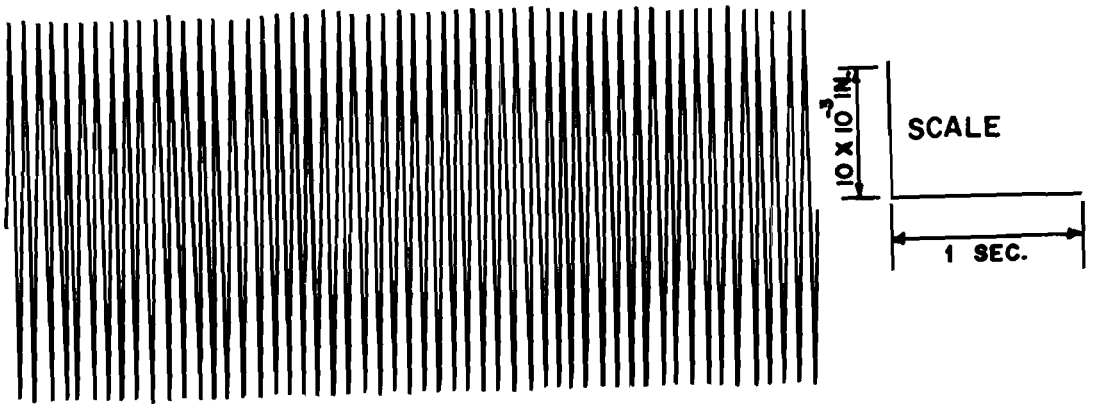

(b) Deflection at Girder 1 midspan, 12.7 Hz

Fig. 3.3 Typical dynamic response - Bridge 4, Series-C.

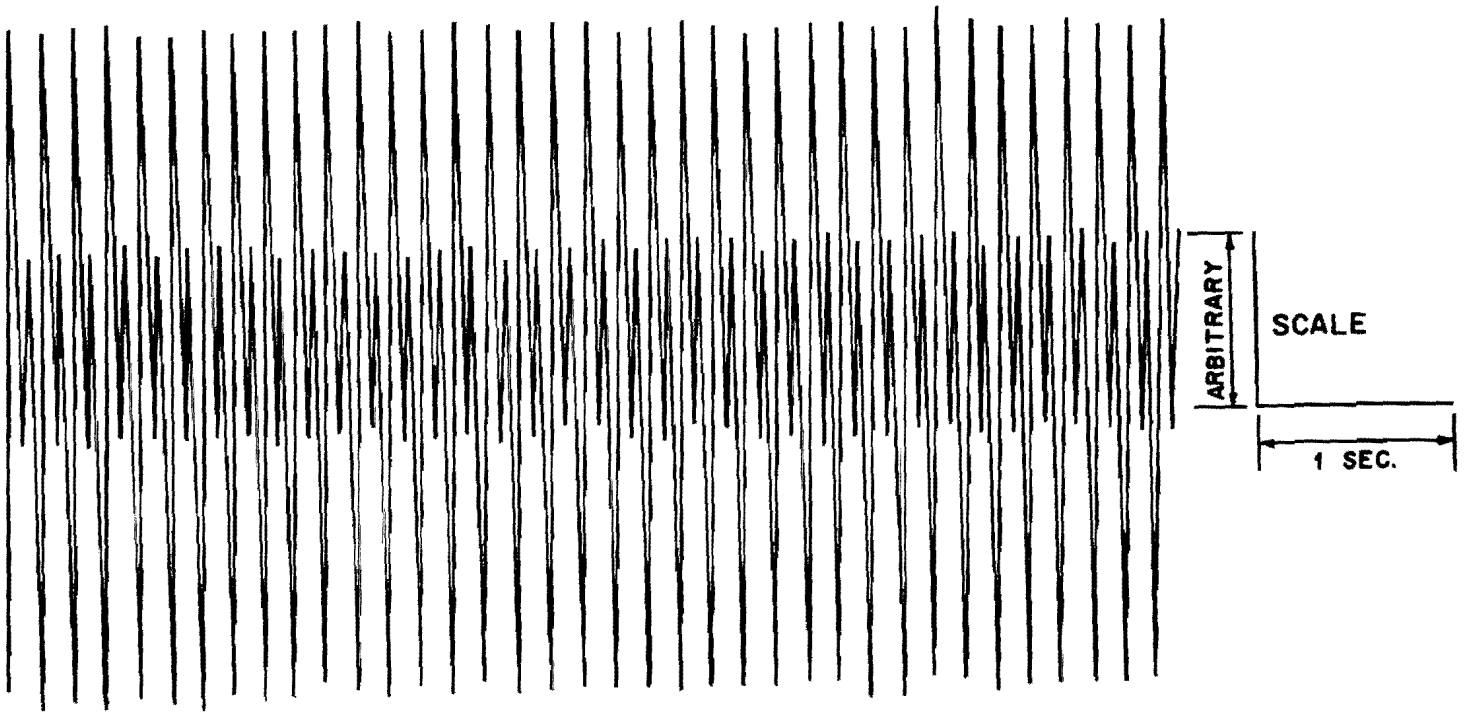

Fig. 3.4 Typical dynamic response showing presence of second harmonic (Bridge 3, Series-A, Girder 1 midspan strain due to load at midspan of Girder 1, driving frequency = 6 Hz).

function X(f) which provides the amplitude and phase information of the harmonics (i.e. the sinusoids) constituting the function x(t).

In order to determine X(f) digitally, x(t) is replaced by $x(n\Delta t)$, which is a set of N values of x(t) measured (i.e. sampled) at Δt time intervals (Fig. 3.5). Δt is called the sample interval. If T be the time length (also called time window) over which the data are sampled, then the total number of samples, N (see Fig. 3.5), is given by

$$N = T/\Delta t \tag{3.5}$$

Values of T, N and Δt have to be finite for practical considerations. This, in effect, assumes that the function x(t) is periodic with period T. This assumed repetition of the signal after period T is shown in dotted lines in Fig. 3.5.

X(f) is a complex quantity. For real functions of time, as in the present investigation, the real part of X(f) is symmetrical about $f_s/2$ (called folding frequency), and the imaginary part is antisymmetrical about $f_s/2$.[9] Therefore, X(f) values need to be calculated only in the frequency range of 0 to $f_s/2$ to define X(f) completely over its period. From this, if f_{max} is the maximum desired frequency in the spectrum, then

$$\begin{aligned} f_{max} &= f_s/2 = N\cdot\Delta f/2 \\ \therefore\ f_{max}/(N/2) &= \Delta f \end{aligned} \tag{3.6}$$

or

$$N = \frac{2f_{max}}{\Delta f} \tag{3.7}$$

where Δf is the desired frequency resolution in the frequency domain.

3.3.2.2 Definitions

If the Fourier transforms of data lengths $x_1(t)$ and $x_2(t)$ are given by

$$X_1 = A_1(f)\cdot e^{j\theta_1(f)} \tag{3.8a}$$

and

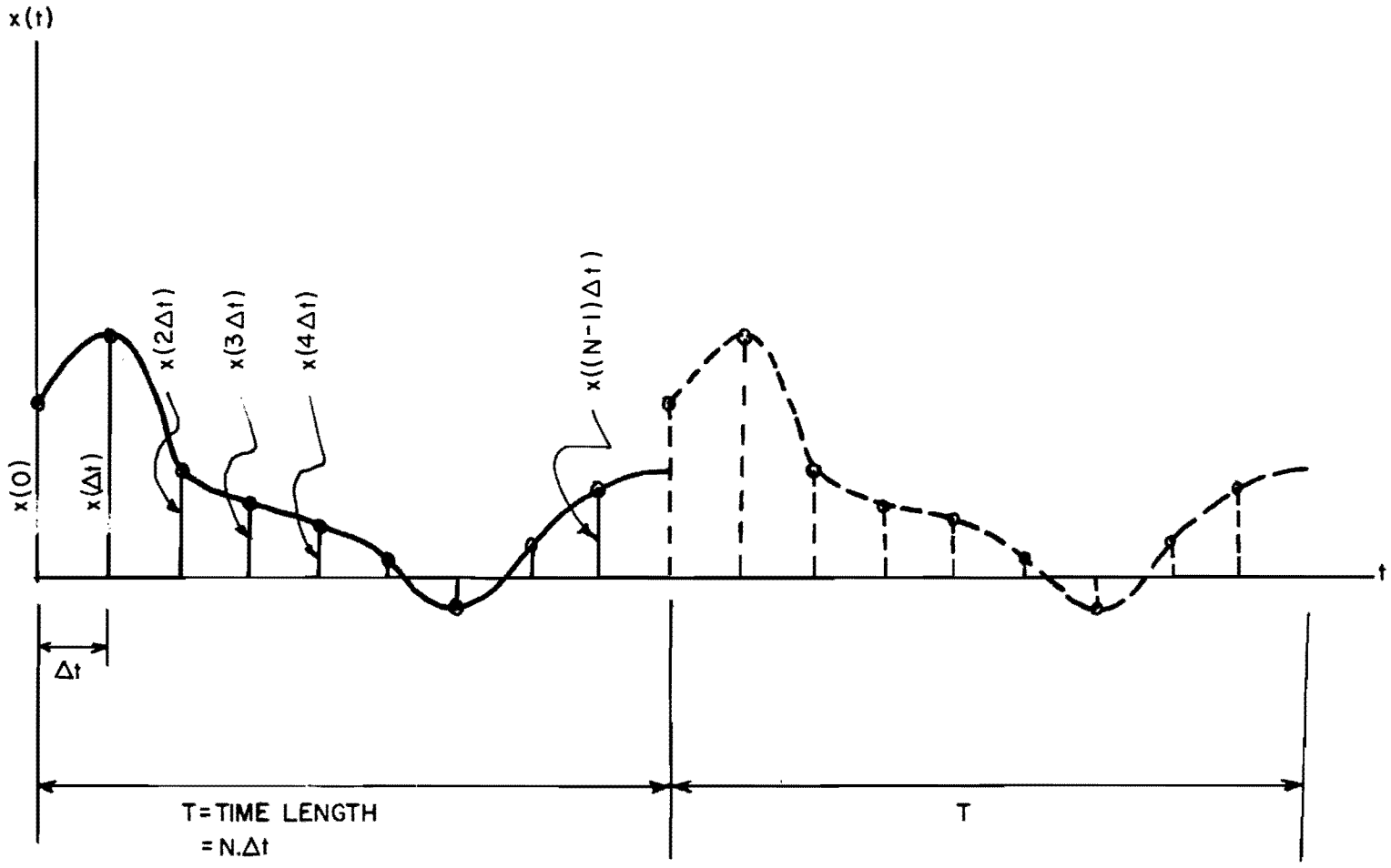

Fig. 3.5 Sampling continuous time data signal.

$$X_2 = A_2(f) \cdot e^{j\theta_2(t)} \tag{3.8b}$$

then the cross-power spectrum P_{12} of data $x_1(t)$ and $x_2(t)$ is defined as

$$P_{12} = \frac{1}{\delta f} \sum_{(f - \frac{\delta f}{2})}^{(f + \frac{\delta f}{2})} A_1 A_2 e^{j(\theta_1 - \theta_2)} \tag{3.9}$$

Where δf is the resolution realized in the final analysis. For convenience Eq. 3.9 is rewritten as

$$P_{12} = B_{12} e^{j\varphi_{12}} \tag{3.10}$$

where B_{12} and φ_{12} are functions of f and are called the cross-power amplitude spectrum and the cross-power phase spectrum, respectively. In other words, the cross-power amplitude spectrum of two functions $x_1(t)$ and $x_2(t)$ gives the product of the amplitudes (i.e., $A_1 \cdot A_2$) of the harmonics of $x_1(t)$ and $x_2(t)$ for any frequency f and the cross-power phase spectrum gives the phase difference of these two harmonics.

The auto-power spectrum P_{11} of a data length $x_1(t)$ is defined by

$$P_{11} = \frac{1}{\delta f} \sum_{(f - \frac{\delta f}{2})}^{(f + \frac{\delta f}{2})} A_1^2 \tag{3.11}$$

P_{11} gives the information of the amplitude squared values of the harmonics, averaged over a frequency band width δf.

The squared coherency function K_{12} of a set of data $x_1(t)$ and $x_2(t)$ is defined by

$$K_{12} = \frac{B_{12}^2(f)}{P_{11}(f) \cdot P_{22}(f)} \tag{3.12}$$

where $P_{22}(f)$ is the auto-power spectrum of $x_2(t)$ and $P_{11}(f)$ and $B_{12}(f)$ are defined as above.

Plots of K_{12} vs. f are called the coherency spectrum. The coherency function is a measure of the signal-to-noise ratio in the recorded data in a frequency band width δf centered at f. The coherency function is constrained to lie between the limits of zero and unity. Zero coherence corresponds to a totally incoherent or noisy situation, while unity implies a perfectly coherent situation. In this experiment high values of coherence are observed in those frequency bands where the signal-to-noise ratio is large, and vice versa.

3.3.2.3 Data Analysis

The actual spectral analysis is performed by computer programs developed by Smith.[41] First the analog data were digitized (i.e. sampled). This operation is schematically shown in Fig. 3.6. The aliasing filter was first adjusted to the required cut-off frequency (i.e. $f_{aliasing}$ in Table3.1) to prevent overlapping of spectra. The particular length of data to be digitized was determined from the data book. The analog signal was displayed on the oscilloscope A and the exact location of the desired data on the analog tape was determined. Then from the main control (MC) a command was given to the computer to get ready to receive signals. The time window and the sampling frequency were also specified in this command. Next the control was switched to the subcontrol (SC). The play-back switch of the analog recorder was turned on. As soon as the exact footage of the analog tape was reached on the counter as determined above, the subcontrol switch was turned on to inform the computer to receive the signal. The signal was digitized in the analog-to-digital converter and stored on the digital tape. Control was returned to the main control from which a command was given to display the digital data on the oscilloscopes A and B to check that the right length of data was digitized. The digital data were then printed out. These digitized data were then input to the spectral analysis computer program, which employs Fast Fourier Transforms to initially transform the time data length. The program output gave both printouts and plots of auto-power spectra, cross-power phase and amplitude spectra and coherency spectra.

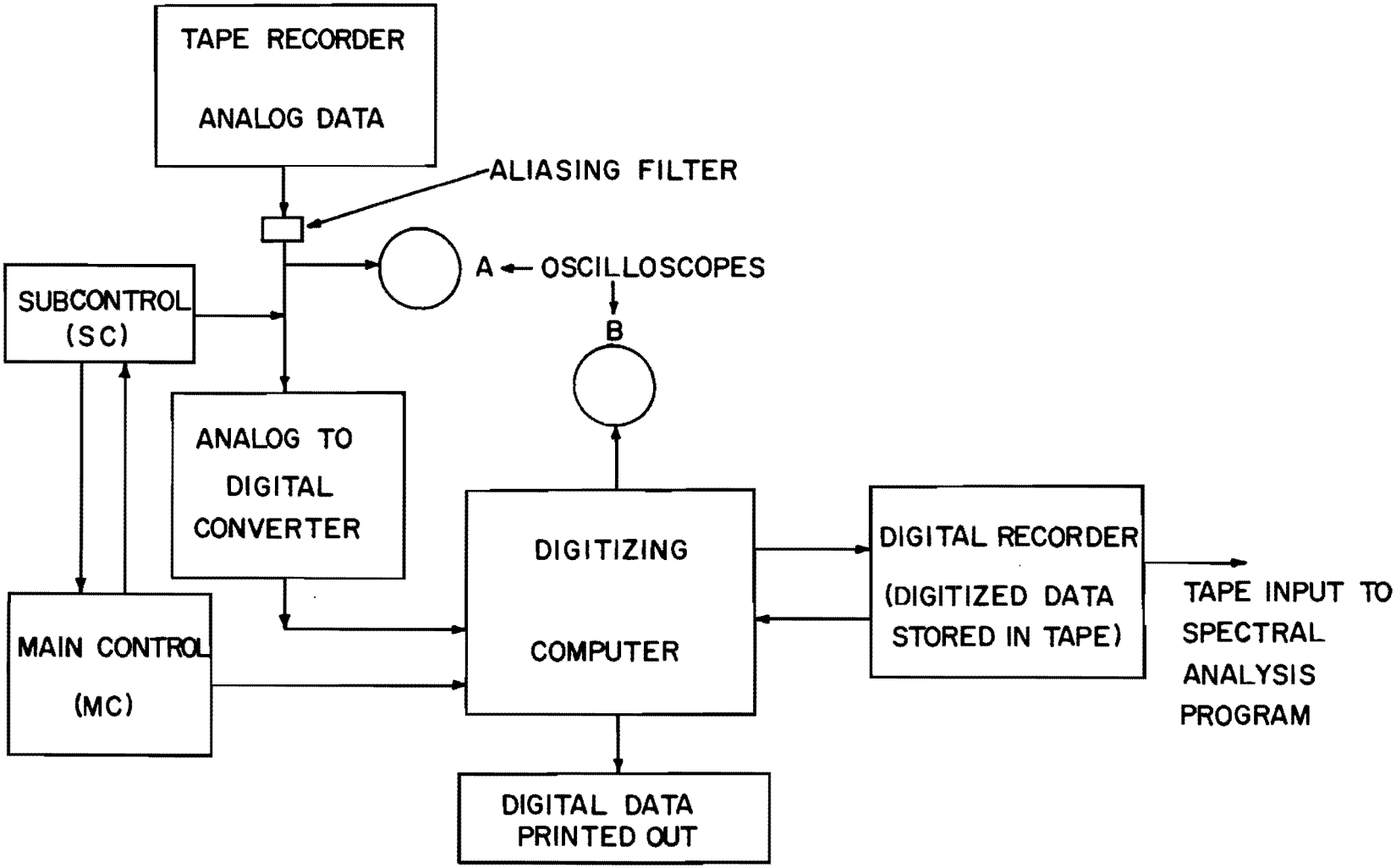

Fig. 3.6 Digitizing analog data.

For this analysis the chosen values of frequency resolution, frequency range, etc., are given in Table 3.1.

TABLE 3.1. VALUES OF THE PARAMETERS FOR SPECTRAL ANALYSIS

Quantities	Cyclic Data	Impact Data
Frequency resolution δf	0.5 Hz	0.5 Hz
Number of elementary band widths, m for "m-averaging"	20	5
Elementary band width ($\Delta f = \delta f/m$)	0.025 Hz	0.1 Hz
Time data length ($T = 1/\Delta f$)	40 sec.	10 sec.
$f_{max} = f_{aliasing}$	100 Hz	400 Hz
$f_{sampling} = 2f_{max}$	200 Hz	800 Hz

3.3.2.4 Determination of Natural Frequencies and Mode Shapes

When the bridge vibrates freely, then the predominant frequencies of vibration are the fundamental frequencies (i.e. the natural frequencies) of the bridge. At these frequencies, the harmonics of the response signal will have relatively large amplitudes. As the auto-power spectrum is basically a relationship between the harmonic amplitude squared values and the corresponding frequencies, the peak values in such a spectrum will occur at the natural frequencies of the bridge. Figure 3.7a shows a typical auto-power spectrum of the midspan girder deflection of an interior girder due to impact on midspan of the same girder. The girder is expected to vibrate only in the longitudinal mode. The data indicate one prominent peak at 9.5 Hz, which is the natural frequency for the longitudinal mode. Figure 3.7b shows the same spectrum for an exterior girder due to impact on midspan of

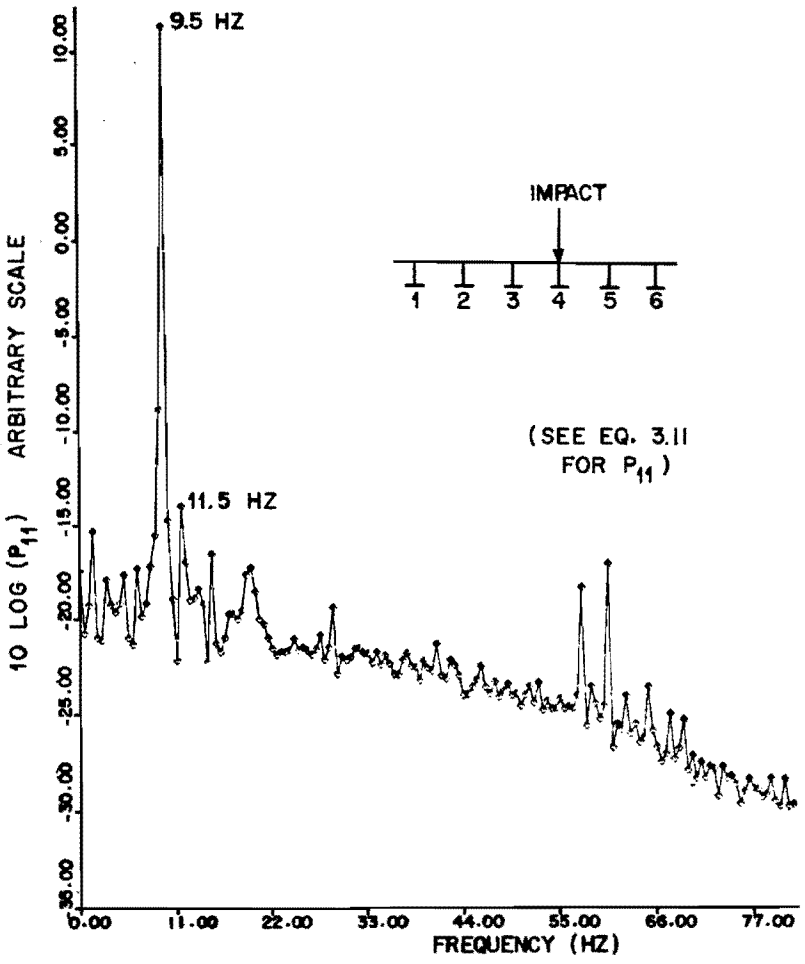

(a) Girder 4 midspan deflection, impact at midspan of Girder 4

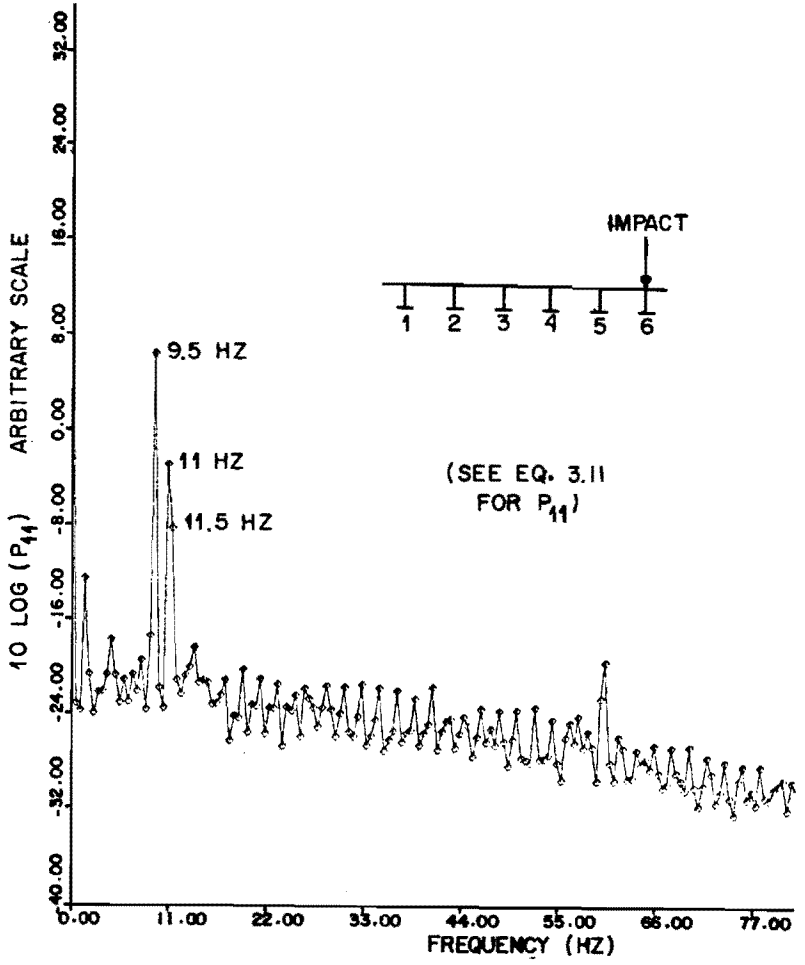

(b) Girder 6 midspan deflection, impact at midspan of Girder 6

Fig. 3.7 Auto-power spectra of Bridge 3 responses due to impact loads.

the same girder. Both torsional and longitudinal modes are expected to be significant. Presence of two prominent peaks in Fig. 3.7b confirms this. The frequencies corresponding to these peaks are 9.5 Hz and 11 Hz. The former is the same as found for the longitudinal mode with the interior girder tests, while the latter corresponds to the frequency of the torsional mode. In Section 3.3.1, the natural frequencies found by direct analysis of the same signals were 9.69 and 11.34 Hz. There is a slight discrepancy in the results of the two analyses because the spectral analysis procedure resolution chosen is only 0.5 Hz. Because more precise values were computed by direct analysis, this method was used to compute the natural frequencies of Bridges 1, 2, and 3. In Bridge 4, direct analysis could not be used effectively because interior girder responses due to impact on the midspan interior girder showed significant beating effect. A typical response is shown in Fig. 3.8. Under such circumstances, the longitudinal and the torsional frequencies could not be separated out by direct analysis. Similarly, the spectral analysis was ineffective because the signals were of too short a duration and too noisy. Because of these reasons neither the natural frequencies nor the damping coefficient for Bridge 4 could be determined from the experiment.

To find the fundamental mode shapes, the auto-power and cross-power phase spectra of the bridge response signals (i.e. midspan deflections or strains of the girders) were computed. The auto-power and phase spectral values corresponding to the fundamental frequencies were determined. In each case the coherency values at the corresponding frequencies were checked. This is important, especially for small signals, where the signal-to-noise ratio may be high. The smaller the coherency value, the larger the signal distortion due to noise. An acceptable value of coherency is a matter of judgment and depends on how much accuracy is required. Where a qualitative estimate is desired (such as mode shapes), coherency values as low as 0.75 were considered satisfactory. For reasonable accurate quantitative estimates (as in the case of load distribution) a value of more than 0.95 was considered adequate.

The ratio of the square root of the auto-power spectral value of any girder to that of a reference girder gives the relative amplitude for the girder. The reference girder response was chosen as the one having the

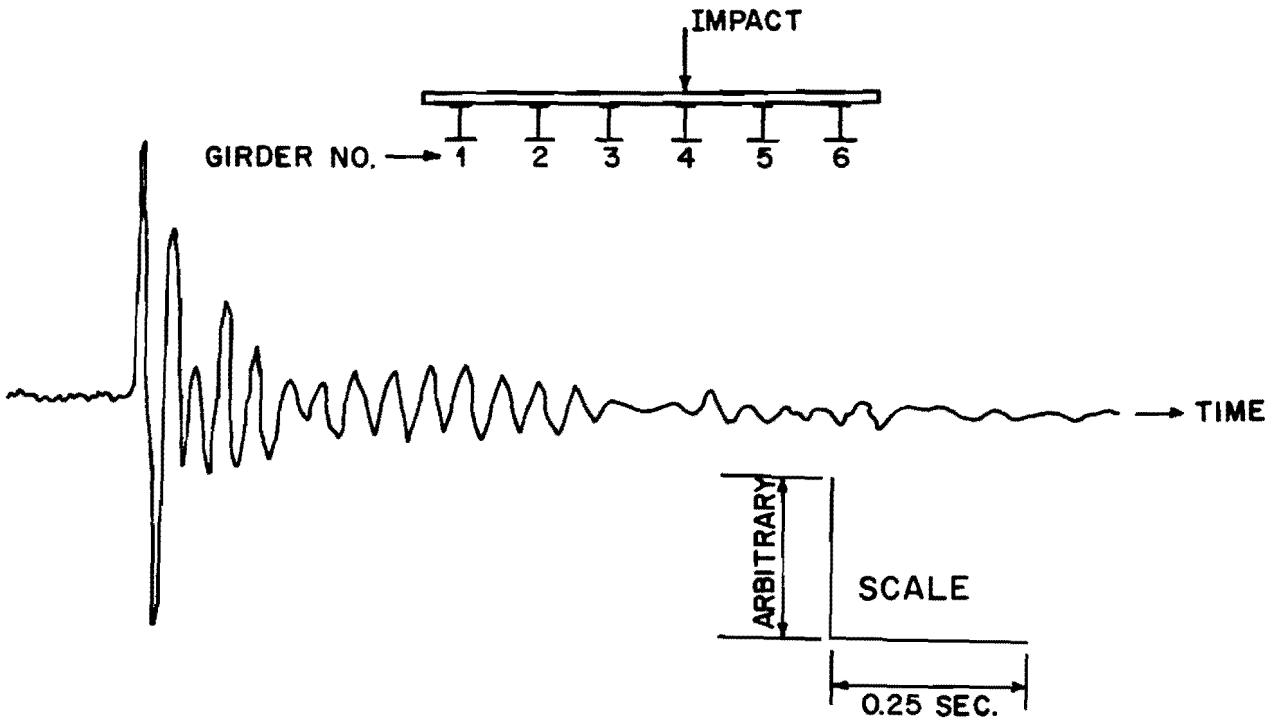

Fig. 3.8 Bridge 4, Girder 3 midspan deflection due to impact on midspan Girder 4.

largest auto-power spectral value. Typical relative amplitude and phase distribution for a straight and a skew bridge at their fundamental frequencies are shown in Figs. 3.9a and 3.9b. From these figures it may be noted that at the lower fundamental frequency (9.5 Hz in Fig. 3.9a and 10 Hz in Fig. 3.9b) the amplitudes are almost uniformly distributed and all the girders are nearly in the same phase. This implies that at this frequency the bridge vibrates vertically like a beam. This has so far been referred to as the longitudinal mode of vibration. At the higher fundamental frequency (11.5 Hz in Fig. 3.9a and 12 Hz in Fig. 3.9b) the amplitude distribution is symmetrical with maximum values at the exterior girders, decreasing almost linearly towards the center of the bridge. The responses of Girders 1, 2 and 3 are almost in the same phase, but nearly 180 degrees out of phase from those of Girders 4, 5 and 6. Therefore, the lower natural frequencies correspond to the longitudinal mode and the higher correspond to the tortional mode of vibration.

3.3.2.5 Cyclic Data

Any periodic function may be considered to be constituted of a set of sine and cosine functions, called harmonics. If T_p is the time period of the function, then the frequency of any harmonic of that function is always an integer multiple of $1/T_p$. That is the frequencies of the consecutive harmonics are separated by $1/T_p$ Hz. If the auto-power spectrum of such a time function is computed with averaging band width δf (same as frequency resolution) less than $1/T_p$, then it is obvious that δf times spectral density (i.e. auto-power spectral value) at a given frequency will give the exact amplitude square of the harmonic corresponding to that frequency. In the present analysis minimum $1/T_p = 4$ Hz (the driving frequency) and $\delta f = 0.5$ Hz (the frequency resolution). Therefore, the requirement that $1/T_p$ be greater than δf is satisfied. However, the presence of noise and slight variations in the driving frequency (i.e., the load frequency) makes the actual data signal an approximately periodic one. To estimate the effect of noise, auto-power spectra were computed for an actual load signal (at frequency 4 Hz), taking the averaging frequency band width (δf) as 0.5 Hz and 0.125 Hz. The amplitudes of first, second, third and fourth harmonics (with frequencies 4 Hz, 8 Hz, and 16 Hz, respectively) were

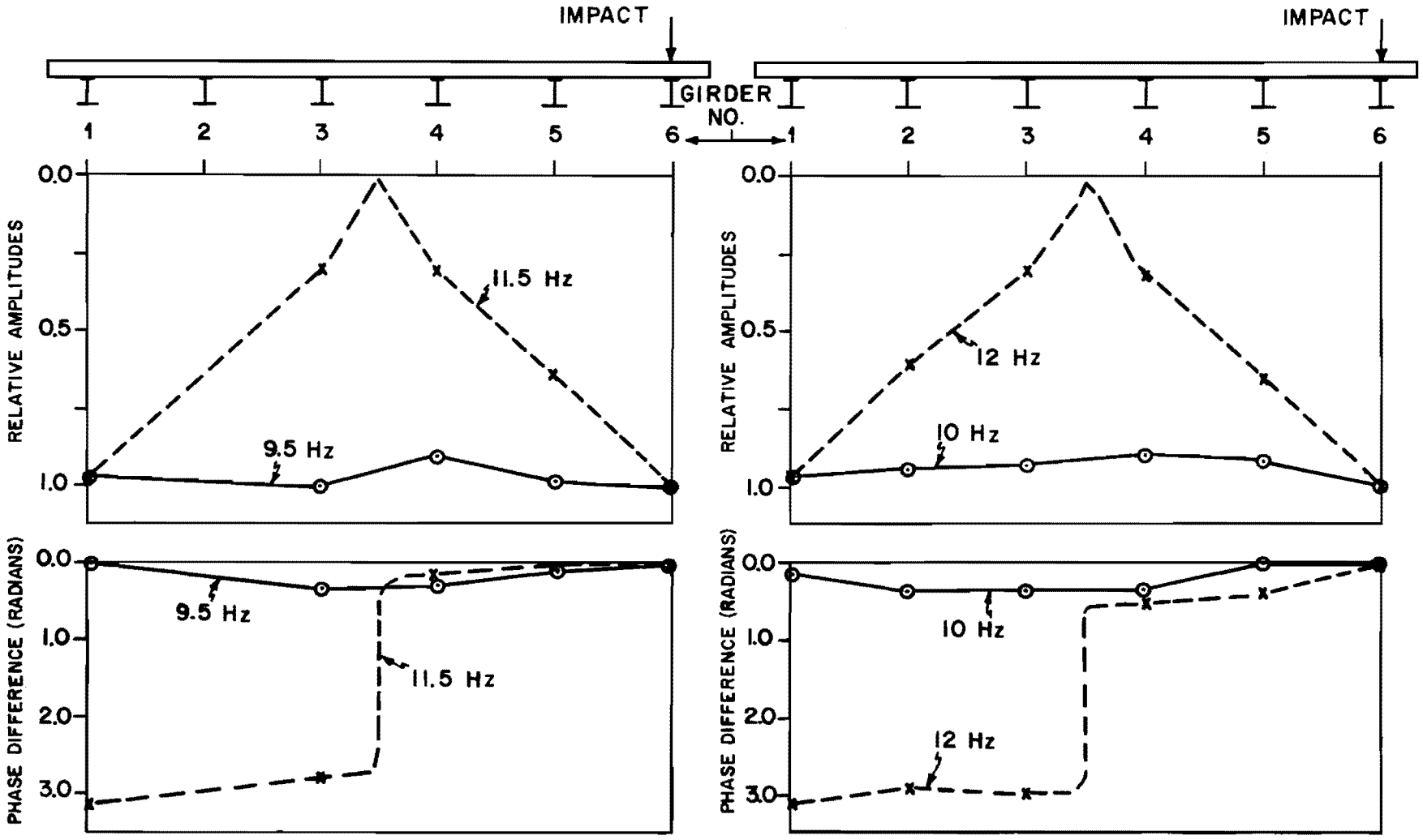

(a) Straight bridge (Bridge 3, Test Series-B)

(b) Skew bridge (Bridge 2, Test Series-B)

Fig. 3.9 Relative girder responses and phase angles due to impact at midspan of reference Girder 6.

calculated from these spectra, in the same manner as described above. The difference between these two sets of values was 0.04, 0.2, 12.5, and 52.5 percent of the latter set for first, second, third, and fourth harmonics, respectively. For $\delta f = 0.125$ Hz, the amplitudes of second, third, and fourth harmonics were 9.7, 1.2, and 1.8 percent of the first harmonic amplitude, respectively. From this it may be noted that the effect of noise is small for first and second harmonics. For higher harmonics, the amplitudes being very small (i.e., signal-to-noise ratio is small), signal distortion due to noise is high.

In the spectral analysis the amplitudes of deflection and strain per unit amplitude of load were calculated by taking the square root of the ratios of deflection (or strain) and load spectral values at the desired frequency. To express these ratios in in./kip (or strain/kip) corresponding calibrations were taken into account. These ratios are not affected by the variation of the frequency of the exciting load as long as these variations are small, so that the amplification of the response signals (i.e., deflections and strains) can be considered to remain the same within the range of variation. Results obtained in this manner were compared with those from direct analysis in some cases where the presence of higher harmonics was negligible. Agreement was found to be excellent.

Cyclic data of Bridges 1, 2, and 3 were analyzed by the spectral analysis method. Direct analysis was not very effective for treatment of cyclic data for these bridges because the data signals showed a significant presence of higher harmonics in many cases. Considerable error may be introduced if the harmonics are not separated out in the analysis. To demonstrate this, results from two driving frequencies (7.5 Hz and 6 Hz) are considered. Load and bridge response auto-power spectra for these cases are shown in Figs. 3.10 and 3.11. It should be noted that the vertical scales in these figures are logarithmic. The amplitude of response per unit load at any given frequency is obtained by taking the square root of the ratio of the corresponding auto-power spectra values. Sample calculations are shown below.

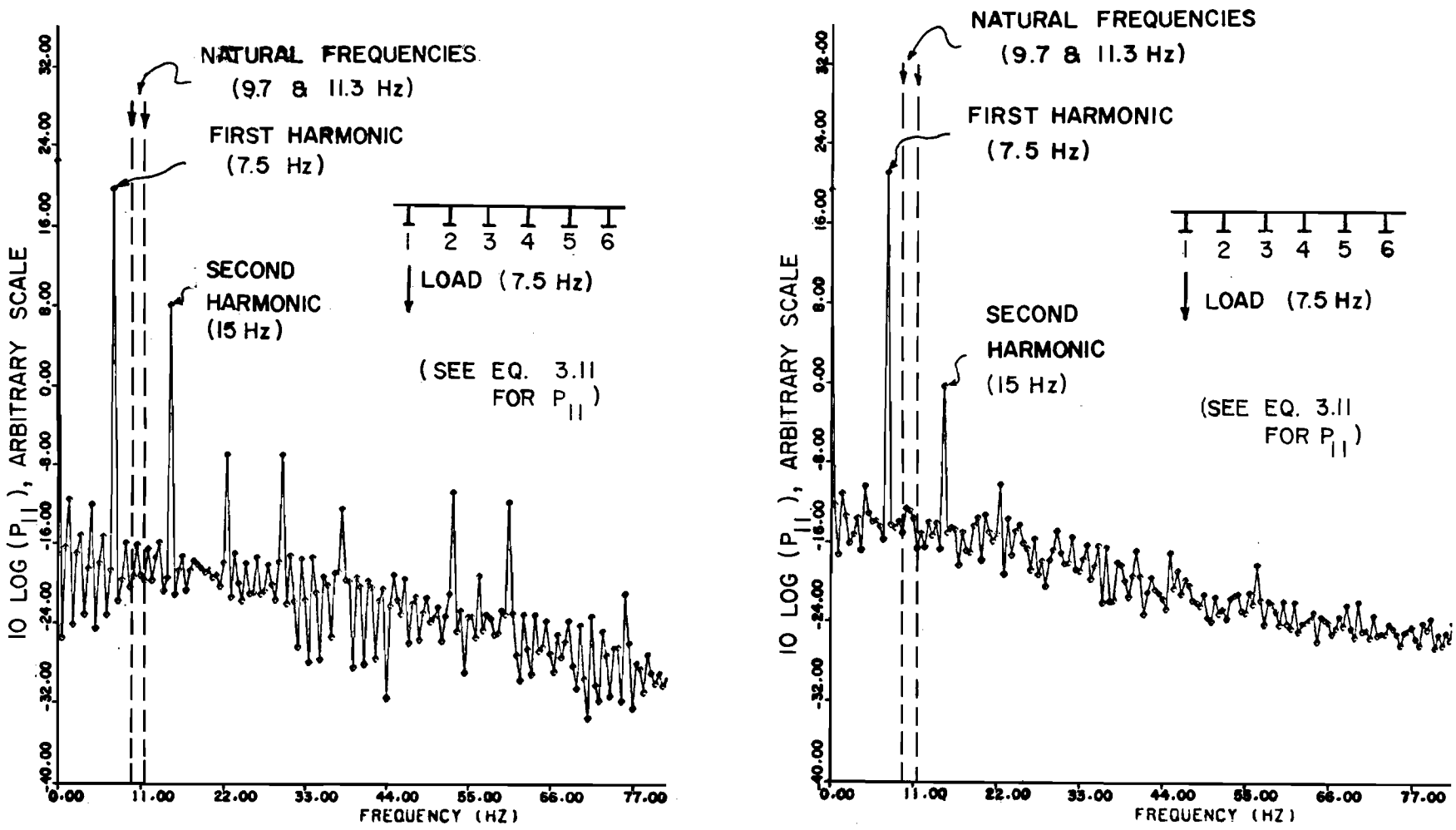

(a) Load at Girder 1 midspan

(b) Girder 1 response at midspan

Fig. 3.10 Auto-power spectra of cyclic load and corresponding bridge response, Bridge 3, Series-A, driving frequency = 7.5 Hz.

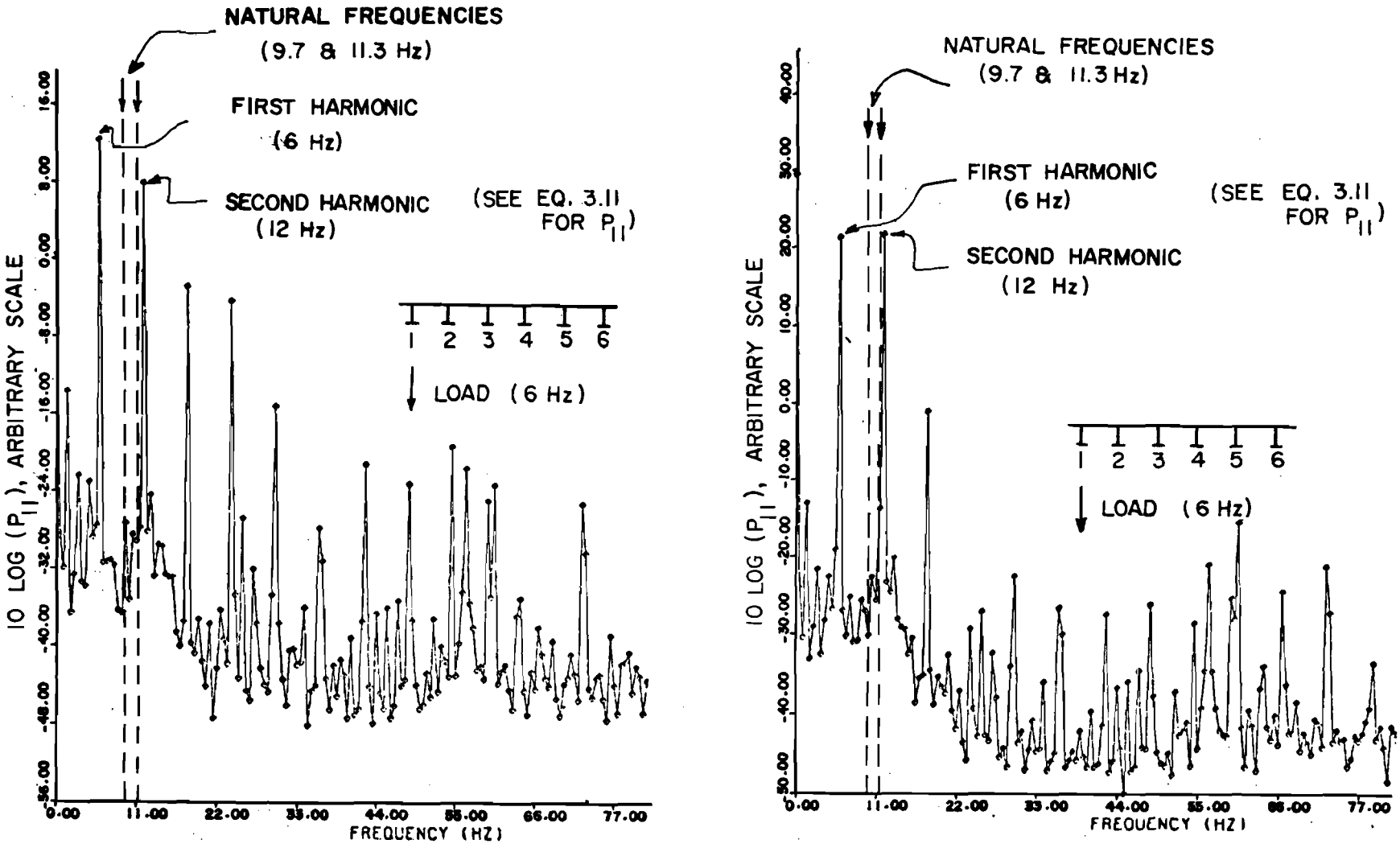

(a) Load at Girder 1 midspan

(b) Girder 1 response at midspan

Fig. 3.11 Auto-power spectra of cyclic load and corresponding bridge response, Bridge 3, Series-A, driving frequency = 6 Hz.

From Fig. 3.10a, auto-power spectral values for load are determined as:

at 7.5 Hz 10 $\log_{10}$ (P_{11}) = 19.7 units

at 15 Hz 10 $\log_{10}$ (P_{11}) = 8.1 units

Corresponding responses are determined from Fig. 3.10b as

at 7.5 Hz 10 $\log_{10}$ (P_{11}) = 21.0 units

at 15 Hz 10 $\log_{10}$ (P_{11}) = -0.4 units

Using the antilogarithm relations then:

at 7.5 Hz P_{11} for load = 92.38 units

at 15 Hz P_{11} for load = 6.3 units

at 7.5 Hz P_{11} for response = 124.0 units

at 15 Hz P_{11} for response = 0.92 units

The amplitude of load at 7.5 Hz is the square root of the corresponding P_{11} or $\sqrt{92.38}$ = 9.6 units.

Similarly,

the amplitude of load at 15 Hz = 2.5 units

the amplitude of response at 7.5 Hz = 11.16 units

and

the amplitude of response at 15 Hz = 0.96 units

From these values, the amplitude of response per unit load at 7.5 Hz is determined as 11.16/9.6 = 1.16 units. Similarly, the amplitude of response per unit load at 15 Hz is 0.96/2.5 or 0.39 units. This shows that, with a driving frequency of 7.5 Hz, the ratio of the girder response to load at the first harmonic (i.e., at 7.5 Hz) is 1.16/0.39 or three times higher than at the second harmonic (i.e., at 15 Hz). Similar calculations based on Fig. 3.11 with a driving frequency of 6 Hz show that the amplitude of response per unit load for the first harmonic (at 6 Hz) is only 0.57 that for the second harmonic (at 12 Hz). Thus, it can be seen that the response amplitude per unit load can vary widely between harmonics and with different driving frequencies.

In direct analysis the harmonics are not separated. Response per unit load at the driving frequency, as calculated by this method, corresponds approximately to the ratio of the average of the amplitudes of response at different harmonics to the average of the amplitudes of load at different harmonics. To give some quantitative idea about the possible error which may result from use of direct analysis when the presence of higher harmonics in the signals is significant, the ratio of the average response amplitude to the average load amplitude values was calculated for the cases shown in Figs. 3.10 and 3.11. In these calculations the third and higher harmonic values are neglected because their quantitative effects are insignificant.

From the previous calculations the average of the load amplitudes at the first and second harmonics (i.e., at 7.5 Hz and 15 Hz) for a driving frequency of 7.5 Hz is equal to (9.6 + 2.5)/2 or 6.05 units. The corresponding average response is (11.16 + 0.96)/2 or 6.06 units. Therefore, for the 7.5 Hz driving frequency, direct analysis procedures would indicate the ratio of the average of response amplitudes to the average of load amplitudes or 6.06/6.05 = 1.0 unit. This value is 1/1.16 or 0.86 that determined by spectral analysis for the first harmonic (i.e., 7.5 Hz).

By similar calculations for the case with 6 Hz driving frequency, the direct analysis average ratio would be 1.28 times the spectral analysis first harmonic amplitude ratio. This shows that for the example cases considered, the direct analysis will give considerable error. At 7.5 Hz driving frequency it will be an underestimation and at 6 Hz driving frequency it will be an overestimation. As there is no prior knowledge of the possible extent of this error, it is necessary to separate out the harmonics to determine a meaningful response of the bridge at any frequency of excitation.

From the auto-power spectra of load and bridge responses, it appears possible to determine bridge response at the higher harmonic frequencies. This should not be done, since the third and higher harmonic values are so small that their quantitative values should not be relied on. In some cases the second harmonic values were large enough and bridge response for such cases was calculated. However, since the second harmonic amplitudes are

generally less than 10 to 20 percent of the first harmonic amplitude, the calculated bridge response at the second harmonic is much less reliable than at the first harmonic.

CHAPTER 4

COMPUTER SIMULATION

4.1 General

Essentially, three different approaches have been used to analyze slab and girder bridges under static loads. In procedures proposed by Lightfoot,[24] Hendry and Jaeger,[17] and Newmark,[31] the slab and girder system is replaced by an equivalent grillage or a system of primary (longitudinal) and secondary (cross) members. In a second approach, the structural system is replaced by an elastically equivalent plate having different flexural rigidities in two orthogonal directions. The problem is then solved applying orthotropic plate theory.[45] Massonnet's[26] work is an example of this method. A detailed presentation of this method is given by Rowe.[34] A third approach is the finite element method, where the structure is idealized as an assemblage of deformable elements linked together at the nodal points where continuity and equilibrium are established. The works of Mehrain,[28] Gustafson[16] and Sawko[36] provide examples of this method.

Under dynamic loads the analysis of bridges becomes a much more complex problem. Simply supported bridges are usually idealized as a single simple beam.[11,49] Walker and Veletsos[49] mentioned an analytical procedure[32] to solve simple span multigirder bridges by treating the bridge as a plate continuous over flexible beams. Cabera et al.[14] reported a generalized analysis technique of the dynamics in a two-dimensional field for a homogeneous plate. Consideration was given to vehicle loads moving on an uneven surface. A list of references concerning the behavior of highway bridges under the passage of heavy vehicles may be found in the works of Veletsos and Huang.[46] Cabera[14] gives a historical summary of different works related to dynamics of bridge decks.

Because of the extreme complexity involved in a two-dimensional dynamic analysis of bridges of the type studied herein, no effort was made in this study to theoretically investigate the dynamic aspects of the problem. However, a carefully verified computer program was available to study major bridge characteristics under static loads. In this study the ability of this program to determine the effects of diaphragms was checked and numerous extensions of the test variables were studied. The following sections present a short description of the basis of the analysis, describe the input parameters for the computer program and summarize the program accuracy evaluation.

4.2 Discrete Element Model[47]

A mechanical model consisting of a tridirectional system of rigid bars and elastic joints was developed by Vora and Matlock[47] to simulate anisotropic skew plates plus slab and girder systems in which the grid beams may run in any three directions. A model of the plate consists of elastic joints connected by rigid bars in the directions a, b and c (see Fig. 4.1a). The model of a grid beam in a particular direction consists of elastic joints connected by rigid bars running in that direction (Fig. 4.1b). The plate and the grid beam models are connected at the elastic joints so that the deflections for both models at these joints are the same. The stiffnesses, loads and restraints are lumped at the elastic joints. The only function of the rigid bars is to transfer bending moments from one elastic joint to the other. To analyze this plate and grid system the following assumptions are made.

(1) There is no axial deformation in the middle plane of the plate. That is, the middle plane remains neutral during bending.

(2) The neutral plane of the plate and grid beams are at the same level.

(3) A normal to the middle plane remains normal before and after bending.

(4) The normal stresses in the direction perpendicular to the plate are neglected.

(5) Each elastic joint is of infinitesimal size and composed of an elastic but anisotropic material. Curvature appears at the joint as a concentrated angle change.

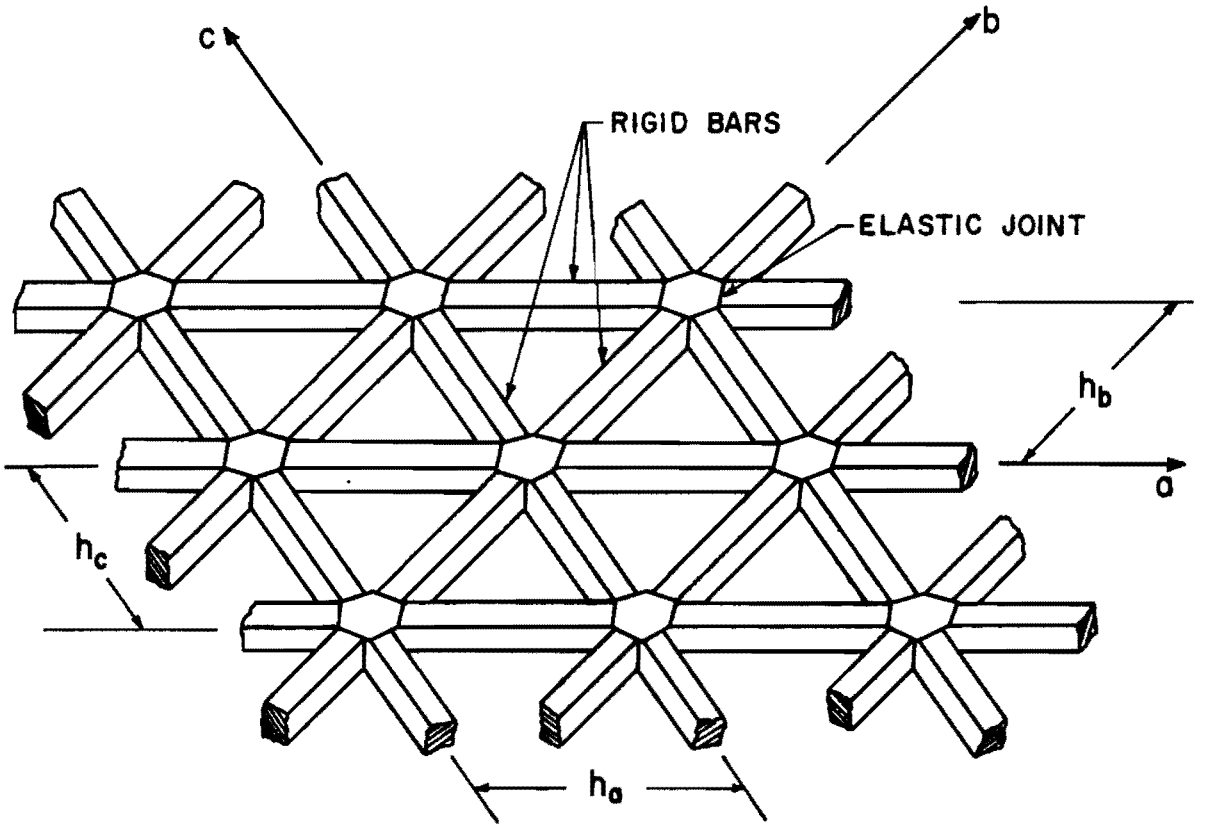

(a) Plate model

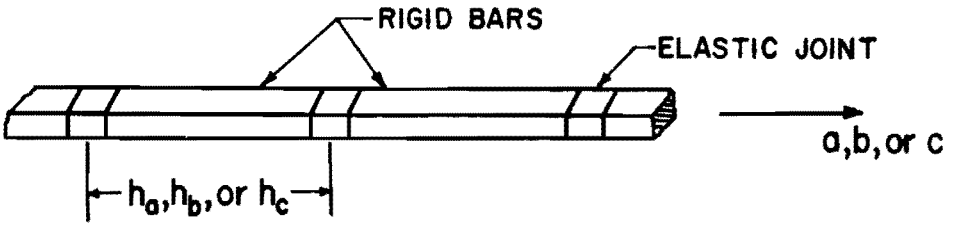

(b) Grid-beam model

Fig. 4.1 Discrete element models.

(6) The rigid bars of the model are infinitely stiff and weightless. They transfer bending moments by means of equal and opposite shears. They do not transfer twisting moments. They do not deform due to inplane forces.

(7) The stiffnesses of the plate and of beams may vary from point to point.

(8) The elastic joint spacings h_a and h_c (Fig. 4.1a) need not be equal but must remain constant. The spacing in the b direction h_b (Fig. 4.1a) is equal to the length of the diagonal of the parallelogram having sides h_a and h_c.

4.3 Principle of Analysis[47]

By applying the equations of equilibrium and conditions of compatibility, the vertical force $P_{i,j}$ at any joint i,j is expressed as a function of the known elastic and geometrical properties of the model and of the unknown deflections at it and 18 surrounding joints, as shown in Fig. 4.2a. In general form this may be written as

$$\sum R_{m,n} \cdot \delta_{k,\ell} = F_{i,j} \tag{4.1}$$

Where $R_{m,n}$ are the known functions of geometric and elastic properties of the discrete element model at different joints m,n (joint m,n and k,ℓ is not always the same for all m,n and k,ℓ values), and $\delta_{k,\ell}$'s are unknown deflections at joints k,ℓ. k varies from i - 2 to i + 2 and ℓ varies from j - 2 to j + 2 (Fig. 4.2a). Equation 4.1 may be considered as an operator and is applied successively to each joint of the slab and beam model (Fig. 4.2b). The number of unknown deflections will always be more than the number of equations thus obtained. The difference is made up by the additional equations obtained from the boundary conditions of the model. By solving this set of simultaneous equations, deflections at all the joints are obtained. Forces such as moments, twisting moments, etc. are then calculated by putting these known deflections into the conditions of compatibility. The mathematical formulation and the computer program based on this principle has been presented by Vora.[47]

4.4 Input Parameters and Their Evaluation

Alani[3] has discussed in detail the evaluation of input parameters for different kinds of bridges. In this section only a short guideline for

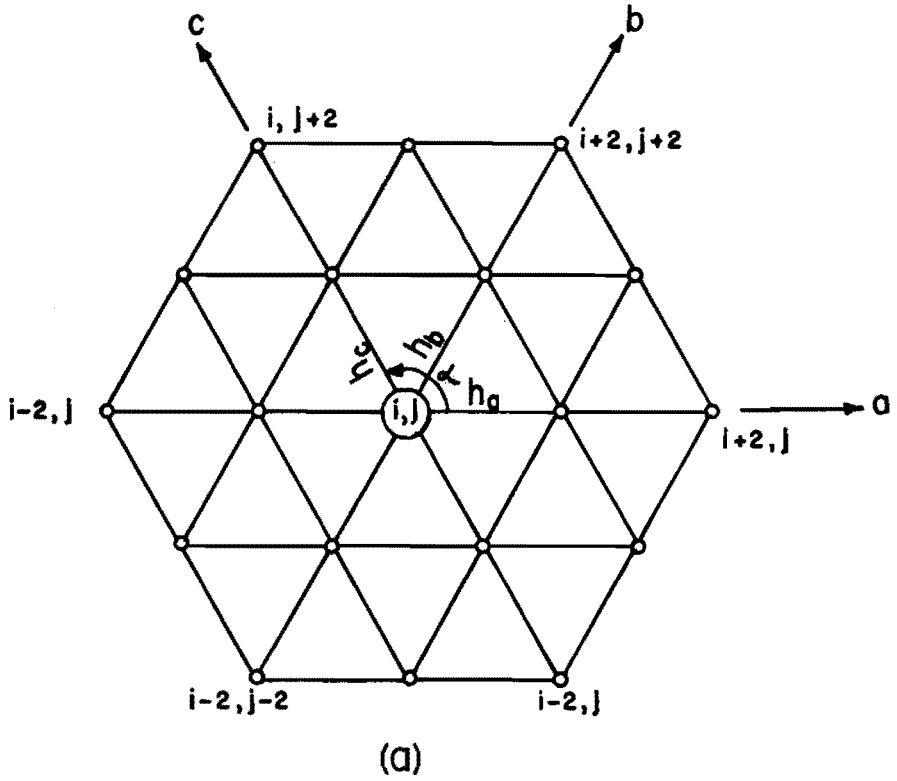

(a)

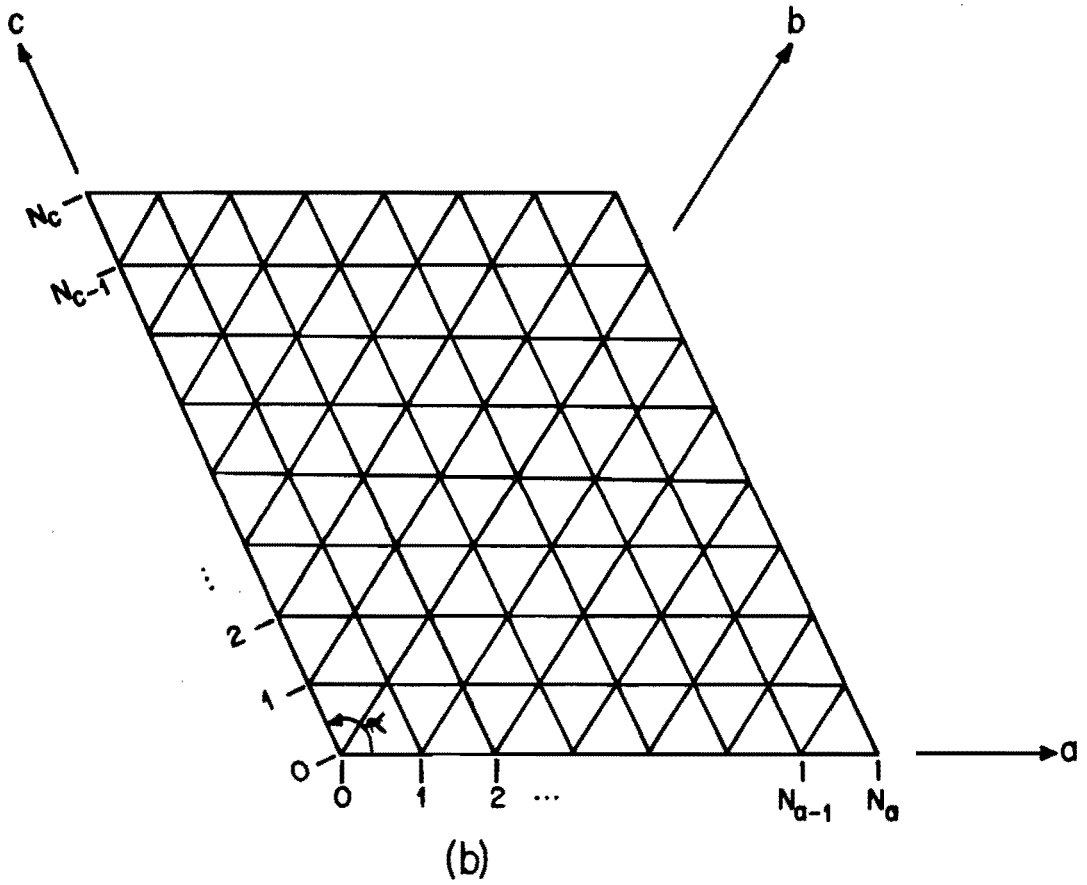

(b)

Fig. 4.2 Operator and model.

the evaluation of these parameters for prestressed concrete girder and slab bridges is presented.

4.4.1 Length and Number of Increments

The desired numbers of increments N_a and N_c (Fig. 4.2b) are determined from the consideration of computation cost and desired accuracy. Previous studies[3,47] indicate about four to seven increments between girders and about 20 to 50 increments along the span are sufficient for accuracy and reasonable for computation cost.

4.4.2 Angle between Axes a and c (α in Fig. 4.2.b)

The axes are chosen parallel to the lines of support and to the center lines of the longitudinal girders determining the angle α.

4.4.3 Boundary Conditions

Nonyielding simply supported boundary conditions are simulated by introducing very large spring constants (1×10^8 lbs./in. or more) at girder support nodes.

4.4.4 Loads

All loads are input at the nodes of the grid. In the case of loads which occur inside the grid, the loads are distributed to the surrounding nodes assuming that the grid is stiff and is simply supported on the surrounding nodes.

4.4.5 Slab Stiffnesses

In this study the slab stiffnesses are evaluated with respect to two orthogonal directions. The formulas for evaluation of these stiffnesses are given by Vora[47] as functions of modulus E_c, Poisson's ratio ν_c, and the thickness of the slab. E_c has been determined according to the ACI Building Code 318-71.[2] The Poisson's ratio for concrete is taken as 0.16.

4.4.6 Beam Flexural Stiffnesses

These values are taken as the product of the gross transformed moment of inertia of the section and the concrete modulus of elasticity. For the

cross beams (i.e. diaphragms) the area of the reinforcing steel was neglected. For composite sections, the flange widths are calculated according to the ACI Building Code 318-71.[2]

4.4.7 Beam Torsional Stiffnesses

Diaphragm torsional stiffnesses are neglected. The torsional stiffness of the girder flange is included in the slab. Additional torsional stiffness due to the girder and the connection between the girder and flange is obtained from the product of an additional torsional rigidity factor K and the concrete shear modulus G. K and G are calculated as follows:[3]

$$K = K_1 + K_2 \tag{4.2a}$$

where

$$K_1 = \beta d e^3 \tag{4.2b}$$

$$K_2 = 0.156\ Q^2 \tag{4.2c}$$

and

$$G = \frac{E_c}{2(1 + \nu_c)} \tag{4.3}$$

β, d, e and Q are as shown in Fig. 4.3a, Fig. 4.3b, and Fig. 4.3c. E_c and ν_c values are evaluated as before.

Additional girder torsional stiffnesses cannot be directly input in the program. To overcome this difficulty, these torsional stiffnesses are transformed to equivalent slab torsional stiffnesses. They are then input in the slab grid at joints common to the girder and the slab. The equivalent stiffness is approximately obtained by dividing the girder torsional stiffness by 4 times the grid length in the direction perpendicular to the girder. This transformation is necessary because the program input for slab torsional stiffness is 1/4 the stiffness per unit length.

4.5 Verification of the Program

For program verification studies, all input data except the longitudinal girder stiffnesses were determined as stated in Section 4.4. The girder flexural stiffnesses were obtained experimentally from the auxiliary tests (Sec. 2.7).

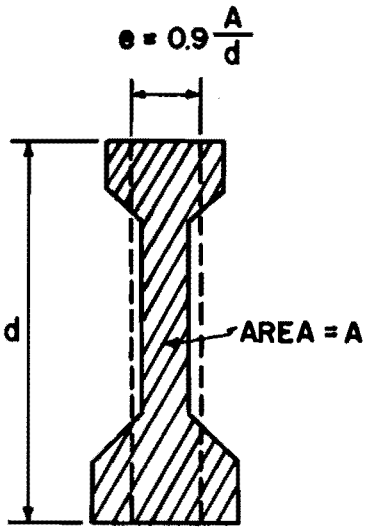

(a) Prestressed concrete girder section

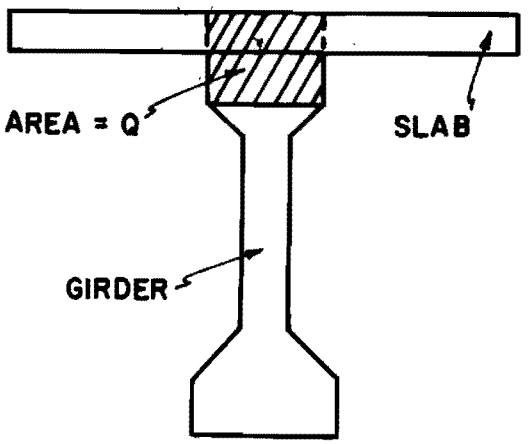

(b) Composite section of slab and girder

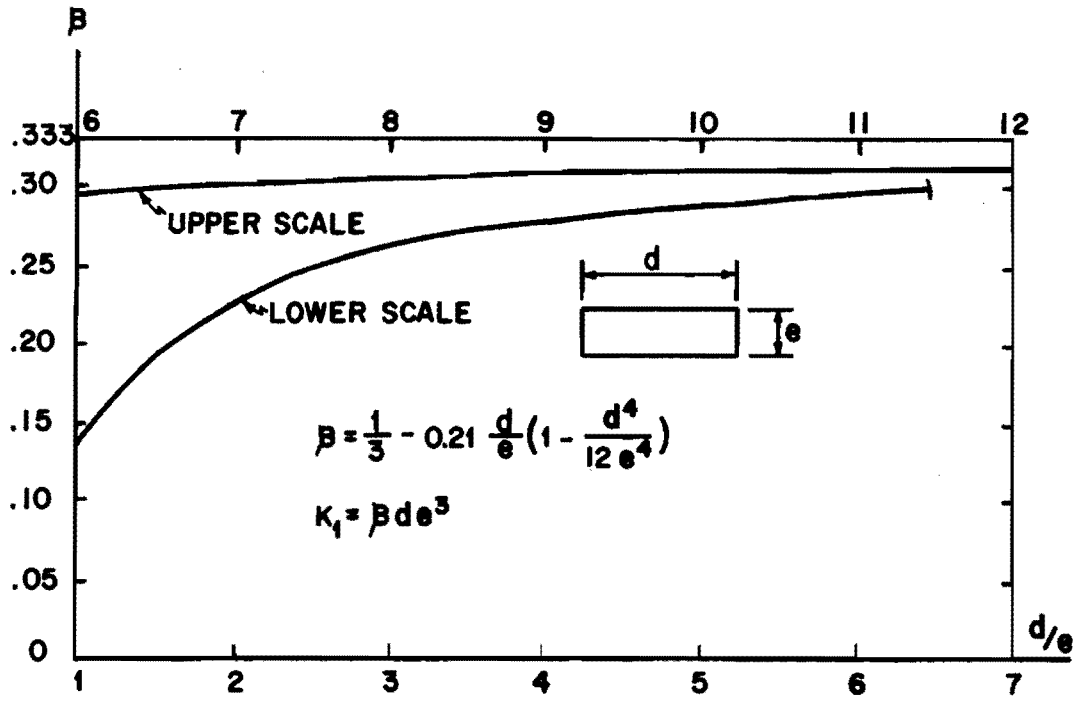

(c) Coefficient β

Fig. 4.3 Quantities to evaluate girder torsional stiffness (taken from Ref. 3).

Girder torsional stiffnesses, used in this analysis were determined experimentally earlier.[7] The torsional stiffness contributed by the flange was determined from Eq. 4.2b. For the slab β was taken as equal to 0.33. For this case, d and e refer to the flange width and the slab thickness, respectively. This part of the torsional stiffness was then deducted from the experimental value to obtain input torsional stiffness for the girders.

Theoretical and experimental relative moment and deflection distributions across mid and 3/4 spans due to truck and point loads, for skew and straight bridges are shown in Fig. 4.4, 4.5 and 4.6. In these figures TA, TB and TC are standard truck loads (see Figs. 2.25 and 2.26 for their location and Fig. 2.20c for model truck load) and F1, F2, etc. are point loads of 1 kip magnitude (see Figs. 5.1 and 5.2 for load locations). Relative moments and deflections are given by

$$\text{Relative moment} = M/\Sigma M \tag{4.4}$$

$$\text{Relative deflection} = \delta/\Sigma\delta \tag{4.5}$$

where M and δ are the moment and deflection of any girder at a given section (at 3/4 span and midspan in this case) and ΣM and $\Sigma\delta$ are the sum of these quantities for all girders across the same span section. These figures show an excellent correlation between the theoretical and experimental values. Similar agreement was reported in previous investigations.[3,47] Therefore, it was concluded that both skew and straight bridges can be analyzed by this program with sufficient accuracy.

The percentage change in the distribution coefficients caused by the removal of the diaphragms was chosen as the basic criterion for assessing ability of the program to determine diaphragm effectiveness. The distribution coefficients are defined as

$$\text{D.C. (moment)} = M_{max}/\Sigma M \tag{4.6}$$

$$\text{D.C. (deflection)} = \delta_{max}/\Sigma\delta \tag{4.7}$$

M_{max} and δ_{max} are the maximum girder moment and deflection at a given span location. ΣM and $\Sigma\delta$ are defined as before. Percentage increase of these from Series-A (all diaphragms in) to Series-B (no interior diaphragms) or Series-C (no diaphragms) is calculated as

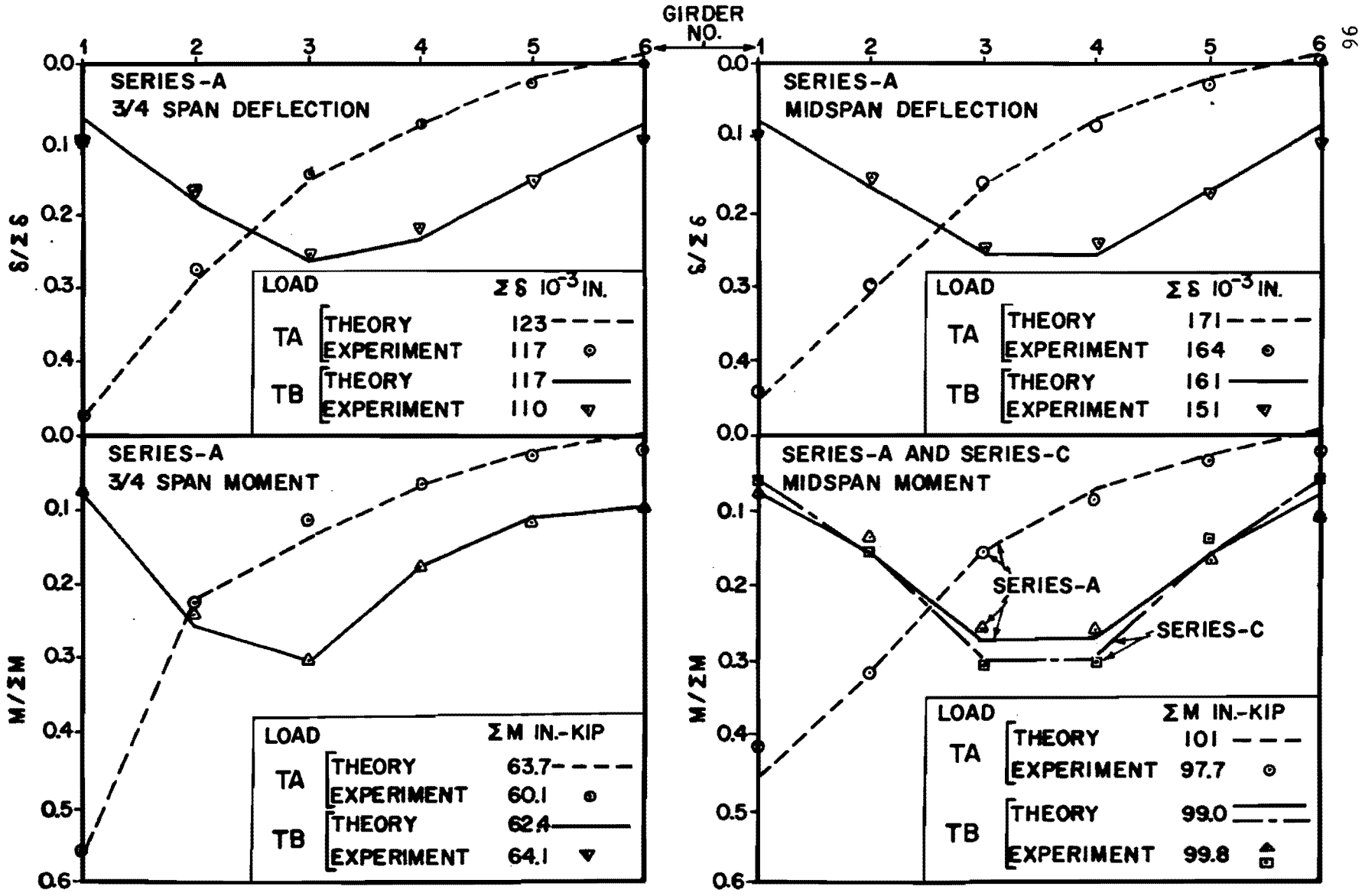

Fig. 4.4 Bridge 2 (45° skew, 172 in. span), $\delta/\Sigma\delta$ and $M/\Sigma M$ distribution.

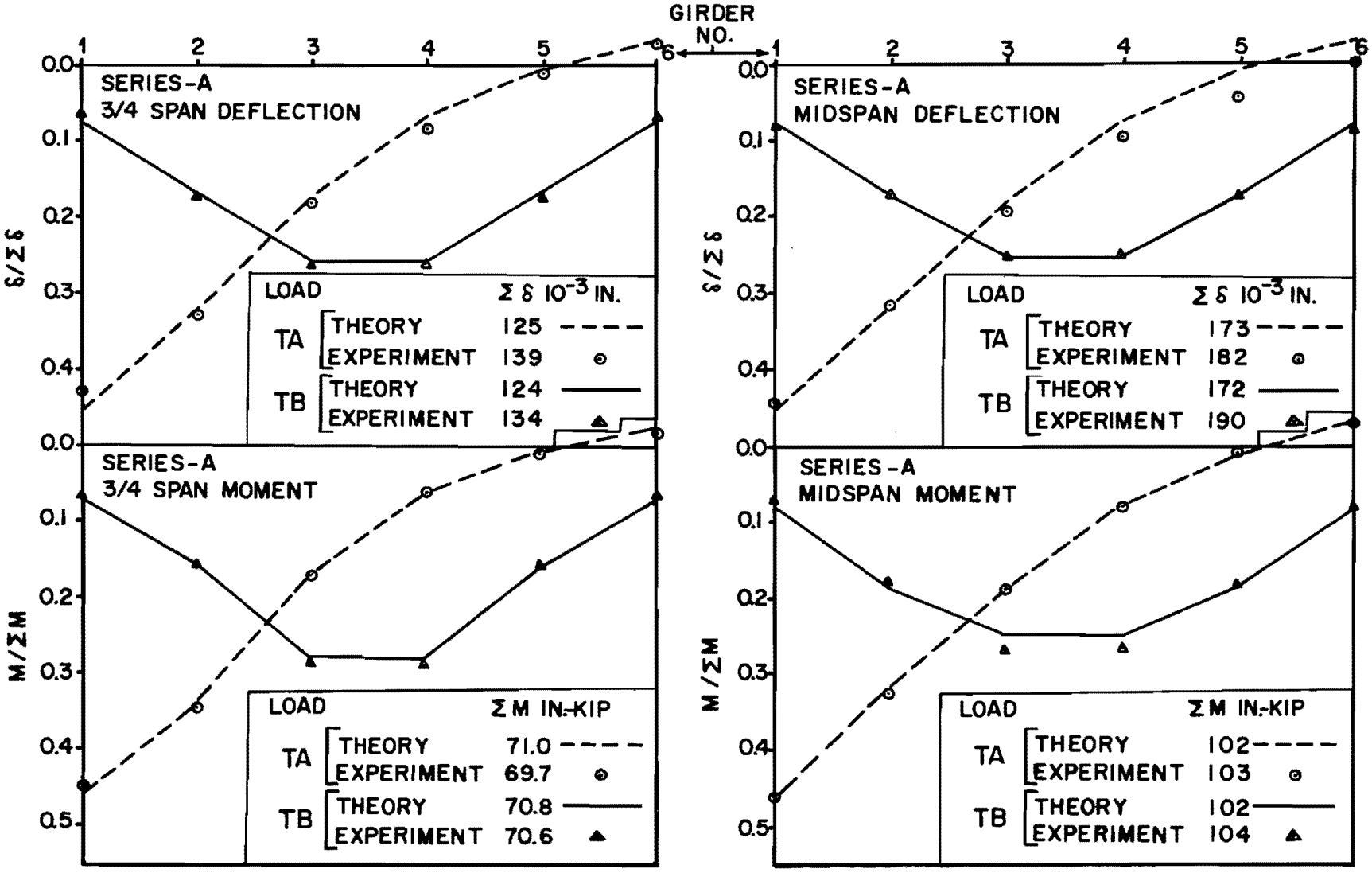

Fig. 4.5 Bridge 3 (straight, 172 in. span), $\delta/\Sigma\delta$ and $M/\Sigma M$ distribution.

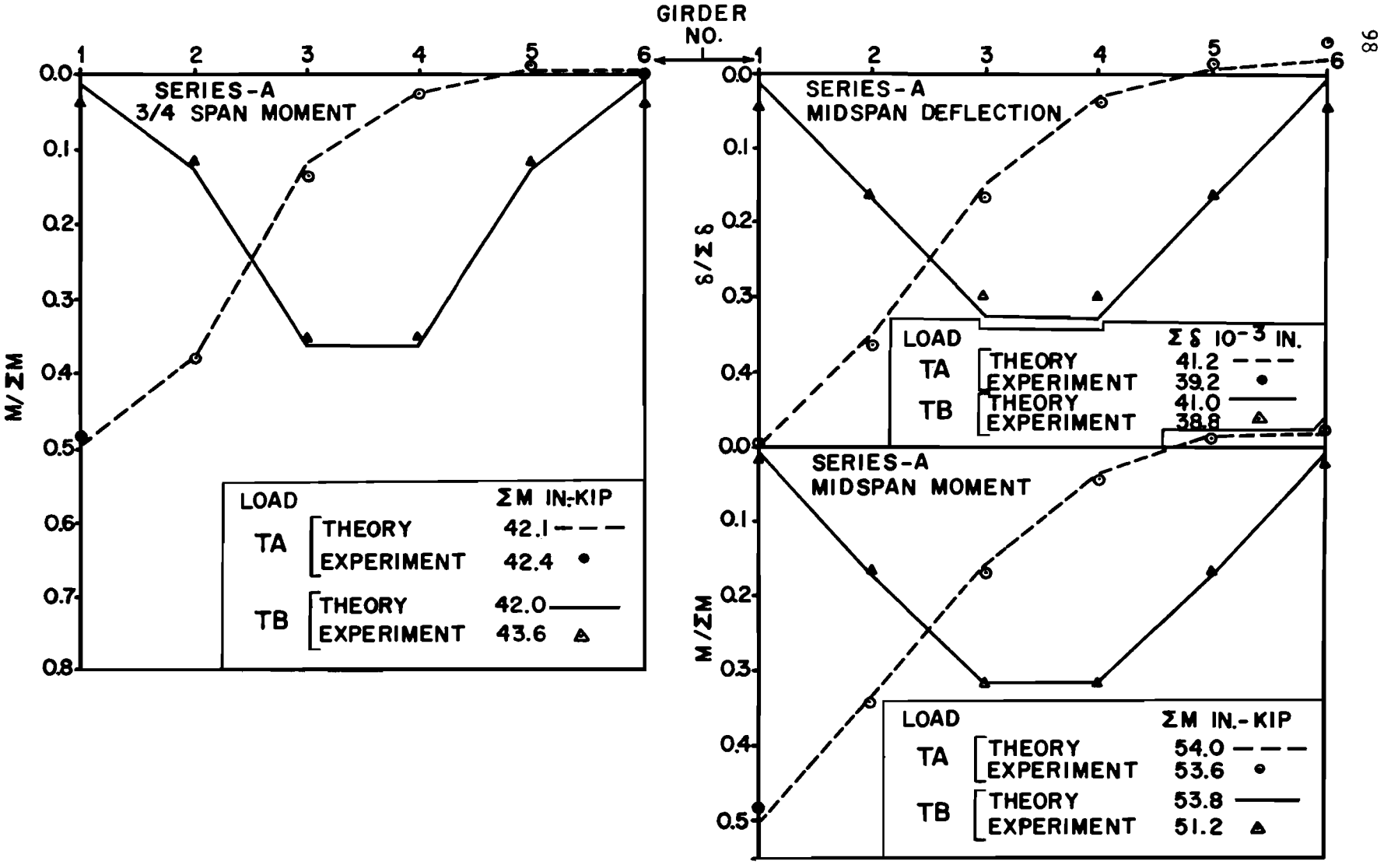

Fig. 4.6 Bridge 4 (straight, 107 in. span), $\delta/\Sigma\delta$ and $M/\Sigma M$ distribution.

$$\text{Percentage increase} = \left[\frac{\text{D.C. (Series-B or C)}}{\text{D.C. (Series-A)}} - 1\right] \times 100 \qquad (4.8)$$

Figures 4.7 and 4.8 show the percentage changes of these distribution coefficients at 3/4 span and midspan for all four bridges and for different loads. Legends A to B and A to C at the top of these figures indicate that the changes are from Series-A to B and from Series-A to C, respectively.

In skew bridges (Fig. 4.7a and Fig. 4.7b), though the calculated and experimental changes in distribution coefficients due to different loads show a similar trend, agreement in their quantitative values is very poor. This discrepancy is even more apparent in Bridge 1, where Type D1 (Fig. 2.7) interior diaphragms were used. It appears that the effective stiffness of Type D1 diaphragms is larger than that calculated on the basis of the cross section of the diaphragm alone. This is probably due to partial composite action between the diaphragm and the slab. In the case of staggered diaphragms (Figs. 2.3 and 2.4), moments from one diaphragm to the other are transferred through the slab and also through torsion in the girders. The approximate nature of inputting girder torsional stiffness in the program may be a possible reason for this disagreement. At this stage it appears that more work is needed to improve the ability of the program to determine diaphragm effects in skew bridges.

There is an apparent contradiction if the program is accurate enough to determine distribution characteristics for skew bridges, but not accurate enough to detect diaphragm effectiveness. To clarify this, the results shown in Fig. 4.4 (lower right) should be reexamined. In this figure the relative moment distribution plots for both Series-A and Series-C (i.e., with all the diaphragms in position and without any diaphragm cases) are shown. In both the cases the theoretical results agree very well with experimental values. For Series-A the maximum theoretical value of $M/\Sigma M$ is 7 percent higher than that obtained from the experiment. For Series-C the maximum theoretical value of $M/\Sigma M$ is about 3 percent lower than that obtained from the experiment. As the bridge distribution characteristics are measured by the distribution coefficient values (i.e., maximum $M/\Sigma M$ in this case) and these values obtained from theory agree very well with the experiment values, the program is considered accurate enough to determine the

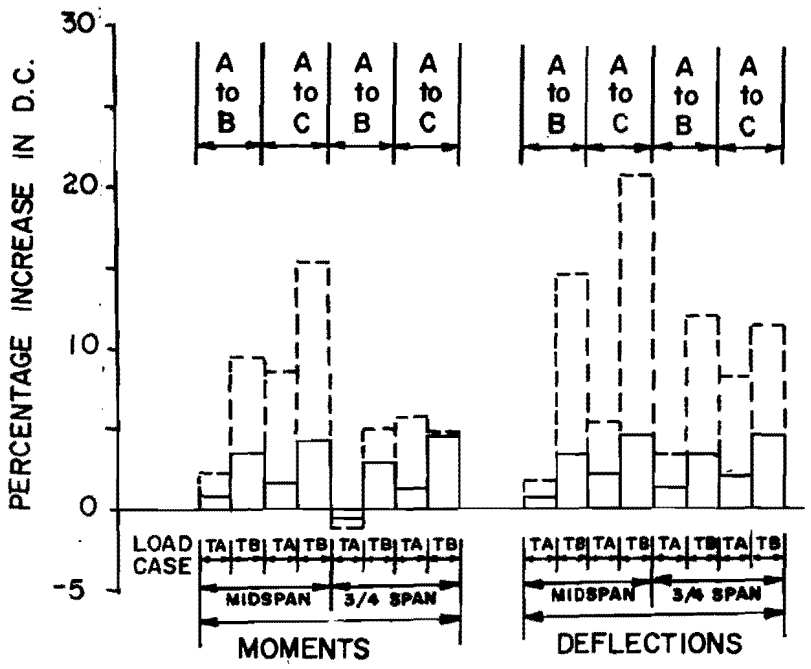

(a) Bridge 1, 45° skew, 172 in. span, Type D1 Diaphragms at 1/3 & 2/3 spans

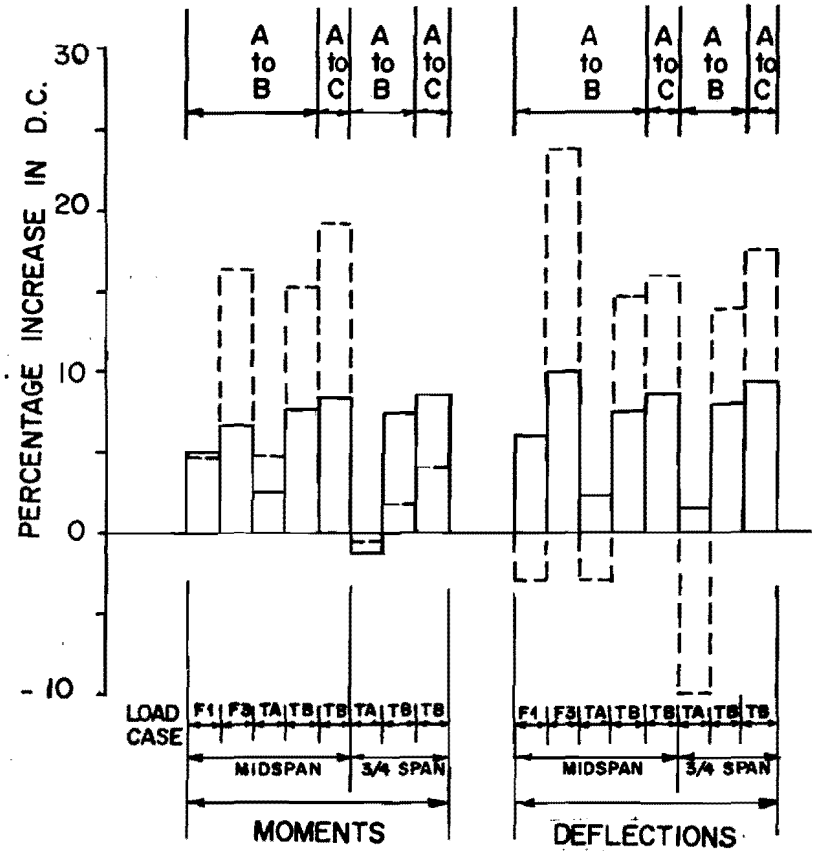

(b) Bridge 2, 45° skew, 172 in. span, Type D2 and Type D3 diaphragms at 1/3 & 2/3 spans

$$D.C.(M) = \frac{M_{max}}{\Sigma M}; \quad D.C.(\delta) = \frac{\delta_{max}}{\Sigma \delta}$$

EXPERIMENT ⬚ ; THEORY ▯

Fig. 4.7 Percentage increase in distribution coefficient due to diaphragm removal, skew bridges.

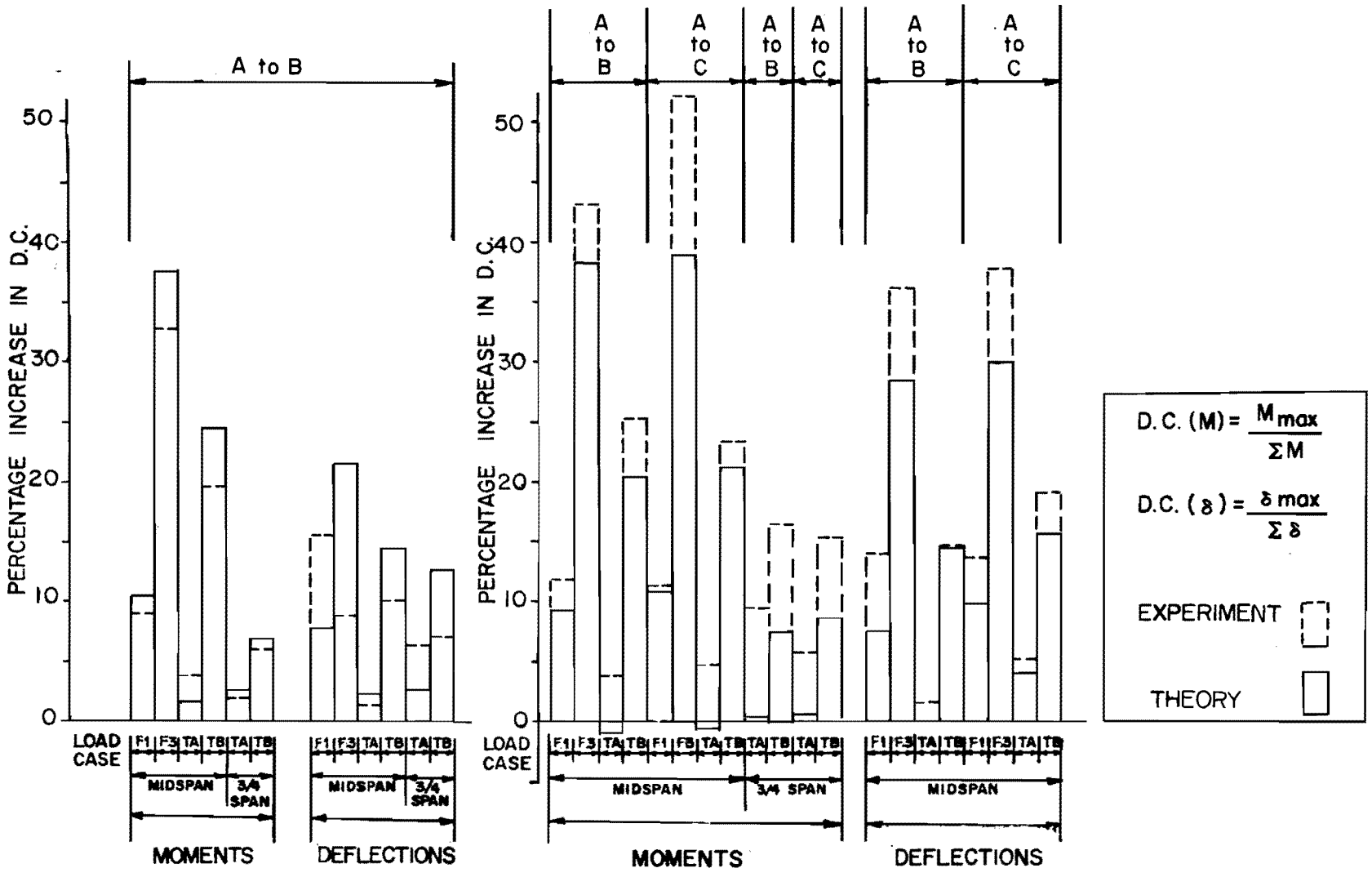

(a) Bridge 3, straight, 172 in. span, Type D2 diaphragms at midspan

(b) Bridge 4, straight, 107 in. span Type D2 diaphragms at midspan

Fig. 4.8 Percentage increase in distribution coefficient due to diaphragm removal, straight bridges.

distribution characteristics of skew bridges. On the other hand the diaphragm effectiveness is measured by the change in the distribution coefficients caused by the removal of diaphragms. For the example case these changes are 8 percent and 19 percent in theoretical and experimental values, respectively. This shows that the program cannot reliably measure the effectiveness of the diaphragms in skew bridges, although the accuracy of the program is sufficient for determination of the bridge moment and deflection distribution characteristics.

In straight bridges, where diaphragms are at midspan and continuous, the agreement between the theoretical and experimental results is much better (Figs. 4.8a and 4.8b). Due to experimental errors and errors in estimating input parameters, the scatter in the variation of these quantities (i.e., moments and deflections) can be expected to be much larger than in the actual quantities themselves. In view of this fact, it is considered that the accuracy of this program is acceptable in determining diaphragm effectiveness in a straight bridge.

CHAPTER 5

RESULTS AND DISCUSSION

5.1 General

In this chapter the reduced experimental data are presented to document the role of diaphragms. The computer program was used to extend and generalize some of the experimental findings. The results are discussed under the following headings:

5.2 Diaphragm effectiveness in static load distribution
5.3 Diaphragm effectiveness under dynamic loads
5.4 Diaphragm effectiveness under lateral impacts
5.5 Overload and ultimate truck load tests
5.6 Slab end static load tests
5.7 Slab punching
5.8 Stresses in diaphragms.

5.2 Diaphragm Effectiveness in Static Load Distribution

The effect of diaphragms in distributing service loads was determined from static point load and truck tests. The normalized values of experimental girder moments and deflections at different transverse sections along the span (i.e., at 1/4, mid and 3/4 points) are tabulated in Appendix B. In these tables point loads are of 1 kip magnitude (i.e., 1.89 times the model scale standard rear wheel load). These point loads are designated by a letter and a number which give the grid coordinates of the point of application as shown in Figs. 5.1 and 5.2. For truck loads, the magnitude corresponds to the AASHO standard HS20-44 truck and includes a 25 percent impact factor (obtained from the AASHO formula for an 80 ft. span). The location and designation of truck loads have been given in Figs. 2.25 and 2.26 of Chapter 2.

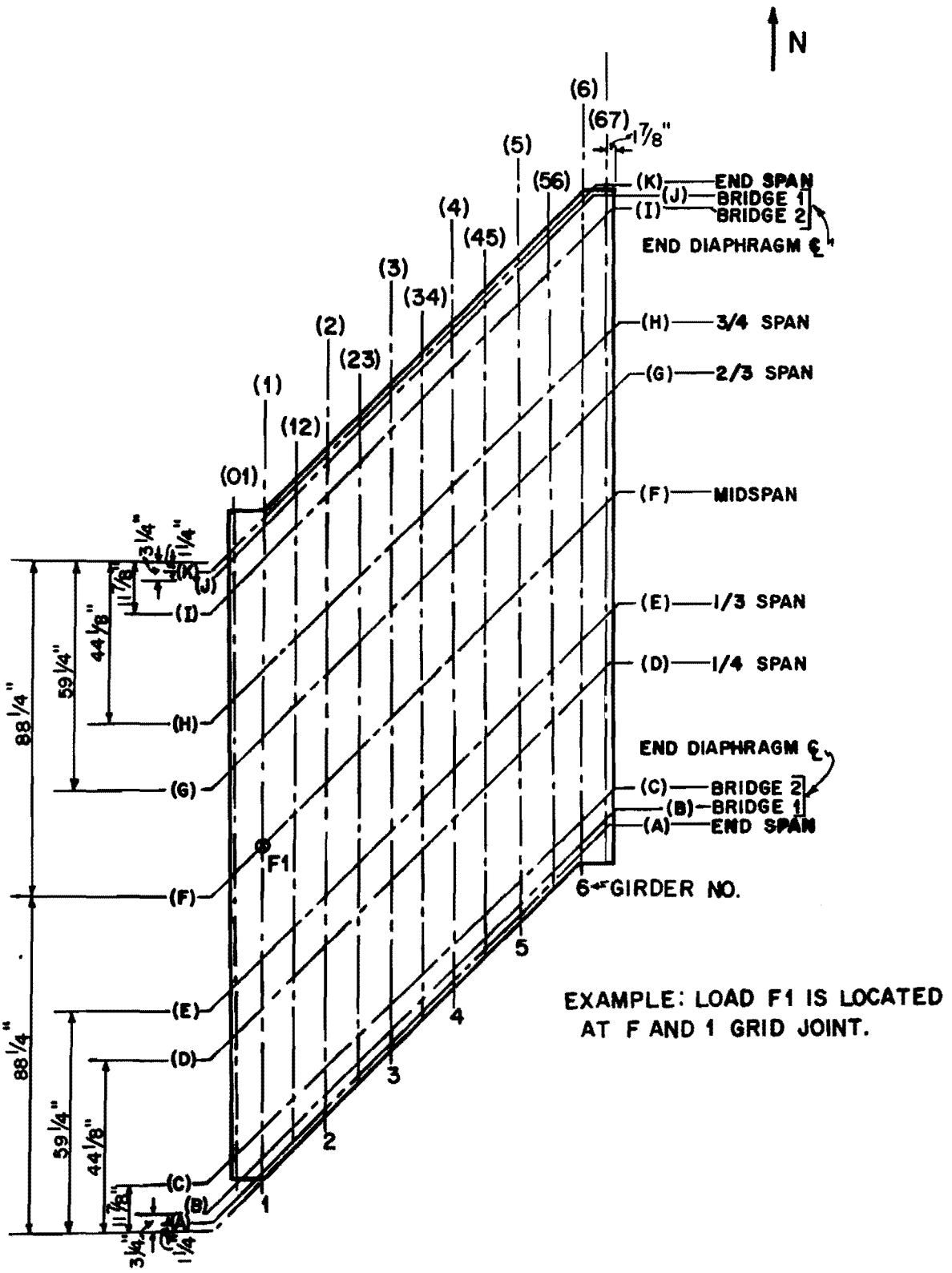

Fig. 5.1 Reference grids for point loads, Bridges 1 and 2.

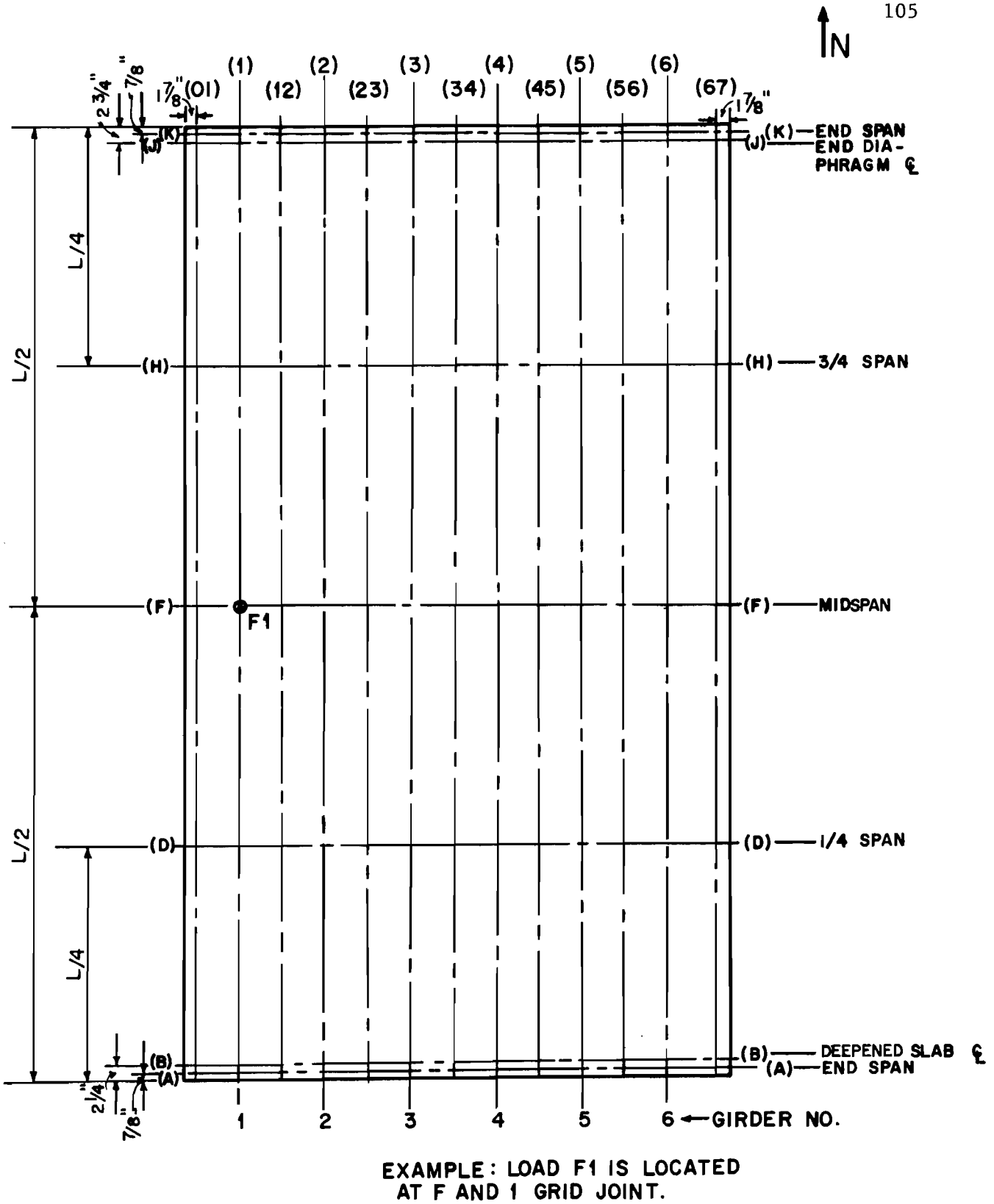

Fig. 5.2 Reference grids for point loads, Bridges 3 and 4.

Under a given static load the sum of all the girder moments or of all the girder deflections at any given transverse section (e.g., at midspan, etc.) can be considered to be essentially independent of the presence or absence of diaphragms. Therefore, variations in the maximum normalized moments and deflections were chosen as the measure of distribution. These maximum normalized quantities were defined in Chapter 4 as moment distribution coefficients and deflection distribution coefficients. Percentage changes of these distribution coefficients from one test series to the other (i.e., as the diaphragms are removed) were chosen as the index of diaphragm effectiveness in load distribution. Figures 5.3 through 5.10 show, in the lower part of each figure, the distribution coefficient values at midspan for test Series-A (i.e., with all diaphragms in position) and also for either Series-B or Series-C (i.e., after the interior diaphragms or all the diaphragms are removed) whichever is larger, for different truck and point loads. Percentage changes in these distribution coefficient values from Series-A to Series-B or Series-C are given at the top of each figure. From these figures the following observations can be made:

5.2.1 Distribution Coefficients - Skew Bridges (Bridges 1 and 2, Figs. 5.3 through 5.6)

5.2.1.1 Point Loads

(1) The percentage increase in distribution coefficients is greater when the loads at midspan are directly above the girder than when the loads are placed in between the girders.

(2) For loads at midspan and directly above the girders, the percentage increase is greater for interior than for exterior girders.

(3) For loads at 3/4 span (i.e., H1, H3, etc.), although the changes in deflection distribution coefficients do not show any definite trend, the moment distribution coefficients (Fig. 5.4) show the largest increase with the load on the interior girder (i.e., load H3).

(4) With few exceptions (as in a few cases in Figs. 5.3 and 5.5), removal of the diaphragms always increases the distribution coefficient value.

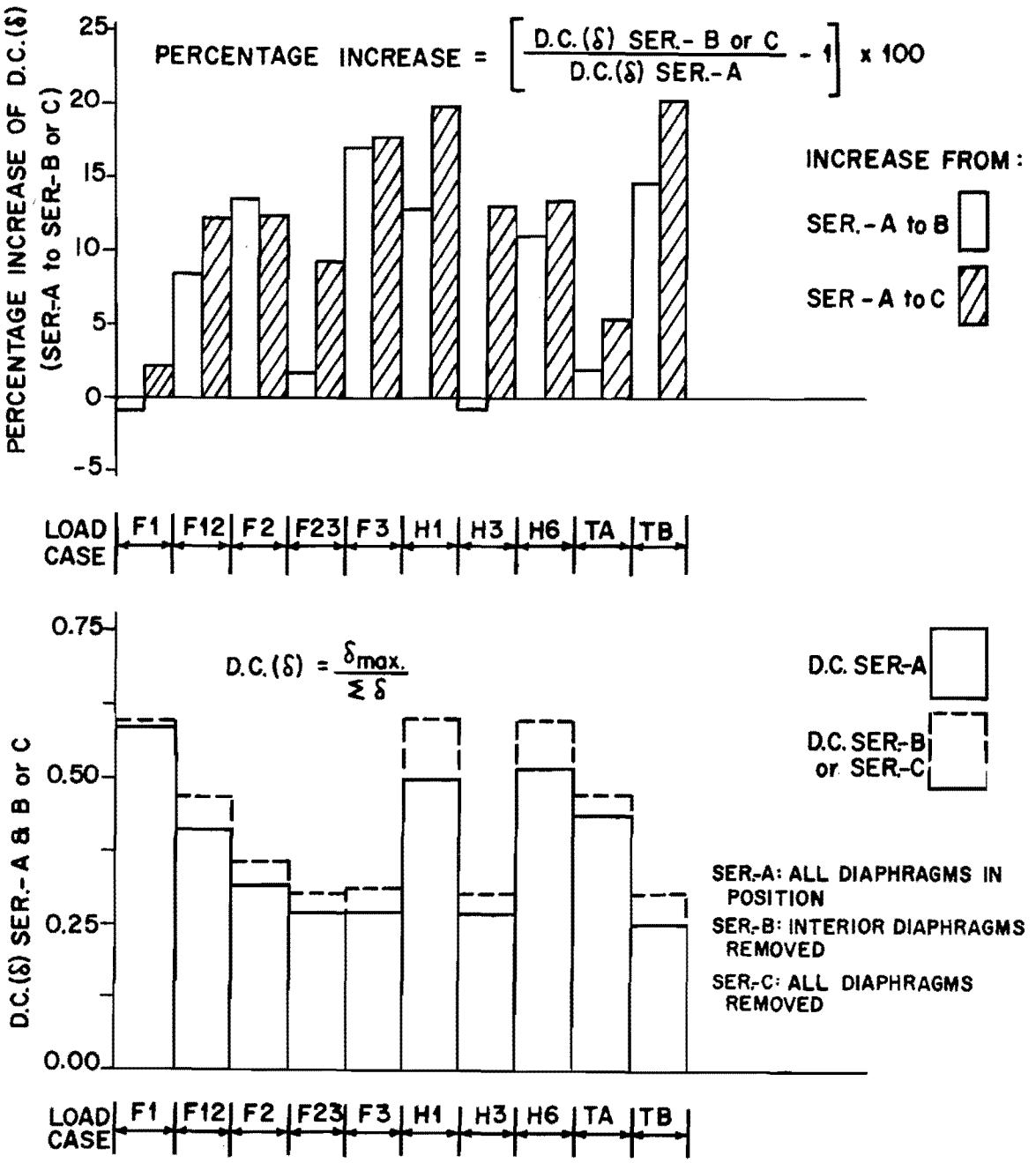

Fig. 5.3 Bridge 1 (45° skew, 172 in. span, Type D1 diaphragms at 1/3 points of span); deflection distribution coefficients and their percentage increases due to diaphragm removal.

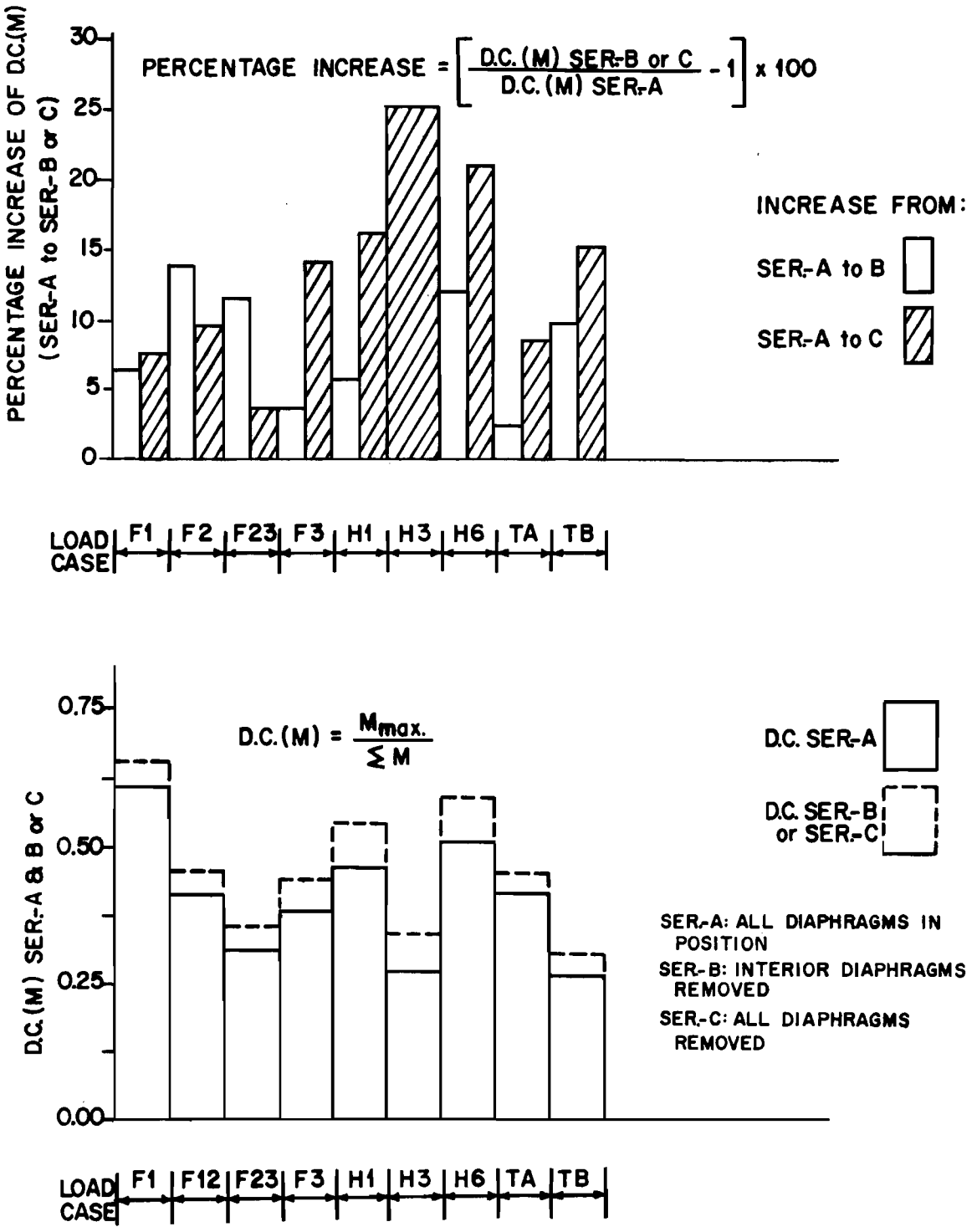

Fig. 5.4 Bridge 1 (45° skew, 172 in. span, Type D1 diaphragms at 1/3 points of span); moment distribution coefficients and their percentage increases due to diaphragm removal.

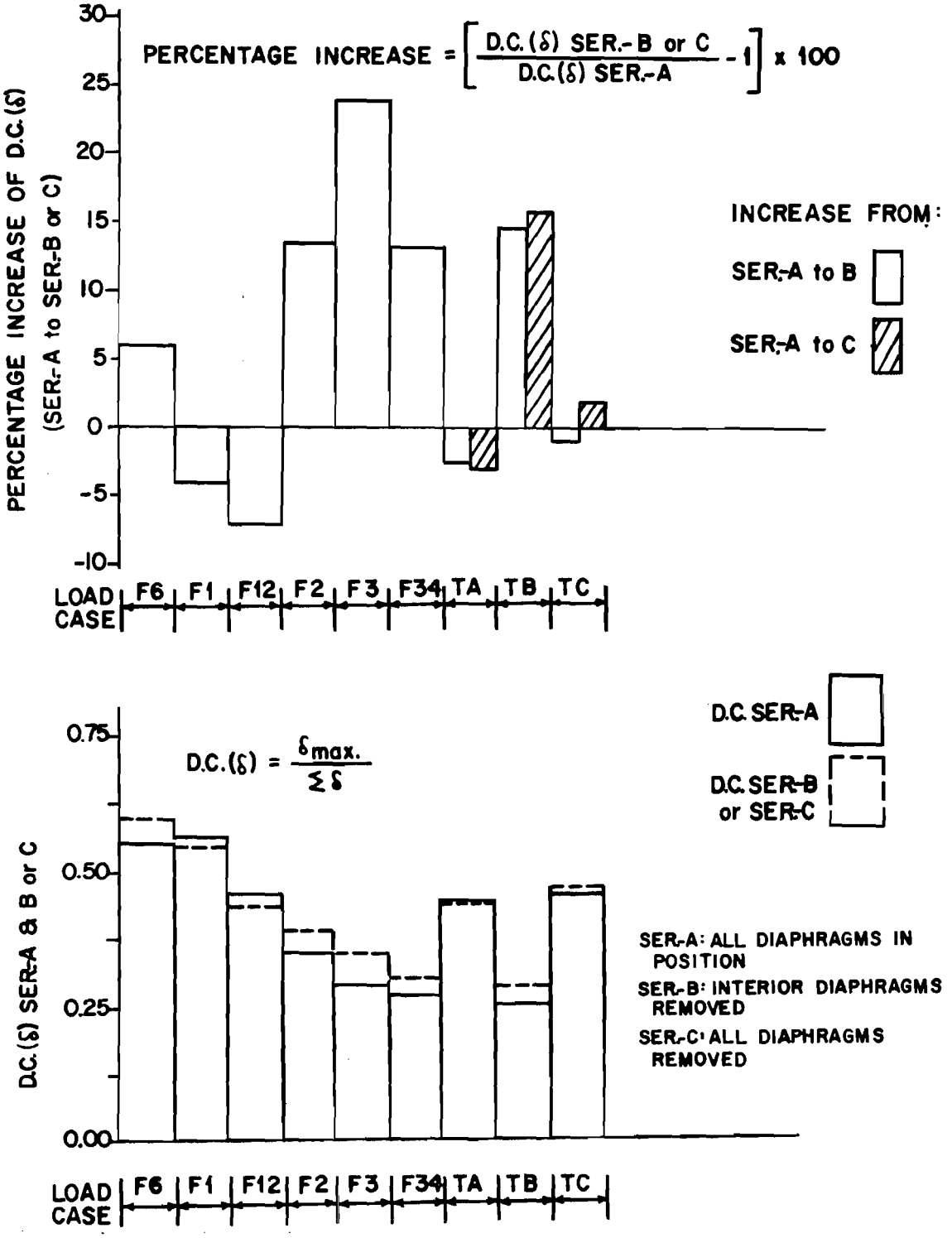

Fig. 5.5 Bridge 2 (45° skew, 172 in. span, Type D2 and Type D3 diaphragms at 1/3 points of span); deflection distribution coefficients and their percentage increases due to diaphragm removal.

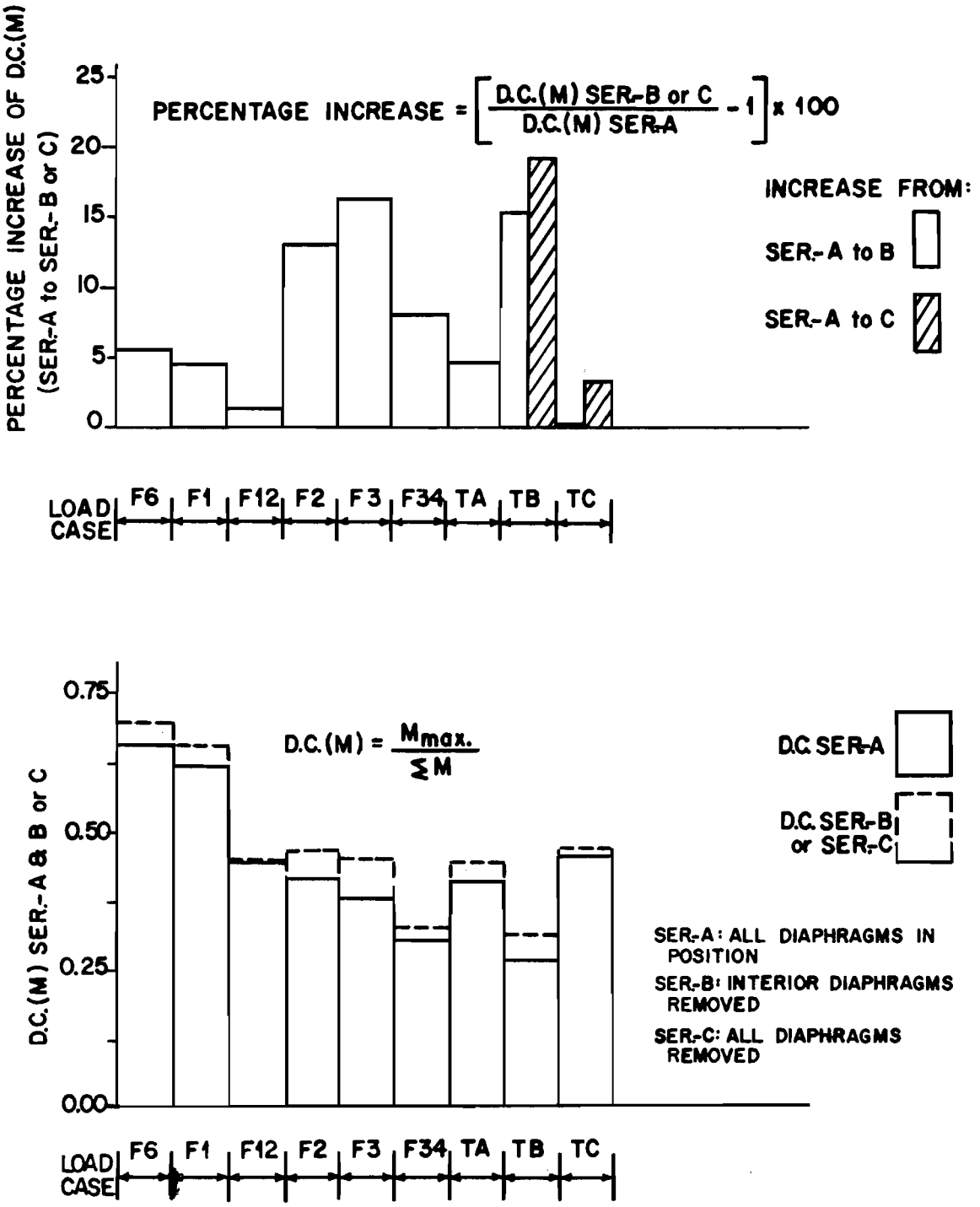

Fig. 5.6 Bridge 2 (45° skew, 172 in. span, Type D2 and Type D3 diaphragms at 1/3 points of span); moment distribution coefficients and their percentage increases due to diaphragm removal.

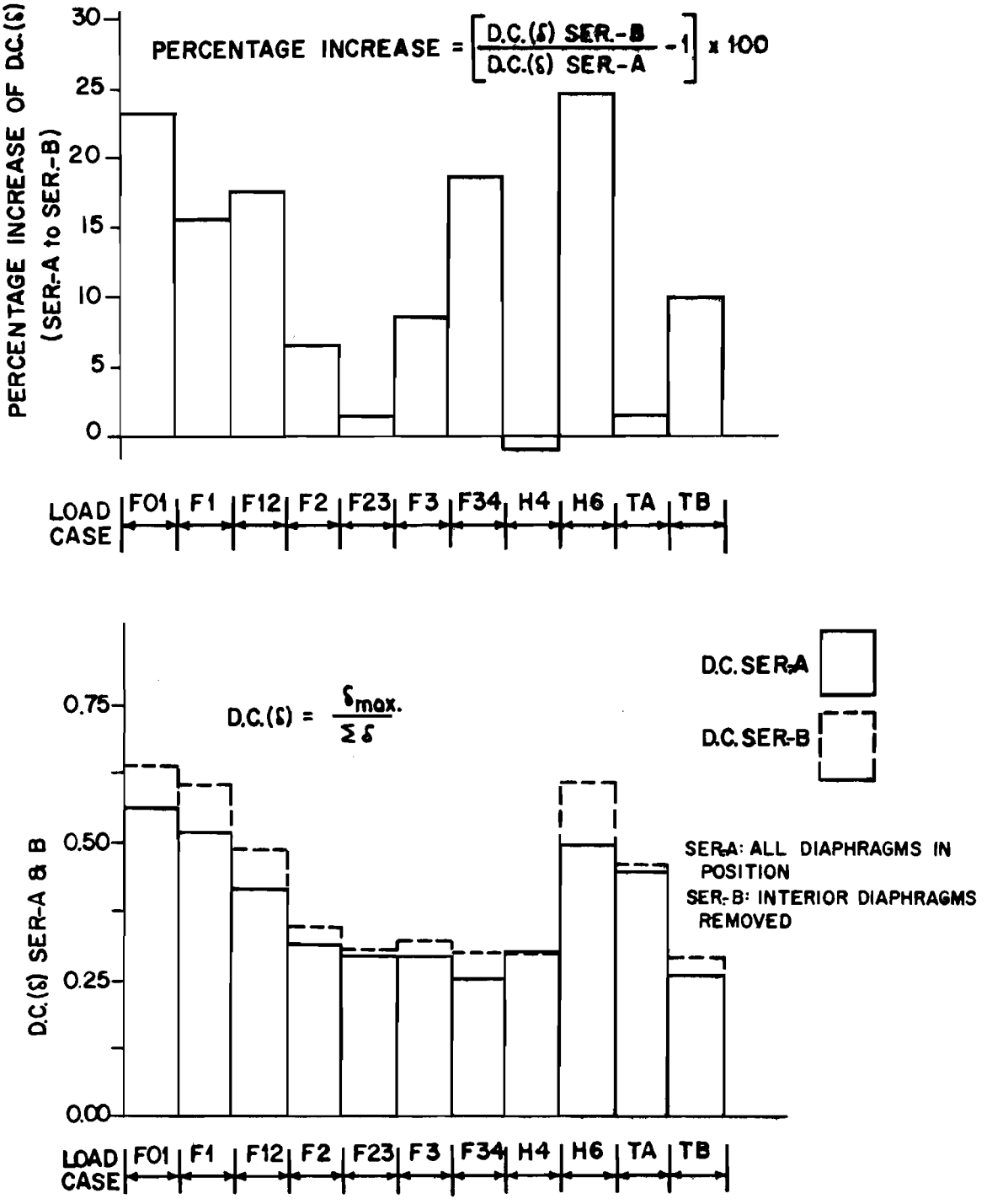

Fig. 5.7 Bridge 3 (straight, 172 in. span, Type D2 diaphragms at midspan); deflection distribution coefficients and their percentage increases due to diaphragm removal.

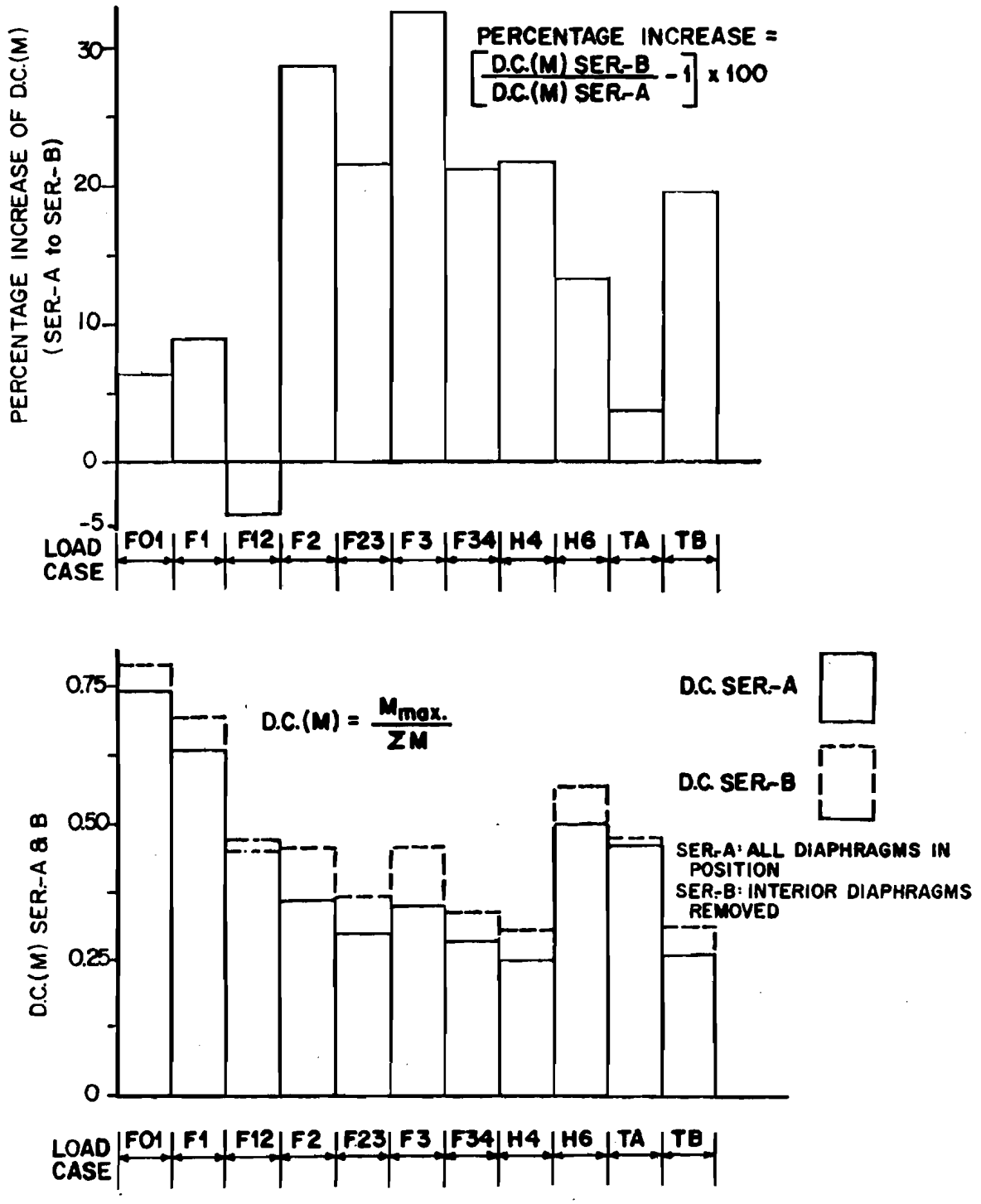

Fig. 5.8 Bridge 3 (straight, 172 in. span, Type D2 diaphragms at midspan); moment distribution coefficients and their percentage increases due to diaphragm removal.

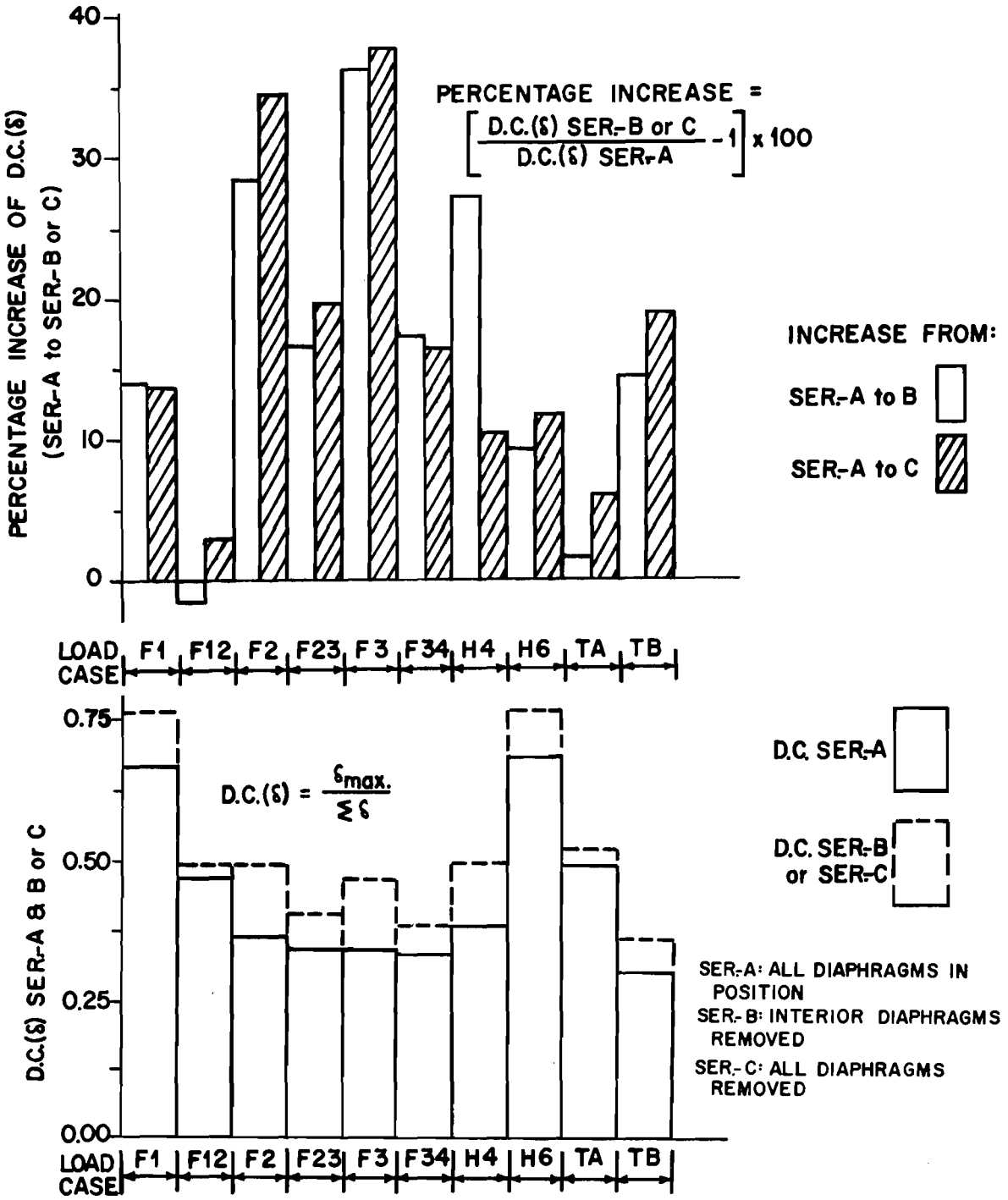

Fig. 5.9 Bridge 4 (straight, 107 in. span, Type D2 diaphragms at midspan); deflection distribution coefficients and their percentage increases due to diaphragm removal.

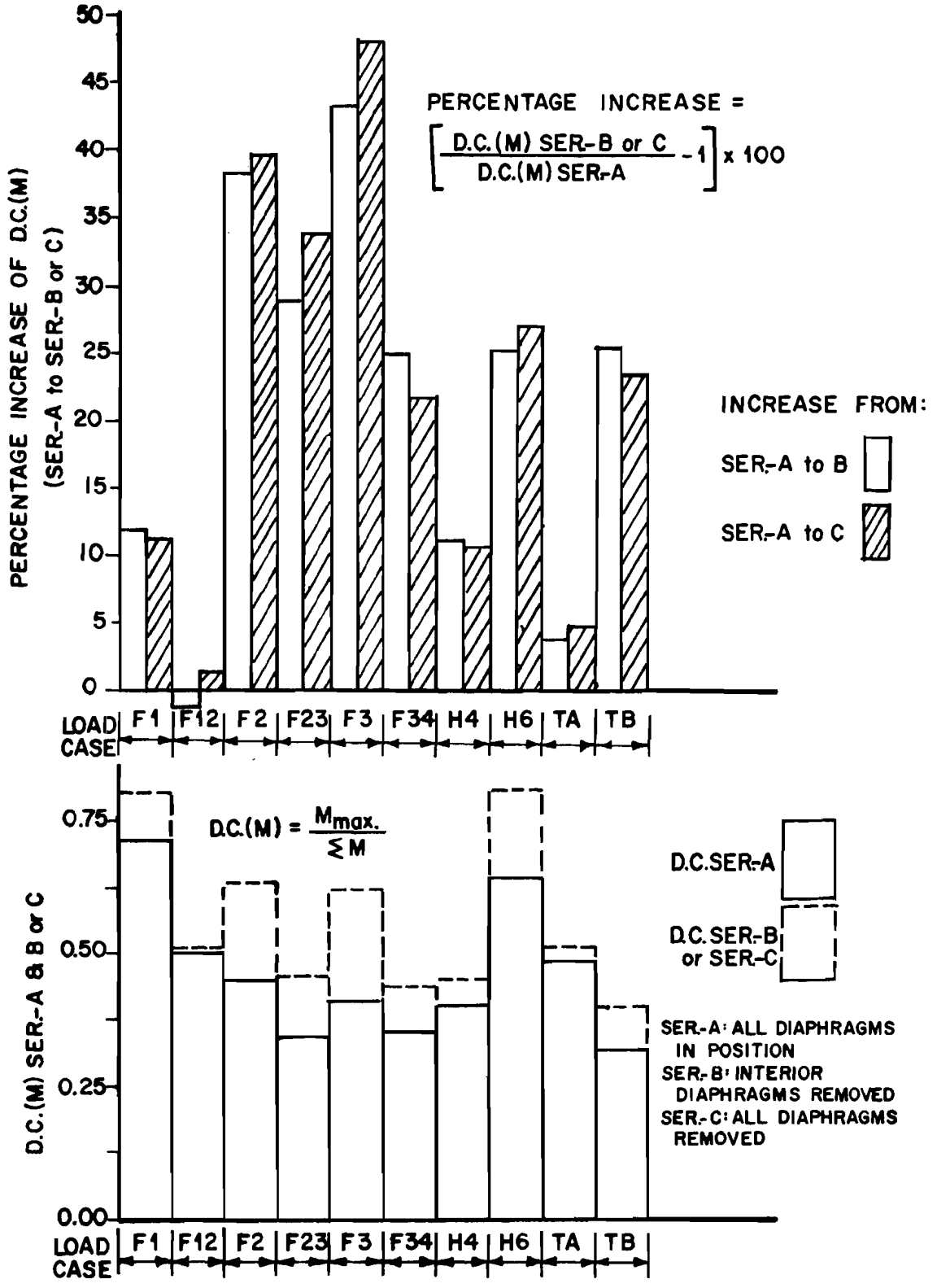

Fig. 5.10 Bridge 4 (straight, 107 in. span, Type D2 diaphragms at midspan); moment distribution coefficients and their percentage increases due to diaphragm removal.

(5) For point loads at midspan, larger percentage increases in the distribution coefficients are associated with smaller distribution coefficient values. Therefore, these changes are relatively less important. This is true for moment distribution coefficients with loads at the 3/4 span, also. Deflection distribution coefficients for loads at the 3/4 span show no definite trend.

5.2.1.2 Truck Loads

(1) Larger percentage increases in distribution coefficients are associated with the smaller distribution coefficients (i.e., with relatively less important load cases).

(2) Percentage increases in distribution coefficients for side truck loads (TA, TC) are small (all less than 9 percent). Sometimes the distribution coefficients decrease, as in Fig. 5.5.

(3) Because truck loads are the most realistic design cases among the various load cases studied, and, because only the central truck load (TB) produces any important change in distribution coefficient values due to removal of diaphragms, this case was chosen as the criterion to compare the performance of end and interior diaphragms. Figures 5.4 and 5.6 show that removal of end diaphragms increased the moment distribution coefficient by about 5.5 percent for Bridge 1, and about 4 percent for Bridge 2 (obtained from the difference of Series-A to B and Series-A to C percentage changes). Removal of only the interior diaphragms caused an increase of about 10 percent for Bridge 1 and 15 percent for Bridge 2. The ratio of interior diaphragm stiffness to end diaphragm stiffness is 0.32 for Bridge 1 and 1.8 for Bridge 2. Thus, the diaphragm effects do not vary linearly with their stiffness, and typical end diaphragms appear about 1/2 to 1/4 as effective as interior diaphragms. Similar consideration of the deflection distribution coefficients (Figs. 5.3 and 5.5) shows that end diaphragms are about 1/3 to 1/12 as effective as interior diaphragms.

(4) Bridge 1 and Bridge 2 are geometrically identical and have essentially the same member stiffnesses except for the stiffnesses of the interior diaphragms (see Table 2.4). The stiffness of the Type D2 and

Type D3 interior diaphragms in Bridge 2 was 5.7 times that of the Type D1 interior diaphragms in Bridge 1. For the most sensitive truck load case TB, removal of interior diaphragms caused about 15 percent increase in the deflection distribution coefficient in both Bridge 1 and Bridge 2. Corresponding increases in moment distribution coefficients are 10 percent and 15 percent, respectively, for Bridge 1 and Bridge 2. This indicates that very minimal changes in distribution coefficients accompanied very substantial increases in interior diaphragm stiffness. The data were insufficient to make any direct comparison between Type D2 and Type D3 (See Figs. 2.7 and 2.8) interior diaphragms. However, as their stiffnesses are the same except near the haunched ends, no significant difference between these two types of diaphragms would be expected as far as load distribution is concerned.

5.2.2 Distribution Coefficient - Straight Bridges (Figs. 5.7 through 5.10)

5.2.2.1 Point Loads

For point loads at midspan in Bridge 3, the percentage increases in deflection distribution coefficients do not show any general trend. For all other point load cases, larger increases in coefficients are associated with small distribution coefficients. The changes in distribution coefficients in Bridge 3 are generally greater than those in skew Bridges 1 and 2, while those in Bridge 4, which has a shorter span, are even greater than those of Bridge 3. This indicates that for point loads, the diaphragms in straight bridges were more effective than those in larger span bridges.

In Bridge 4 (Figs. 5.9 and 5.10) where the percentage changes are largest, the end diaphragms have almost no effect on load distribution.

5.2.2.2 Truck Loads

Larger percentage increases in distribution coefficients are again associated with smaller values of distribution coefficients. Percentage increases in coefficients for side truck loads are very small (all values less than 6.5 percent). If load case TB is again taken as a criterion:

(1) Percentage increases for moment distribution coefficients are higher than for deflection distribution coefficients.

(2) Removal of interior diaphragms caused 19.6 percent and 25.5 percent increase in moment distribution coefficients for Bridge 3 and Bridge 4, respectively.

(3) Removal of the end diaphragms caused a 2 percent decrease in the moment distribution coefficient (Fig. 5.10).

5.2.3 Distribution Factors

Because the larger changes in distribution coefficients were shown in Section 5.2.2 to accompany the smaller values of distribution coefficients, the load distribution role of diaphragms can be better understood when the effect of diaphragms on a design procedure such as distribution factors is studied. The distribution factor for any individual girder is defined as the fraction of a single wheel load carried by that girder, when a wheel load, an axle load or multiple axle loads are applied on the bridge so as to cause maximum moment on the girder concerned. The distribution factor for truck loads is defined in the same manner, except the function is that of a row of wheel loads (of rear, center and front axle). To calculate the distribution factor values, the experimental influence lines for midspan girder moments and deflections were plotted for all test series as shown in Figs. 5.11 through 5.18. Moments and deflections due to wheel loads and axle loads, positioned to produce maximum effects (see Fig. 5.19) were then obtained from these influence lines. These moments and deflections were then compared to values for a single girder loaded with a single wheel or single row of wheel loads. These ratios are termed the distribution factors.

The lower portions of Figs. 5.20 through 5.23 show the deflection and moment distribution factors DF(δ) and DF(M) for Series-A and also for the larger value of either Series-B or C. The current AASHO distribution factor for bridges of these dimensions is also shown for comparison. In the upper portions of these figures, percentage increases of these distribution factors due to diaphragm removal (i.e., from Series-A to Series-B or C are given.

Although these bar charts indicate that large percentage increases in distribution factor values may be found for single wheel loads, they are

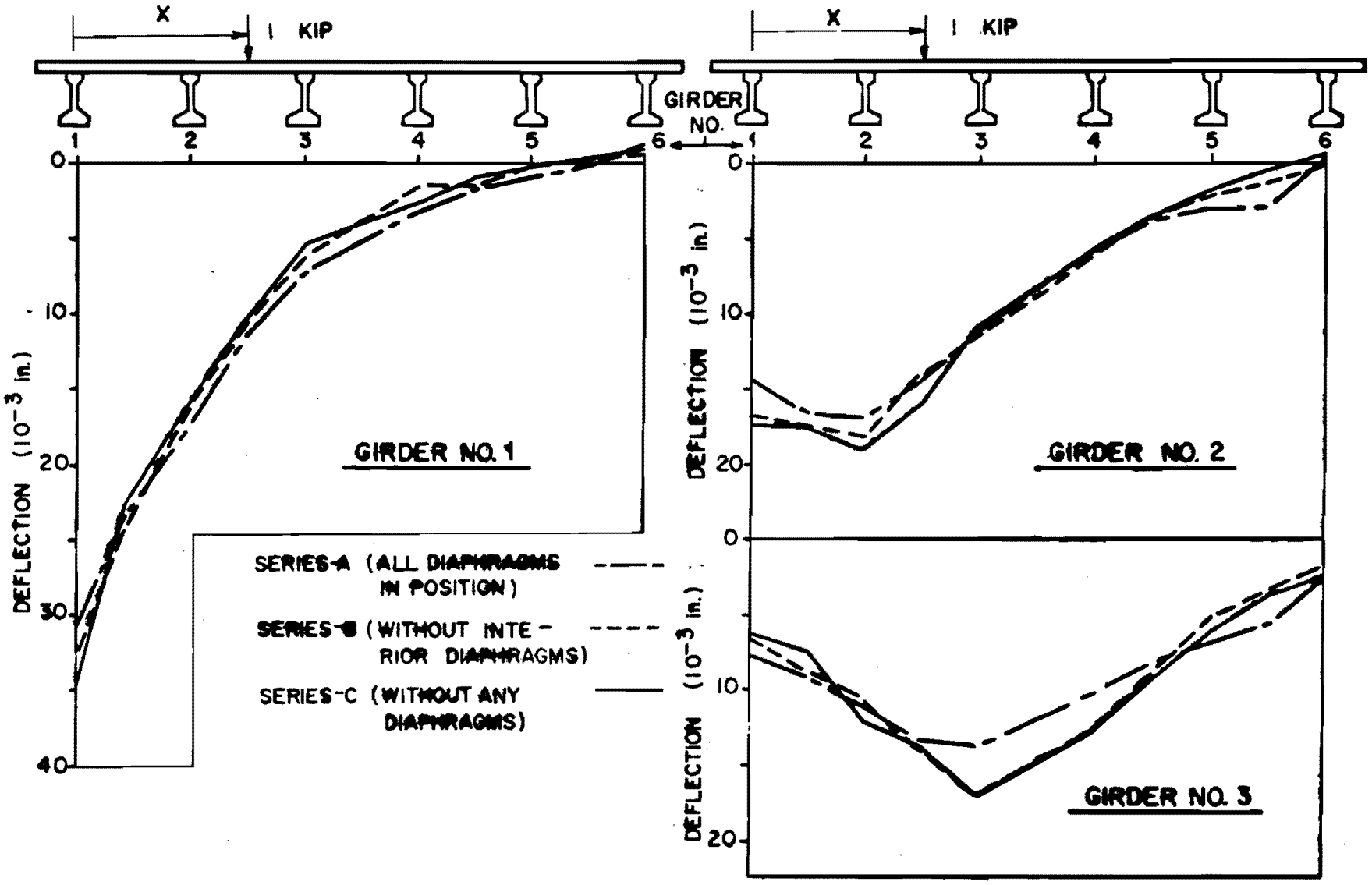

Fig. 5.11 Bridge 1, experimentally determined influence lines for midspan girder deflection due to 1 kip point load at midspan moving across the bridge.

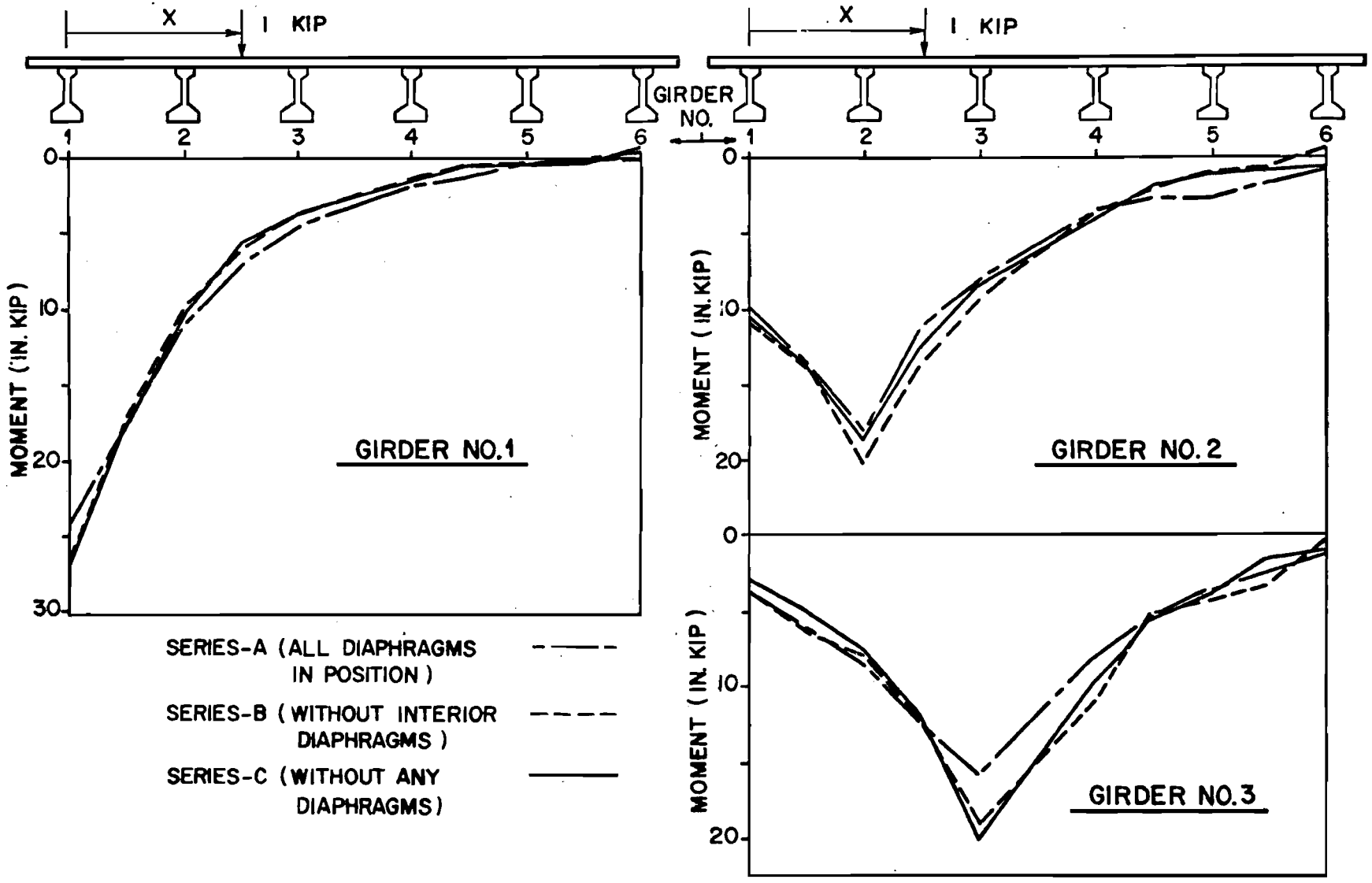

Fig. 5.12 Bridge 1, experimentally determined influence lines for midspan girder moment due to 1 kip point load at midspan moving across the bridge.

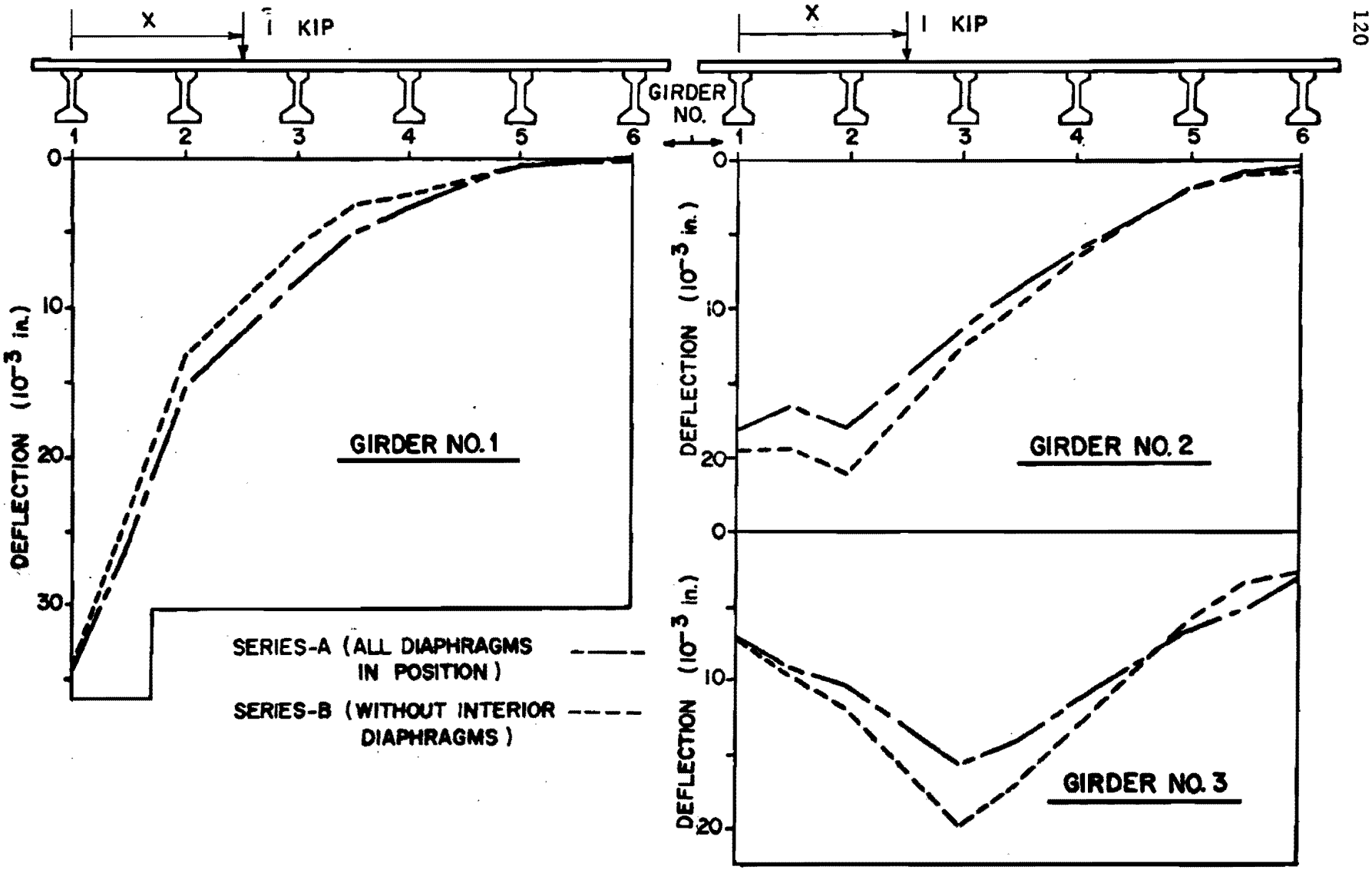

Fig. 5.13 Bridge 2, experimentally determined influence lines for midspan girder deflection due to 1 kip point load at midspan moving across the bridge.

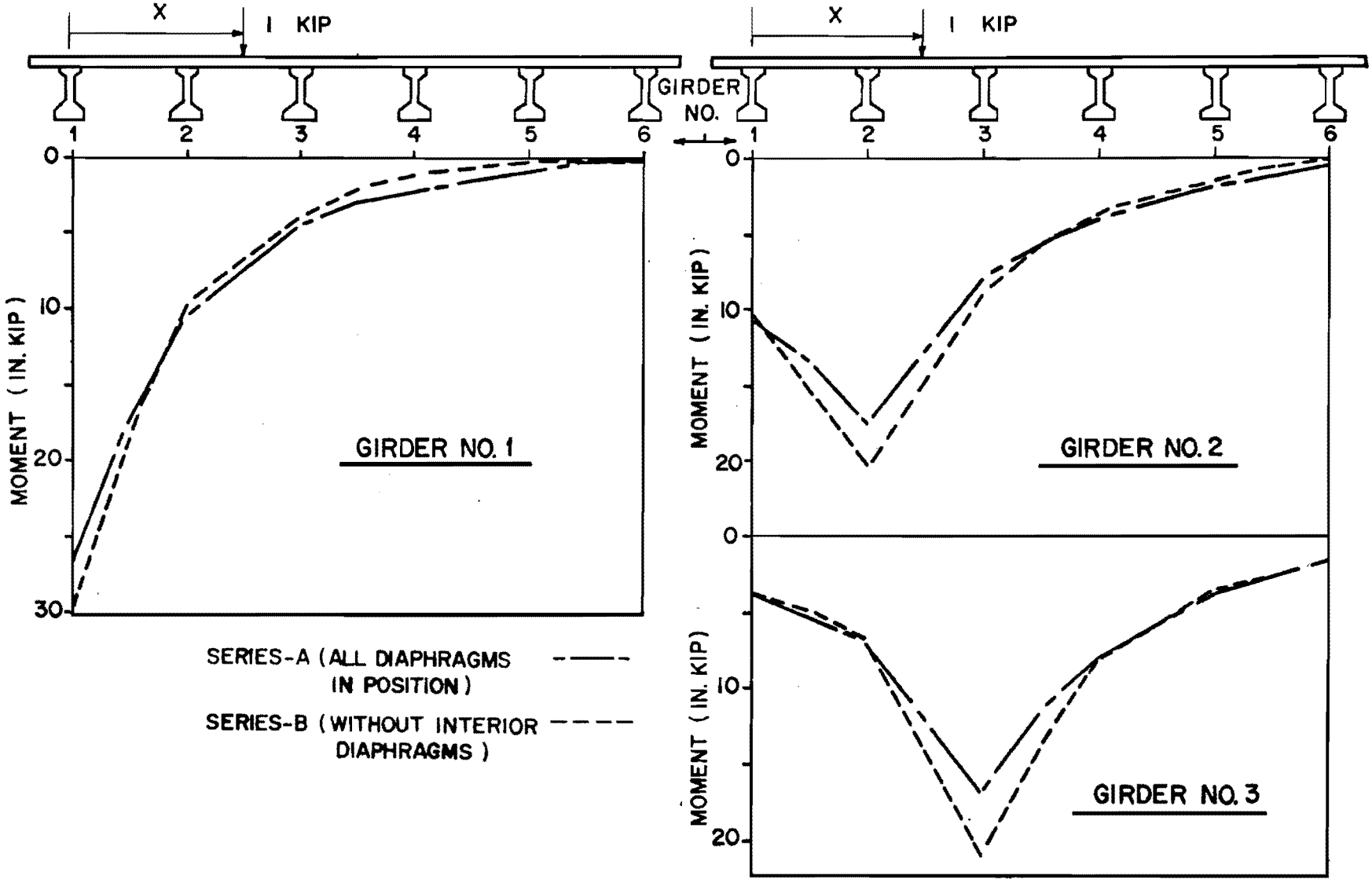

Fig. 5.14 Bridge 2, experimentally determined influence lines for midspan girder moment due to 1 kip point load at midspan moving across the bridge.

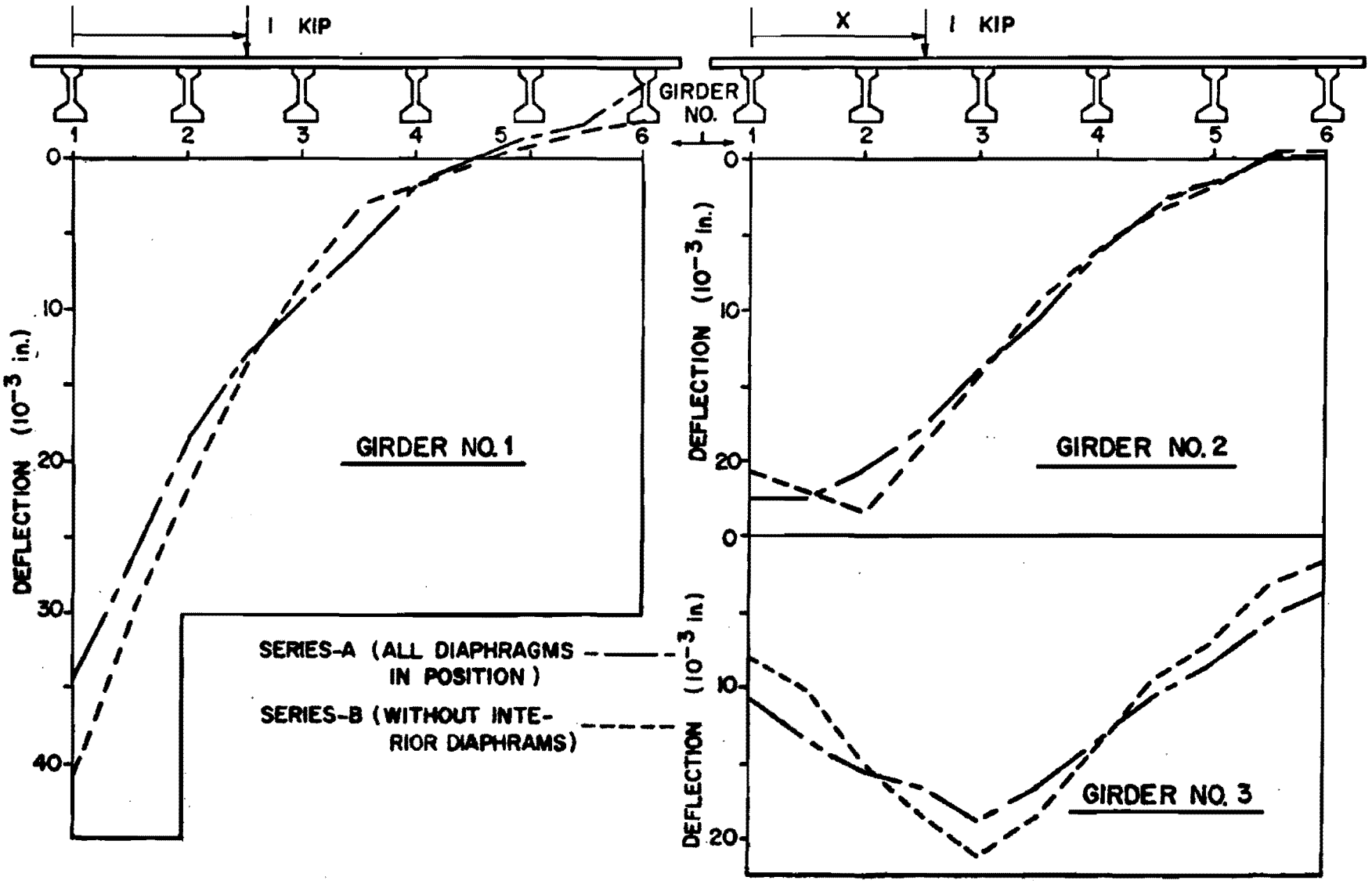

Fig. 5.15 Bridge 3, experimentally determined influence lines for midspan girder deflection due to 1 kip point load at midspan moving across the bridge.

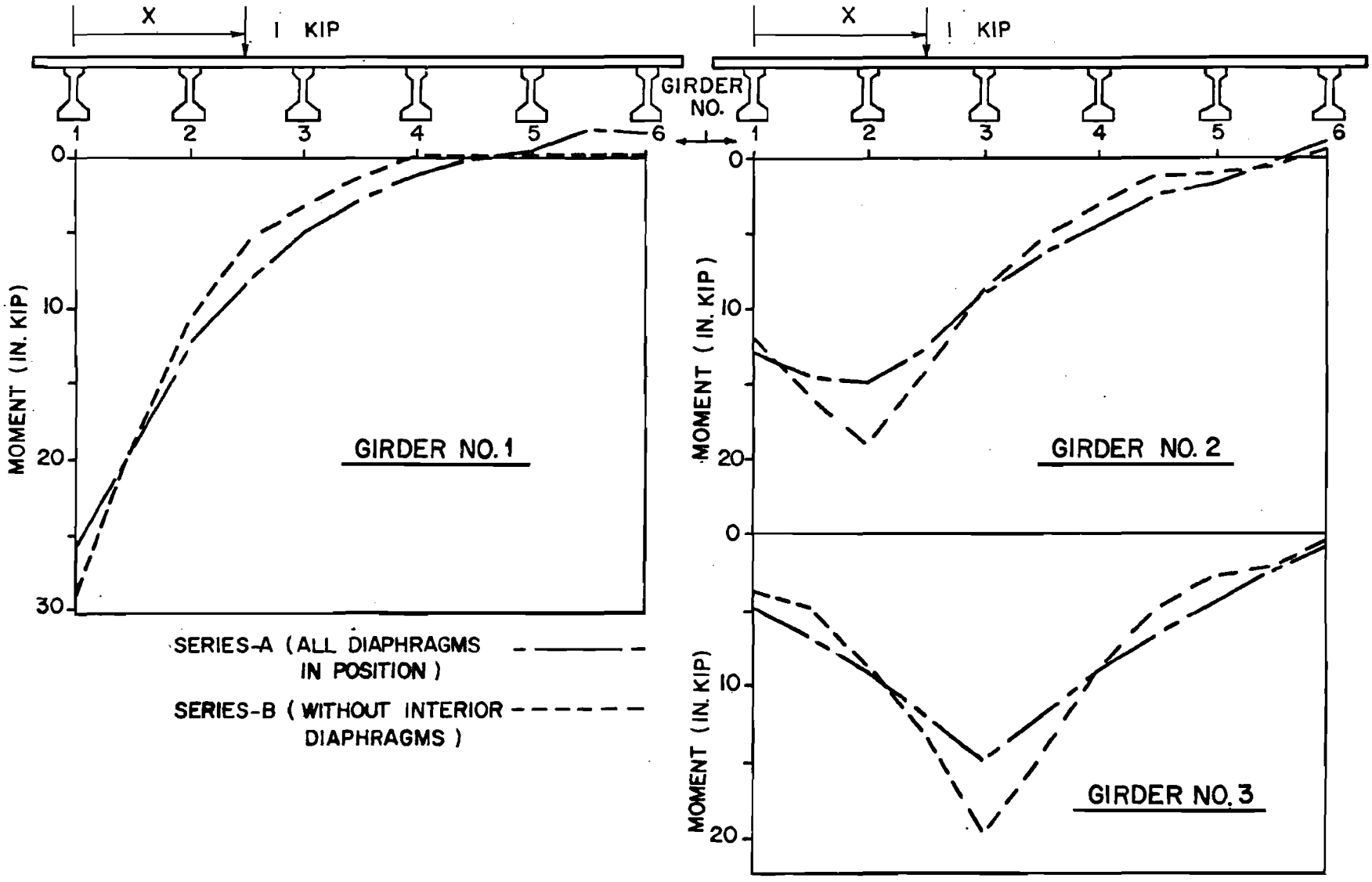

Fig. 5.16 Bridge 3, experimentally determined influence lines for midspan girder moment due to 1 kip point load at midspan moving across the bridge.

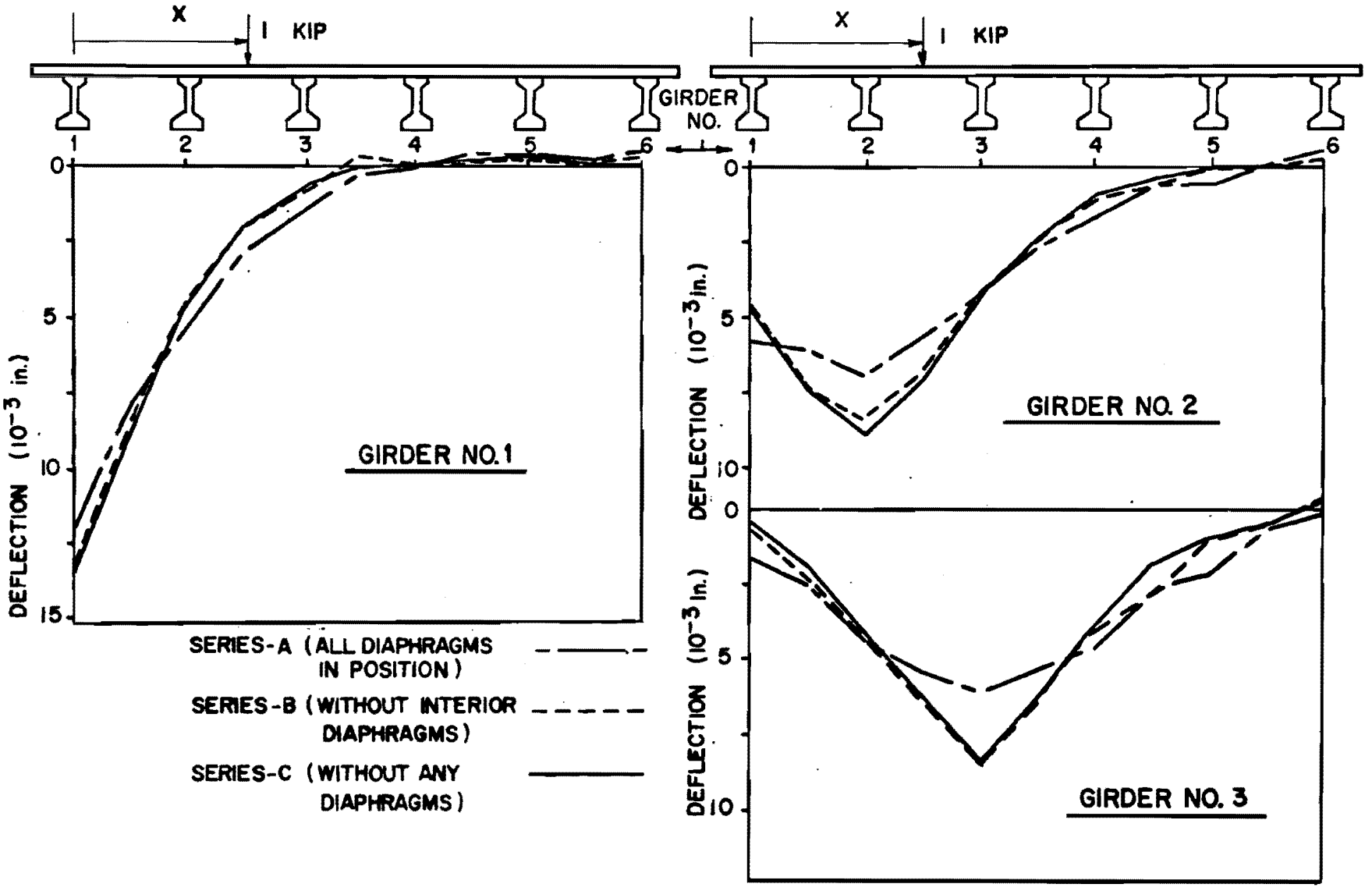

Fig. 5.17 Bridge 4, experimentally determined influence lines for midspan girder deflection due to 1 kip point load at midspan moving across the bridge.

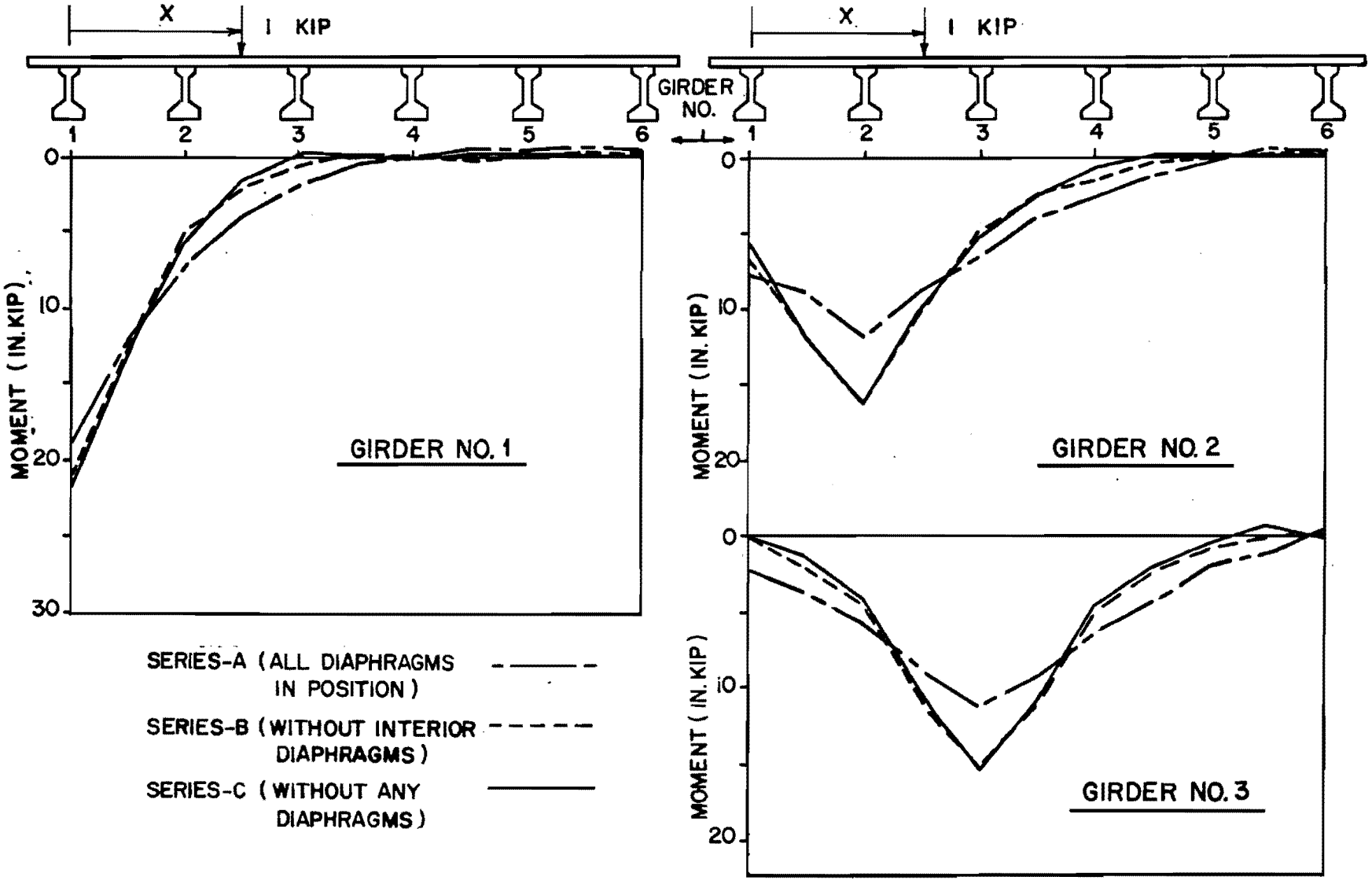

Fig. 5.18 Bridge 4, experimentally determined influence lines for midspan girder moment due to 1 kip point load at midspan moving across the bridge.

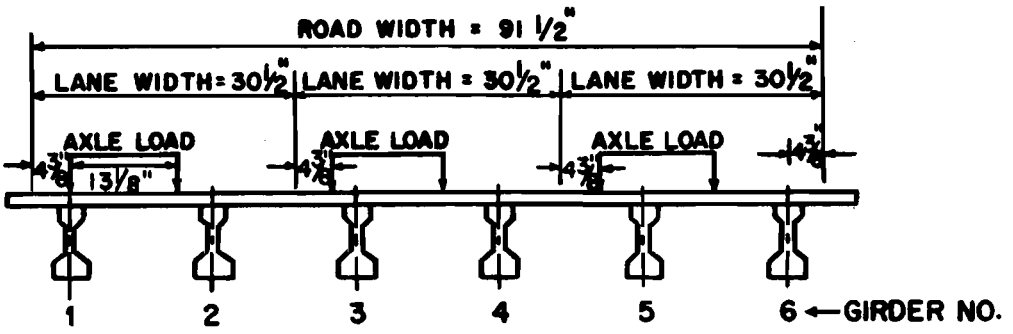

(a) For maximum effect on Girder 1

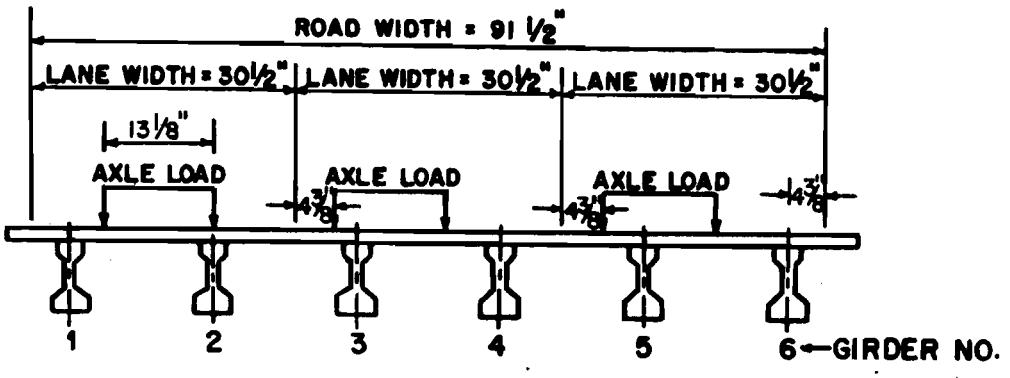

(b) For maximum effect on Girder 2

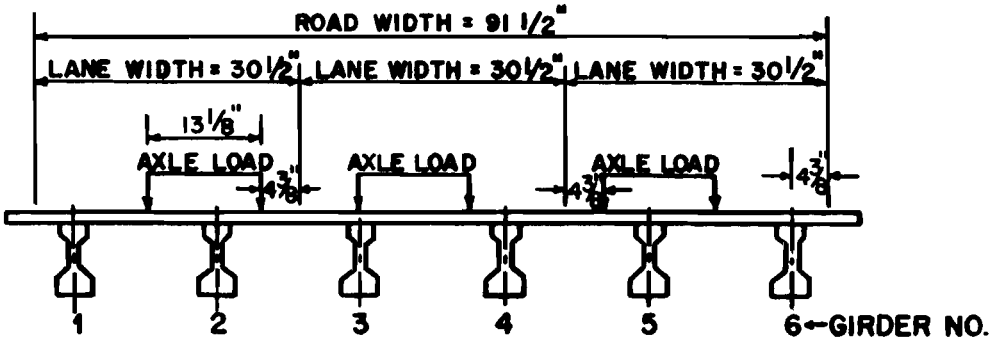

(c) For maximum effect on Girder 3

Fig. 5.19 Midspan wheel and axle load transverse locations for maximum effect on girders.

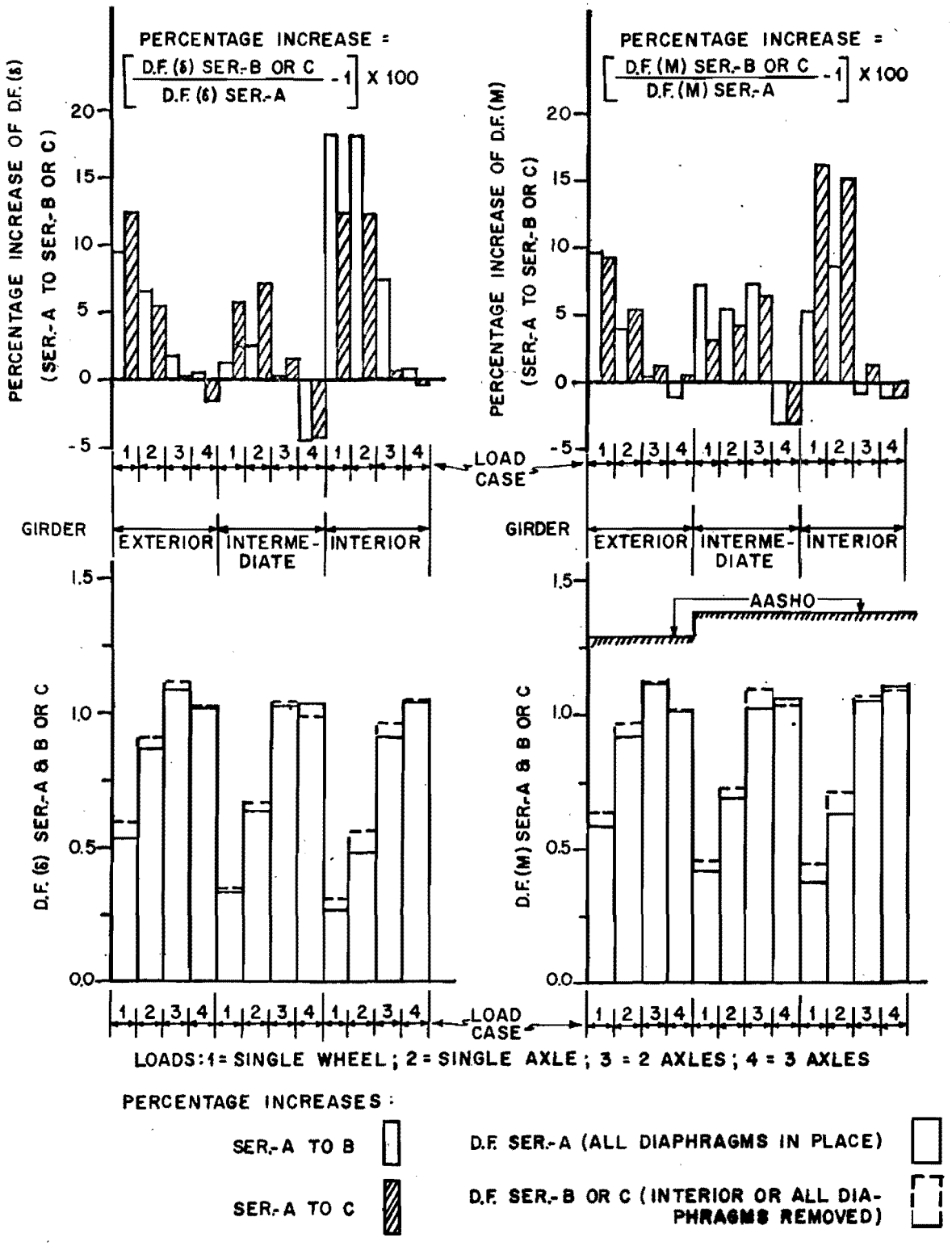

Fig. 5.20 Bridge 1 (45° skew, 172 in. span, Type D1 diaphragms at 1/3 points of span): moment and deflection distribution factors and their percentage increases due to diaphragm removal.

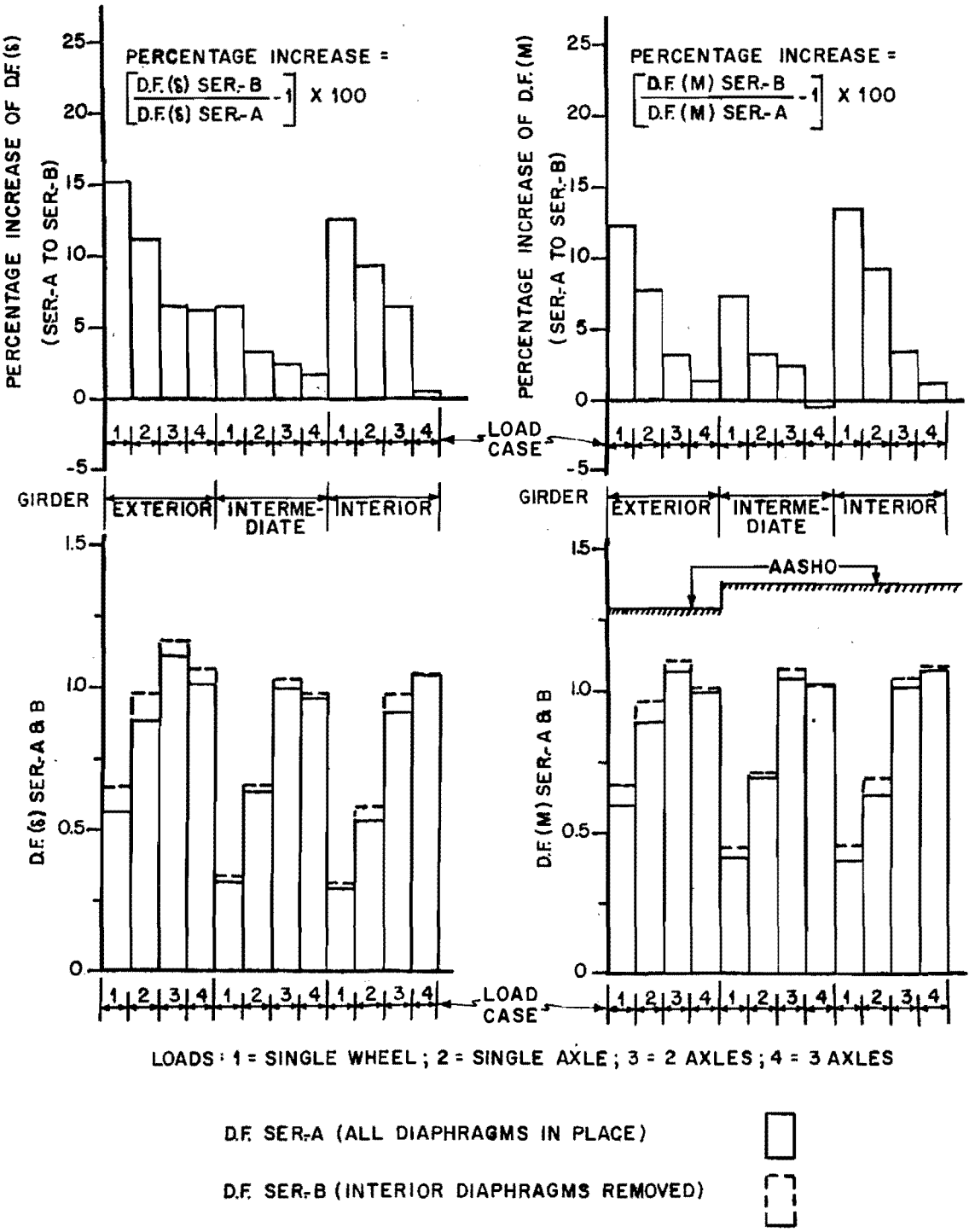

Fig. 5.21 Bridge 2 (45° skew, 172 in. span, Type D2 and Type D3 diaphragms at 1/3 points of span); deflection and moment distribution factors and their percentage increases due to diaphragm removal.

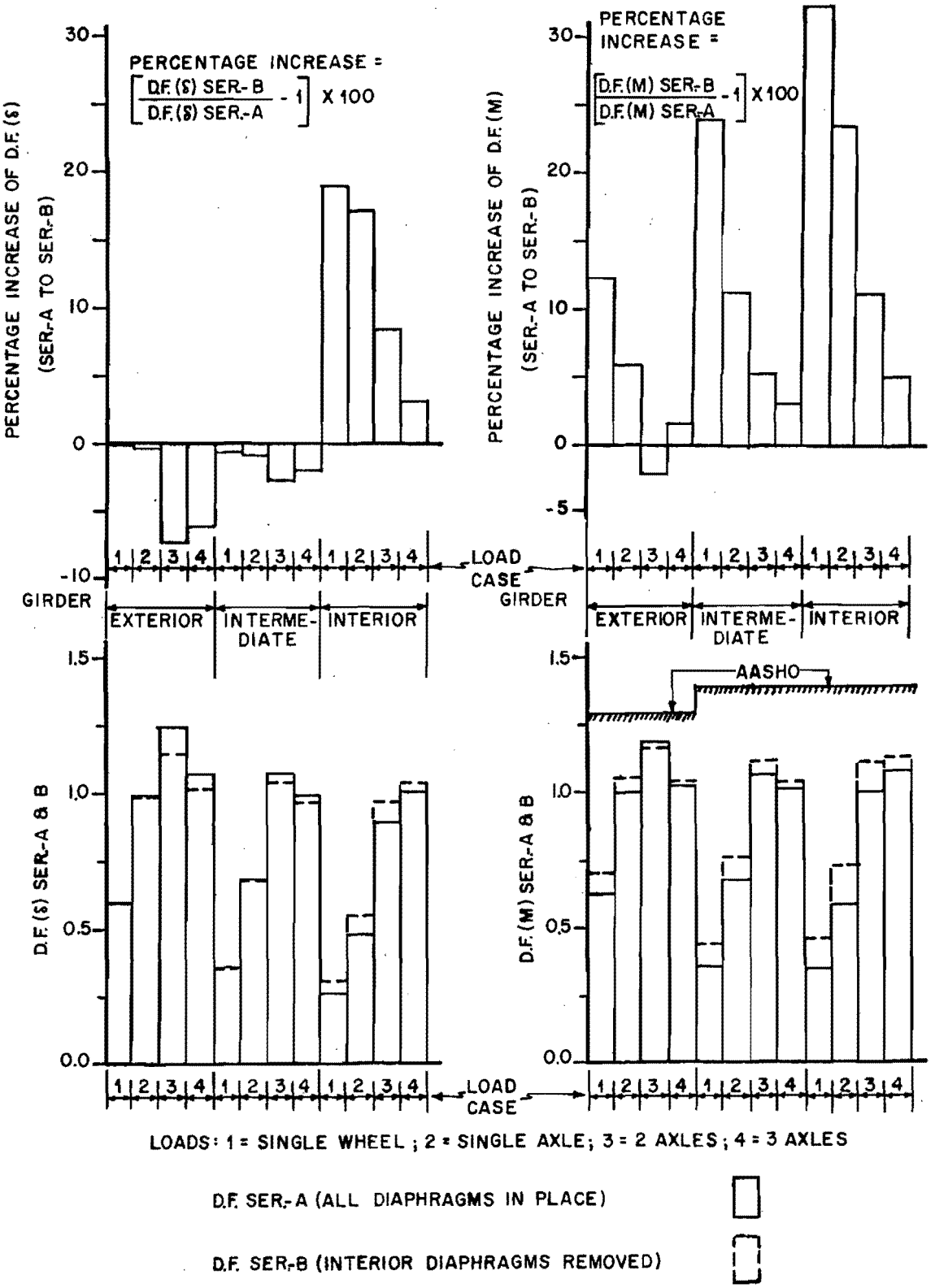

Fig. 5.22 Bridge 3 (straight, 172 in. span, Type D2 diaphragms at midspan); deflection and moment distribution factors and their percentage increases due to diaphragm removal.

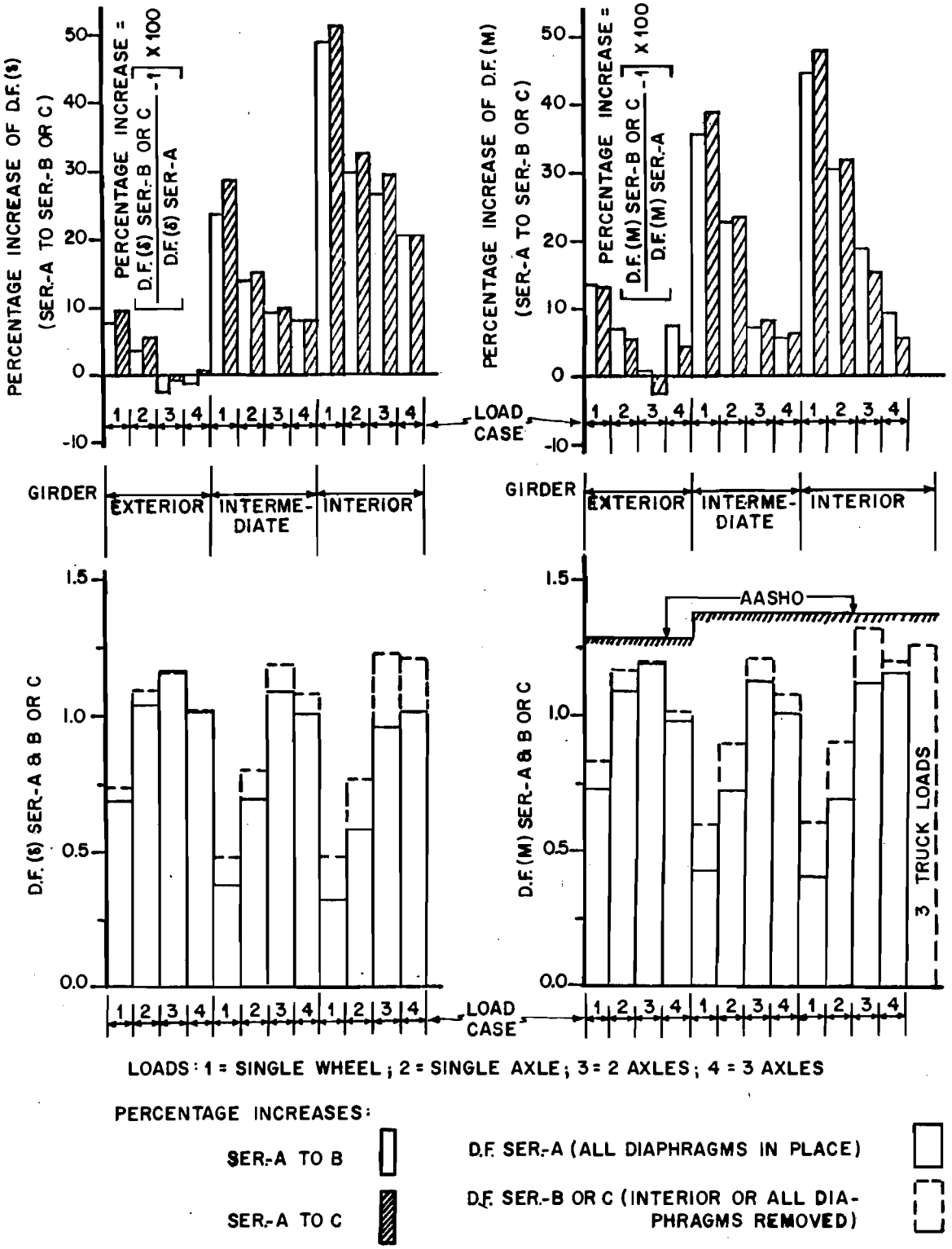

Fig. 5.23 Bridge 4 (straight, 107 in. span, Type D2 diaphragms at midspan); deflection and moment distribution factors and their percentage increases due to diaphragm removal.

always associated with small, noncritical values of distribution factors and, therefore, are not important. For axle loads, distribution factor values for exterior girders are generally comparable with the design distribution factor and their percentage increases in values are usually small. The highest bar in the lower set of charts represents the most critical fraction of a wheel load which the girder would have to be designed for. Percentage increases in these critical design distribution factors for Bridges 1, 2 and 3 are essentially negligible (all less than 6 percent). Only the Bridge 4 interior girder shows any considerable increase in the governing design distribution factor. For Series-A of this case, the maximum interior girder distribution factor is equal to 1.163 (corresponding to a 3-axle load) and for Series-B it is equal to 1.337 (due to a 2-axle load). This gives a 15 percent increase in the critical distribution factor for an interior girder, when the interior diaphragms are removed. However, both values are less than the present AASHO requirements.

In Bridge 4 (Fig. 5.23), for the cases where the diaphragms show the greatest effect, the percentage increase in distribution factor from Series-A to Series-B and that from Series-A to Series-C is almost the same for different loadings. This indicates that exterior diaphragms are not necessary from midspan load distribution considerations.

Ordinarily no distinction is made in design between exterior, intermediate and interior girders and all the girders are designed for the same maximum moment in this type of bridge. The highest Series-A (with diaphragms) measured distribution factors for Bridge 1 to Bridge 4 are 1.11, 1.08, 1.19 and 1.19, respectively. The largest values measured with diaphragms removed in Series-B or C are 1.12, 1.11, 1.17 and 1.34, giving increases in critical distribution factors as 1, 3, -2 and 12 percent for Bridges 1, 2, 3 and 4, respectively. The maximum distribution factors for Series-B or Series-C for Bridge 1 and Bridge 2 are less than the maximum Bridge 3 distribution factor, which is in turn less than that of Bridge 4. This indicates that the load distribution in skew bridges (Bridge 1 and 2) is slightly more favorable than that in a straight bridge of the same span (Bridge 3) while for a shorter span (Bridge 4) the distribution gets worse.

Figure 5.23 (lower right) shows that the measured distribution factor obtained from a 3-axle load is close to that obtained from 3 truck loads (see Fig. 2.27 for location of the truck loads T1, T2 and T3). For the bridges tested diaphragms had very little beneficial effect on critical load distribution for Bridges 1, 2 and 3. Indeed, Bridge 3 has an increased critical distribution factor when diaphragms are provided. The maximum reduction (about 11 percent) in critical distribution factor due to the provision of diaphragms was observed in the shorter span straight bridge (Bridge 4). In any case, whether the diaphragms were provided or not, the AASHO distribution factors (shown in hatched lines in Figs. 5.20 through 5.23) were always conservative, and even more so for longer spans (in Bridges 1, 2 and 3).

5.2.4 Scatter in Experimental Results

In spite of taking all possible precautions, some errors in experimental tests are unavoidable. It was impossible to find any definite quantitative measure for all the variables reported. However, an approximate indication of the possible scatter in the experimental results can be determined. Since for any given load, the sum of the moments or deflections of all the girders across any transverse section may be considered almost independent of the presence or absence of diaphragms, the ratio of these sums for Series-A to those for Series-B or Series-C should be very close to 1. The scatter of these ratios about their mean value may then be considered as an indication of experimental errors. The calculated mean and standard deviation (σ) of the ratio of these sums are

$$\text{Mean} = 1.015$$
$$\sigma = 0.08$$

This gives a coefficient of variation (σ/Mean) of approximately 8 percent. Since the distribution coefficients and the distribution factors are calculated for maximum quantities only, their coefficient of variation may be expected to be less than 8 percent.

5.2.5 Generalization of Results

The computer program outlined in Chapter 4, was employed to study in a general way diaphragm effects in load distribution for straight bridges

with one diaphragm at midspan. The effect of the location of diaphragms and the effect of skew angle were also studied.

5.2.5.1 Diaphragm Effect on Load Distribution in Straight Bridges

Previous studies (discussed in Chapter 1) indicate that diaphragms are more effective for shorter spans, wider beam spacings, and larger girder stiffness to slab stiffness ratios and that the most effective location of diaphragms is at midspan. Based on these previous investigations and on the experimental results, a range of bridge parameters was chosen from the current design drawings of the Texas Highway Department. Span lengths of 40 and 60 ft., maximum and minimum girder spacings as generally occur within that span range, slab thicknesses corresponding to those spacings, and the most commonly used girder types (Type 54 and Type C) were chosen. All bridges had six prestressed concrete girders. To calculate the girder and slab stiffnesses, the modulus of elasticity of the girder and slab concrete was taken as 4.5×10^6 psi and 3.5×10^6 psi, respectively. In all cases the diaphragm stiffness was chosen as 10 percent of girder stiffness. Bridges were analyzed for two standard HS20-44 AASHO[1] truck loads. One analysis was made assuming diaphragms at midspan and end spans. Another analysis was made with all the diaphragms removed. Truck loads were transversely positioned in conformity with AASHO specifications, to find the maximum moment distribution factor for the exterior girder and for the interior or intermediate girder (whichever was larger). For the case with all the diaphragms in position the load locations for maximum effect on interior or intermediate girders were not exactly known. However, with a few trials, values close to the maximum were easily obtained. The moment distribution factors were then obtained by dividing these maximum values by the maximum moment produced in a simply supported single beam of the same span due to three wheel loads (those of front, center and rear axles). The results thus calculated, are summarized in Table 5.1, where Series-A and Series-C refer to cases with all diaphragms in position and without any diaphragms, respectively. Also included in this table are the distribution factors as recommended by AASHO.[1] In Table 5.2 the ratios of the Series-A distribution factor to the Series-C distribution factor and the AASHO

TABLE 5.1 DISTRIBUTION FACTORS

Case	L (ft.)	S (ft.)	EI_S 10^8 lbs. in.^{2} per in.	EI_G 10^{12} lbs. in.^{2}	Series	Calculated DF		AASHO DF	
						Exterior Girders	Interior Girders	Exterior Girders	Interior Girders
1	40	7.6	1.260	1.203	A	1.072	1.127	1.288	1.381
					C	1.045	1.242		
2	40	7.6	1.260	1.945	A	1.076	1.163	1.288	1.381
					C	1.047	1.282		
3	60	7.6	1.260	1.203	A	1.177	1.069	1.288	1.381
					C	1.129	1.159		
4	60	7.6	1.260	1.945	A	1.192	1.128	1.288	1.381
					C	1.126	1.249		
5	60	6.67	1.114	1.128	A	1.141	1.032	1.188	1.211
					C	1.081	1.061		
6	60	6.67	1.114	1.839	A	1.161	1.054	1.188	1.211
					C	1.078	1.139		

TABLE 5.2 DISTRIBUTION FACTOR RATIOS

Case	S/L	$\frac{EI_G}{EI_S \cdot L}$	Series-A to Series-C			AASHO to Series-C	
			Exterior Girder	Interior Girder	Design Girder	Exterior Girder	Interior Girder
1	0.190	19.9	1.026	0.908	0.908	1.233	1.112
2	0.190	32.2	1.028	0.907	0.907	1.230	1.077
3	0.127	13.3	1.043	0.922	1.011	1.141	1.193
4	0.127	21.5	1.059	0.904	0.954	1.143	1.106
5	0.111	15.6	1.055	0.973	1.055	1.090	1.143
6	0.111	22.4	1.077	0.925	1.016	1.093	1.063

distribution factor to the Series-C distribution factor are given for comparison. In Table 5.2 the different bridge parameters are expressed in commonly used nondimensional ratios.

These tables indicate that diaphragms always increased the distribution factors for exterior girders and decreased them for interior (or intermediate) girders. As it is common practice to proportion prestressed girders for the largest distribution factor, these factors in Table 5.1 (calculated values) are underlined for convenience. It may be noted that in some cases (cases 3, 4 and 6 in Table 5.1) the exterior girder governs the design when the diaphragms are present, but when the diaphragms are removed an interior girder governs the design. The ratios of these governing design distribution factors are also given in Table 5.2 for comparison with and without diaphragms. The results indicate that except for cases 1 and 2 (i.e., 40 ft. span bridges) changes in the design distribution factors are small. In fact, for cases 3, 5 and 6, the provision of diaphragms increased the design distribution factor values.

Diaphragms are generally considered more effective for large S/L and $EI_G/(EI_S \cdot L)$ ratios. Values of S/L = 0.19 and $EI_G/(EI_S \cdot L) = 32.2$ are on the higher side in the normal range of slab and girder bridges. Even for this case diaphragms reduced the critical distribution factor by only 9.3 percent. For medium and small S/L ratios (less than about 0.12) diaphragms may increase the critical distribution factor. For the cases analyzed, the results also indicate that in bridges without any diaphragms the AASHO[1] design distribution factors are always conservative by 6 to 23 percent.

5.2.5.2 Effective Diaphragm Location

In shorter spans (40 to 60 ft.) only one interior diaphragm at midspan is usually used. In the longer span ranges, common practice is to use 2 or 3 interior diaphragms (located at 1/3 spans or 1/4 spans and midspan). To determine the most effective diaphragm location in the span range of 60 ft. to 130 ft., several straight bridges were analyzed for a uniformly distributed line load plus a point load (proportioned from AASHO HS20-44 lane loading) applied on an interior girder. Commonly used slab thickness and

girder spacing (7 in. and 7 ft., respectively) were used. These values were kept constant for all the cases, while the location and number of interior diaphragms were varied. Standard Texas Highway Department Type-C, Type-54 and Type-72 prestressed concrete girders were considered. Stiffness of each diaphragm (EI_D) in all the cases was chosen as 15 percent of the corresponding girder stiffness (EI_G). The point load was moved along the span to produce maximum moment in each case. Percentage reductions of maximum moments from Series-C to Series-A (i.e., from the "no" diaphragm case to the "with" diaphragms case) were calculated. The results are summarized in Table 5.3, where the bridge parameters are expressed in non-dimensional ratios.

The results (Table 5.3) from this simple load case illustrate that generally one diaphragm at midspan is as effective as two such diaphragms at 1/3 spans, and is two-thirds as effective as three such diaphragms at mid and 1/4 spans. Considering the number of diaphragms, it may therefore be said that the most effective diaphragm location is at midspan. This is in agreement with previous findings reported in Chapter 1 and, therefore, no further analysis is considered necessary.

5.2.5.3 Effect of Angle of Skew

An 80 ft. span bridge with 6 standard Type-C girders was analyzed for a uniformly distributed line load plus a concentrated load at midspan (proportioned as before), acting on an interior girder (girder 3). Girder spacing of 7 ft. and slab thickness of 7 in. was used. Keeping the girder spacing (measured normal to the girder center line) constant, the skew angle was varied from 0^{o} to 60^{o}. Only end diaphragms parallel to the line of support with stiffness 15 percent of the girder were used. Calculated maximum moments and deflections and the sums of these quantities for all the girders across the midspan were expressed as a ratio to the same quantities for the zero degree skew bridge (i.e., right bridge). These values are shown in Figs. 5.24a and 5.24b. It may be seen that with increasing angle of skew (α) both the maximum values and the sum of these quantities decrease. The rate of decrease is faster with increasing α. Whereas the change in the sum of deflections ($\Sigma\delta$) and moments (ΣM) are almost the same, δ_{max} decreases

TABLE 5.3 EFFECTIVE DIAPHRAGM LOCATION

S/L	$\frac{EI_G}{EI_S.L}$	$\frac{EI_D}{EI_G}$	Interior Diaphragms No. and Location in the Span	Percentage Reduction in M_{max}
0.117	16.4	0.15	1 @ mid	19.6
0.117	16.4	0.15	3 @ mid, 1/4, 3/4	29.3
0.117	16.4	0.15	2 @ 1/3, 2/3	21.4
0.088	12.3	0.15	1 @ mid	14.1
0.088	12.3	0.15	3 @ mid, 1/4, 3/4	21.1
0.088	12.3	0.15	2 @ 1/3, 2/3	14.5
0.088	17.9	0.15	1 @ mid	19.2
0.088	17.9	0.15	3 @ mid, 1/4, 3/4	27.6
0.088	17.9	0.15	2 @ 1/3, 2/3	21.3
0.070	14.3	0.15	1 @ mid	15.6
0.070	14.3	0.15	3 @ mid, 1/4, 3/4	24.0
0.070	14.3	0.15	2 @ 1/3, 2/3	14.0
0.054	28.7	0.15	1 @ mid	16.8
0.054	28.7	0.15	3 @ mid, 1/4, 3/4	23.9
0.054	28.7	0.15	2 @ 1/3, 2/3	15.9
			1 @ mid	17.1
		Average	2 @ 1/3, 2/3	17.4
			3 @ mid, 1/4, 3/4	25.2

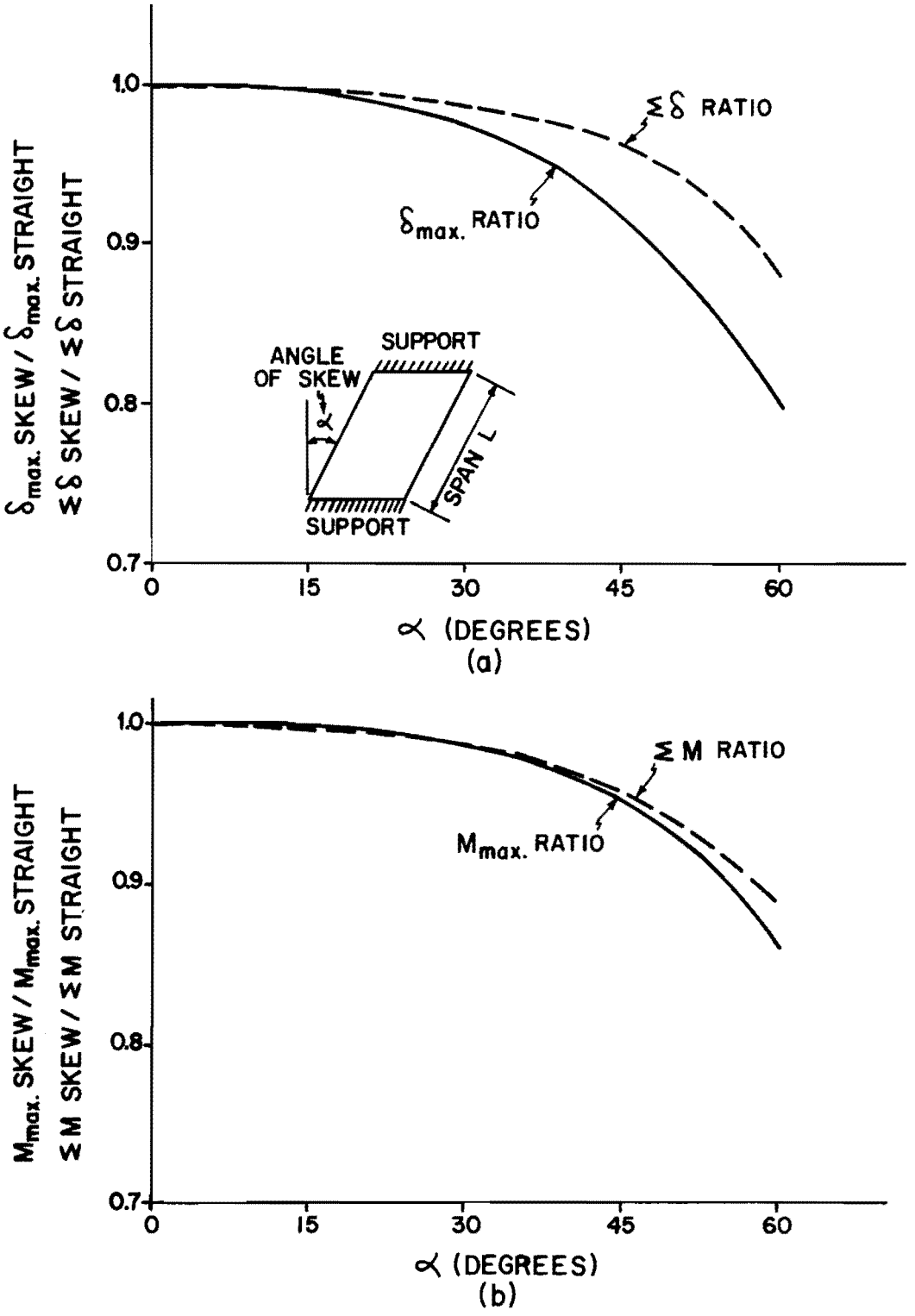

Fig. 5.24 Effect of skew angle on moment and deflection.

faster than M_{max}. In both cases the maximum quantities (δ_{max} and M_{max}) decrease faster than the sum of the quantities ($\Sigma\delta$ and ΣM), as α increases.

Similar findings have been reported in earlier investigations.[16,30] Therefore, it may be inferred that if a straight bridge without any interior diaphragms is safe for a given load, a skew bridge of the same proportions will be safer.

5.3 Diaphragm Effectiveness under Dynamic Loads

Problems associated with dynamic loads are not only the distribution of loads but also the amplification of the effects due to the loads. Apart from these, another factor needing attention is the discomfort to the pedestrian or rider which may be caused by excessive bridge vibration. The effect of diaphragms on these bridge characteristics under dynamic loads is examined in the following sections.

5.3.1 Dynamic Amplification and Distribution

Dynamic amplification of bridge response is a function of the natural frequencies and damping characteristics of the bridge. If the fundamental longitudinal and torsional mode natural frequencies and the damping characteristics do not change significantly upon removal at diaphragms, then it may be concluded that diaphragms have little effect on dynamic amplification. Average values of the natural frequencies and coefficients of damping, obtained from several impact tests, are summarized in Table 5.4 for three bridge models. For consistency, the coefficient of damping in all cases was determined after three cycles of initial oscillations. Test results showed a decrease in the coefficient of damping with decreasing amplitude of response. For instance, the measured values of the damping coefficient for a case in Bridge 3, Series A, determined after 3, 5, and 10 cycles of initial oscillations were 1.2, 0.9, and 0.6 percent of the critical, respectively. The data in Table 5.4 show no significant change in the quantities between test series, indicating that the dynamic amplifications are independent of the presence or absence of the diaphragms.

Available literature indicates that the most important cause of bridge vibration is the initial oscillation of the vehicle as it enters the bridge.

TABLE 5.4 NATURAL FREQUENCIES AND COEFFICIENTS OF DAMPING

Quantity	Series	Bridge 1	Bridge 2	Bridge 3
Natural Frequency	A	9.9	9.8	9.7
Longitudinal Mode	B	10.0	9.8	9.7
(f_L, cycles/sec)	C	10.0	---	---
Natural Frequency	A	12.1	11.7	11.3
Torsional Mode	B	12.0	11.6	11.3
(f_T, cycles/sec)	C	11.9	----	----
Coefficient of damping C	A	2.4	1.4	0.9
Percent of	B	1.9	1.3	1.0
critical C_{cr})	C	2.1	---	---

The range of these frequencies has been indicated as 1 to 3 Hz;[11] for the model scale of this investigation, the corresponding range is about 2 to 7 Hz. Since this range is less than the longitudinal natural frequencies, f_L, and since for a given bridge the results indicate that the torsional frequency f_T is higher than f_L, it may be expected that within the normal frequency range of excitation the longitudinal mode will be excited more than the torsional mode. In the longitudinal mode of vibration the inertial forces are evenly distributed across the bridge. The dynamic effects may be considered to be caused by two kinds of forces -- the inertia force and the applied load. Since the effect due to the former can be considered to be more evenly distributed than that due to the latter, the total effect can be considered to be more evenly shared by the girders than the effect due to the live load alone. In other words, moments and deflections due to dynamic loads can be expected to be more evenly distributed than those due to static loads. This implies that as far as distribution is concerned, diaphragms should be less effective under dynamic loads than under static loads.

These hypotheses were verified by the experimental results obtained from the cyclic loads. Figures 5.25 through 5.39 show the distribution of measured girder midspan deflection and moment amplitudes when excited at

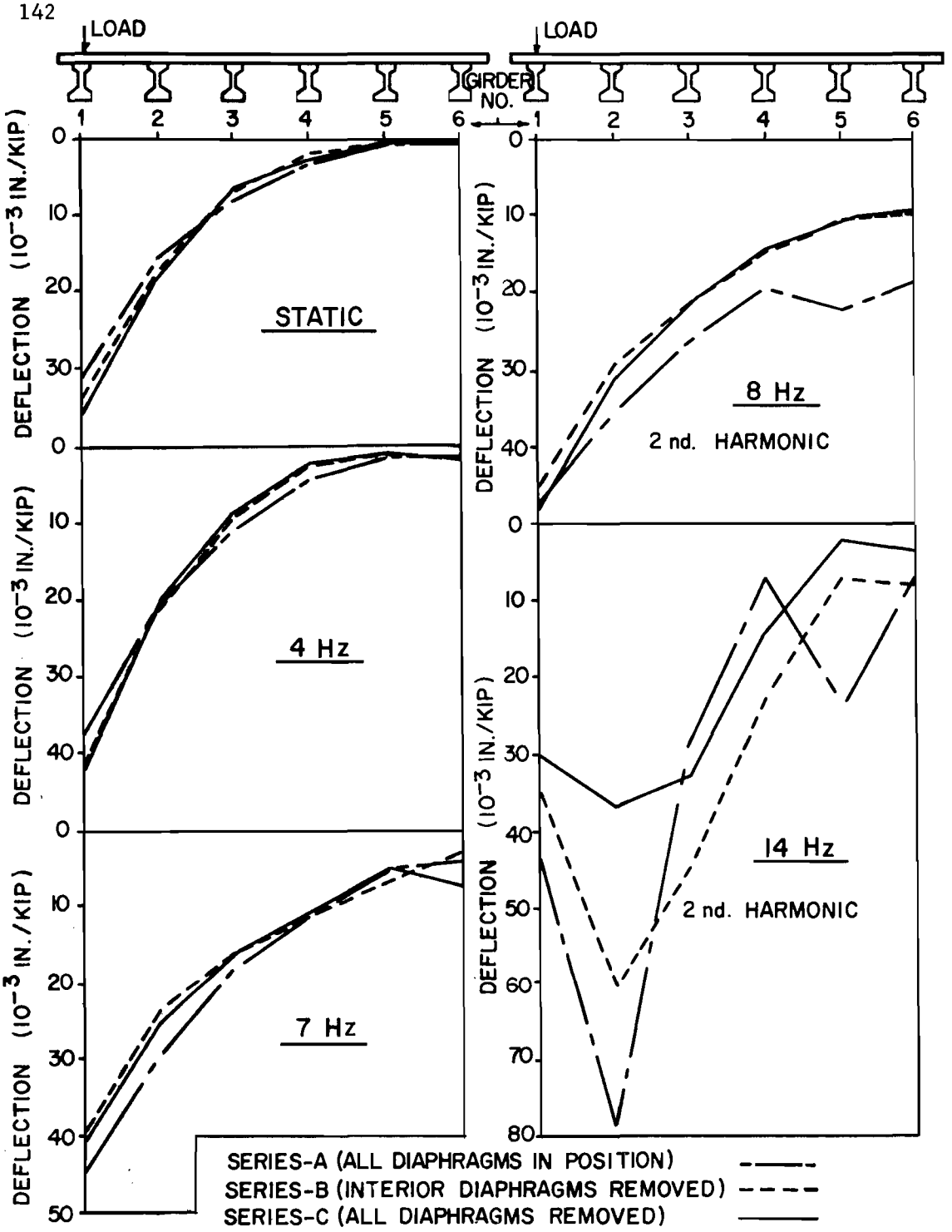

Natural Frequencies: f_L = 9.9 Hz

f_T = 12.1 Hz

Fig. 5.25 Bridge 1 (45° skew, 172 in. span, Type D1 diaphragms at 1/3 points of span); midspan girder deflection amplitudes due to cyclic load of 1 kip amplitude at F1.

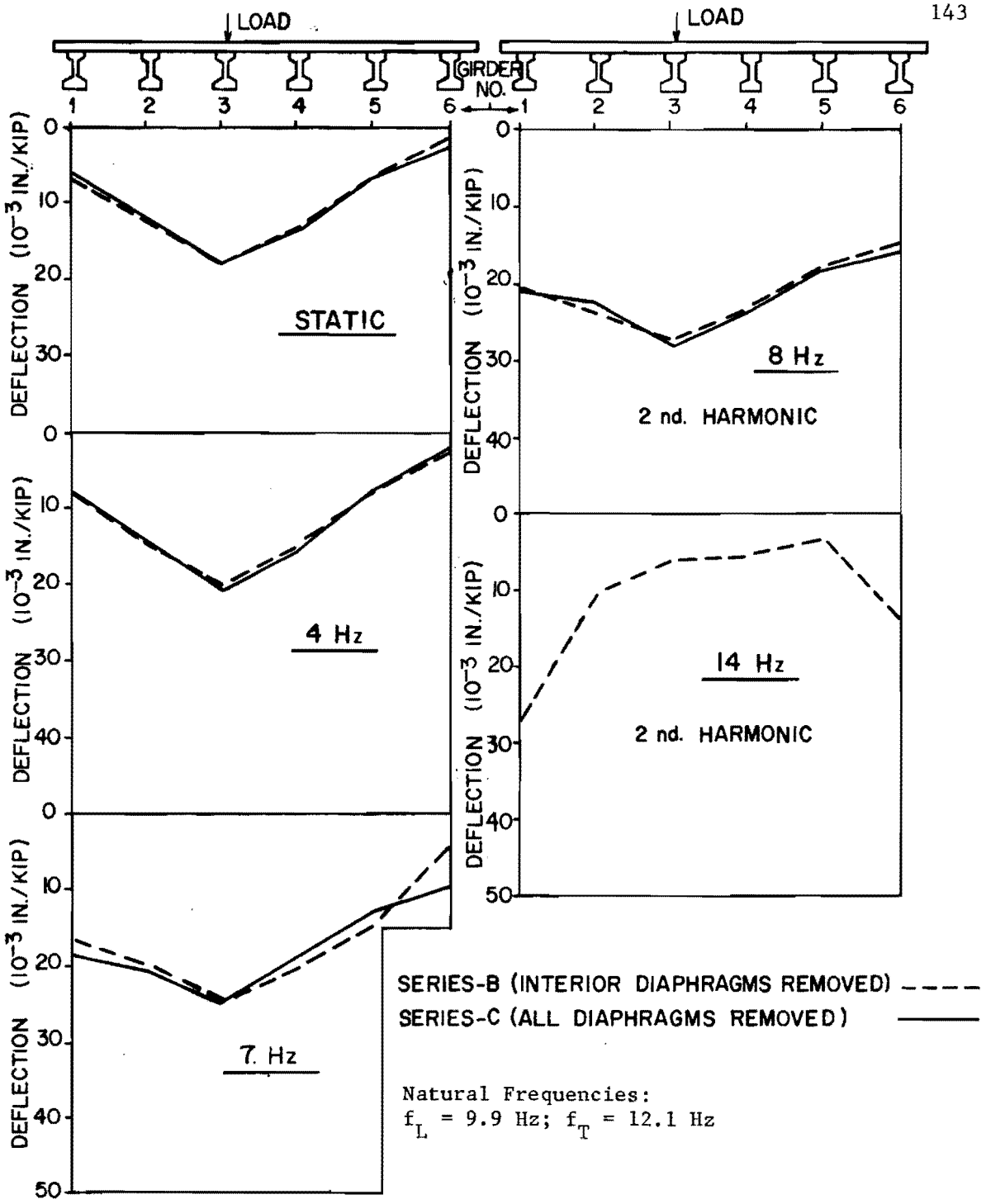

Fig. 5.26 Bridge 1 (45° skew, 172 in. span, Type D1 diaphragms at 1/3 points of span); midspan girder deflection amplitudes due to cyclic load of 1 kip amplitude at F3.

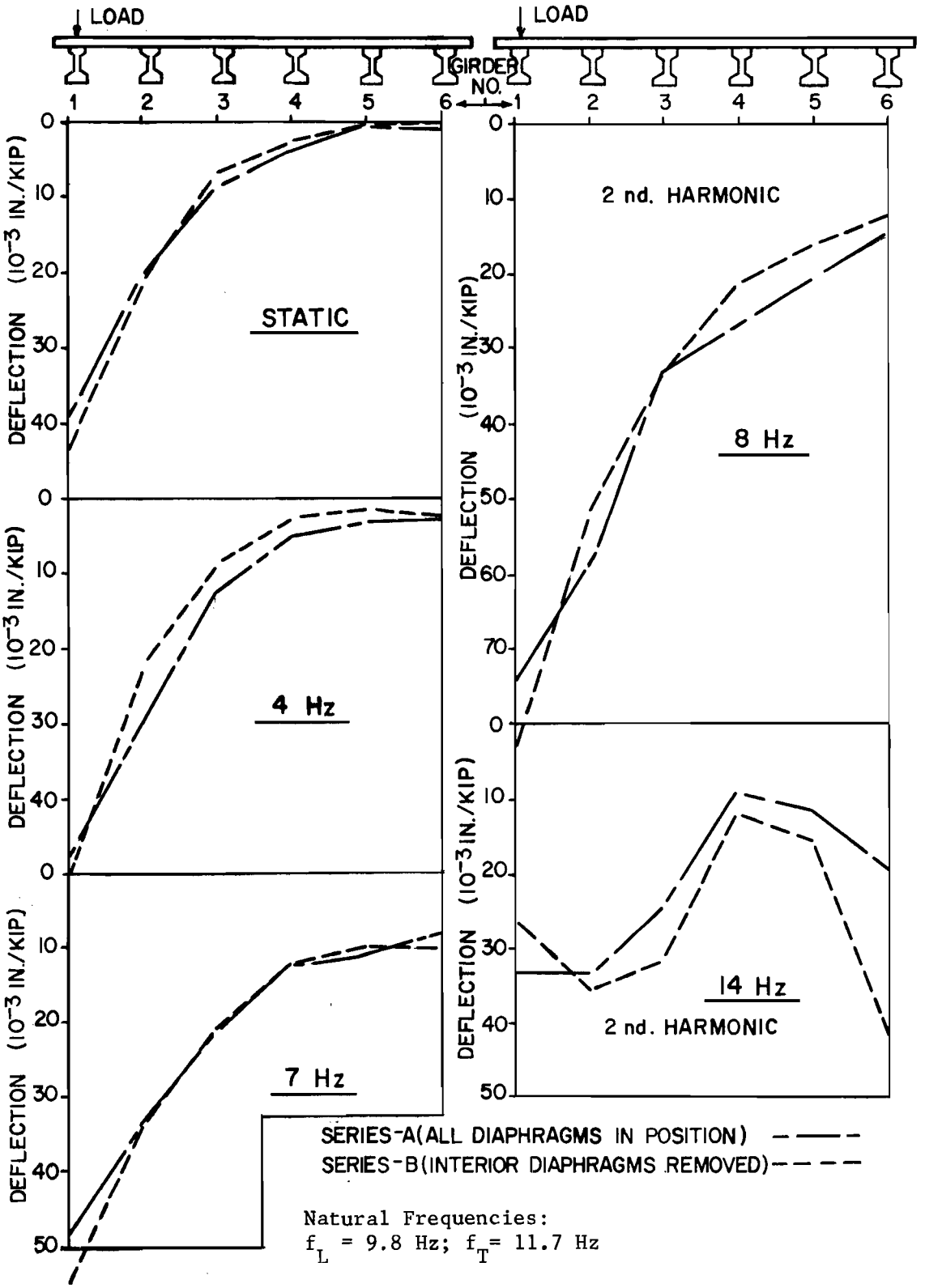

Fig. 5.27 Bridge 2 (45° skew, 172 in. span, Type D2 and Type D3 diaphragms at 1/3 points of span); midspan girder deflection amplitudes due to cyclic load of 1 kip amplitude at F1.

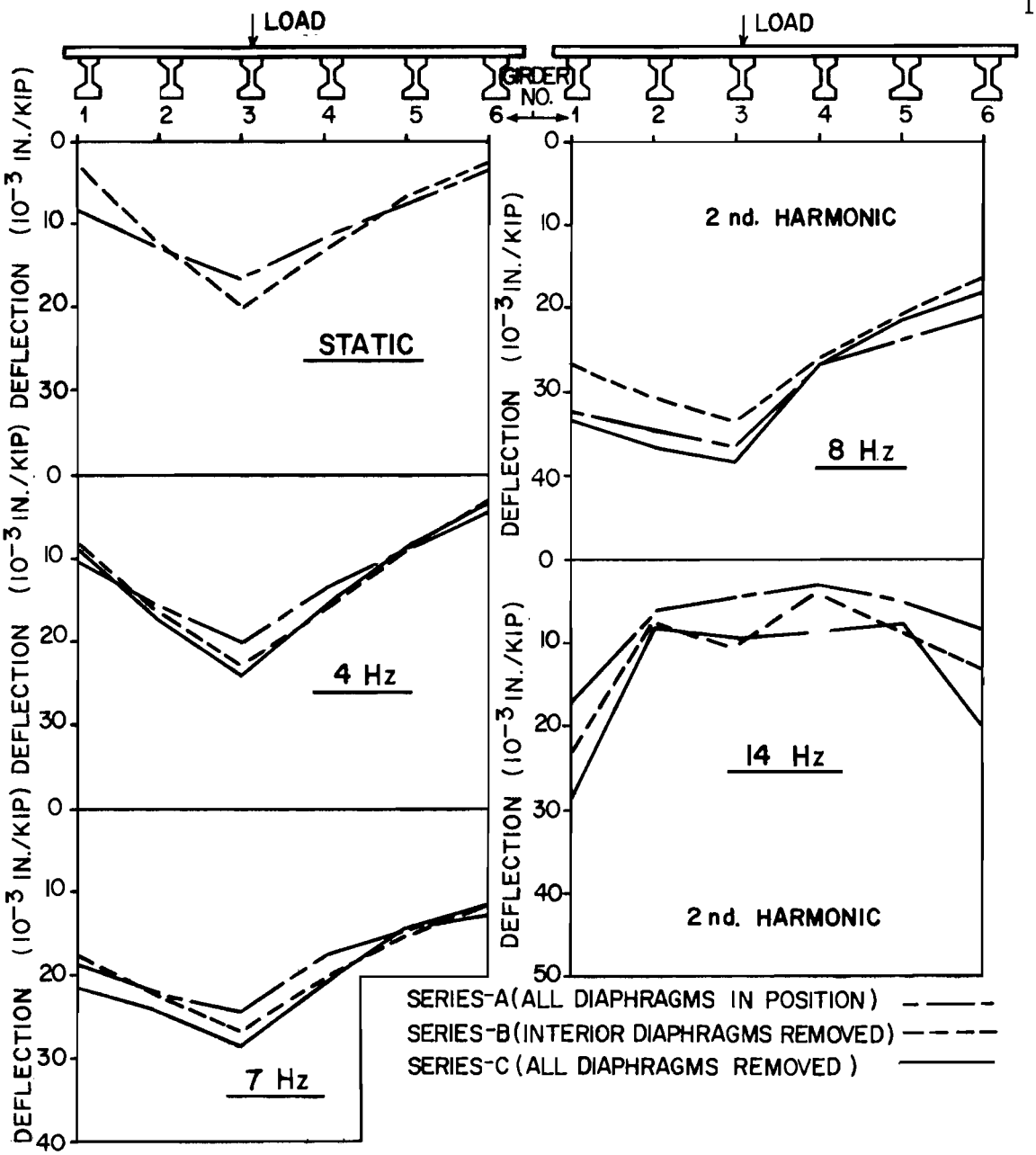

Natural Frequencies:

f_L = 9.8 Hz; f_T = 11.7 Hz

Fig. 5.28 Bridge 2 (45° skew, 172 in. span, Type D2 and Type D3 diaphragms at 1/3 points of span); midspan girder deflection amplitudes due to cyclic load of 1 kip amplitude at F3.

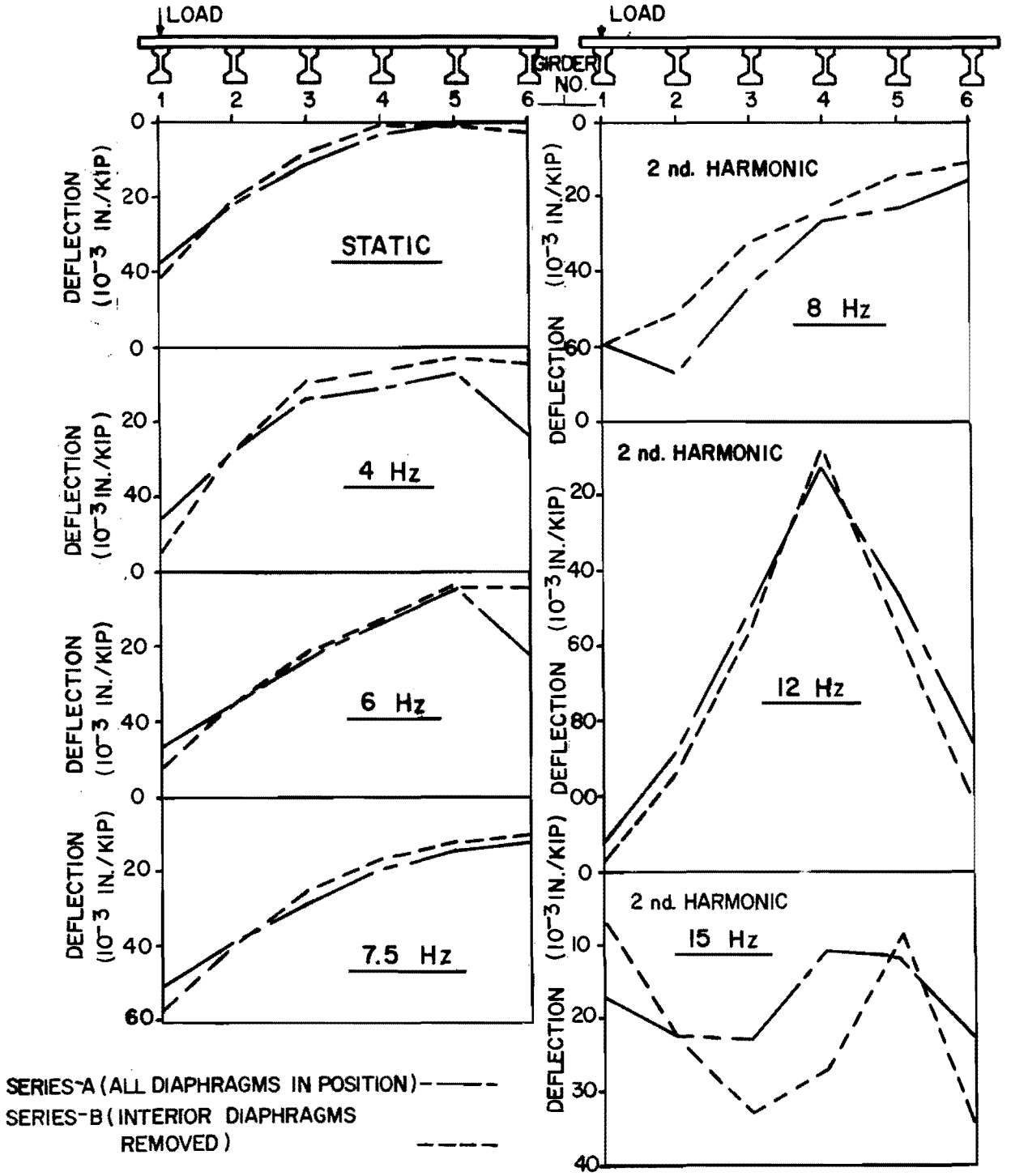

Natural Frequencies: f_L = 9.7 Hz; f_T = 11.3 Hz

Fig. 5.29 Bridge 3 (straight, 172 in. span, Type D2 diaphragms at midspan); midspan girder deflection amplitudes due to cyclic load of 1 kip amplitude at F1.

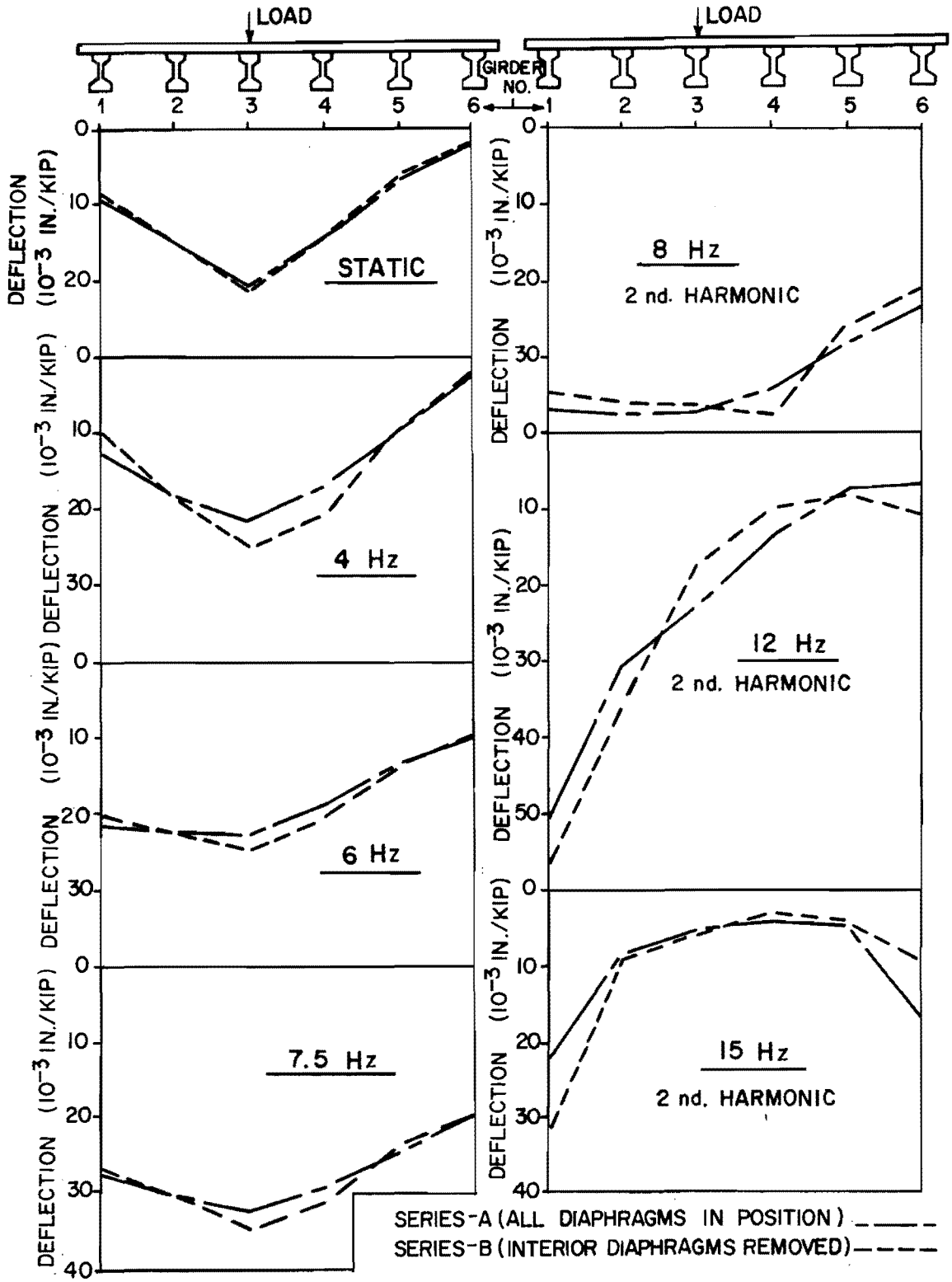

Natural Frequencies: f_L = 9.7 Hz; f_T = 11.3 Hz

Fig. 5.30 Bridge 3 (straight, 172 in. span, Type D2 diaphragms at midspan); midspan girder deflection amplitudes due to cyclic load of 1 kip amplitude at F3.

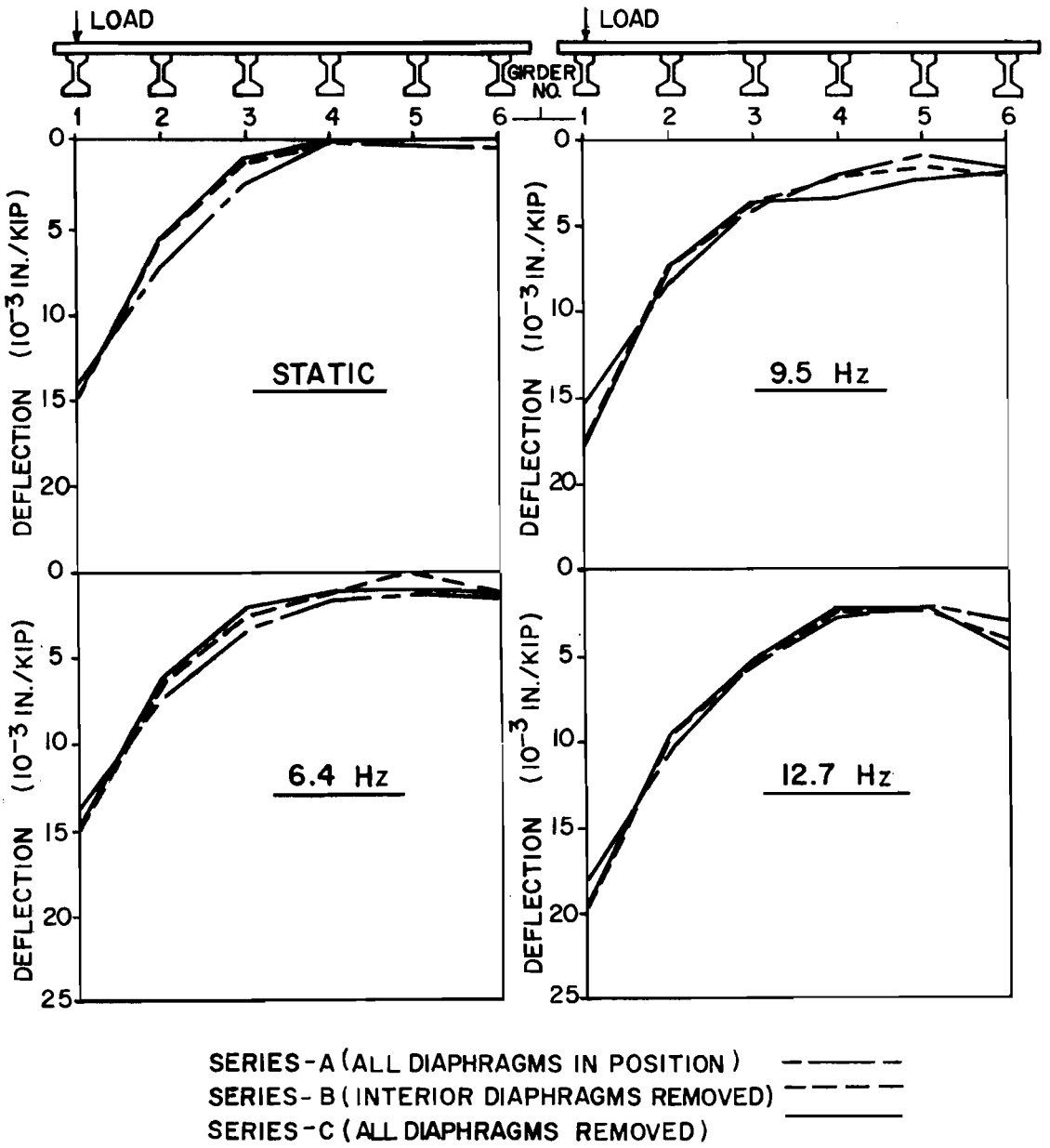

Natural Frequencies: f_L = 25.5 Hz

Fig. 5.31 Bridge 4 (straight, 107 in. span, Type D2 diaphragms at midspan); midspan girder deflection amplitudes due to cyclic load of 1 kip amplitude at F1.

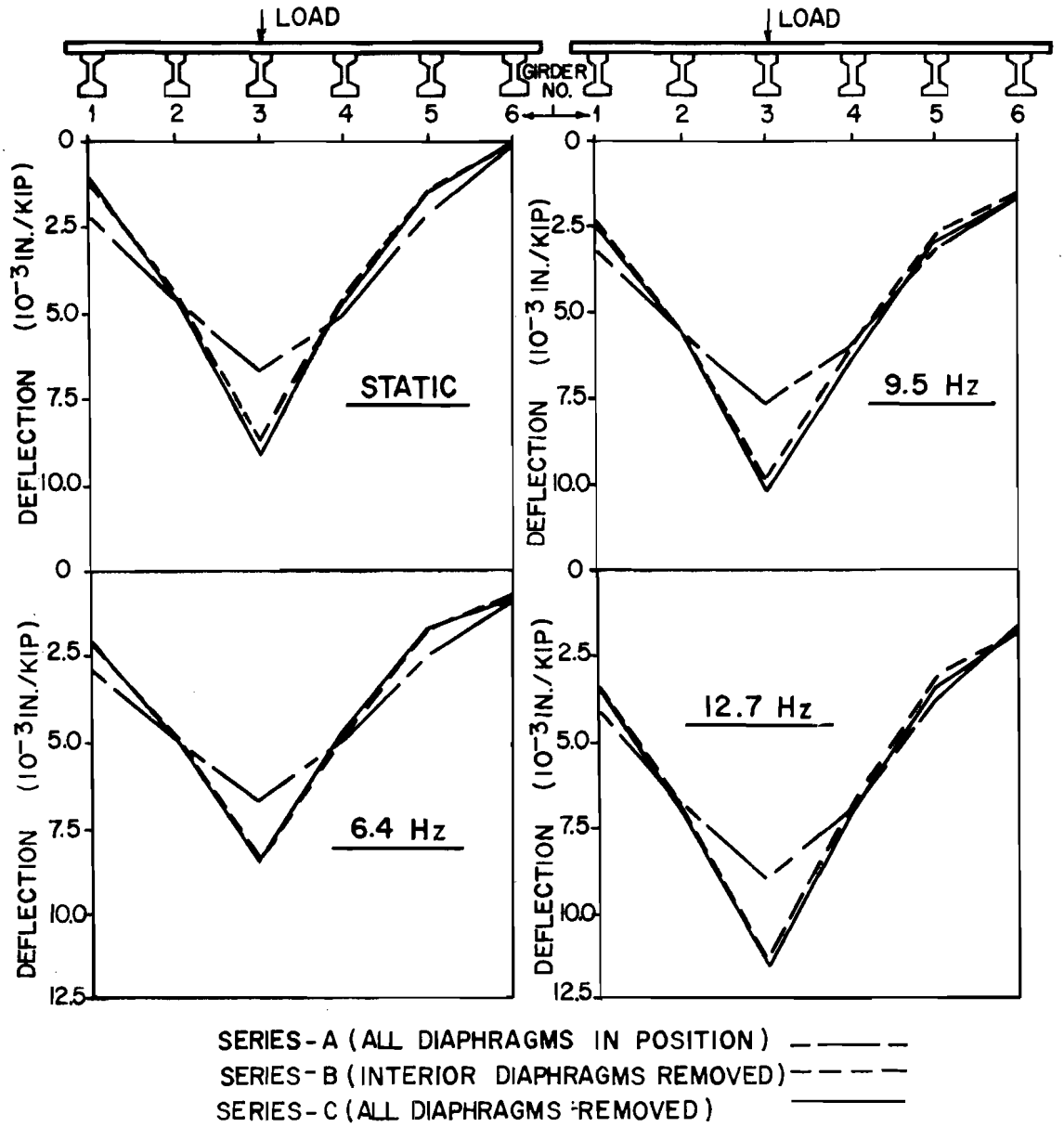

Natural Frequencies: f_L = 25.5 Hz

Fig. 5.32 Bridge 4 (straight, 107 in. span, Type D2 diaphragms at midspan); midspan girder deflection amplitudes due to cyclic load of 1 kip amplitude at F3.

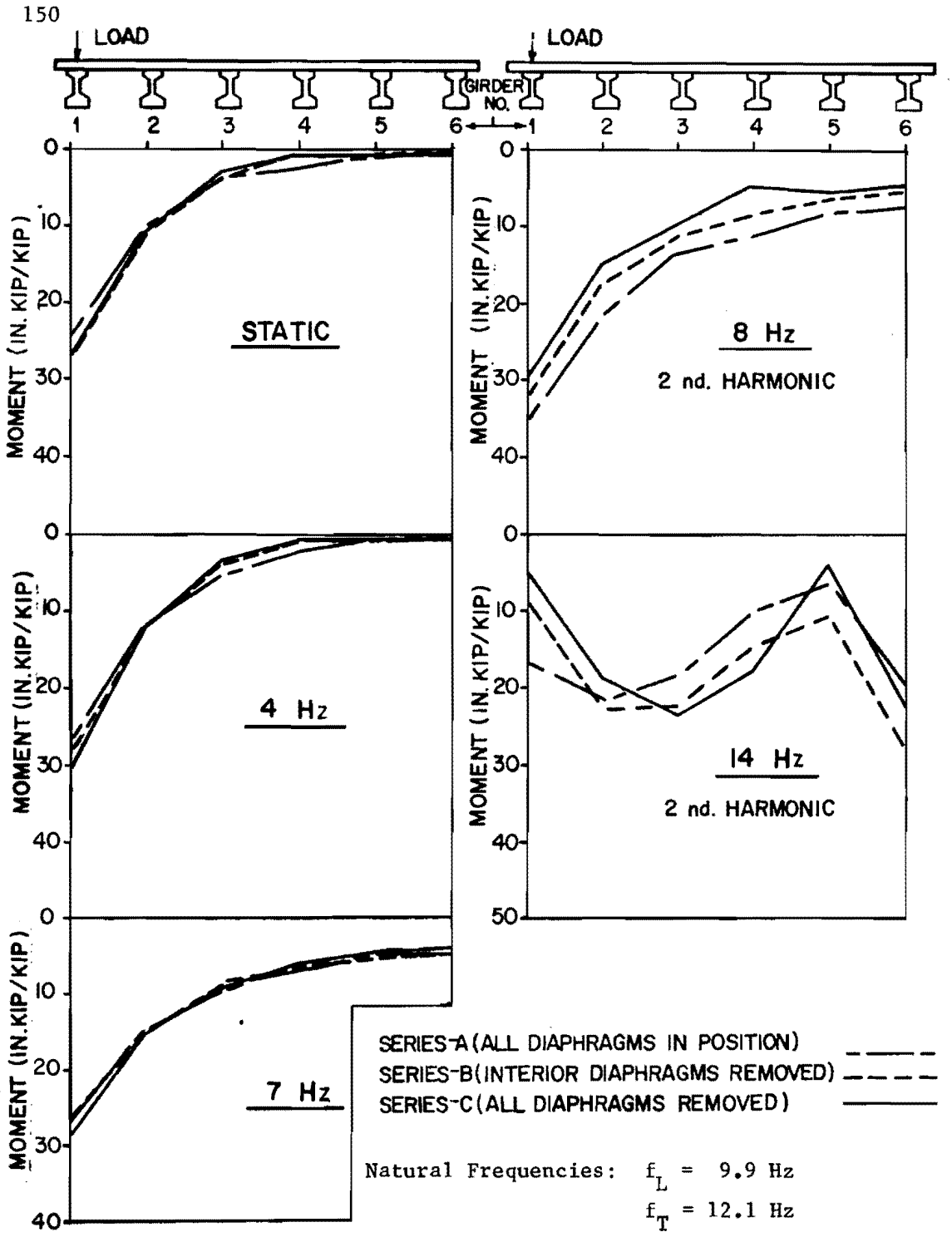

Fig. 5.33 Bridge 1 (45° skew, 172 in. span, Type D1 diaphragms at 1/3 points of span); midspan girder moment amplitudes due to cyclic load of 1 kip amplitude at F1.

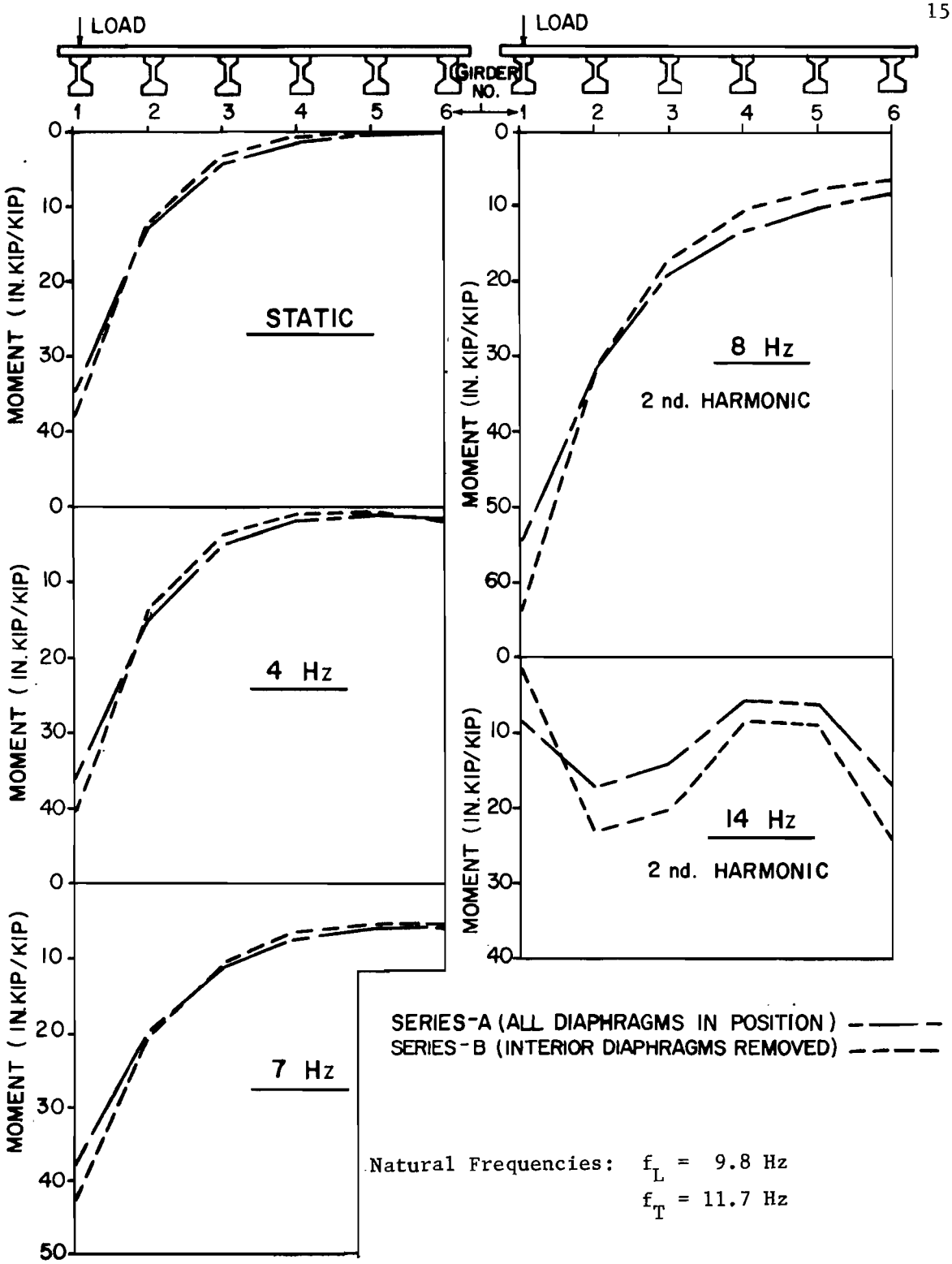

Fig. 5.34 Bridge 2 (45° skew, 172 in. span, Type D2 and Type D3 diaphragms at 1/3 points of span); midspan girder moment amplitudes due to cyclic load of 1 kip amplitude at F1.

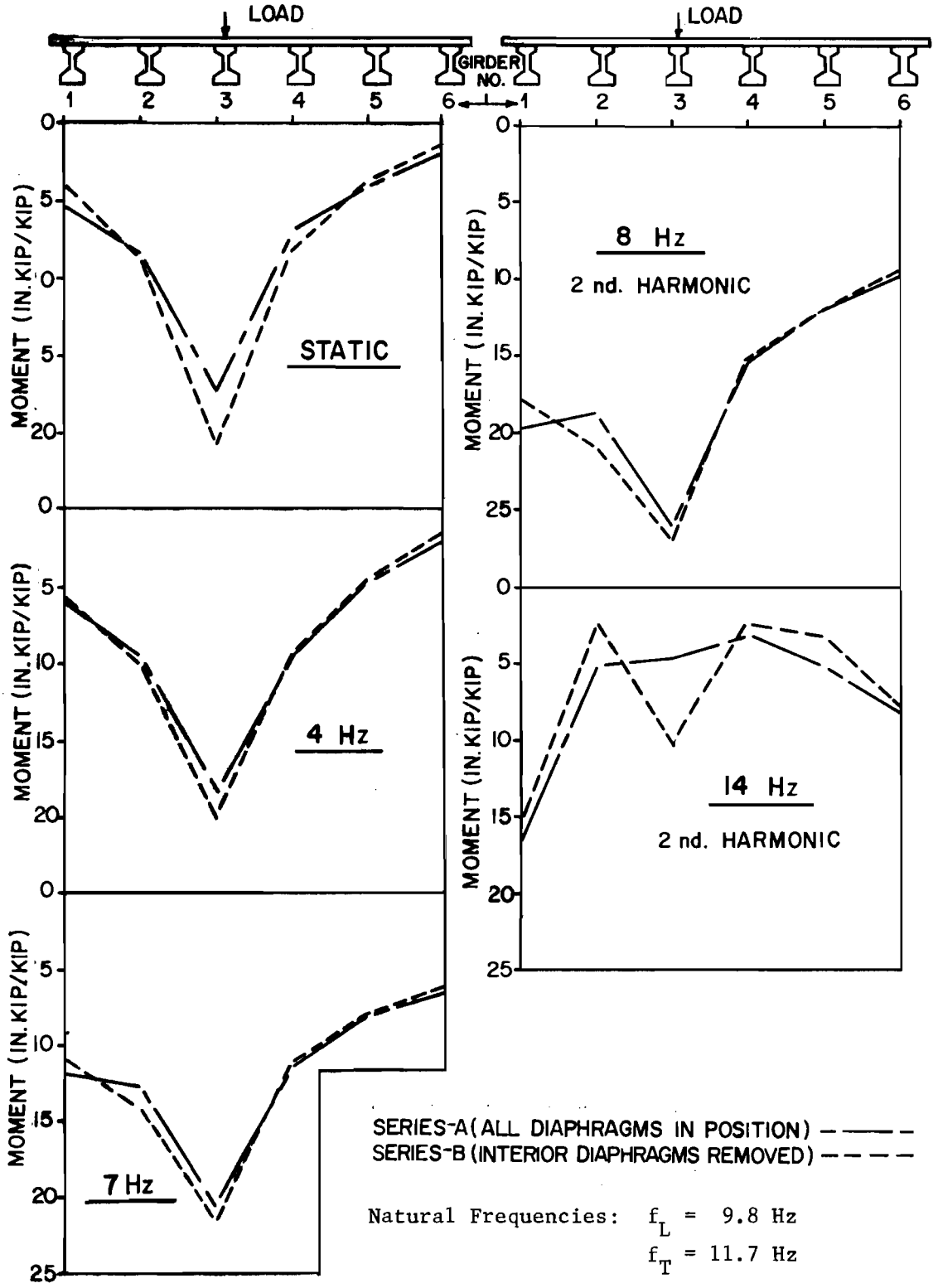

Fig. 5.35 Bridge 2 (45° skew, 172 in. span, Type D2 and Type D3 diaphragms at 1/3 points of span); midspan girder moment amplitudes due to cyclic load of 1 kip amplitude at F3.

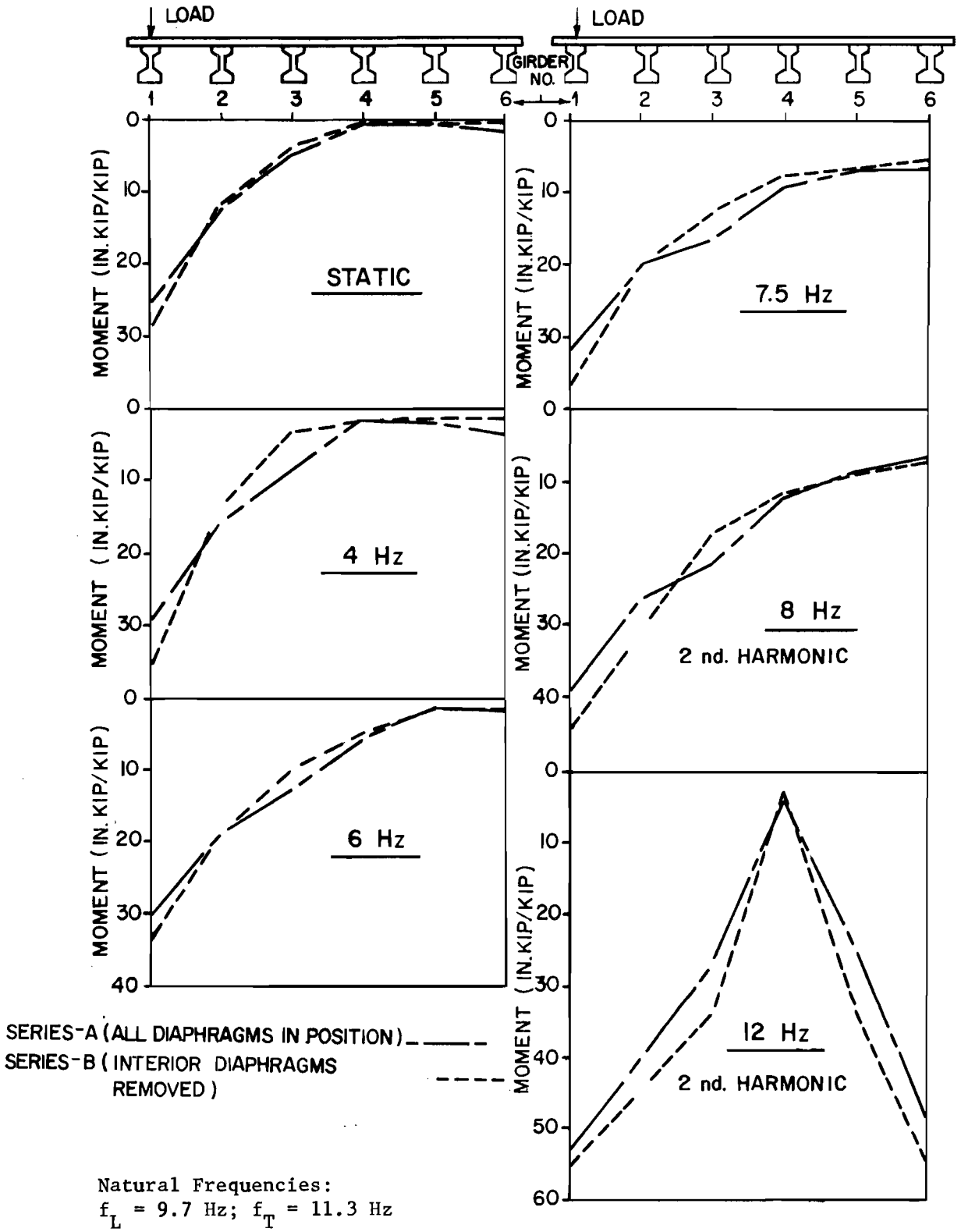

Natural Frequencies:
f_L = 9.7 Hz; f_T = 11.3 Hz

Fig. 5.36 Bridge 3 (straight, 172 in. span, Type D2 diaphragms at midspan); midspan girder moment amplitudes due to cyclic load of 1 kip amplitude at F1.

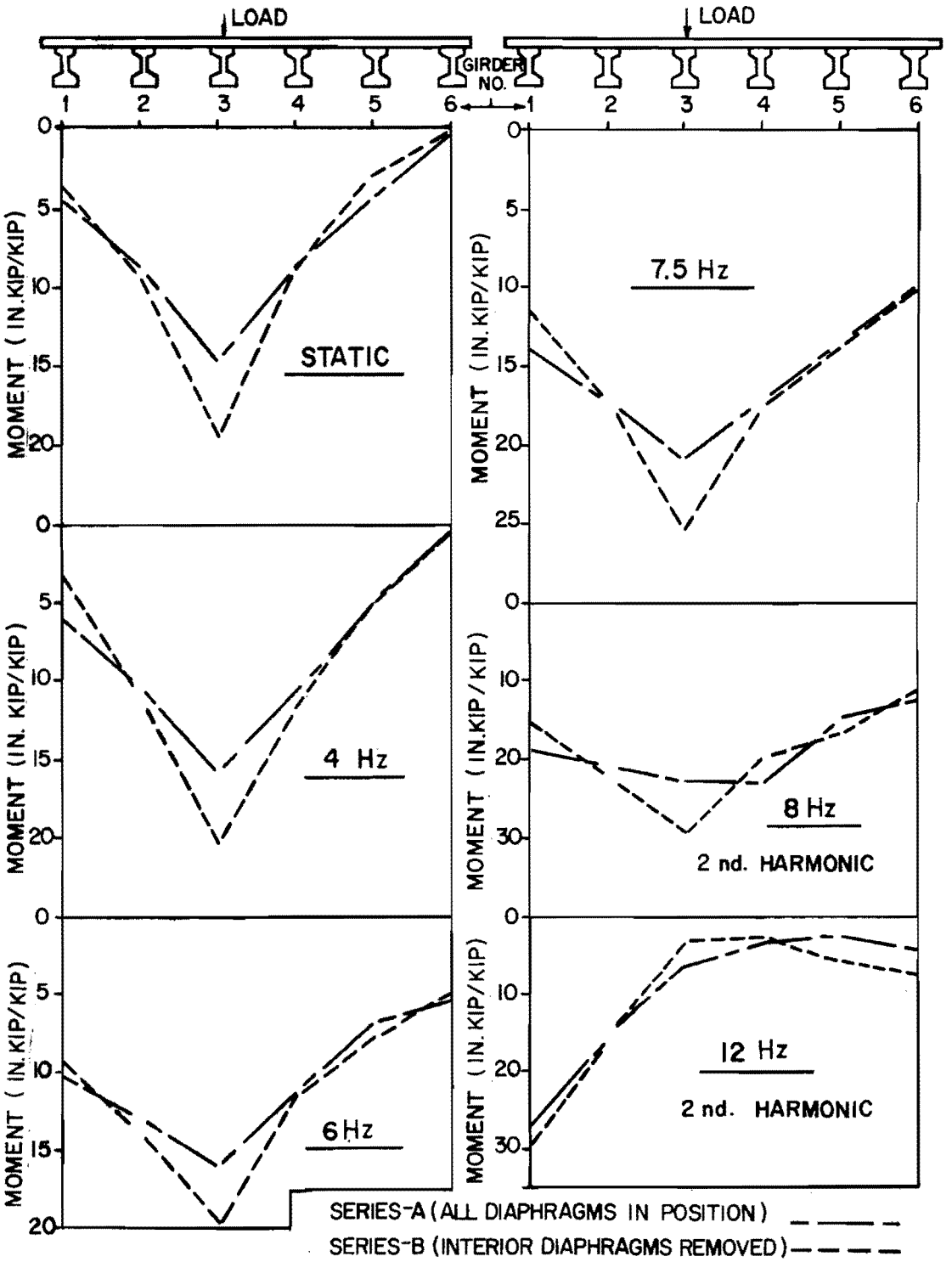

Natural Frequencies: f_L = 9.7 Hz; f_T = 11.3 Hz

Fig. 5.37 Bridge 3 (straight, 172 in. span, Type D2 diaphragms at midspan); midspan girder moment amplitudes due to cyclic load of 1 kip amplitude at F3.

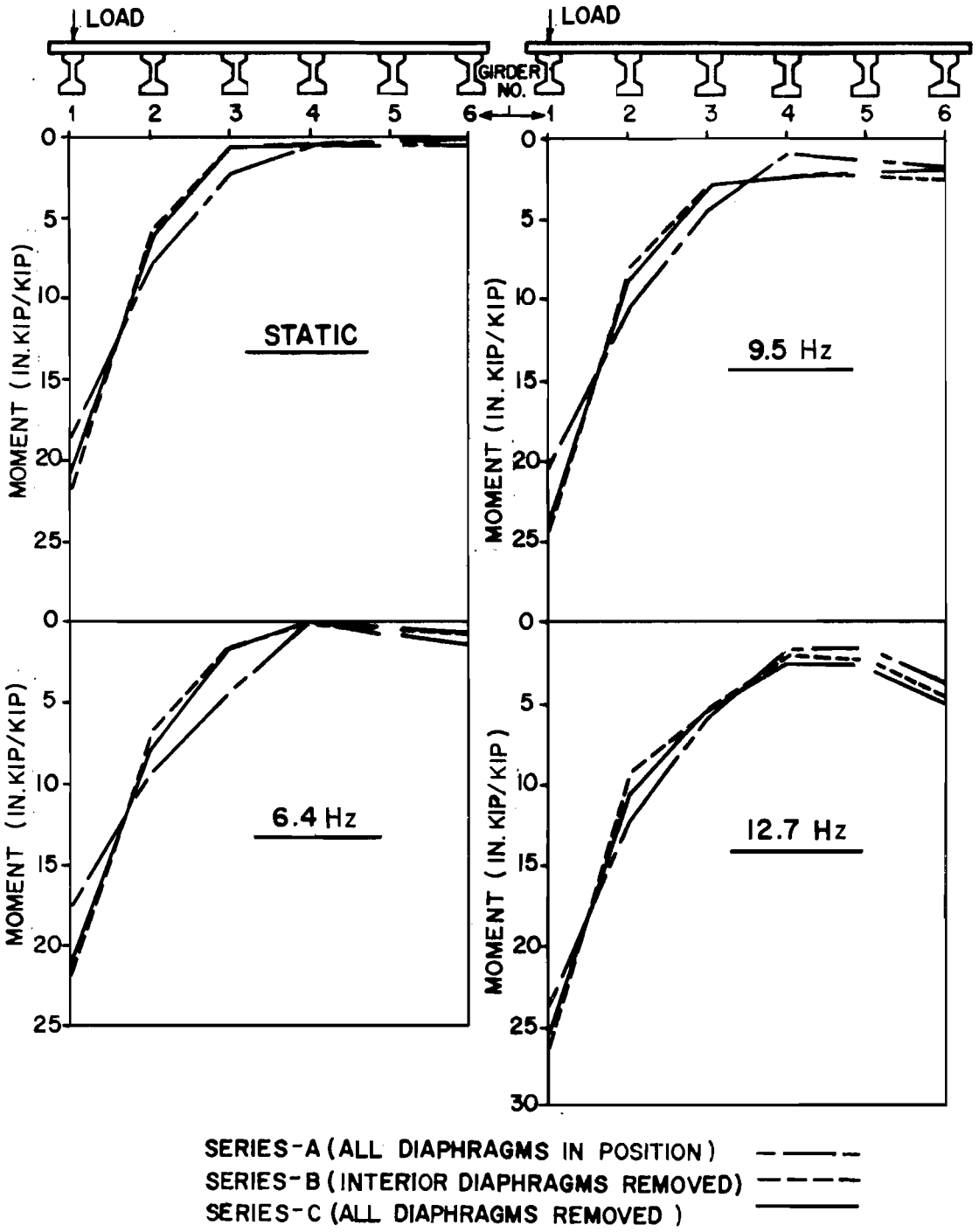

Natural Frequencies: f_L = 25.5 Hz

Fig. 5.38 Bridge 4 (straight, 107 in. span, Type D2 diaphragms at midspan); midspan girder moment amplitudes due to cyclic load of 1 kip amplitude at F1.

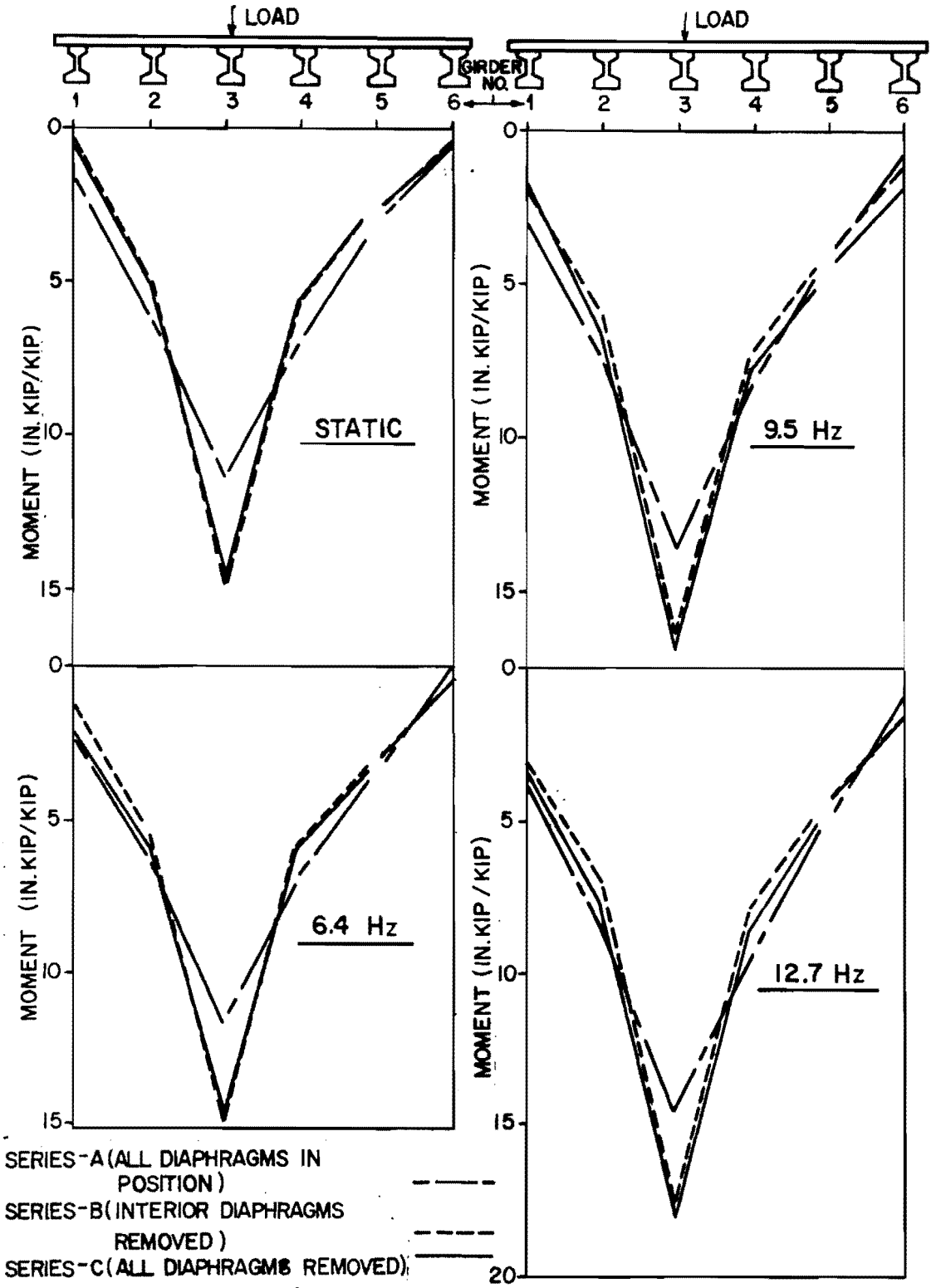

Natural Frequencies: f_L = 25.5 Hz

Fig. 5.39 Bridge 4 (straight, 107 in. span, Type D2 diaphragms at midspan); midspan girder moment amplitudes due to cyclic load of 1 kip amplitude at F3.

different frequencies by a load of 1 kip amplitude. In each case the corresponding static distribution for a 1 kip load is also given. Results obtained from the less reliable second harmonics are also given. The results cover a range of driving frequencies from 4 to 15 Hz, with most of the values below 10 Hz. This is consistent with realistic prototype load frequencies. Included on each figure are the natural frequencies for convenient reference.

These figures indicate:

(1) The moment and deflection amplitudes increase as the exciting frequency approaches the natural fundamental frequencies.

(2) These amplitudes decrease for exciting frequencies greater than the natural frequencies. (Figure 2.25, 14 Hz case, is an exception. Values in this figure and also in Fig. 5.33, 14 Hz case, were very doubtful and are not considered in the following discussions.)

(3) With increasing frequencies the effects are more evenly shared by the girders except when the exciting frequency is equal to the torsional frequency. The more uniform distribution is apparent when the load acts on the interior girder (Figs. 5.26, 5.28, 5.30, 5.32, 5.35, 5.37, and 5.39), the case where the diaphragms are most effective. This is to be expected as loads acting on the inner girder excite the torsional frequency less.

(4) When the exciting frequency is very near to the torsional mode natural frequency (12 Hz cases in Figs. 5.29, 5.30, 5.36, and 5.37), excitation of this mode is very high and distributions are nonuniform. This is more pronounced when the load acts on Girder 1 (exterior girder). However, even in this case, change from Series-A to Series-B does not show any large difference. That is, interior diaphragms have no special role at this frequency. This is to be expected, since even though the distribution in the torsional mode case is nonuniform, this does not cause any transverse bending of the bridge at midspan (see Fig. 1.2b).

(5) In Bridge 4, where the diaphragms show the largest effect, the Series-B and Series-C distributions are virtually identical, indicating that exterior diaphragms essentially play no role in the dynamic load distribution (Figs. 5.32 and 5.39).

If the change in the sum of amplitudes of moments or deflections at midspan as load is changed from static to dynamic is considered as the measure of dynamic amplification, the ratio of the sum for Series-B or C to the sum for Series-A will indicate the diaphragm effect on dynamic amplification. A value of this ratio close to 1 means a very small effect of diaphragms.

These ratios were calculated for all available load cases (74 cases, with frequency range 4 to 15 Hz and loads at F1 and F3) and the results are shown in Fig. 5.40. The mean value of this ratio is 1.012 and the coefficient of variation is about 10 percent. This confirms the hypothesis that the diaphragms do not play any significant role in dynamic amplification. Neither the mean nor the variance seems significant since the coefficient of variation for the same ratios under static loads was found to be 8 percent.

Since the total response (i.e., the sum of the quantities) does not show any significant change from Series-A to Series-B or C, the maximum response due to any load case was chosen as an index of distribution. To verify the second hypothesis (i.e., the diaphragms are less effective under dynamic loads than under static loads) the ratios of the maximum response due to any given load, for Series-B or C, to that due to the same load for Series-A were calculated. Comparisons were then made of these ratios between the dynamic case and the static case, for each load location (F1 and F3) and for both moments and deflections. This was done by computing new ratios of dynamic to static relationships. To verify the hypothesis the value of these new ratios should be less than 1. The results are summarized in Fig. 5.41. The mean value is obtained as 0.979 with a coefficient of variation of 11.8 percent. It should be emphasized that this coefficient of variation is not due to the experimental scatter alone. The value of the ratio of these ratios depends on the dynamic frequency and also on the location of the load. This coefficient of variation includes, in addition to the experimental scatter, any variations in these load characteristics. Figures 5.42 and 5.43 show the frequency distributions of the numerator and denominator of the ratios shown in Fig. 5.41. As expected, the mean value for the static case is greater than that for the dynamic case (1.172 and 1.136, respectively).

These results do not prove that the diaphragms are always less effective under dynamic loads. However, they indicate that in the normally expected frequency range the role of diaphragms is not significantly different under dynamic loads from that under static loads and, on the average, diaphragms are less effective under dynamic loads as far as load distribution is concerned.

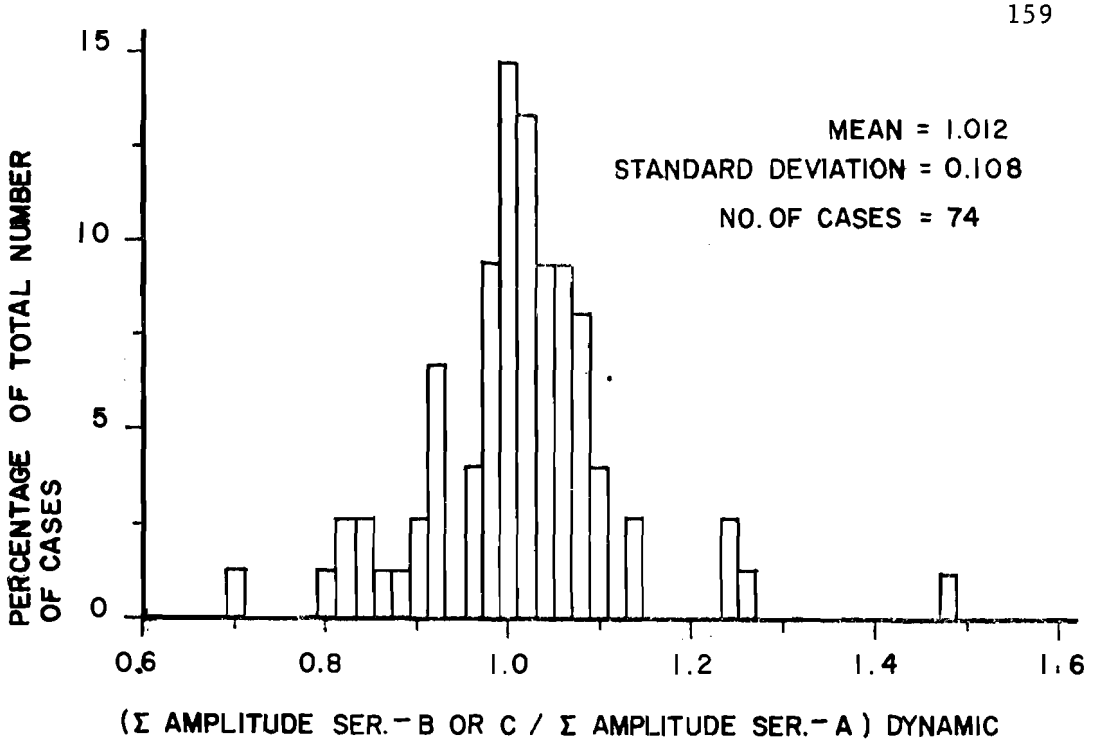

Fig. 5.40 Diaphragm effect on dynamic amplification.

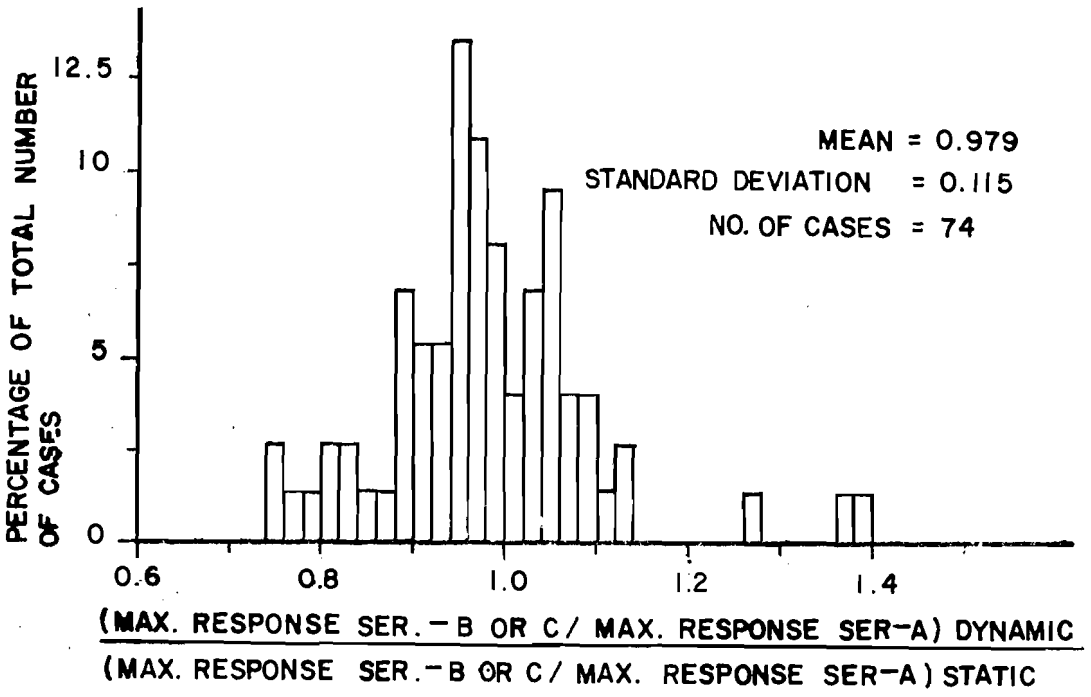

Fig. 5.41 Comparison of diaphragm effects on dynamic and on static load distribution.

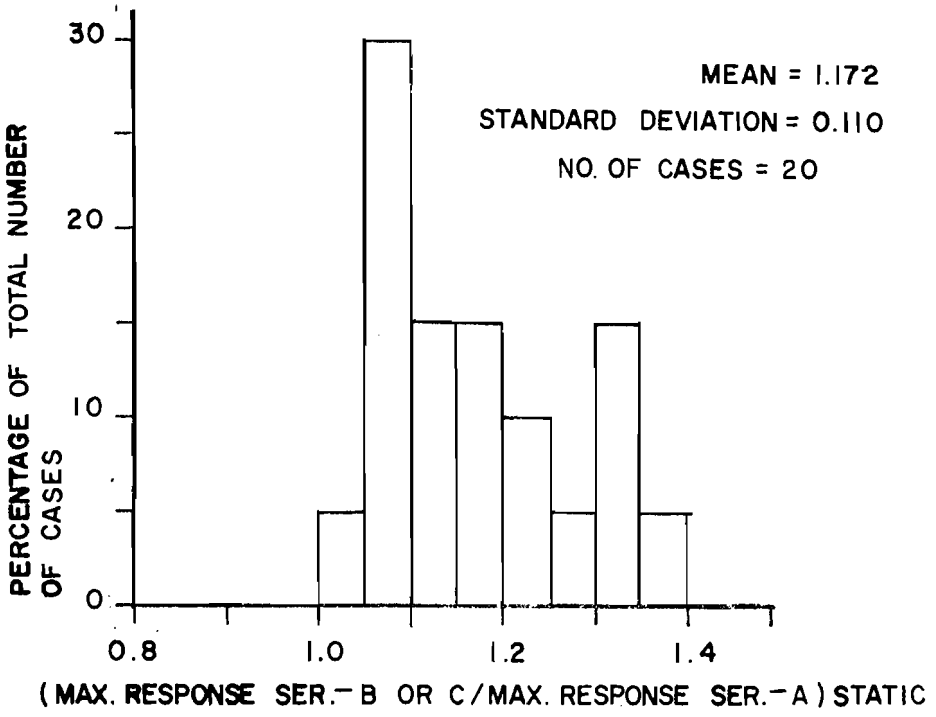

Fig. 5.42 Diaphragm effect on static load distribution.

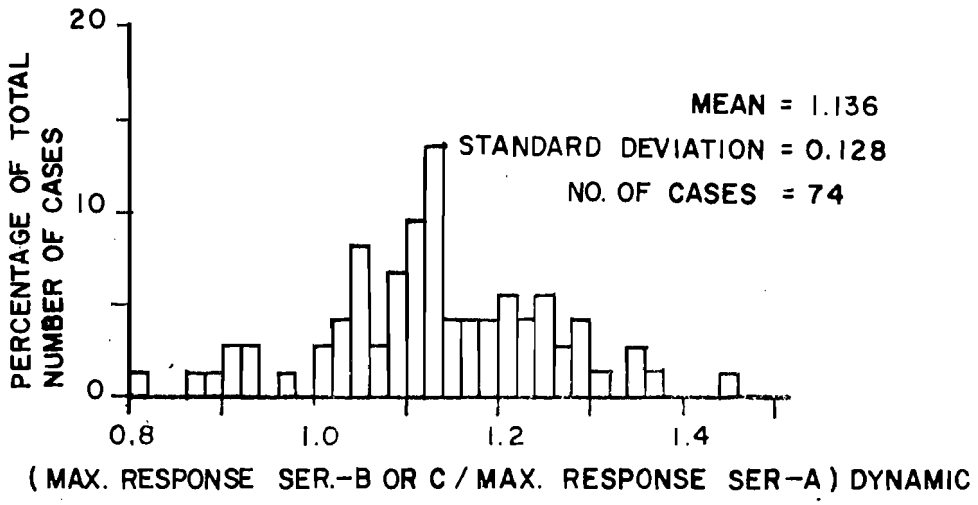

Fig. 5.43 Diaphragm effect on dynamic load distribution.

5.3.2 Effect of Diaphragms on Pedestrians' and Riders' Comfort

Human response to vibration is thought to be largely a function of the acceleration of the bridge motion. This acceleration is proportional to the square of the frequency and to the amplitude of the dynamic part of the bridge motion. The frequency of the bridge vibration depends on the natural frequencies of the bridge and the frequencies of vehicle oscillation. The latter is obviously independent of the diaphragms. The fundamental natural frequencies of the bridges have been shown to be unaffected by the presence or absence of diaphragms. Although the diaphragms affect the amplitude of deflection to a slight extent (reduce it at the loading point and increase it away from the loading point) this change in the amplitude of deflection and its effect on human response to vibration can be considered negligible because human response to vibration varies with the logarithm of the acceleration amplitude. Therefore, for all practical purposes it may be stated that the diaphragms do not play a significant role with regard to a pedestrian's or rider's comfort.

5.4 Diaphragm Effectiveness under Lateral Impacts

For extremely heavy impacts due to collision of an overheight vehicle passing under the bridge, the whole bridge may be displaced from the supports and collapse.* Under such circumstances, whether diaphragms are provided or not does not matter. With relatively smaller impacts the bridge may not collapse but the exterior (and possibly some interior) girders will be damaged. The possible extent of damage under such circumstances with and without diaphragms was studied. The different tests performed and the location of diaphragms during the testing were given in Table 2.6 and Fig. 2.28.

Bridge 2: The results of the impact tests conducted on Girder 1 and Girder 6 are not discussed in detail because the concrete strength of Girder 1 was considerably less than that of Girder 6. The bottom flange of Girder 1 (with all the diaphragms) was completely shattered, whereas Girder 6 (without any diaphragms), which was impacted more times (see Table 2.6) was less

*Such a case was reported in Texas Highways, Vol. 19, No.2, February, 1972.

damaged. These results were suspect because of the difference in girder concrete strengths. However, with equal strength girders and for equal impacts, damages caused to Girder 2 (with all the diaphragms) and Girder 5 (without any diaphragms) are shown in Figs. 5.44a and 5.44b. The maximum crack width in Girder 2 was about 2 in., exposing 15 prestressing strands, whereas in Girder 5 cracks were much finer (width not precisely measured but less than 1/16 in.), widespread along the beam and no strand was exposed. Girder 2 was not only more highly damaged, but the forces transferred through the diaphragms caused diagonal shear cracks at the bottom flange of the next girder (i.e., Girder 3) as shown in Fig. 5.44c. The girder without any diaphragms showed cracks along the interface of the girder and the slab (Fig. 5.44b), while the girder with all the diaphragms did not show this.

Bridge 3: In this bridge girders were impacted with an increasing height of fall (see Table 2.6) until failure. A failure criterion arbitrarily chosen was widespread visual damage. Figures 5.45a and 5.45b show that for equal impacts the damage caused to the girder with all the diaphragms (i.e., Girder 1) is obviously considerably more than the girder without any diaphragms (i.e., Girder 6). In the former case some reinforcement in the web and 13 strands in the bottom flange were exposed. In the latter case the maximum crack width was about 0.02 in. Equivalent failure of Girder 6 occurred at a much higher height of fall (44 in. as against 29 in. for Girder 1) by crushing of concrete at the impacting point, exposing 10 strands (Fig. 5.45c). As in Bridge 1 the girder slab interface cracked. No such cracking was observed when the diaphragms were present (i.e., Girder 1).

The measured impacting force and corresponding lateral deflection of the bottom flange at the point of impact are plotted against the height of fall in Figs. 5.46 and 5.47. While these figures are only general indications, they show that for equal impact (i.e., equal height of fall, since the impacting weight was the same), the impacting force was greater and the lateral deflection of the bottom flange was less for the girder with diaphragms than the one without. To give some rough quantitative idea, the impact test potential energies (i.e., height of fall times the impacting weight) corresponding to first cracking and to failure were both about 33 percent less when the diaphragms were present than in the cases without diaphragms.

(a) Girder 2, with diaphragms at 1/3 points of the span

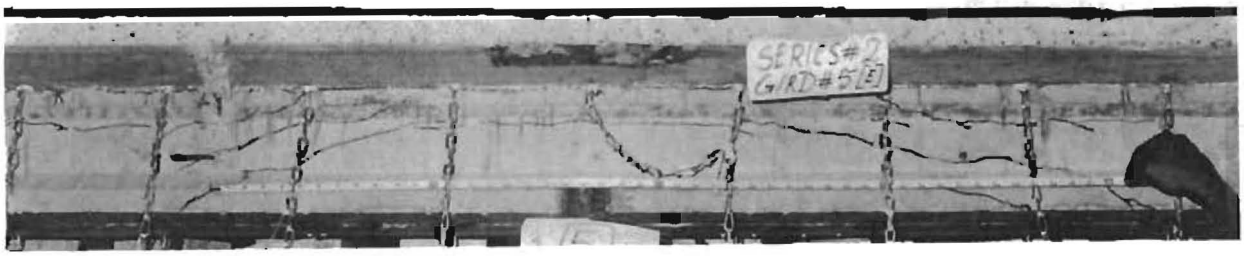

(b) Girder 5, without any diaphragms

(c) Diagonal crack in Girder 3 due to impact on Girder 2, with diaphragms at 1/3 points of the span

Fig. 5.44 Bridge 2, damages in girders due to equal lateral impacts.

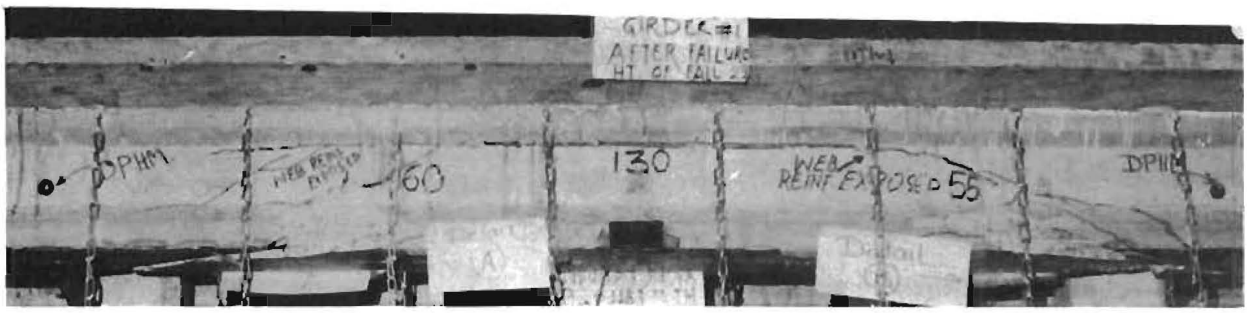

(a) Girder 1 after failure, with diaphragms at 1/3 points of the span (height of fall = 29 in.)

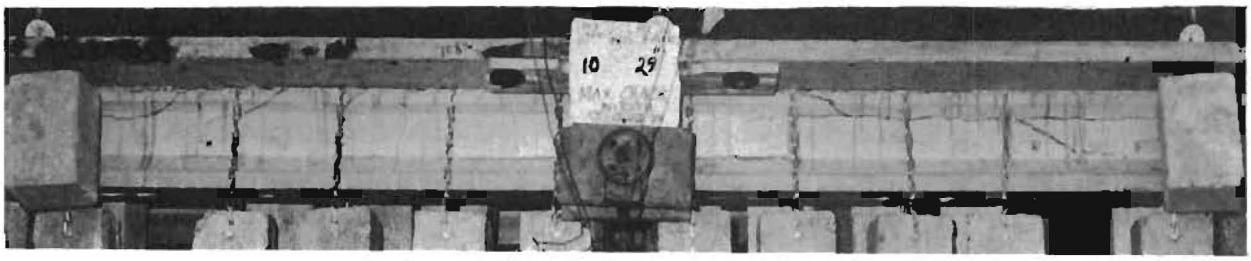

(b) Girder 6, without any diaphragms (height of fall = 29 in.)

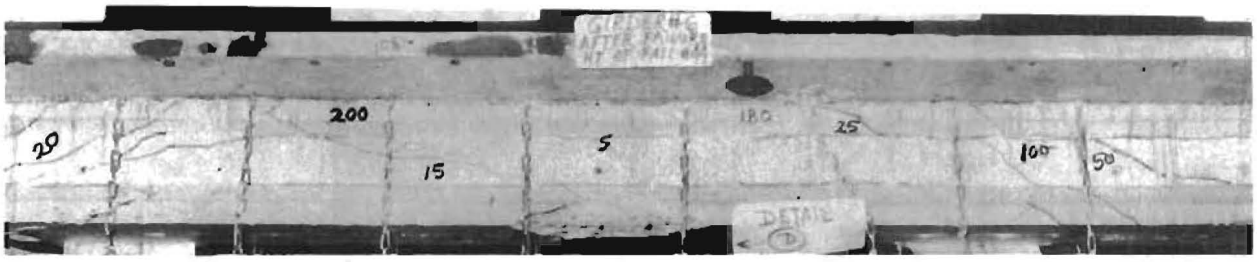

(c) Girder 6 after failure, without any diaphragms (height of fall = 44 in.)

Fig. 5.45 Bridge 3, girder damages due to lateral impacts (crack widths are shown in 10^{-3} inches).

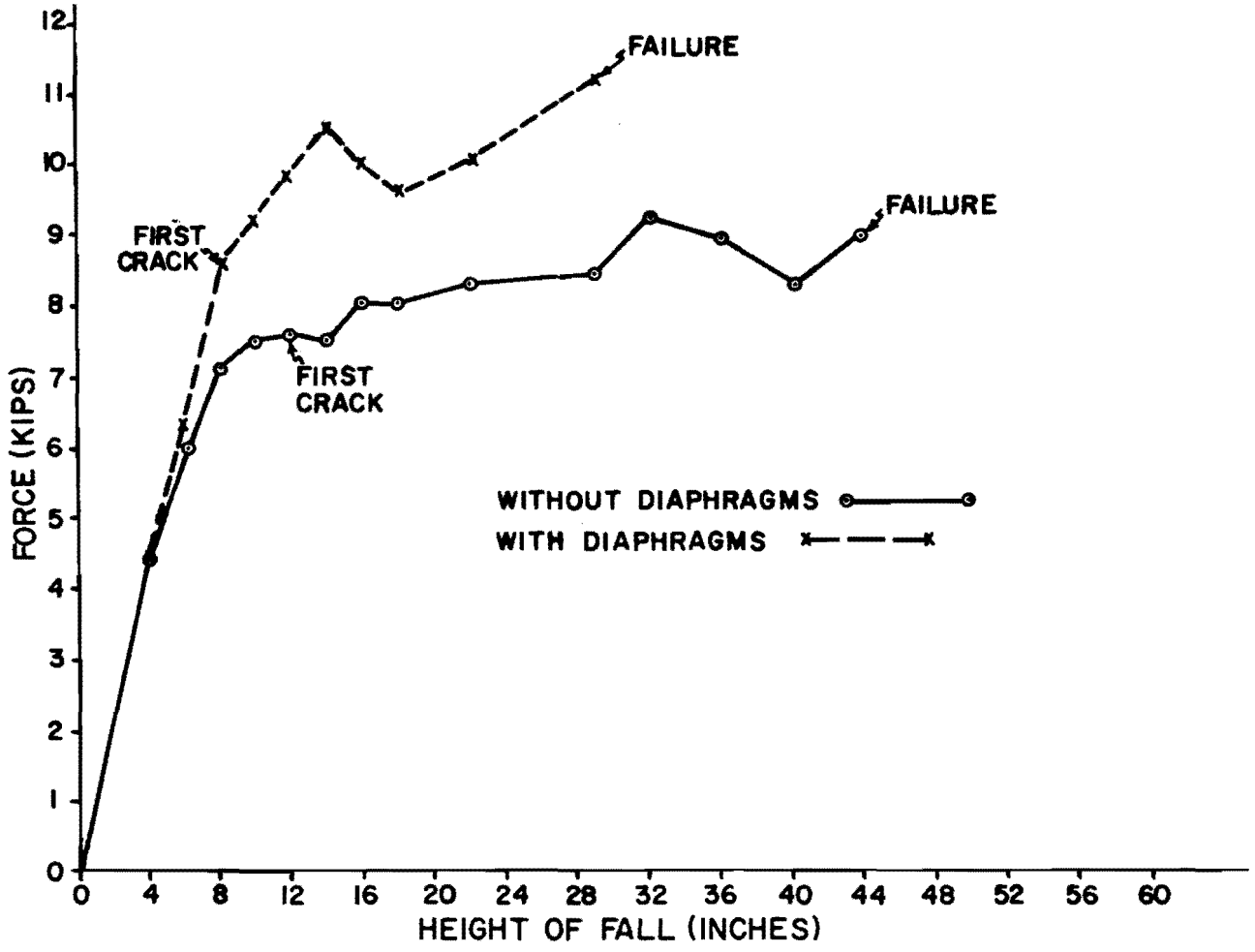

Fig. 5.46 Bridge 3, impacting forces due to different heights of fall.

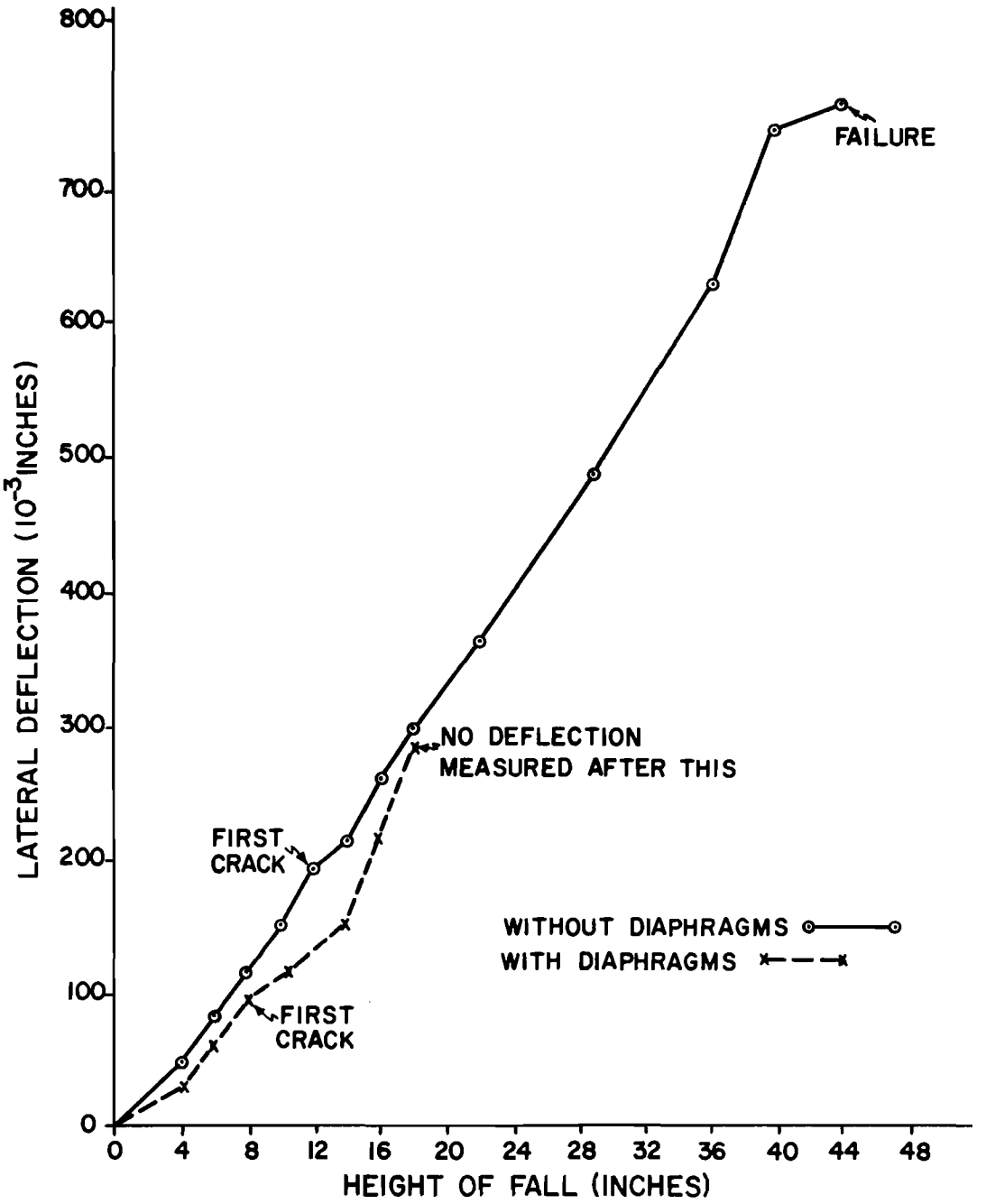

Fig. 5.47 Bridge 3, lateral deflections of bottom flange for different heights of fall.

After the lateral impacts, Girders 2 and 5 of Bridge 2 and Girders 1 and 6 of Bridge 3 were loaded with single vertical point loads at midspan. The girders were loaded simultaneously up to 10 kips each in Bridge 2 and 2.5 kips each in Bridge 3. The load deflection plots are shown in Figs. 5.48 and 5.49. In the earlier stages of loading (2.5 to 3 kips) the girders with diaphragms show about 25 percent less stiffness than the girders without diaphragms. This is because the bottom flange of the girders with diaphragms was considerably more damaged than that of the girders without diaphragms. As the load increased, the deflection of the girder without diaphragms increased faster (Fig. 5.48). At about 8.5 kips load the deflections of the two girders were almost equal. Beyond this load Girder 5 (without diaphragms) showed larger deflection than Girder 2 (with). The ultimate load capacity of Girder 2 was found to be about 11 percent higher than Girder 5. In both cases failure occurred with some separation of the slab and girder at the interface.

These tests indicate that the diaphragms make the girders more rigid when resisting lateral impacts. However, in doing so they reduce the energy absorption capacity of the girder, making them more susceptible to damage from lateral impacts. The point load ultimate tests indicate that even though the damage was greater, the ultimate load capacity of the girder with diaphragms was somewhat higher. As wide cracks always develop through the girder tension zone near ultimate load, the damages in the bottom flange of the girders did not significantly affect their ultimate load-carrying capacity. Such damages, however, are very important from the consideration of serviceability, repair, and especially corrosion of prestressing strands. The results indicate that the presence of diaphragms causes greater problems. Crack patterns indicate that when the diaphragms are present, most of the major damage is due to diagonal tension from torsion. In prestressed concrete girders the prestressing force helps to reduce the effect of such diagonal tension. Reinforced concrete girders do not have this beneficial compressive force. As such their performance under lateral impacts can be expected to be relatively worse when diaphragms are provided. However, in the case of steel girders, because of the large inherent ductility, such adverse effects due to the presence of diaphragms are not expected.

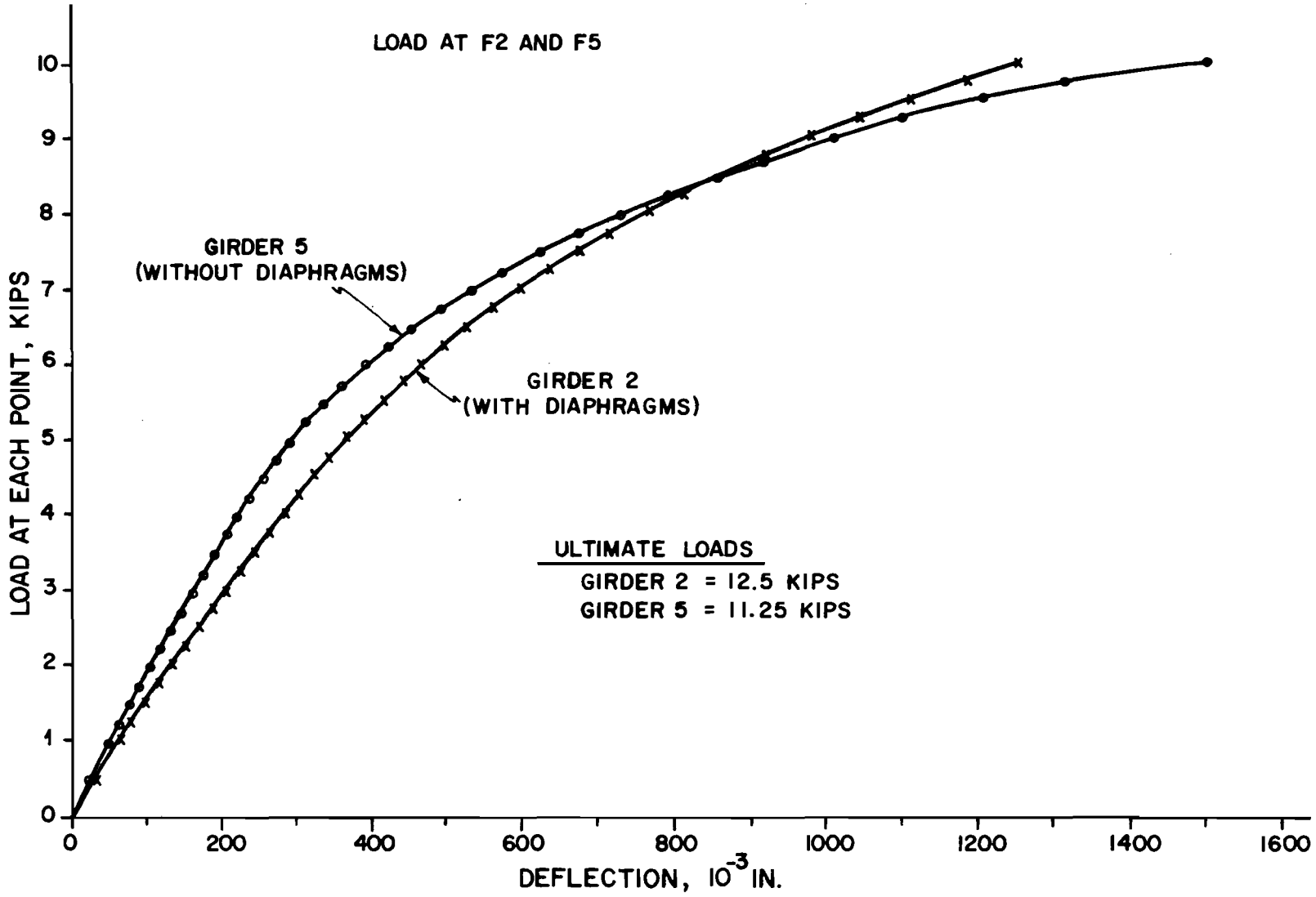

Fig. 5.48 Bridge 2, midspan girder deflections due to point loads at midspan (tested after lateral impacts).

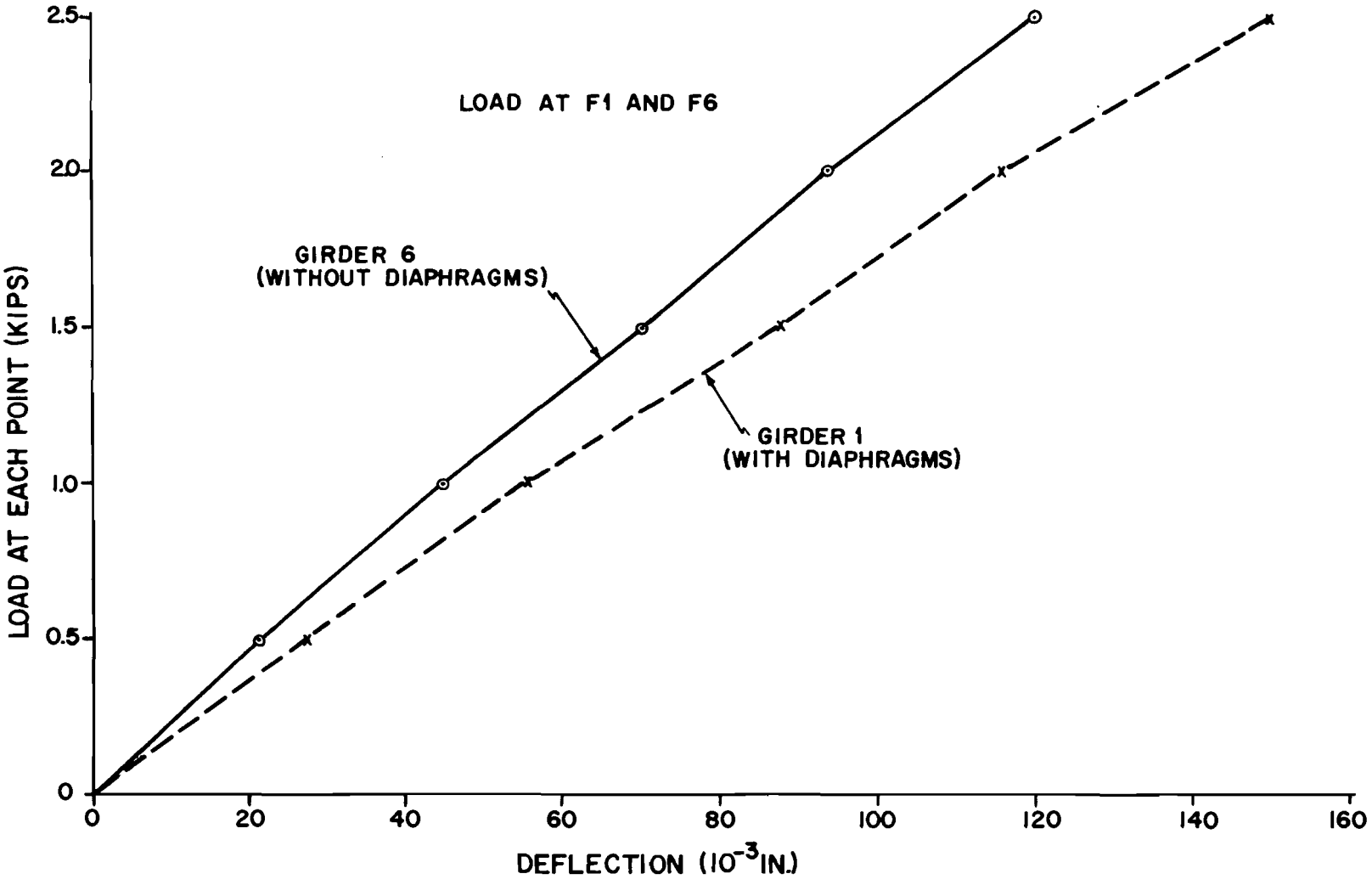

Fig. 5.49 Bridge 3, midspan girder deflection due to point loads at midspan (tested after lateral impacts).

5.5 Overload and Ultimate Truck Load Tests

Tests were conducted after all the diaphragms were removed to check the bridge ultimate load capacities without diaphragms.

Bridge 1: Truck loads TA, TB and TC (see Fig. 2.25 for their location) were applied. All the loads were increased to 3 times standard truck loads (which includes 25 percent impact factor). Then the side truck load TA was increased until failure while trucks TB and TC were held at 3 times service load. Near ultimate load, flexural tension cracks propagated through the girder under truck TA and into its flange. Just before failure some crushing of concrete at the top of the flange was noted. At a load level of 9 TA + 3 (TB + TC), a sudden failure was observed. The flange completely separated from the girder which broke into two pieces (see Fig. 5.50) under the release of energy stored in the loading girder.

The load deflection relationships are shown in Fig. 5.51, where X and Y are used as standard truck load multipliers as shown in that figure. These results indicate that the bridge behaved essentially elastically up to X = Y = 2. The large change in deflection from X = Y = 2 to X = Y = 3 indicates that somewhere in this load range the girders cracked. This becomes clear from the load vs. midspan girder strain plots (Fig. 5.52), which show that in the load range X = Y = 2.2 to X = Y = 2.6 all the girders cracked. The deflection differences between the load case X = 0, Y = 1 and the case X = 1, Y = 1 show that the Grider 6 deflection was not affected by application of truck TA, when the bridge behaved elastically. After cracking in the higher load stages, increases in truck TA caused additional downward deflection in Girder 6. This means that a somewhat better load distribution exists at higher loads. Because of the unknown nonlinear behavior of the girder deflections, no accurate quantitative estimate could be made from the deflection values about the change in load distribution characteristics at overloads. However, an approximate estimate may be obtained from Girder 1 (maximum loaded girder) strains. Before cracking the moment at midspan of Girder 1 due to a single truck load TA was 93.1 x 0.453 or 42.3 in.-kip (obtained from Appendix B, Table B2, Series-C). After cracking the change in Girder 1 midspan strain due to application of

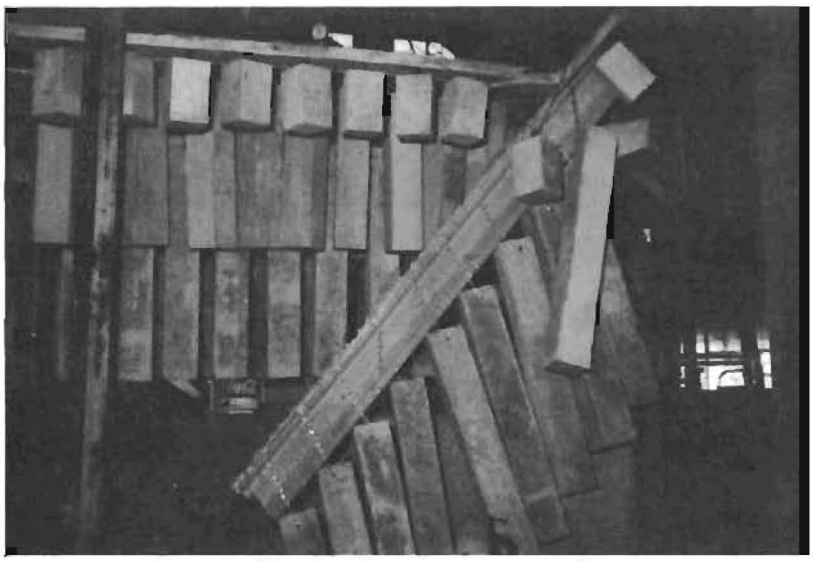

Fig. 5.50 Bridge 1 after failure.

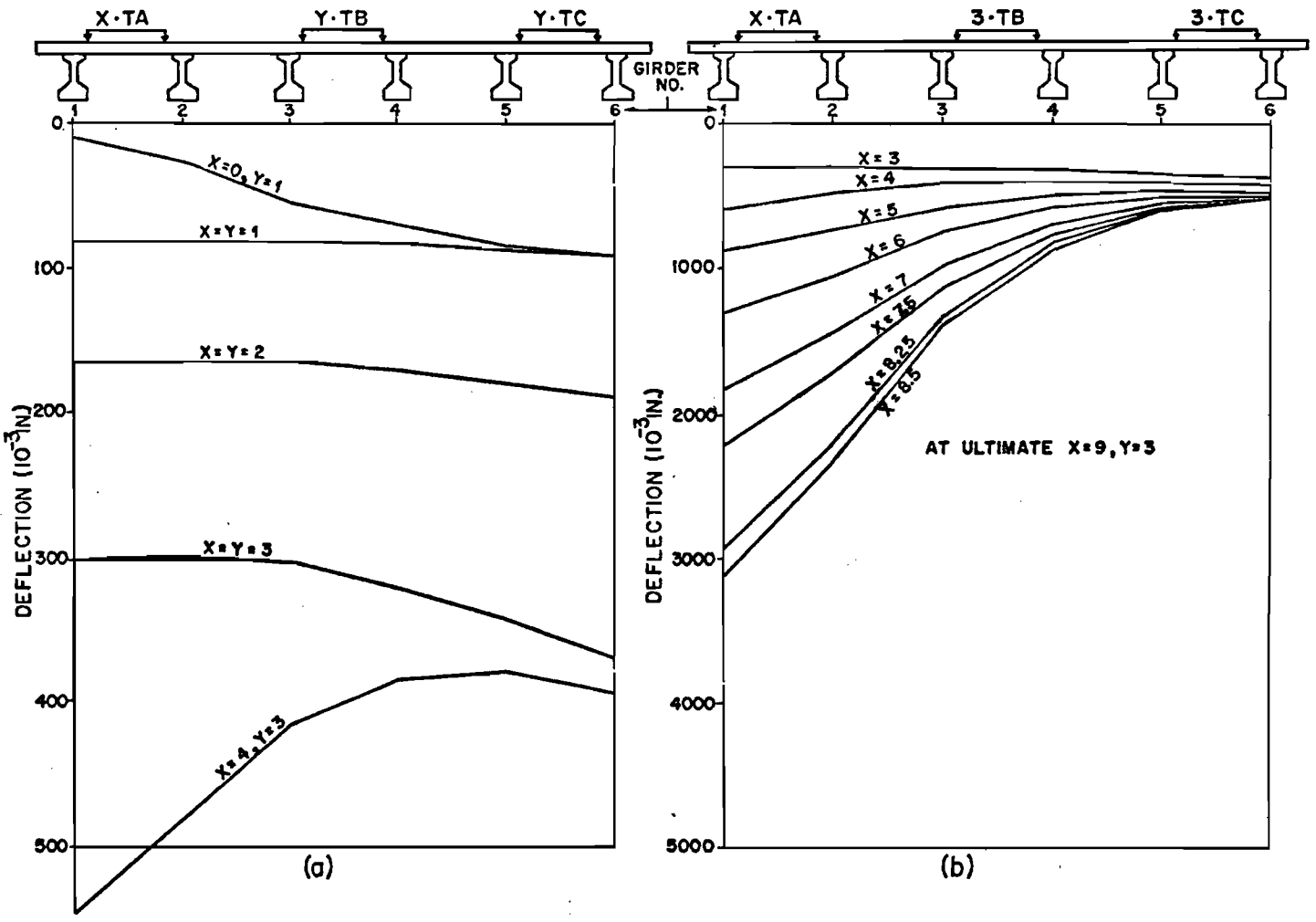

Fig. 5.51 Bridge 1 (45° skew, 172 in. span, no diaphragms); ultimate load test, midspan girder deflections.

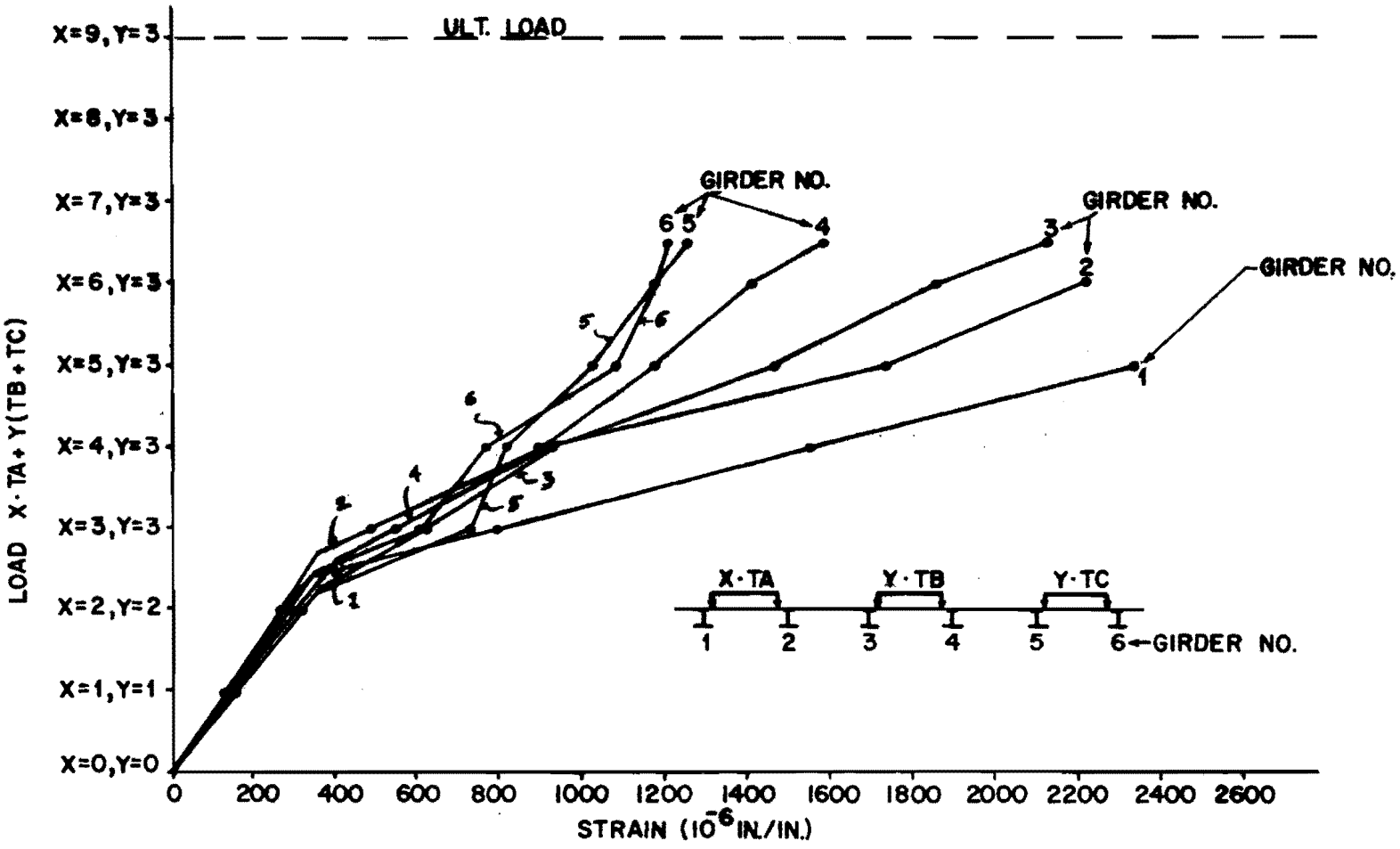

Fig. 5.52 Bridge 1 (45° skew, 172 in. span, no diaphragms); ultimate load test, midspan strains.

2 TA (from Fig. 5.52, from X = 3, Y = 3 to X = 5, Y = 3) is (2340 - 800) = 1540 micro in./in. A girder moment-strain curve for an identical girder with exactly the same strain gage location was previously experimentally determined by Barboza.[7] Using this moment-strain relationship the change in girder moment due to strain change from 800 to 2340 micro in./in. is obtained as (204 - 158) or 46 in.-kip. Therefore, after cracking the change in Girder 1 midspan moment due to a single truck TA is 46/2 or 23 in.-kip in contrast to 42.3 in.-kip when all the girders were uncracked. This shows that the moment coming to Girder 1 due to TA after cracking is about (23/42.3) or 0.54 that before cracking. Corresponding experimental values of $M/\Sigma M$ for Girder 1 due to TA shows that this ratio is about 0.72 that before cracking. This discrepancy indicates the aforementioned results are very approximate. However, both the changes in the absolute values and in the relative values are very significant, indicating considerable load redistribution occurred after cracking of the girders.

Bridge 4: This bridge was loaded with design truck loads (including 25 percent impact factor) T1, T2 and T3 to produce a maximum moment in Girder 3. Load locations are shown in Fig. 2.27. Maintaining the side truck loads constant at design service load level, the central truck load T2 was increased. When T2 reached 8.5 times the design service load value, the bridge held the load for about 5 minutes, then suddenly failed, breaking all the prestressing strands in Girder 3. At its interface this girder and its flange separated over about a 24 in. length near the midspan. Large cracking in Girder 4, moderate cracking in Girders 2 and 5 and absolutely no sign of any damage in Girders 1 and 6 was observed.

Deflection plots in Fig. 5.53 show that up to about X = 3 (X is a truck load multiplier as shown in Fig. 5.53) the bridge behaved elastically. A larger increase in deflection between X = 3 and X = 3.5 indicate that somewhere in this load range both Girders 3 and 4 cracked. This is more clearly seen from the strain plots (Fig. 5.54), which indicate that first cracking occurred at X = 3.25. Girders 1 and 6 deflections were unaffected by central truck load T2 throughout the loading range, indicating no appreciable change in load distribution to Girder 1 and 6 occurred at higher loads. Since almost no change occurred in Girder 1 and 6 strains due to T2, this was confirmed.

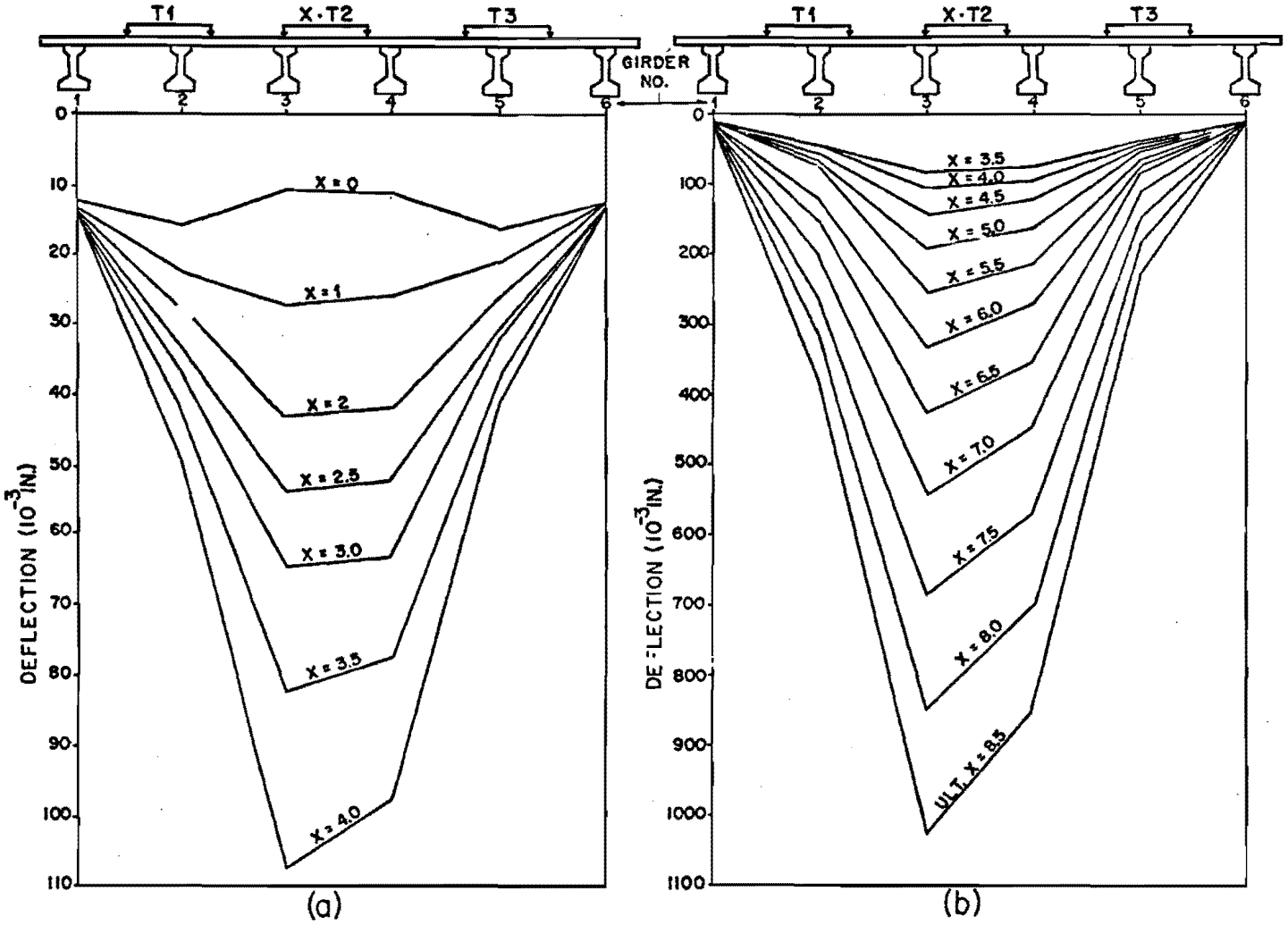

Fig. 5.53 Bridge 4 (straight, 107 in. span, no diaphragms); ultimate load test, midspan girder deflections.

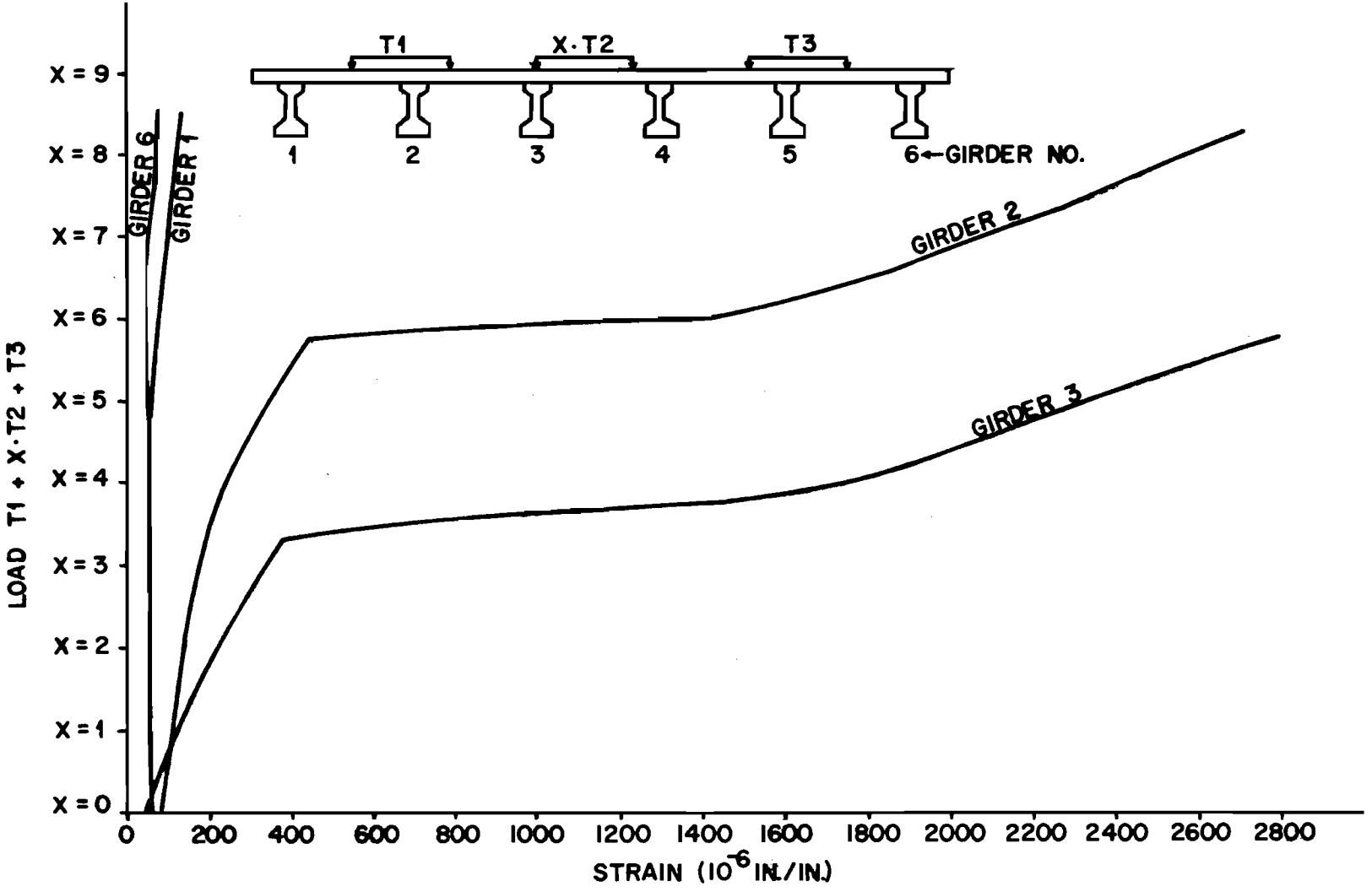

Fig. 5.54 Bridge 4 (straight, 107 in. span, no diaphragms); ultimate load test, midspan girder strains.

However, after the first cracking in Girder 3, the rate of change of strain in Girder 2 (see Fig. 5.54) showed a considerable increase. Girder 3 cracked at X = 3.25. From X = 0 to X = 3.25, the change in midspan strain in Girder 2 was (184 - 81) or 103 micro in./in. Average change in midspan strain of Girder 2 in this loading range was 103/3.25 or 31.7 micro in./in. per truck load T2. In the load range of X = 3.25 to X = 5.75 (i.e., after cracking of Girder 3 and before cracking of Girder 2) average midspan Girder 2 strain was (411 - 184)/(5.75 - 3.25) or 91 micro in./in. due to one truck load T2. Since before cracking of a girder section the moment-strain relationship may be considered approximately linear, the above results indicate that a considerable increase in load distribution to Girder 2 occurred between X = 3.25 to X = 5.75. As the total midspan moment due to a single truck load T2 at any stage of loading remains essentially constant, a large increase in Girder 2 moment indicates a proportionate decrease in the moment of the maximum loaded girder (i.e., Girder 3). That is to say, a considerable load redistribution occurred at higher loads. No quantitative estimate for the change in Girder 3 moment after cracking could be made because of the unknown moment-strain relationship for these girders beyond cracking moment.

AASHO[1] requires a minimum ultimate load capacity of 1.5 dead load plus 2.5 (live load = impact factor). For the type of bridges considered, the maximum live load corresponds to three truck loads with a 10 percent reduction factor (Sec. 1.2.8 and 1.2.9 of AASHO). The model standard truck loads including impact factor are shown in Fig. 2.20c. The dead load of the model bridges (including model scale compensating dead loads) is 114 lbs. per in. The span of Bridge 1 is 172 in. and that of Bridge 4 is 107 in. From these values, the required total ultimate moment at the midspan section is obtained from statics as 1315 in.-kip and 607 in.-kip for Bridge 1 and Bridge 4, respectively. The experimental ultimate load for Bridge 1 was 15 truck loads plus the dead load of the bridge and that for Bridge 4 was 10.5 truck loads plus the bridge dead load. Corresponding total ultimate moments are obtained from statics as 1935 in.-kip and 730 in.-kip for Bridge 1 and Bridge 4, respectively. This shows that the experimental ultimate capacity of Bridge 1 is 1.47 times the AASHO requirement and that

of Bridge 4 is 1.20 times the AASHO requirement. The test loads, particularly in Bridge 4, were much more nonuniform than the design truck loads. Even so the experimental ultimate moments for both bridges without diaphragms are more than the design requirements indicating more than adequate strength for the type of bridges tested.

Bakir[5] tested a bridge identical to Bridge 1 (see Fig. 2.3) of this investigation with the same types and locations of diaphragms. The bridge was loaded with 3 truck loads, TA, TB and TC as shown in Fig. 2.25. Initially the truck loads TB and TC were applied and both were increased to 3 times the standard truck load. Maintaining these loads at this level, the side truck load TA was applied and was increased to near failure conditions. During this test all the diaphragms were present. The loads were then removed and the interior diaphragms were taken out. The bridge was then reloaded after the truck direction and location were interchanged so that the main loading would be applied to the previously lightly damaged side of the bridge. All the trucks were increased to 3 times the standard truck load. Maintaining TB and TA at this load level, the side truck TC was then increased to failure.

By comparing girder deflections and strains for these tests Bakir[5] concluded that the removal of the interior diaphragms did not decrease the ultimate strength of the bridge. On the contrary for a given overload he observed somewhat lower girder strains and deflections when the diaphragms were removed. However, he mentioned that the observed increase in stiffness was probably due to minor differences in girder stiffnesses and not necessarily due to the removal of the diaphragms. From a similar test on a 30^{o} skew bridge of the same type Barboza[7] found that neither the girder deflections at ultimate load conditions nor the ultimate strength were appreciably affected by the presence of interior diaphragms. However, it should be pointed out that in both the ultimate tests conducted by Bakir and Barboza, the diaphragms were discontinuous and located at 1/3 points of the span and the bridge was loaded with three lines of trucks. With continuous diaphragms at midspan and with less evenly distributed loading, a greater effect of diaphragms may be found.

In general the truck load ultimate tests indicate that the bridges behaved elastically up to considerable overloads. Among all the bridges tested, load distribution in Bridge 4 was found to be the most nonuniform. Even in this bridge, the results indicate that the overload application of two equivalent design vehicles in addition to the normal three design truck loads did not cause any permanent damage to the bridge. This is probably enough of a safety factor to permit crossing of heavy individual loads under emergencies. Results show considerable redistribution of loads after cracking at higher loads. The ultimate capacities were found to be more than adequate even without any diaphragms. The ultimate tests reported here showed no significant effect of diaphragms on the bridge behavior at overload and ultimate load conditions.

5.6 Slab End Static Load Tests

Four different kinds of approach slab edges were tested. They were: (a) standard slab with end diaphragm; (b) standard slab without end diaphragm; (c) slab with extra reinforcement and no diaphragm, and (d) deepened slab with no diaphragm. The standard slab section details were as called for in the Texas Highway Department drawings (see Appendix A, Figs. A1 and A2). The end diaphragm slab with extra reinforcement and deepened slab details is shown in Figs. 2.8 and 2.10. The test results are summarized in Table 5.5. Load designations are as discussed in Sec. 5.2 of this chapter. Reference grids for loads are shown in Figs. 5.1 and 5.2. Figure 5.55 shows the results with grouping for different types of slab edge conditions. The bridge number and the angle of skew of the bridge are shown by a number followed by the skew angle in degrees. For example, 3 - 0^{o} means Bridge 3, zero degree skew. Edge distance of 0.88 in. for the straight bridges (i.e., 0^{o} skew) and 1.25 in. for the 45^{o} skew bridge correspond to wheel loads applied at the extreme edge, i.e., the outer edge of the loading block (as in Fig. 2.20a) flush with the slab edge. In other cases load distances from the slab edge are equal to the diaphragm center line distance from the edge.

The measured ultimate load for the unsupported edge with increased reinforcement in Bridge 3 with the load placed 0.88 in. from the edge (shown with a "?" mark) is doubtful. Near the ultimate load in this case the load

TABLE 5.5

END SPAN WHEEL LOAD TESTS

Bridge No.	Load at*	Distance from Edge (in.)**	Cracking Strain (10^{-6} in./in.)	Cracking Load (Wheel Load)	Ultimate Load (Wheel Load)	Failure Mode	Remarks
2	J34	3.25	218	2.02	5.20	Flexure	Standard Slab
2	B34	3.25	---	----	5.20	Flexure	Standard Slab
2	A45	1.25	---	----	4.85	Flexure	Standard Slab
3	J12	2.75	157	3.12	16.60	Flexure	With End Diaphragm
3	B12	2.15	160	1.04	9.90	Flexure	Deepened Slab
3	B56	2.15	104	0.95	8.50	Flexure	Additional Reinforcement
3	K23	0.88	189	3.32	10.90	Shear	With End Diaphragm
3	A23	0.88	141	0.85	6.34	Flexure	Deepened Slab
3	A45	0.88	---	----	4.73?	Flexure	Additional Reinforcement
3	J56	2.75	---	----	7.38	Flexure	Standard Slab
3	K45	0.88	---	----	6.15	Flexure	Standard Slab
4	A56	0.88	---	4.00†	5.68	Flexure	Additional Reinforcement
4	A23	0.88	210	1.08 4.00†	5.22	Flexure	Standard Slab
4	A12	0.88	---	4.00†	6.15	Flexure	Deepened Slab

* See Figs. 5.1 and 5.2, for load locations.

One wheel load = 0.528 kip
[without any impact factor]

** Distance measured along the girder.

† Load at first crack observed.

? Uncertain value, load cell slipped

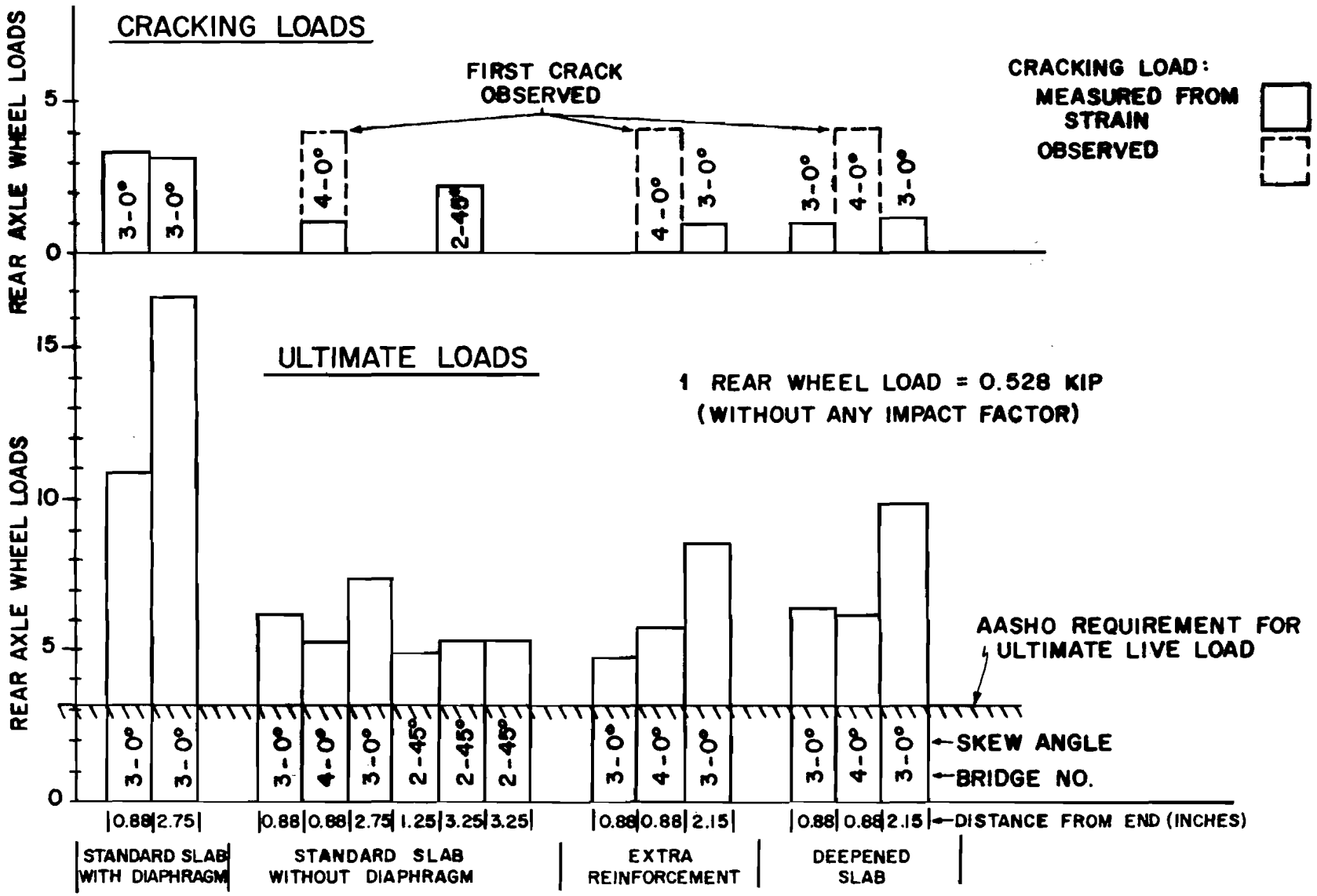

Fig. 5.55 Cracking and ultimate wheel loads for slab at approach span.

cell slipped off and the recorded load was probably less than the actual. The results show considerable reductions in ultimate strength when the end diaphragms are removed. This reductionwas to some extent compensated for when extra reinforcement was provided. With deepened slab some additional gain in the ultimate strength was obtained.

AASHO specifications do not indicate any ultimate capacity requirement for the slab. However, for prestressed concrete members it requires the computed ultimate capacity should be not less than 1.5 dead load + 2.5 (live load + impact). Neglecting the dead load of the slab (which is very small in this case) and considering an impact factor of 25 percent[1] for Bridges 1, 2, and 3 (for Bridge 4 this factor will be slightly higher) the required ultimate live load is obtained as 3.12 times the rear wheel load. This load is shown in Fig. 5.55 by a horizontal line. It may be seen from this figure that the ultimate loads in all the cases are considerably higher than required. That is, in terms of ultimate load the results show more than adequate strength for all the cases including standard slabs without end diaphragms. In terms of serviceability, however, cracking load becomes an important factor. The cracking loads computed from strain readings (Fig. 5.55) indicate that except for the cases with end diaphragms all other edge sections cracked at about 1 wheel load. In a few cases where visual observations were made, the first crack was not visible until 4 service wheel loads were applied. This suggests that, for the cases studied, the cracks are extremely fine at service loads and may not be harmful.

AASHO[1] specifies design moments for the interior portion of the slab. It does not provide any recommendation for the design of unsupported slab edges. For such cases it requires that the edges should be supported by diaphragms or any other suitable means. Until further criteria for serviceability and some further data on full scale tests can be developed, it is suggested that end diaphragms or other suitable stiffeners be provided for supporting the free edge of the slab.

5.7 Slab Punching Tests

The results of the slab punching tests are summarized in Table 5.6, where ultimate loads are expressed in terms of model rear wheel service loads without impact factor (one wheel load = 528 lbs.).

TABLE 5.6 PUNCHING TESTS ON SLAB

Bridge No.	Loading Block	Ultimate Wheel Load (Test)	Ultimate Wheel Load (ACI)
2	3.75 in. x 2.20 in.	16.1	7.3
2	3.63 in. x 1.75 in.	14.8	6.9
3	3.63 in. x 1.75 in.	12.1	5.9

It can be seen that the punching shear strength of the slabs is more than adequate. As AASHO specifications do not specify any requirements for slab shear capacity, the test results are compared with those calculated on the basis on ACI Building Code [2] requirements for two-way shear (Sec. 11.10.1.6). It may be seen from Table 5.6 that actual strengths are about 100 percent higher than predicted by the ACI formulas. In Bridge 3 one ultimate wheel load test was carried out on the side edge of the bridge (Load location was at H01. See Fig. 5.2 for grid coordinates.) The failure was in flexure and the ultimate load was 5.21 times the rear wheel load.

5.8 Stresses in Diaphragms

Diaphragm stresses were measured under service loads only. All the overload and ultimate load tests (except end span loadings as discussed in Sec. 5.6) were conducted after the removal of the diaphragms.

5.8.1 Interior Diaphragms

For all the service load cases (as in Appendix B) the diaphragm top and bottom fiber stresses were determined. In Bridge 2, some additional tests were conducted by applying a 1 kip point load directly above the diaphragm midspan (at G12 and D56 in Fig. 5.1). In all the bridge tests, the maximum diaphragm stresses were found to be due to truck loads TA, TB or TC. Maximum tensile and compressive stresses in interior diaphragms for all the bridges under service loads are given in Table 5.7. Modulus of rupture (cracking stress), calculated from the formula given in Sec. 9.5.2.2 of the ACI Building Code[2] (modulus of rupture = $7.5\sqrt{f'_c}$, where f'_c = compressive

TABLE 5.7 INTERIOR DIAPHRAGM STRESSES

Bridge No.	Modulus of Rupture (psi)	Maximum Tensile Stress (psi)	Maximum Compressive Stress (psi)
1	415	194	197
2	470	460	303
3	445	897	433
4	405	403	296

strength of concrete in psi) is also included in the table. The tensile stresses obtained from strain readings in the tests are calculated on the assumption of an uncracked section. In the table the large tensile stress for Bridge 3 indicates that the section has already cracked and the value 897 psi is not the real stress in the concrete. In general, results indicate that the stresses in the diaphragms are small. However, except for Type D1 (see Fig. 2.7a) diaphragms (as in Bridge 1), interior diaphragms can be expected to crack under service loads.

Under dynamic loads the exact maximum stresses could not be determined, as the record was made from an oscillograph, one channel at a time. From these records the phase angle between the upper and the lower gages in the diaphragms could not be determined. Strains measured due to load at F3 in Bridge 1 indicate that the maximum strain amplitude per kip amplitude of load at 4 Hz was 50 percent higher and at 7 Hz 30 percent lower than that under static load. Strains measured at the upper and lower reinforcement levels of the diaphragms of the full scale bridge showed very small values under both static and dynamic loads (see Sec. 2.10, Chapter 2 for tests). The maximum recorded strain was under dynamic load and its peak-to-peak value (i.e., double amplitude), was found to be less than 10 micro in./in., which would correspond to about 45 psi. Although the full scale bridge (see Fig. 2.30) is not exactly of the same type as considered in the present investigation (see Figs. 2.3 through 2.9), the results obtained from the prototype give an indication that the stresses in diaphragms under service loads are very small.

5.8.2 End Diaphragms

The measured stresses in the end diaphragms were negligible except for the end span loadings. Under service loads, highest stresses were observed when a 1 kip load (i.e., 1.89 times a rear wheel load) was applied directly on the top of the diaphragm midspan. In Bridges 1, 2, and 3 (no measurement was done in Bridge 4) the highest measured tensile stresses were 538 psi, 461 psi, and 300 psi, respectively. Corresponding moduli of rupture of concrete (calculated as in Sec. 5.8.1) are 426 psi, 458 psi and 466 psi, respectively, for Bridges 1, 2, and 3. As wheel load impact factors of 100 percent or more may be expected on bridge decks,[4] it appears that the diaphragms parallel to the support in skew bridges of the type tested (Bridge 1) may be expected to crack. However, because of very low stress levels the crack widths can be expected to be very fine. In other bridges, where the exterior diaphragms were normal to the girders (as in Bridge 2 and Bridge 3), chances of cracking are relatively less.

Compressive stresses in end diaphragms under service loads were found to be negligible in all the cases. Maximum observed compressive stress was only 310 psi.

CHAPTER 6

IMPLEMENTATION

6.1 Interior Diaphragms

The results show that the only beneficial role of the interior diaphragms is to distribute the live load somewhat more evenly. Within the practical range of bridge excitation, the diaphragms become less important under dynamic loads.

Since the distribution of the dead load is not affected by diaphragms, the effect of diaphragm inclusion on the total design moment of the girders will be significantly less than considerations based on live load moment alone. To illustrate the extent that diaphragms might reduce the total design moments of girders, ratios of the live load moment to the total girder moment were calculated for different types of slab and girder bridges of various spans. The total dead loads of these bridges (all are of 28 ft. roadway width and designed for HS20-44 loads) were obtained from a survey reported by Walker and Veletsos.[49] Girder dead load moments were calculated assuming all the bridges had five girders. The live load moments were calculated using AASHO[1] formulas for load distribution and impact factors. Fig. 6.1 shows that in all types of bridges the proportion of live load moment to the total design moment decreases very rapidly with increasing span.

Diaphragms were found to be more effective in distributing loads in bridges with larger S/L (i.e., girder spacing to span ratio), and $EI_G/(EI_S \cdot L)$ (i.e., girder stiffness to slab stiffness ratio values. Computer analysis of a prestressed concrete girder and slab bridge with S/L and $EI_G/(EI_S \cdot L)$ ratios of 0.19 and 32, respectively, showed less than a 10 percent reduction of live load moment when interior diaphragms were provided. The maximum reduction in live load moment found experimentally in the model studies was 11 percent (Bridge 4).

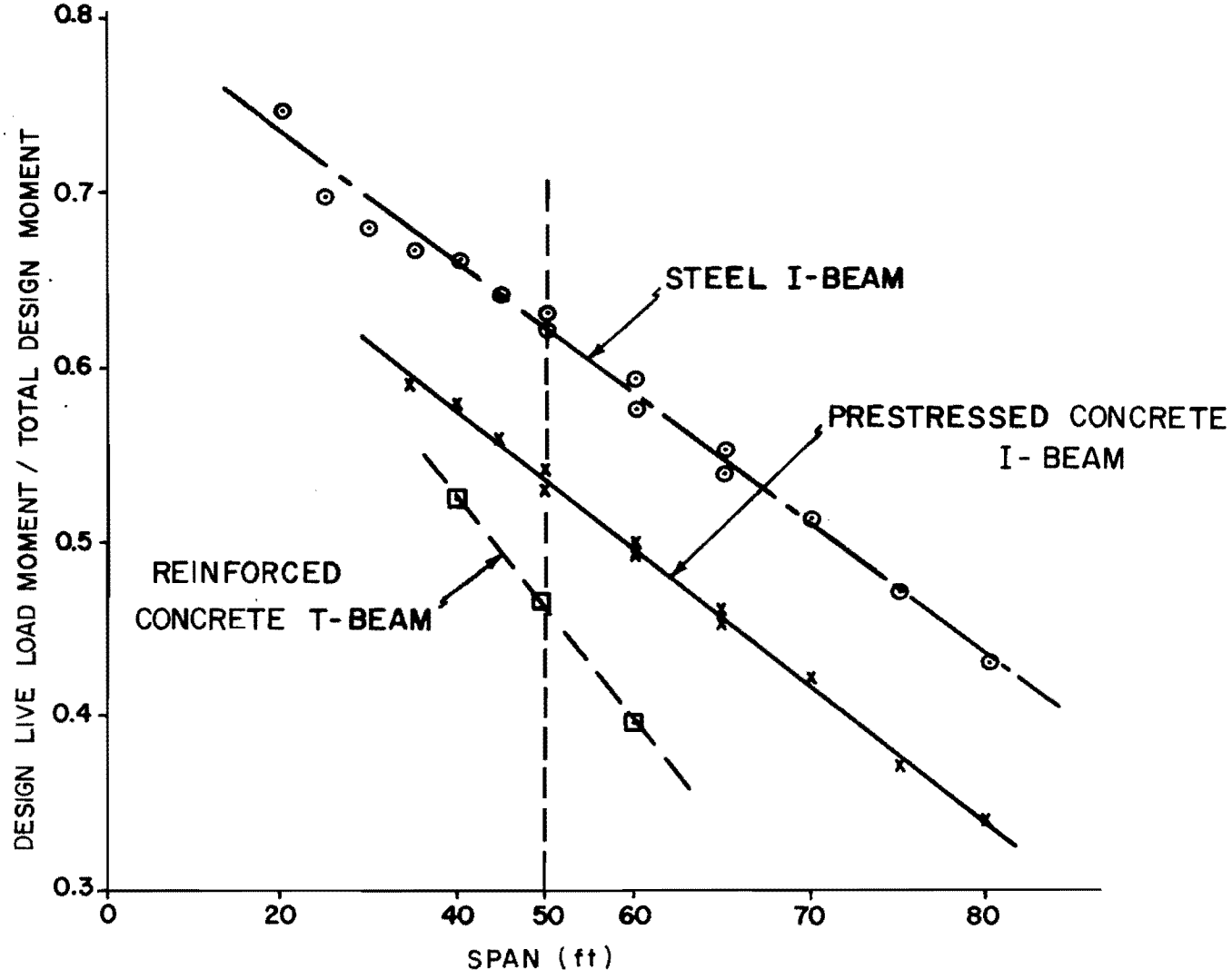

Fig. 6.1 Proportion of live load design moment for different bridge types.

The prototype span for this bridge is 50 ft. For a prestressed concrete bridge of this span, Fig. 6.1 indicates the proportion of live load moment as 0.54 (actual calculation for this bridge shows 0.51). Thus the reduction in total design moment for a girder due to the provision of interior diaphragms is the product 11 x 0.54 = 5.9 percent. While this may not be the absolute maximum possible reduction, it indicates the order of magnitude of the maximum possible reduction in the girder design moment due to provision of interior diaphragms.

A special load case sometimes considered important by the designer is that of a very heavy single vehicle crossing the bridge under emergency situations. In such cases, the maximum reduction in design moment due to provision of interior diaphragms will occur when the vehicle occupies the center lane. This corresponds closely to the truck load TB as shown in Fig. 2.26. For this case the experimental maximum reduction in live load moment was 21 percent in model Bridge 4. Assuming an extreme case with the overload vehicle three times as heavy as a standard HS20 truck load (i.e., total weight of 108 tons in prototype scale), the corresponding total load design moment reduction is only 15 percent.

Such reductions in girder design moment can only be realized if a detailed analysis is carried out. If the girders are designed using AASHO coefficients, no savings are possible. Even if a detailed analysis is carried out and the reduction in design moment is taken advantage of, a question exists as to whether the cost of providing the diaphragms is really justified.

This economics question can be studied by comparing the cost of two different bridges designed for the same loads and the same safety factors. In the first bridge interior diaphragms are provided while in the second bridge interior diaphragms are omitted, but the girder strength is increased to compensate for the reduced load distribution so that both have the same safety factor. The extreme case chosen for this analysis is the 50 ft. span prototype of model Bridge 4 loaded with the 108T extreme overload single vehicle. This is the case where the effect of diaphragms was found to be most pronounced. Under this load the bridge with diaphragms has a 15 percent lower girder design moment. To compensate for this in the second bridge

(without diaphragms) the girder strengths must be increased 15 percent. Since the number of prestressing strands in a girder of this type (Type C) can be considered approximately proportional to its strength, the required 15 percent increase in strength can roughly be obtained by increasing the number of prestressing strands by 15 percent. Bridge 4 prototype girders have 14 strands; a 15 percent increase would be approximately 2 strands. Thus, the bridge without interior diaphragms will have roughly the same safety factor as the one with the diaphragms if two additional strands are provided in each girder of the bridge without diaphragms. In some extreme cases girder depths might have to be increased, but this would not be the usual case.

Realistic cost estimates obtained from local contractors indicate that the cost of a single interior diaphragm for this type of bridge varies from $50 to $150. Assuming an average cost of $100 per diaphragm, the cost of interior diaphragms per girder in the bridge case being studied is equal to $100 x 5/6 or $83 (a total of 5 diaphragms were used in Bridge 4, which had 6 girders). Information obtained from a local prestressing yard indicates that the type of strands (7 wire, 1/2 in. φ strands) used in the bridge concerned cost about 10¢ per ft. in place. From this, the cost of two additional strands for a 50 ft. long girder is $10, which is less than 1/8 the cost of providing the interior diaphragms. This simple example clearly demonstrates that even under this very extreme loading condition where the diaphragms might be found most effective, their provision cannot be justified for structural safety and economics. The same comparison with ordinary AASHO truck loads indicates the diaphragms to be 20 times as costly as additional strands.

To approximate the possible percentage saving in the superstructure cost, the cost of the total superstructure including the slab, the girders and the diaphragms for the example case was estimated from recent twelve month average bids for Texas Highway Department bridges. The estimated cost for the total superstructure for Bridge 4 is $14,500. The estimated cost of one row of five diaphragms at midspan is $500, which corresponds to 3.5 percent of the total superstructure cost. Thus in this example, even if no other

saving in time or convenience results from omission of diaphragms about 3.5 percent of the superstructure cost can be saved. In addition it appears that the elimination of interior diaphragms will significantly reduce the superstructure construction time and thus result in added benefits.

Recent construction of prestressed concrete girder and slab bridges on Interstate Highway 35 in Austin indicate that interior diaphragms are not necessary for construction purposes. Figure 6.2 shows typical construction stages. Precast prestressed girders are erected and held in position with temporary timber bracings and tiedowns (Fig. 6.2a). Figure 6.2b shows placement of the deck slab formwork with end diaphragms cast at only one end of the girders, and with temporary braces at the interior of the span and at the other end of the span (Fig. 6.2c). Thus, the diaphragms are not a construction necessity.

Results discussed in Chapter 5 showed that even without the diaphragms the girders are conservatively overdesigned when load distribution is determined according to AASHO[1] specifications. This is even more pronounced with skew bridges. Further, it was found that if the interior diaphragms are provided, they make the girders more susceptible to damage from lateral impact. Thus, whether the design is based on a detailed analysis or on AASHO[1] load distribution formulas, interior diaphragms should not be provided in simply supported prestressed concrete girder and slab bridges of this type where the slab is continuous over the girders which are composite.

6.2 End Diaphragms

It was shown that the end diaphragms act as a supporting member for the free end of the slab at the approach span. As far as ultimate load capacity is concerned, the test results indicate an adequate strength even without the diaphragms. However, observed cracking at low loads (of about one service wheel load without any impact factor) makes the slab edge without diaphragms of questionable serviceability. Thickening the slab or providing additional reinforcement increased the ultimate strength but did not significantly improve cracking load capacity.

As the use of inverted T bent caps (Fig. 6.2c) is not uncommon, it appears that the web of this type of bent cap can be used as a suitable

(a) Erected girders with temporary timber braces and tie downs

(b) Formwork in progress with only one diaphragm (at one end of the span) cast

(c) Temporary braces at the end of the span

Fig. 6.2 Construction of prestressed concrete girder and slab bridges.

supporting member for the edge of the slab. With development of appropriate details, end diaphragms might be removed.

The AASHO[1] specifications provide formulas for the design moment for slabs in the interior span only (where the slab is continuous). Slabs designed for this moment will not have the intended safety factor at the free edges of the slab, unless some adequate supporting members, such as end diaphragms, are provided. Therefore, unless a suitable criterion for serviceability requirements is developed, it is suggested that the end diaphragms be provided as indicated in AASHO[1] specifications.

CHAPTER 7

SUMMARY, CONCLUSIONS AND RECOMMENDATIONS

7.1 Summary of the Investigation

The object of this investigation was to study the role of diaphragms in simply supported prestressed girder and slab bridges, in order to develop more rational rules for the provision of diaphragms. For this purpose, four 1/5.5 scale microconcrete models of Texas Highway Department standard prestressed concrete girder and slab bridges were tested. Variables considered in the experiments were--span and skew angle of the bridges; stiffness, location and number of diaphragms. Service level bridge behavior was examined under static, dynamic, and impact loads, as the diaphragms were incrementally removed. Finally, two bridges were tested to failure under truck loads to examine their behavior under overload and ultimate load conditions, while the other two bridges were tested to failure under lateral impacts and various ultimate wheel loads. A computer program was verified using the experimental results and was used to generalize the study.

7.2 Summary of Results

The findings of this investigation are:

(1) Load distribution under static service loads: The provision of diaphragms increased the design moment for exterior girders and reduced the design moment for interior girders. In reducing the design moment diaphragm effectiveness was found to be greater in bridges with large girder spacing-to-span ratios (S/L) and large girder stiffness to slab stiffness ratios ($EI_G/(EI_S \cdot L)$). In distributing loads diaphragms are most effective when they are located at midspan. When located at the end of the span, their effect on load distribution is negligible. The provision of diaphragms produced a maximum of 5 to 8 percent reduction in design moment when standard AASHO truck loads governed the design. A maximum reduction of 15 percent was

noted for the very special case of an extremely heavy single overload vehicle (108T) governing the design. Cost analyses indicated that it was substantially more economical to increase the prestressed girder strength than to provide diaphragms to decrease the design moment. For all the cases studied including that where neither interior nor end diaphragms were provided, it was found that the AASHO load distribution factors are conservative.

(2) Static overloads and ultimate loads: Results indicate that the bridges of this type, even without diaphragms, can carry considerable overloads without causing any permanent damage to the girders. Bridge ultimate flexural capacities without any diaphragms were found to be more than adequate. Considerable reduction in load distribution to the maximum loaded girder was observed under overloads after first cracking.

(3) Unsupported slab edges: For the bridges tested, ultimate load capacities of the slab edges (such as the slab at the approach span and between the girders) were found to be adequate even without any end diaphragms. In such cases, however, very early cracking was noted (at about 1 service wheel load). Thickening the slab or providing extra reinforcement (see Fig. 2.10) increased the ultimate load capacity but did not improve the cracking load to any significant extent. Results indicate that the cracks were very fine at service loads (could not be visually detected). End diaphragms increased both cracking loads and ultimate loads to a great extent.

(4) Dynamic loads: Free vibrations after vertical impacts on the bridges indicated two significant modes of vibration: the longitudinal and torsional modes (Figs. 1.2a and 1.2b). Natural frequencies for these modes of vibrations were found to be independent of the presence or absence of diaphragms. No effect of diaphragms was observed on the damping coefficient of bridge vibration. The presence or absence of diaphragms did not influence the dynamic amplifications of the bridges when subjected to sustained cyclic loads. Load distribution characteristics of the diaphragms did not show any significant change under such loads. Indeed, on an average, within the normal frequency range of bridge excitation, the diaphragms were found to be slightly less effective under dynamic loads than under static loads.

(5) Lateral impacts: By making the girders more rigid laterally, the diaphragms reduced the energy absorption capacity of the girders, and thereby made the girders more vulnerable to damages from lateral impacts.

(6) Stresses in diaphragms: Under service loads the compressive stresses in the diaphragms were found to be very low (highest observed stress = 433 psi). However, diaphragms cast monolithically with the slab can be expected to have tensile cracks.

7.3 Conclusions and Recommendations

7.3.1 Interior Diaphragms

The only important function of interior diaphragms was that of distributing the loads more evenly across the bridge. However, for this type bridge under no circumstances would significant reductions in design girder moment be expected because of the provision of interior diaphragms. In fact, the provision of diaphragms may even increase the design moment. Cost studies indicated that it is more economical to increase the girder strength by providing extra strands than to decrease the design moment by providing diaphragms. The design distribution factors recommended by AASHO[1] are conservative even without any diaphragms. The interior diaphragms do not seem to be necessary for construction purposes for prestressed concrete girder and slab bridges. Tests indicated that provision of diaphragms increased the intensity of girder damages from lateral impacts. Therefore, whether a detailed analysis is carried out or AASHO[1] load distribution formulas are followed for the design, it is recommended that interior diaphragms should not be provided in simply supported prestressed concrete girder and composite, transversely continuous slab bridges.

7.3.2 End Diaphragms

The only significant role of end diaphragms is that of a supporting member for the otherwise free slab edge at the approach span. If the slab is designed in accordance with the AASHO formula, unsupported slab edges will have considerably less safety margin than intended in AASHO.[1] The test results indicate a possibility of an alternate design by thickening the end slab or by providing additional reinforcement in the slab in the approach

span zone. To make such a design feasible it is necessary to determine a suitable design criterion and develop a reliable method. Until this is done satisfactorily, it is suggested that the exterior diaphragms be provided as recommended in AASHO.[1] Wherever inverted T bent caps are used, it appears that the web of such a bent cap may suitably be used as a supporting member for the slab to replace the end diaphragms, with development of suitable details.

B I B L I O G R A P H Y

1. American Association of State Highway Officials, Standard Specifications for Highway Bridges, Tenth Ed., 1969.

2. American Concrete Institute, Building Code Requirements for Reinforced Concrete (ACI 318-71), Detroit, Michigan, 1971.

3. Alani, A. F., and Breen, J. E., "Verification of Computer Simulation Methods for Slab and Girder Bridge Systems," Research Report No. 115-1F, Center for Highway Research, The University of Texas at Austin, August 1971.

4. Al-Rashid, Nasser I., Lee, Clyde E., and Dawkins, William P., "A Theoretical and Experimental Study of Dynamic Highway Loading," Research Report 108-1F, Center for Highway Research, The University of Texas at Austin, May 1972.

5. Bakir, N. N., "A Study of a 45^{o} Skew Simply Supported Bridge," M.S. thesis, The University of Texas at Austin, May 1970.

6. Balog, L., Discussion on the paper No. 2381, entitled "Highway Bridge Floors - A Symposium," Transactions, ASCE, V. 114, 1949.

7. Barboza, N. J., "Load Distribution in a Skewed Prestressed Concrete Bridge," M.S. thesis, The University of Texas at Austin, August 1970.

8. Bendat, J. S., and Piersol, A. G., Measurement and Analysis of Random Data, John Wiley and Sons, Inc., New York, 1966.

9. Bergland, G. D., "A Guided Tour of the Fast Fourier Transform," IEEE Spectrum, July, 1969.

10. Biggs, John M., Introduction to Structural Dynamics, McGraw-Hill Book Company, New York, 1964.

11. Biggs, J. M., Suer, H. S. and Louw, J. M., "The Vibration of Simple Span Highway Bridges," Journal of the Structural Division, ASCE, Vol. 83, No. ST 2, March 1957.

12. Bramer, C. R., and others, "Effectiveness of Diaphragms in Steel Stringer Bridges," Highway Research Program, North Carolina State University at Raleigh, June 1966.

13. Buth, E., and others, "Evaluation of a Prestressed Panel, Case in Place Concrete Bridge, Research Report 145-3, Texas Transportation Institute, Texas A & M University, College Station, Texas, September 1972.

14. Cabera, Francesco M. Y., and Menditto, Giovanni, "Influence of Travel Surface Unevenness on the Dynamics of a Bridge Deck Traversed by Several Moving Loads in Tandem," Construzioni in Cemento Armato, Italcementi, 1971.

15. Carpenter, J. E., and Magura, D. D., "Structural Model Testing - Load Distribution of Concrete I-Beam Bridges," Journal of PCA Research and Development Laboratories, September 1965.

16. Gustafson, W. C., and Wright, R. N., "Analysis of Skewed Composite Girder Bridges," Journal of Structural Division, ASCE, V. 94, No. ST4, April 1968.

17. Hendry, A. W., and Jaeger, L. G., The Analysis of Grid Frameworks and Related Structures, Chatto and Windus, London, 1958.

18. Hendry, A. W., and Jaeger, L. G., "Load Distribution in Highway Bridge Decks," Discussion by the authors, Transactions, ASCE, V. 123, 1958.

19. Jenkins, G. M., and Watts, D. G., Spectral Analysis and Its Applications, Holden-Day, Inc., San Francisco, 1968.

20. Kinnier, H. L., "A Dynamic Stress Study of the Weyer's Cave Bridge," Vibration Survey of Composite Bridges, Progress Report No. 2, Virginia Council of Highway Investigation and Research, Charlottesville, Virginia, August 1963.

21. Kumar, Brajendra, "Effects of Transversals in T-Beam and Slab Bridges," Institution of Engineers (India), Journal V. 46, No. 3, Pt. C12 November 1965.

22. Leyendecker, E. V., "Behavior of Pan Formed Concrete Slab and Girder Bridges," Ph.D. dissertation, The University of Texas at Austin, June 1969.

23. Lount, A. M., "Distribution of Loads on Bridge Decks, "Journal of Structural Division, ASCE, V. 83, No. ST4, July 1957

24. Lightfoot, E., and Sawko, K., "Grid Frameworks Resolved by Generalized Slope-Deflections, Engineering, (London), V. 187, January 1959.

25. Makowski, Z. S., Discussion on the paper entitled "Distribution of Loads on Bridge Decks" by A. M. Lount, Journal of the Structural Division, ASCE, V. 84, January 1958.

26. Massonnet, C., "Methode de Calcul des Ponts a Poutres Mulliples Tenant Compte de leur resistance a la torsion" (Method of Calculation of Bridges with Several Longitudinal Beams, Taking into Consideration Their Torsional Resistance), Zurich, International Association for Bridge and Structural Engineering Publications, V. 10, 1950.

27. Mattock, A. H., and Kaar, P. H., "Precast-Prestressed Concrete Bridges 6. Test of Half-Scale Highway Bridge Continuous Over Two Spans," Journal of the Portland Cement Association Research and Development Laboratory, V. 3, No. 3, September 1961.

28. Mehrain, M., "Finite Element Analysis of Skew Composite Girder Bridges," Report No. 67-28, Structural Engineering Laboratory, The University of California, Berkeley, California, November 1967.

29. Mirza, S. M., White, R. N. and Roll, R., "Materials for Structural Models," Preprints, ACI Symposium, Models for Concrete Structures, Dallas, Texas, March 1972.

30. Newmark, N. M., "Design of I-Beam Bridges," Highway Bridge Floors - A Symposium, Paper No. 2381, Transactions, ASCE, V. 114, 1949.

31. Newmark, N. M., "A Distribution Procedure for the Analysis of Slabs Continuous over Flexible Beams," Bulletin No. 304, University of Illinois Engineering Experiment Station, 1938.

32. Oran, C., and Veletsos, A. S., "Analysis of Static and Dynamic Response of Simple-Span, Multi-Girder Highway Bridges," Civil Engineering Studies, Structural Research Series No. 221, Department of Civil Engineering, University of Illinois, Urbana, Illinois, 1958.

33. Ramesh, C. K., Kalani, M., and Donde, P. M., "Study of Cross-Girders in a Skew Bridge Deck System," Indian Concrete Journal, V. 44, No. 11, November 1970.

34. Rowe, R. E., Concrete Bridge Design, John Wiley and Sons, New York, 1962.

35. Sandars, W. W., Jr., Munse, W. H., "Load Distribution in Steel Railway Bridges," Journal of the Structural Division, ASCE, December 1969.

36. Sawko, F., and Cope, R. J., "The Analysis of Skew Bridge Decks - A New Finite Element Approach," The Structural Engineer, V. 47, No. 6, June 1969.

37. Schwartz, Mischa, Information Transmission, Modulation, and Noise, McGraw-Hill Book Company, Inc., New York, 1959.

38. Self, M. W., Experimental Investigation of the Influence of an Interior Diaphragm on the Behavior of a Model Prestressed Concrete Bridge Under Static and Dynamic Loading, Engineering and Industrial Experiment Station, College of Engineering, University of Florida, Gainesville, July 1969.

39. Sengupta, Sobhan, "The Effect of Diaphragms in Prestressed Concrete Girder and Slab Bridges," Ph.D. dissertation, The University of Texas at Austin, January 1974.

40. Sithichaikasem, S., and Gamble, W. L., "Effects of Diaphragm in Bridges with Prestressed Concrete I-Section Girders," Civil Engineering Studies, Structural Research Series No. 383, University of Illinois, Urbana, Illinois, February 1972.

41. Smith, Donald E., "A Digitally Implemented Spectral Analysis for Use in the Study of Fluctuations in Turbulant-Like Plasmas," M.S. thesis, The University of Texas at Austin, August 1970.

42. Stuart, R. D., An Introduction to Fourier Analysis, John Wiley & Sons, New York, 1961.

43. Thomas, F. G., and Short, A., "A Laboratory Investigation of Some Bridge Deck Systems," Proc. of Institution of Civil Engineers, V. 1, Part 1, 1952.

44. Thomson, W. T., Mechanical Vibrations, Second Edition, Prentice-Hall Inc., Englewood Cliffs, N. J., 1953.

45. Timoshenko, S., and Woinowsky-Krieger, S., Theory of Plates and Shells, McGraw-Hill Book Company, Inc., New York, 1959.

46. Veletsos, A. S., Huang, T., "Analysis of Dynamic Response of Highway Bridges," Journal of the Engineering Mechanics Division, ASCE, October 1970.

47. Vora, M. R., and Matlock, H., "A Discrete Element Analysis for Anisotropic Skew Plates and Grids," Research Report No. 56-18, Center for Highway Research, The University of Texas at Austin, August 1970.

48. Walker, W. H., "Model Studies of the Dynamic Response of a Multiple Girder Highway Bridge," University of Illinois, College of Engineering, Engineering Experiment Station Bulletin No. 495.

49. Walker, W. H., Veletsos, A. S., "Response of Simple-span Highway Bridges to Moving Vehicles," University of Illinois, College of Engineering, Engineering Experiment Station Bulletin No. 486.

50. Wei, Benjamin C. F., "Load Distribution of Diaphragms in I-Beam Bridges," Journal of Structural Division, ASCE, May, 1959.

51. White, R. W., "Similitude Requirements for Structural Models," ASCE Structural Engineering Conference Preprint 469, Seattle, Washington, May 8-12, 1967.

52. White, A., and Purnell, W. B., "Lateral Load Distribution Tests on I-Beam Bridge," Journal of Structural Division, ASCE, V. 83, No. ST 3, May 1957.

53. Wong, A. Y. C., and Gamble, W. L., "Effects of Diaphragms in Continuous Slab and Girder Highway Bridges," Civil Engineering Studies, Structural Research Series No. 391, University of Illinois, Urbana, Illinois, May 1973.

54. Wright, R. N., and Walker, W. H., "Vibration and Deflection of Steel Bridges," AISC Engineering Journal, V. 9, No. 1, January 1972.

55. Zia, P., White, R. N., Van Horn, D. A., "Principles of Model Analysis," Models for Concrete Structures, American Concrete Institute SP 24, Detroit, Michigan, 1970.

A P P E N D I X A

PROTOTYPE BRIDGE PLANS

(Taken from the Texas Highway Department
standard bridge design drawings)

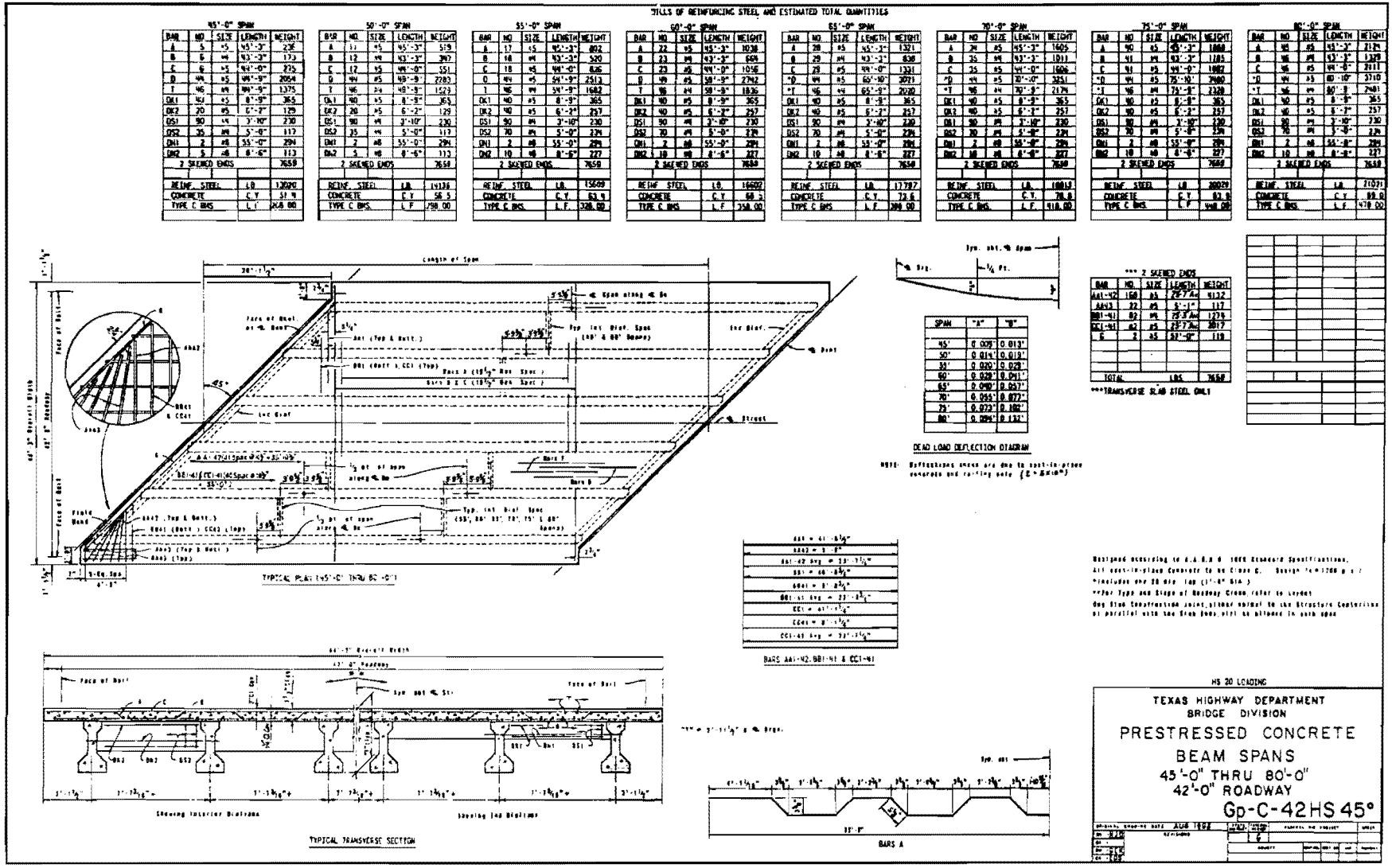

FIG. A1 PROTOTYPE PLAN FOR BRIDGE 1 AND 2 (80 ft. SPAN)

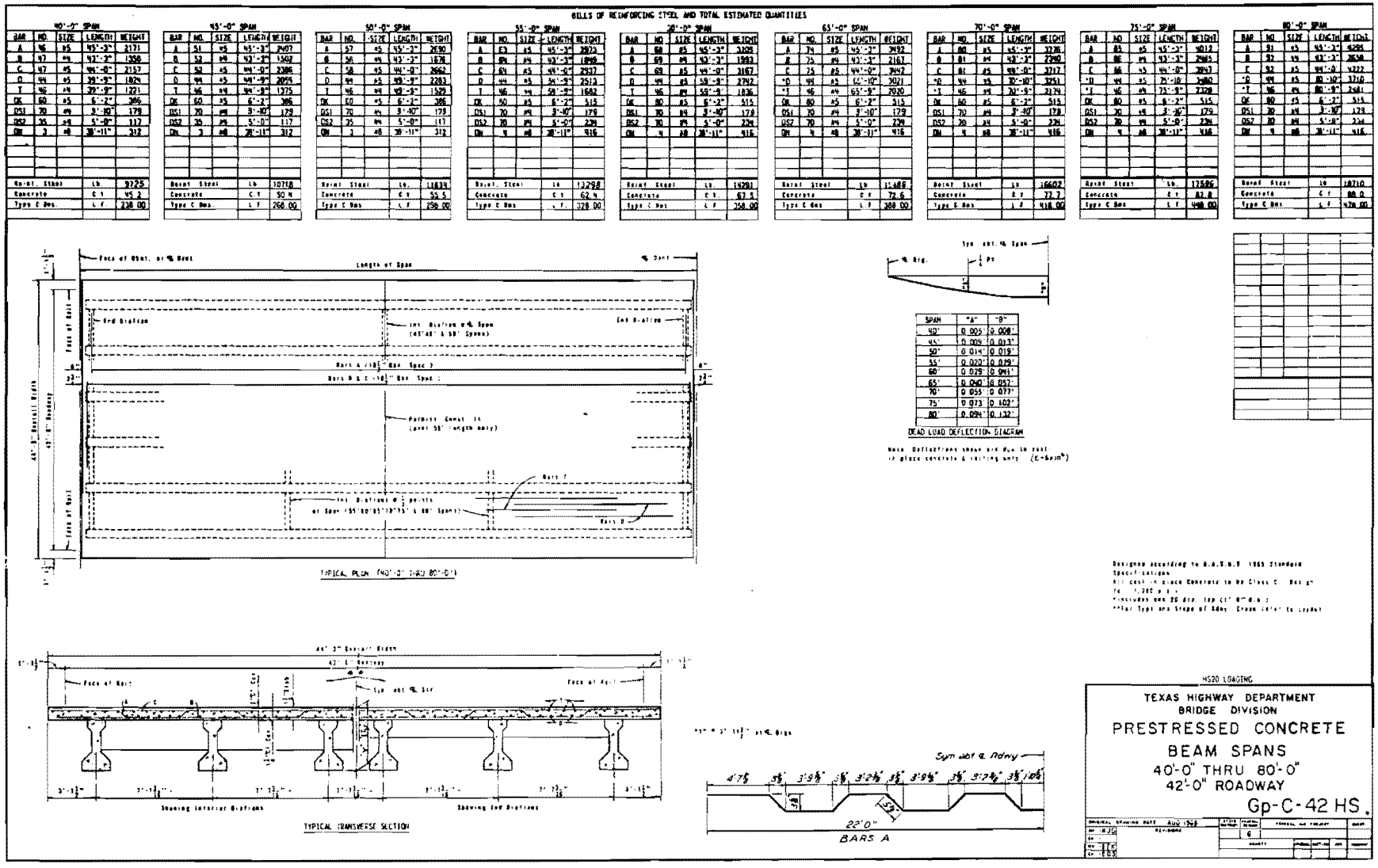

FIG. A2 PROTOTYPE PLAN FOR BRIDGE 3 (80 FT. SPAN) AND BRIDGE 4 (50 FT. SPAN)

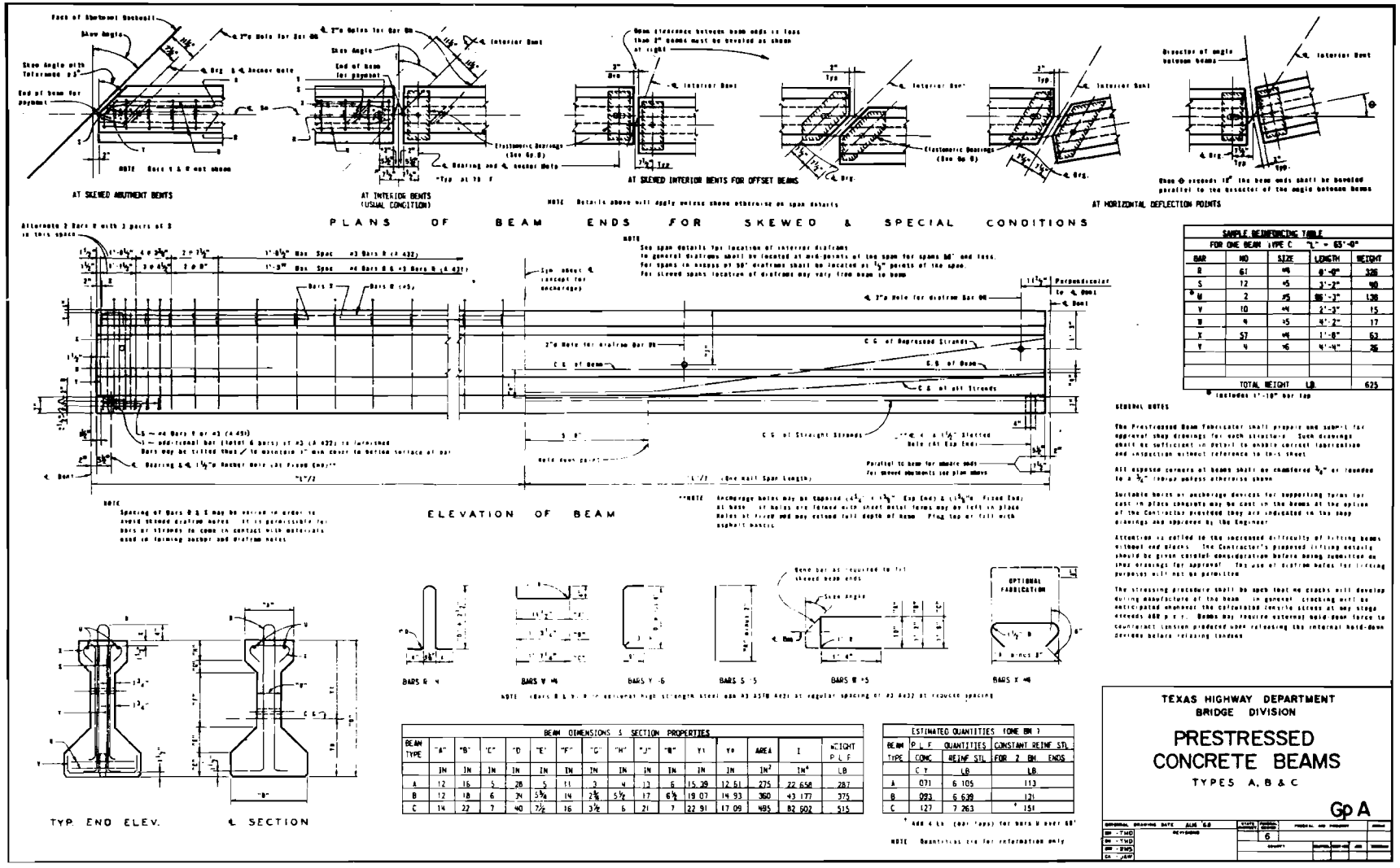

FIG. A3 PROTOTYPE GIRDER DETAILS (OF TYPE-C)

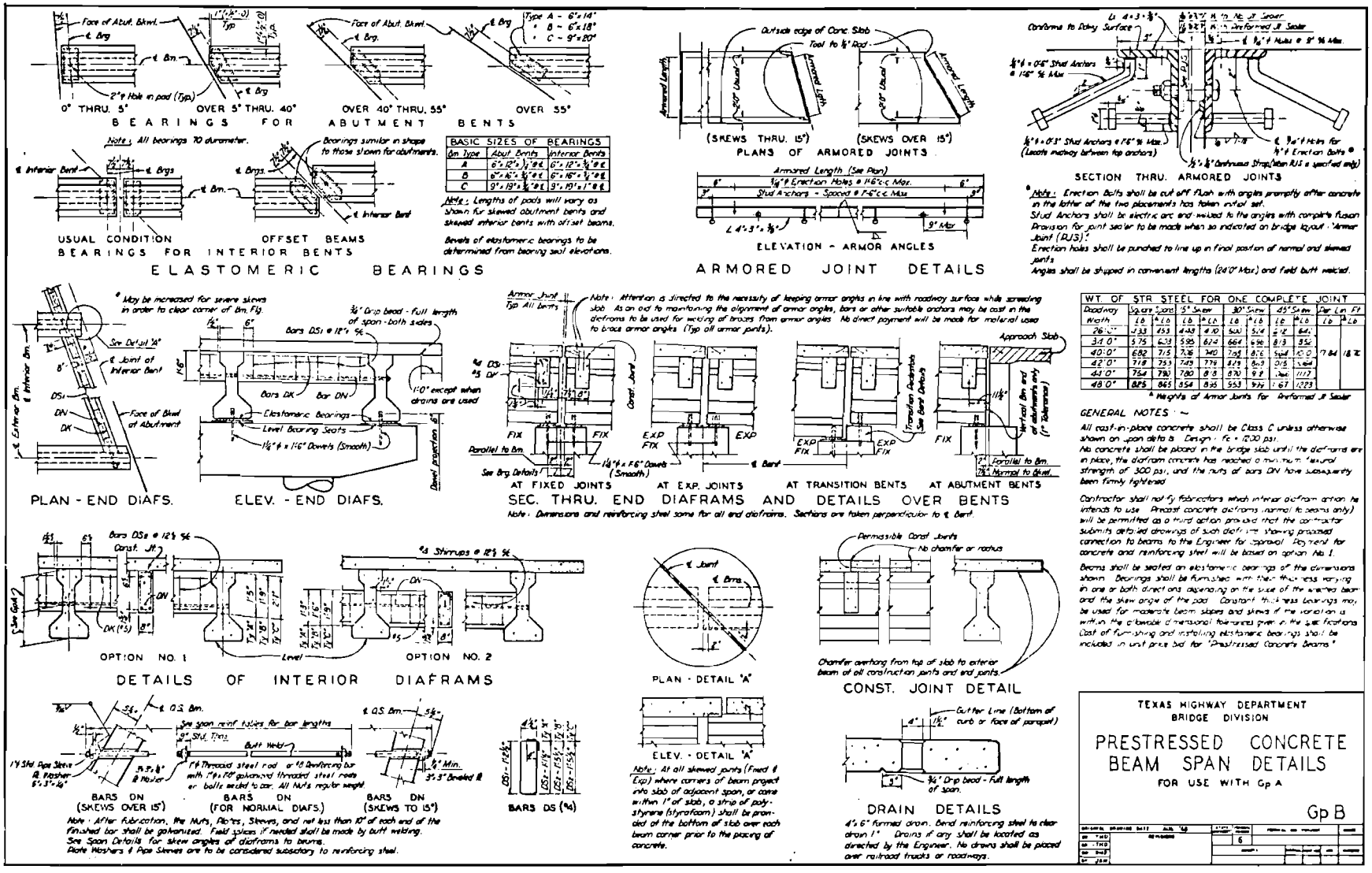

FIG. A4 PROTOTYPE DIAPHRAGM DETAILS

A P P E N D I X B

EXPERIMENTAL MOMENTS AND DEFLECTIONS

Experimental values of relative deflections, relative moments and sums of moments and deflections are given. All point loads are of 1 kip magnitude. See Figs. 5.1 and 5.2 for point load locations. Standard truck load is shown in Fig. 2.20c. Figures 2.25 and 2.26 show location of truck loads.

Notations:

M = moment in any girder at a given transverse section of the bridge (i.e., at 3/4, mid or 1/4 span)

ΣM = sum of all the girder moments at any given transverse section of the bridge

$M/\Sigma M$ = ratio of the moment in a girder to the total moment in all the girders at any transverse section of the bridge

δ = deflection of any girder at a given point along the span (i.e., at 3/4, mid or 1/4 point)

$\Sigma\delta$ = sum of all the girder deflections at any given point along the span

$\delta/\Sigma\delta$ = ratio of the deflection of a girder to the sum of all the girder deflections at a given point along the span

SUM = ΣM or $\Sigma\delta$

T A B L E B1 -- BRIDGE 1, $\delta/\Sigma\delta$ AND $\Sigma\delta$ VALUES

LOAD	SPAN	SER	GIRDER NUMBERS 1	2	3	4	5	6	SUM
F1	3/4	A	.588	.274	.107	.061	-.004	-.026	36.1
		B	.600	.273	.115	.027	-.004	-.012	38.4
		C	.632	.271	.080	.041	-.010	-.013	37.2
	MID	A	.578	.267	.134	.048	-.006	-.021	53.8
		B	.572	.294	.114	.028	.002	-.011	56.9
		C	.590	.292	.103	.040	-.011	-.014	59.1
	1/4	A	.530	.307	.150	.052	-.015	-.023	42.4
		B	.549	.315	.121	.027	.006	-.018	43.0
		C	.553	.324	.112	.031	-.007	-.014	43.9
F12	3/4	A	.454	.290	.173	.070	.012	-.003	36.7
		B	.481	.310	.141	.050	.018	.001	36.8
		C	.497	.300	.126	.071	.011	-.005	35.7
	MID	A	.409	.286	.156	.094	.051	.004	57.9
		B	.443	.321	.161	.058	.019	-.003	54.3
		C	.459	.327	.139	.068	.009	-.003	53.5
	1/4	A	.411	.318	.186	.085	.047	-.008	40.2
		B	.416	.332	.165	.066	.025	-.003	40.7
		C	.436	.347	.156	.057	.013	-.009	38.1
F2	3/4	A	.357	.286	.179	.107	.047	.025	36.7
		B	.351	.309	.193	.106	.033	.008	36.6
		C	.328	.315	.211	.116	.036	-.005	37.0
	MID	A	.306	.303	.196	.121	.054	.021	55.1
		B	.315	.347	.201	.100	.034	.002	52.4
		C	.291	.345	.221	.108	.305	.001	55.3
	1/4	A	.307	.336	.217	.085	.041	.015	38.5
		B	.302	.312	.226	.121	.031	.008	38.2
		C	.278	.322	.246	.117	.037	-.001	39.5
F23	3/4	A	.235	.269	.245	.138	.066	.046	37.4
		B	.233	.265	.241	.161	.074	.027	36.7
		C	.214	.283	.234	.182	.068	.020	37.0

T A B L E B1 -- BRIDGE 1, $\delta/\Sigma\delta$ AND $\Sigma\delta$ VALUES (continued)

LOAD	SPAN	SER	GIRDER NUMBERS 1	2	3	4	5	6	SUM
F23	MID	A	.217	.273	.252	.155	.071	.033	52.7
		B	.198	.277	.266	.166	.065	.029	53.0
		C	.188	.298	.261	.166	.067	.019	54.5
	1/4	A	.207	.243	.264	.178	.073	.034	37.2
		B	.189	.229	.260	.214	.081	.027	38.3
		C	.182	.257	.263	.187	.084	.026	37.8
F3	3/4	A	.160	.238	.248	.180	.102	.072	34.4
		B	.139	.218	.292	.198	.102	.051	38.4
		C	.117	.215	.301	.216	.106	.046	37.8
	MID	A	.141	.219	.266	.199	.111	.065	51.3
		B	.113	.209	.311	.229	.111	.027	54.8
		C	.097	.199	.313	.232	.112	.047	54.4
	1/4	A	.165	.182	.231	.223	.132	.067	36.3
		B	.129	.178	.282	.234	.124	.054	40.1
		C	.092	.174	.281	.256	.141	.056	39.0
H1	3/4	A	.548	.277	.103	.061	.014	-.002	32.1
		B	.605	.271	.122	.025	-.016	-.007	33.7
		C	.679	.266	.070	.021	-.011	-.025	30.3
	MID	A	.494	.277	.148	.071	.022	-.012	40.6
		B	.557	.325	.122	.032	-.016	-.020	40.2
		C	.592	.313	.105	.030	-.014	-.026	38.5
	1/4	A	.451	.337	.183	.064	-.002	-.033	28.9
		B	.508	.340	.147	.035	-.017	-.013	27.3
		C	.577	.347	.110	.035	-.027	-.042	25.2
H3	3/4	A	.094	.206	.325	.219	.107	.049	29.9
		B	.118	.182	.337	.218	.111	.034	32.0
		C	.093	.204	.355	.242	.075	.032	30.5
	MID	A	.104	.177	.267	.245	.146	.061	35.1
		B	.117	.182	.264	.252	.140	.046	37.2
		C	.101	.194	.302	.278	.078	.047	35.1

T A B L E B1 -- BRIDGE 1, $\delta/\Sigma\delta$ AND $\Sigma\delta$ VALUES (continued)

LOAD	SPAN	SER	GIRDER NUMBERS 1	2	3	4	5	6	SUM
H3	1/4	A	.093	.195	.224	.223	.183	.081	21.3
		B	.110	.153	.242	.260	.165	.071	24.0
		C	.104	.173	.264	.306	.097	.056	22.0
H6	3/4	A	0.000	.020	.052	.085	.275	.567	36.9
		B	.003	.001	.023	.085	.302	.587	38.9
		C	.001	-.002	.041	.069	.286	.605	37.5
	MID	A	.007	.020	.067	.105	.282	.520	41.1
		B	-.002	.001	.021	.107	.296	.576	42.9
		C	-.007	-.001	.039	.086	.294	.590	42.4
	1/4	A	.004	.028	.066	.125	.263	.514	26.8
		B	0.000	.003	.029	.105	.285	.578	27.6
		C	-.002	-.001	.039	.115	.259	.590	27.3
TA	3/4	A	.456	.292	.161	.074	.024	-.007	110.0
		B	.471	.308	.144	.062	.017	-.001	111.0
		C	.493	.306	.136	.063	.008	-.006	106.0
	MID	A	.432	.306	.173	.065	.027	-.003	157.0
		B	.440	.321	.155	.070	.015	.001	158.0
		C	.455	.322	.150	.067	.010	-.004	153.0
	1/4	A	.393	.308	.190	.091	.025	-.008	120.0
		B	.416	.327	.173	.072	.013	-.001	117.0
		C	.421	.330	.176	.068	.013	-.008	113.0
TB	3/4	A	.105	.174	.247	.229	.144	.101	108.0
		B	.076	.161	.277	.262	.149	.074	115.0
		C	.064	.156	.269	.275	.146	.090	119.0
	MID	A	.097	.158	.239	.247	.159	.100	151.0
		B	.072	.143	.256	.283	.165	.082	159.0
		C	.059	.143	.260	.298	.165	.075	160.0
	1/4	A	.102	.144	.216	.250	.173	.115	106.0
		B	.070	.127	.245	.282	.185	.090	110.0
		C	.054	.127	.243	.303	.187	.086	117.0

T A B L E B2 -- BRIDGE 1, M/ΣM AND ΣM VALUES

LOAD	SPAN	STR	GIRDER NUMBERS 1	2	3	4	5	6	SUM
F1	3/4	A	.577	.206	.122	.047	.019	.028	19.6
		B	.697	.234	.078	0.000	0.000	-.010	18.9
		C	.673	.211	.096	.019	0.000	0.000	19.3
	MID	A	.615	.249	.093	.030	.019	-.009	39.8
		B	.654	.262	.089	.013	-.018	0.000	41.3
		C	.662	.252	.068	.018	.013	-.013	40.8
	1/4	A	.483	.339	.152	.055	.006	-.030	30.2
		B	.488	.400	.126	.021	-.021	-.014	26.2
		C	.476	.372	.129	.027	.008	-.013	27.7
F12	3/4	A	--	--	--	--	--	--	--
		B	.575	.195	.116	.062	.031	.023	23.8
		C	.576	.212	.131	.057	.016	.008	22.5
	MID	A	--	--	--	--	--	--	--
		B	.433	.341	.160	.068	.013	-.005	39.9
		C	.454	.347	.132	.038	.019	.009	38.9
	1/4	A	--	--	--	--	--	--	--
		B	.365	.341	.192	.067	.024	.012	30.7
		C	.350	.336	.219	.073	.015	.007	25.2
F2	3/4	A	.500	.229	.125	.062	.062	.021	17.7
		B	.418	.230	.172	.123	.033	.025	22.4
		C	.428	.235	.177	.101	.025	.034	21.9
	MID	A	.250	.406	.193	.084	.059	.008	43.9
		B	.220	.462	.186	.102	.021	.008	43.4
		C	.249	.404	.182	.093	.022	.009	41.3
	1/4	A	.238	.270	.301	.159	.032	0.000	23.2
		B	.252	.268	.285	.122	.057	.016	22.6
		C	.237	.260	.313	.137	.053	0.000	24.1
F23	3/4	A	.315	.296	.204	.139	.009	.037	19.9
		B	.270	.304	.226	.130	.043	.026	21.2
		C	.265	.310	.239	.133	.044	.009	20.8
	MID	A	.177	.279	.315	.135	.065	.028	39.5
		B	.152	.352	.307	.134	.051	.005	39.0
		C	.152	.326	.321	.147	.049	.005	37.6

T A B L E B2 -- BRIDGE 1, M/ΣM AND ΣM VALUES (continued)

LOAD	SPAN	SER	GIRDER NUMBERS 1	2	3	4	5	6	SUM
F23	1/4	A	.218	.134	.311	.202	.076	.059	21.9
		B	.173	.191	.327	.227	.082	0.000	20.2
		C	.177	.166	.345	.204	.080	.009	20.8
F3	3/4	A	.181	.287	.207	.126	.081	.117	20.3
		B	.137	.306	.266	.169	.089	.032	22.8
		C	.149	.299	.254	.172	.082	.045	24.7
	MID	A	.107	.191	.383	.195	.080	.044	41.5
		B	.076	.194	.397	.231	.076	.027	48.4
		C	.079	.155	.437	.210	.087	.032	46.4
	1/4	A	.133	.150	.203	.274	.221	.018	20.8
		B	.133	.125	.258	.283	.150	.050	22.1
		C	.120	.160	.256	.288	.128	.048	23.0
H1	3/4	A	.734	.186	.073	.011	.011	-.006	32.6
		B	.732	.190	.067	.010	-.005	.005	35.8
		C	.751	.159	.027	.021	.021	.021	34.7
	MID	A	.461	.335	.134	.036	.017	.008	22.0
		B	.487	.378	.126	.016	0.000	-.008	23.3
		C	.535	.334	.106	0.000	.016	.008	22.6
	1/4	A	.320	.384	.269	.064	-.013	-.026	14.4
		B	.330	.420	.182	.045	.023	0.000	16.2
		C	.341	.390	.171	.049	.024	.024	15.1
H3	3/4	A	.197	.173	.503	.124	.054	.049	34.3
		B	.109	.177	.515	.150	.036	.014	40.6
		C	.089	.173	.530	.211	.038	0.000	54.0
	MID	A	.133	.175	.158	.266	.167	.100	22.1
		B	--	--	--	--	--	--	--
		C	.078	.175	.262	.333	.136	.019	19.0
	1/4	A	.066	.180	.115	.278	.294	.066	11.2
		B	.207	.103	.138	.276	.241	.034	10.7
		C	.152	.152	.109	.326	.283	-.022	8.5
H6	3/4	A	.004	.047	.017	.114	.266	.552	43.4
		B	-.009	0.000	.021	.086	.256	.646	43.0
		C	-.014	.005	.010	.072	.263	.665	38.4

T A B L E B2 -- BRIDGE 1, M/ΣM AND ΣM VALUES (continued)

LOAD	SPAN	SER	GIRDER NUMBERS 1	2	3	4	5	6	SUM
H6	MID	A	-.036	0.000	.018	.142	.356	.520	20.7
		B	-.015	0.000	.030	.130	.274	.581	24.1
		C	-.017	0.000	.008	.101	.279	.629	21.8
	1/4	A	.020	.060	.100	.160	.180	.480	9.2
		B	-.023	-.023	.068	.068	.250	.659	8.1
		C	-.087	0.000	.043	.109	.196	.739	8.5
TA	3/4	A	.555	.219	.118	.059	.029	.021	62.6
		B	.549	.229	.132	.059	.017	.014	65.4
		C	.587	.243	.107	.039	.015	.009	61.6
	MID	A	.417	.292	.160	.081	.049	.002	98.5
		B	.426	.319	.156	.076	.015	.008	97.1
		C	.453	.351	.151	.053	.012	0.000	93.1
	1/4	A	.308	.317	.220	.109	.053	.014	77.9
		B	.339	.341	.215	.077	.021	.008	71.3
		C	.354	.364	.216	.061	.011	-.005	69.2
TB	3/4	A	.092	.222	.322	.167	.105	.092	68.1
		B	.079	.203	.338	.192	.124	.064	77.1
		C	.060	.212	.337	.236	.108	.048	73.3
	MID	A	.077	.144	.264	.253	.170	.093	100.1
		B	.057	.137	.289	.274	.169	.064	103.0
		C	.057	.138	.305	.293	.159	.048	100.1
	1/4	A	.101	.107	.177	.278	.245	.092	60.2
		B	.071	.109	.195	.317	.224	.084	67.6
		C	.065	.111	.215	.335	.224	.059	62.0
TC	3/4	A	--	--	--	--	--	--	--
		B	-.003	.022	.084	.217	.342	.337	83.6
		C	-.002	.020	.076	.228	.355	.323	85.0
	MID	A	--	--	--	--	--	--	--
		B	.001	.020	.059	.151	.350	.420	116.0
		C	.006	.013	.053	.135	.359	.433	115.0
	1/4	A	--	--	--	--	--	--	--
		B	.008	.022	.054	.126	.238	.553	63.7
		C	.006	.020	.046	.118	.234	.576	63.9

T A B L E B3 -- BRIDGE 2, $\delta/\Sigma\delta$ AND $\Sigma\delta$ VALUES

LOAD	SPAN	STR	GIRDER NUMBERS 1	2	3	4	5	6	SUM
F6	3/4	A	-.032	.011	.059	.139	.310	.514	53.8
		B	0.000	.003	.046	.097	.312	.542	58.7
		C	--	--	--	--	--	--	--
	MID	A	-.016	.003	.051	.126	.283	.554	70.1
		B	0.000	.001	.036	.089	.286	.588	74.2
		C	--	--	--	--	--	--	--
	1/4	A	.012	.005	.057	.146	.352	.428	37.1
		B	0.000	.002	-.002	.094	.271	.634	49.8
		C	--	--	--	--	--	--	--
F1	3/4	A	.554	.271	.110	.053	.006	.007	43.7
		B	.483	.327	.122	.049	.014	.005	37.5
		C	--	--	--	--	--	--	--
	MID	A	.556	.292	.108	.045	.002	-.002	62.2
		B	.539	.302	.110	.037	.011	-.003	63.8
		C	--	--	--	--	--	--	--
	1/4	A	.513	.327	.124	.037	-.001	0.000	46.1
		B	.477	.465	.031	.031	-.002	0.000	54.2
		C	--	--	--	--	--	--	--
F12	3/4	A	.492	.282	.131	.076	.016	.003	39.6
		B	.387	.350	.168	.071	.010	.015	34.6
		C	--	--	--	--	--	--	--
	MID	A	.458	.287	.154	.088	.010	.002	56.9
		B	.426	.338	.165	.056	.012	.002	56.9
		C	--	--	--	--	--	--	--
	1/4	A	.417	.326	.174	.087	-.003	0.000	43.7
		B	.485	.367	.079	.055	.014	0.000	39.4
		C	--	--	--	--	--	--	--

T A B L E B3 -- BRIDGE 2, $\delta/\Sigma\delta$ AND $\Sigma\delta$ VALUES (continued)

LOAD	SPAN	SER	GIRDER NUMBERS 1	2	3	4	5	6	SUM
F2	3/4	A	.373	.286	.181	.117	.032	.012	36.0
		B	.205	.392	.258	.117	.025	.003	33.4
		C	--	--	--	--	--	--	--
	MID	A	.298	.345	.195	.123	.035	.005	51.9
		B	.251	.392	.218	.106	.030	.004	53.0
		C	--	--	--	--	--	--	--
	1/4	A	.222	.300	.282	.149	.045	.002	39.0
		B	.336	.369	.127	.146	.023	0.000	37.7
		C	--	--	--	--	--	--	--
F3	3/4	A	.149	.233	.242	.189	.096	.091	44.9
		B	-.001	.203	.372	.239	.110	.074	33.5
		C	--	--	--	--	--	--	--
	MID	A	.147	.203	.280	.202	.107	.061	55.0
		B	.053	.219	.347	.231	.110	.041	56.1
		C	--	--	--	--	--	--	--
	1/4	A	.155	.198	.226	.225	.144	.051	36.7
		B	.119	.221	.187	.266	.155	.053	38.1
		C	--	--	--	--	--	--	--
F34	3/4	A	.095	.179	.241	.241	.149	.095	38.6
		B	-.014	.189	.311	.261	.154	.099	40.6
		C	--	--	--	--	--	--	--
	MID	A	.093	.152	.244	.265	.156	.090	54.4
		B	-.003	.148	.292	.300	.174	.083	54.1
		C	--	--	--	--	--	--	--
	1/4	A	.099	.154	.236	.307	.193	.010	35.5
		B	.044	.176	.167	.310	.206	.097	38.1
		C	--	--	--	--	--	--	--

T A B L E B3 -- BRIDGE 2, $\delta/\Sigma\delta$ AND $\Sigma\delta$ VALUES (continued)

LOAD	SPAN	SER	GIRDER NUMBERS 1	2	3	4	5	6	SUM
TA	3/4	A	.473	.275	.148	.080	.025	0.000	117.4
		B	.427	.315	.153	.075	.024	.006	108.5
		C	.456	.346	.152	.044	.001	.001	110.0
	MID	A	.438	.299	.159	.080	.026	-.002	164.0
		B	.426	.317	.160	.074	.023	.001	163.0
		C	.425	.356	.161	.066	.014	-.001	170.0
	1/4	A	.381	.324	.191	.091	.025	-.012	113.0
		B	.434	.324	.143	.081	.023	-.005	117.0
		C	.442	.340	.144	.065	.017	-.009	120.0
TB	3/4	A	.103	.171	.252	.219	.156	.099	110.0
		B	.010	.191	.287	.267	.154	.090	109.0
		C	.023	.183	.296	.262	.154	.081	108.0
	MID	A	.096	.152	.245	.235	.171	.102	151.0
		B	.045	.152	.281	.277	.169	.077	155.0
		C	.039	.154	.284	.276	.173	.074	150.0
	1/4	A	.100	.136	.233	.238	.191	.102	105.0
		B	.077	.147	.217	.282	.192	.085	106.0
		C	.076	.055	.253	.311	.217	.087	97.0
TC	3/4	A	-.009	.024	.082	.157	.321	.426	136.0
		B	0.000	.016	.071	.158	.314	.441	140.0
		C	-.003	.006	.067	.140	.332	.458	145.0
	MID	A	-.005	.020	.073	.151	.304	.458	178.0
		B	0.000	.017	.074	.147	.308	.455	184.0
		C	-.002	.006	.065	.137	.323	.471	191.0
	1/4	A	.002	.022	.072	.143	.281	.480	123.0
		B	0.000	.023	.032	.143	.297	.505	121.0
		C	-.005	.008	.026	.142	.318	.512	126.0

T A B L E B4 -- BRIDGE 2, M/ΣM AND ΣM VALUES

LOAD	SPAN	SER	GIRDER NUMBERS 1	2	3	4	5	6	SUM
F6	3/4	A	-.045	-.013	.032	.147	.458	.420	28.7
		B	0.000	.006	.028	.128	.397	.441	32.7
		C	--	--	--	--	--	--	--
	MID	A	0.000	.004	.028	.077	.237	.654	52.4
		B	0.000	0.000	.013	.067	.228	.691	55.1
		C	--	--	--	--	--	--	--
	1/4	A	-.026	-.017	.034	.136	.221	.651	21.6
		B	.017	.017	.034	.084	.184	.665	22.0
		C	--	--	--	--	--	--	--
F1	3/4	A	.617	.203	.100	.048	.028	.005	21.4
		B	.662	.169	.080	.048	.040	0.000	22.9
		C	--	--	--	--	--	--	--
	MID	A	.622	.243	.087	.041	.007	0.000	43.5
		B	.651	.223	.075	.039	.008	.004	46.8
		C	--	--	--	--	--	--	--
	1/4	A	.390	.408	.165	.052	.010	-.025	29.2
		B	.411	.376	.134	.061	.024	-.006	30.2
		C	--	--	--	--	--	--	--
F12	3/4	A	.565	.199	.120	.055	.042	.018	20.0
		B	.568	.216	.135	.054	.018	.009	20.4
		C	--	--	--	--	--	--	--
	MID	A	.438	.334	.132	.064	.028	.005	39.9
		B	.444	.363	.114	.062	.013	.004	41.8
		C	--	--	--	--	--	--	--
	1/4	A	.303	.351	.233	.101	.039	-.028	26.5
		B	.313	.354	.211	.068	.048	.007	27.0
		C	--	--	--	--	--	--	--

T A B L E B4 -- BRIDGE 2, M/ΣM AND ΣM VALUES (continued)

LOAD	SPAN	SER	GIRDER NUMBERS 1	2	3	4	5	6	SUM
F2	3/4	A	.423	.228	.138	.098	.065	.049	22.6
		B	.394	.293	.182	.071	.030	.030	18.2
		C	--	--	--	--	--	--	--
	MID	A	.252	.420	.169	.091	.044	.022	41.6
		B	.228	.475	.181	.073	.039	.004	42.7
		C	--	--	--	--	--	--	--
	1/4	A	.245	.232	.285	.166	.086	-.013	27.8
		B	.267	.242	.317	.133	.050	-.008	22.1
		C	--	--	--	--	--	--	--
F3	3/4	A	.154	.316	.179	.162	.077	.111	22.6
		B	.129	.339	.242	.145	.089	.057	22.8
		C	--	--	--	--	--	--	--
	MID	A	.109	.179	.385	.183	.092	.052	43.3
		B	.087	.189	.448	.174	.079	.024	46.7
		C	--	--	--	--	--	--	--
	1/4	A	.115	.144	.163	.288	.221	.067	20.2
		B	.123	.154	.231	.300	.154	.038	23.9
		C	--	--	--	--	--	--	--
F34	3/4	A	.090	.261	.270	.171	.108	.099	20.4
		B	.075	.239	.284	.194	.112	.097	24.6
		C	--	--	--	--	--	--	--
	MID	A	.064	.137	.274	.301	.142	.082	40.2
		B	.043	.132	.321	.325	.128	.051	43.2
		C	--	--	--	--	--	--	--
	1/4	A	.093	.102	.157	.287	.250	.111	19.9
		B	.080	.128	.192	.296	.256	.048	23.0
		C	--	--	--	--	--	--	--

T A B L E B4 -- BRIDGE 2, M/ΣM AND ΣM VALUES (continued)

LOAD	SPAN	STR	GIRDER NUMBERS 1	2	3	4	5	6	SUM
TA	3/4	A	.552	.225	.110	.067	.028	.013	60.1
		B	.550	.241	.127	.055	.024	.003	60.6
		C	--	--	--	--	--	--	--
	MID	A	.415	.308	.153	.081	.030	.013	97.7
		B	.435	.328	.142	.061	.030	.004	96.7
		C	--	--	--	--	--	--	--
	1/4	A	.500	.333	.226	.107	.043	-.010	71.9
		B	.332	.347	.213	.075	.032	0.000	68.6
		C	--	--	--	--	--	--	--
TB	3/4	A	.077	.239	.300	.177	.112	.095	64.1
		B	.051	.217	.305	.227	.122	.078	68.1
		C	.037	.210	.312	.246	.129	.066	64.4
	MID	A	.076	.144	.257	.257	.164	.101	99.8
		B	.051	.144	.296	.285	.158	.067	100.0
		C	.062	.152	.306	.298	.132	.049	94.8
	1/4	A	.083	.114	.157	.271	.262	.114	59.9
		B	.076	.112	.195	.302	.240	.076	61.9
		C	--	--	--	--	--	--	--
TC	3/4	A	-.022	.031	.077	.208	.378	.328	83.2
		B	-.017	.035	.061	.205	.373	.344	85.1
		C	-.013	.025	.061	.199	.365	.363	87.9
	MID	A	0.000	.026	.061	.136	.318	.459	112.0
		B	-.003	.026	.058	.134	.323	.463	114.0
		C	-.002	.017	.048	.132	.331	.474	119.0
	1/4	A	.013	.025	.060	.110	.211	.580	58.1
		B	.017	.029	.058	.117	.226	.553	63.1
		C	.009	.020	.052	.110	.224	.586	63.7

T A B L E B5 -- BRIDGE 3, $\delta/\Sigma\delta$ AND $\Sigma\delta$ VALUES

LOAD	SPAN	SER	GIRDER NUMBERS 1	2	3	4	5	6	SUM
F1	3/4	A	.473	.315	.154	.051	-.004	.011	49.2
		B	.597	.302	.125	.018	-.009	-.034	48.7
		C	--	--	--	--	--	--	--
	MID	A	.522	.338	.161	.056	-.001	-.077	66.6
		B	.603	.303	.118	.021	-.005	-.040	68.1
		C	--	--	--	--	--	--	--
F12	3/4	A	.428	.303	.189	.078	.010	-.007	52.9
		B	.487	.326	.165	.058	-.006	-.029	44.2
		C	--	--	--	--	--	--	--
	MID	A	.407	.342	.205	.080	0.000	-.034	65.8
		B	.479	.349	.158	.047	-.004	-.030	63.8
		C	--	--	--	--	--	--	--
F2	3/4	A	.331	.320	.201	.117	.049	-.016	46.1
		B	.327	.319	.232	.107	.031	-.016	47.1
		C	--	--	--	--	--	--	--
	MID	A	.290	.321	.243	.130	.039	-.024	63.8
		B	.320	.343	.221	.100	.031	-.015	68.4
		C	--	--	--	--	--	--	--
F23	3/4	A	.242	.262	.265	.154	.077	0.000	45.4
		B	.221	.273	.285	.165	.059	-.004	45.7
		C	--	--	--	--	--	--	--
	MID	A	.214	.292	.272	.173	.049	0.000	60.8
		B	.218	.297	.285	.146	.053	.002	64.6
		C	--	--	--	--	--	--	--
F3	3/4	A	.122	.225	.298	.222	.124	.009	42.2
		B	.118	.222	.311	.228	.106	.016	45.6
		C	--	--	--	--	--	--	--
	MID	A	.145	.219	.295	.214	.100	.027	63.9
		B	.118	.221	.321	.216	.096	.028	65.2
		C	--	--	--	--	--	--	--
F34	3/4	A	.050	.168	.283	.283	.168	.050	40.7
		B	.042	.161	.298	.298	.161	.042	40.6
		C	--	--	--	--	--	--	--

T A B L E B5 -- BRIDGE 3, $\delta/\Sigma\delta$ AND $\Sigma\delta$ VALUES (continued)

LOAD	SPAN	SER	GIRDER NUMBERS 1	2	3	4	5	6	SUM
F34	MID	A	.091	.160	.250	.250	.160	.091	66.1
		B	.050	.151	.299	.299	.151	.050	62.0
		C	--	--	--	--	--	--	--
H4	3/4	A	.012	.103	.206	.338	.218	.123	43.6
		B	.038	.111	.224	.343	.180	.104	44.1
		C	--	--	--	--	--	--	--
	MID	A	.037	0.000	.261	.298	.248	.155	40.3
		B	.034	.115	.231	.295	.215	.119	49.5
		C	--	--	--	--	--	--	--
H6	3/4	A	0.000	0.000	.048	.119	.295	.568	44.1
		B	.001	-.003	.006	.084	.290	.622	39.2
		C	--	--	--	--	--	--	--
	MID	A	-.072	0.000	.054	.156	.371	.491	41.8
		B	-.035	-.016	.017	.105	.315	.613	44.6
		C	--	--	--	--	--	--	--
F67	3/4	A	0.000	-.039	0.000	.155	.330	.553	51.5
		B	-.027	-.008	.016	.074	.262	.683	51.2
		C	--	--	--	--	--	--	--
	MID	A	-.095	0.000	0.000	.159	.381	.556	63.0
		B	-.036	-.020	.011	.076	.285	.685	71.5
		C	--	--	--	--	--	--	--
TA	3/4	A	.426	.328	.180	.083	.010	-.026	139.0
		B	.453	.323	.184	.061	.007	-.027	139.0
		C	--	--	--	--	--	--	--
	MID	A	.441	.315	.195	.095	.004	-.050	182.0
		B	.447	.327	.189	.055	.009	-.027	189.0
		C	--	--	--	--	--	--	--
TB	3/4	A	.065	.174	.261	.261	.174	.065	134.0
		B	.065	.156	.279	.279	.156	.065	133.0
		C	--	--	--	--	--	--	--
	MID	A	.082	.170	.249	.249	.170	.082	190.0
		B	.066	.160	.274	.274	.160	.066	182.0
		C	--	--	--	--	--	--	--

T A B L E B6 -- BRIDGE 3, M/ΣM AND ΣM VALUES

LOAD	SPAN	SER	GIRDER NUMBERS 1	2	3	4	5	6	SUM
F1	3/4	A	.570	.332	.136	.032	-.023	-.047	19.4
		B	.596	.342	.103	.002	-.020	-.023	20.3
		C	--	--	--	--	--	--	--
	MID	A	.630	.314	.114	.017	-.027	-.044	41.2
		B	.686	.273	.073	-.005	-.015	-.011	42.8
		C	--	--	--	--	--	--	--
F12	3/4	A	.474	.322	.187	.053	.007	-.043	20.0
		B	.438	.317	.168	.059	.007	.016	21.8
		C	--	--	--	--	--	--	--
	MID	A	.471	.352	.163	.056	.008	-.050	41.2
		B	.453	.384	.113	.047	.011	-.007	42.5
		C	--	--	--	--	--	--	--
F2	3/4	A	.346	.270	.231	.117	.046	-.011	20.2
		B	.348	.289	.255	.119	.018	-.029	19.9
		C	--	--	--	--	--	--	--
	MID	A	.293	.356	.215	.106	.041	-.011	41.7
		B	.258	.358	.209	.063	.023	-.011	41.3
		C	--	--	--	--	--	--	--
F23	3/4	A	.242	.253	.257	.182	.076	-.011	20.1
		B	.214	.289	.282	.187	.038	-.011	19.1
		C	--	--	--	--	--	--	--
	MID	A	.199	.342	.288	.154	.060	-.004	41.6
		B	.142	.367	.344	.123	.032	-.008	38.6
		C	--	--	--	--	--	--	--
F3	3/4	A	.144	.231	.253	.218	.118	.037	21.5
		B	.106	.253	.309	.253	.088	-.009	21.2
		C	--	--	--	--	--	--	--

T A B L E B6 -- BRIDGE 3, M/ΣM AND ΣM VALUES (continued)

LOAD	SPAN	SER	GIRDER NUMBERS 1	2	3	4	5	6	SUM
F3	MID	A	.110	.209	.347	.208	.108	.018	42.8
		B	.070	.207	.460	.201	.069	-.006	42.9
		C	--	--	--	--	--	--	--
F34	3/4	A	.083	.170	.248	.248	.170	.083	19.9
		B	.047	.175	.275	.278	.175	.047	22.8
		C	--	--	--	--	--	--	--
	MID	A	.061	.155	.283	.283	.155	.061	42.2
		B	.028	.129	.343	.343	.129	.028	42.0
		C	--	--	--	--	--	--	--
H4	3/4	A	.005	.047	.172	.527	.187	.062	30.8
		B	.019	.064	.200	.586	.097	.035	29.6
		C	--	--	--	--	--	--	--
	MID	A	.008	.168	.246	.164	.254	.160	20.5
		B	.032	.135	.272	.309	.124	.127	19.7
		C	--	--	--	--	--	--	--
	1/4	A	.028	.131	.230	.177	.223	.211	10.0
		B	.013	.144	.236	.232	.228	.147	11.0
		C	--	--	--	--	--	--	--
H6	3/4	A	-.009	0.000	.014	.065	.234	.696	31.7
		B	0.000	-.005	0.000	.035	.241	.728	31.3
		C	--	--	--	--	--	--	--
	MID	A	-.053	-.030	.044	.168	.372	.499	21.0
		B	0.000	0.000	0.000	.096	.339	.565	21.6
		C	--	--	--	--	--	--	--
	1/4	A	-.027	-.014	.059	.171	.373	.438	10.3
		B	-.013	-.040	.028	.148	.369	.508	10.8
		C	--	--	--	--	--	--	--

T A B L E B6 -- BRIDGE 3, M/ΣM AND ΣM VALUES (continued)

LOAD	SPAN	SER	GIRDER NUMBERS 1	2	3	4	5	6	SUM
TA	3/4	A	.446	.342	.166	.059	.008	-.021	69.7
		B	.455	.338	.159	.045	.005	-.002	70.0
		C	--	--	--	--	--	--	--
	MID	A	.457	.320	.184	.075	.001	-.037	103.0
		B	.475	.354	.148	.038	.002	-.016	102.0
		C	--	--	--	--	--	--	--
	1/4	A	.450	.313	.186	.081	.003	-.032	54.3
		B	.459	.309	.175	.061	.004	-.008	55.0
		C	--	--	--	--	--	--	--
TB	3/4	A	.060	.154	.287	.287	.154	.060	70.6
		B	.036	.160	.304	.304	.160	.036	70.3
		C	--	--	--	--	--	--	--
	MID	A	.066	.172	.262	.262	.172	.066	104.0
		B	.037	.150	.313	.313	.150	.037	102.0
		C	--	--	--	--	--	--	--
	1/4	A	.078	.174	.248	.248	.174	.078	55.1
		B	.049	.178	.273	.273	.178	.049	55.9
		C	--	--	--	--	--	--	--
F67	3/4	A	-.045	-.033	.021	.094	.361	.603	22.0
		B	.032	.006	.021	.043	.289	.610	22.2
		C	--	--	--	--	--	--	--
	MID	A	-.087	-.063	0.000	.088	.326	.736	40.0
		B	-.016	0.000	0.000	0.000	.234	.782	40.4
		C	--	--	--	--	--	--	--

T A B L E B7 -- BRIDGE 4, $\delta/\Sigma\delta$ AND $\Sigma\delta$ VALUES

LOAD	SPAN	SER	GIRDER NUMBERS 1	2	3	4	5	6	SUM
F1	MID	A	.666	.309	.084	.011	-.036	-.033	18.4
		B	.759	.261	.040	-.023	-.021	-.016	17.7
		C	.758	.264	.018	-.013	-.021	-.006	17.9
F12	MID	A	.473	.358	.151	.041	-.009	-.014	16.6
		B	.465	.397	.122	.024	-.003	-.005	18.5
		C	.487	.392	.100	.027	0.000	-.005	18.5
F2	MID	A	.287	.361	.232	.115	.027	-.022	18.9
		B	.253	.463	.232	.058	0.000	-.006	17.8
		C	.248	.486	.234	.047	.001	-.015	18.1
F23	MID	A	.174	.342	.329	.151	.029	-.025	16.3
		B	.102	.343	.399	.133	.026	-.003	19.6
		C	.116	.410	.361	.102	.015	-.003	17.2
F3	MID	A	.073	.231	.340	.266	.089	.002	17.8
		B	.042	.224	.463	.216	.056	0.000	18.3
		C	.034	.236	.469	.215	.046	0.000	17.8
F34	MID	A	.017	.157	.327	.327	.157	.017	16.4
		B	-.016	.132	.384	.384	.132	-.016	17.2
		C	.004	.115	.381	.381	.115	.004	17.3
H4	MID	A	.020	.104	.188	.385	.269	.035	10.1
		B	.009	.075	.154	.491	.243	.029	10.7
		C	0.000	.069	.218	.426	.241	.046	10.8
H6	MID	A	-.033	-.007	-.012	.081	.286	.684	10.8
		B	0.000	-.026	-.021	.017	.282	.748	11.7
		C	-.008	-.012	-.032	.016	.270	.766	12.4
TA	MID	A	.492	.362	.164	.039	-.015	-.042	39.2
		B	.500	.379	.122	.020	-.009	-.012	40.6
		C	.522	.358	.126	.017	-.005	-.016	40.6
TB	MID	A	.042	.159	.298	.298	.159	.042	38.8
		B	.022	.137	.341	.341	.137	.022	40.5
		C	.009	.137	.355	.355	.137	.009	41.2

T A B L E B8 -- BRIDGE 4, M/ΣM AND ΣM VALUES

LOAD	SPAN	SER	GIRDER NUMBERS 1	2	3	4	5	6	SUM
F1	3/4	A	.687	.326	.041	-.010	-.011	-.032	13.8
		B	.818	.296	-.001	-.068	-.007	-.038	11.7
		C	.705	.248	.034	-.012	.031	-.005	13.8
	MID	A	.712	.278	.068	-.014	-.022	-.022	26.8
		B	.797	.237	.009	-.007	-.017	-.019	26.6
		C	.792	.189	-.001	.010	.008	.003	28.0
F12	3/4	A	.540	.385	.125	.025	-.012	-.063	12.1
		B	.485	.405	.122	.024	-.024	-.012	12.1
		C	.548	.511	.132	-.015	-.115	-.061	9.9
	MID	A	.499	.370	.160	.045	-.037	-.037	23.9
		B	.493	.465	.083	.006	-.023	-.023	25.3
		C	.506	.483	.059	-.024	-.018	-.006	24.3
F2	3/4	A	.286	.375	.246	.105	0.000	-.012	12.8
		B	.260	.441	.276	.054	0.000	-.032	11.8
		C	.288	.504	.256	.032	-.049	-.031	12.0
	MID	A	.269	.452	.229	.079	0.000	-.029	25.8
		B	.185	.624	.177	.027	-.011	0.000	25.7
		C	.212	.631	.168	.017	-.011	-.017	25.6
F23	3/4	A	.172	.306	.292	.188	.053	-.011	13.7
		B	.104	.371	.374	.131	.020	0.000	14.4
		C	.086	.435	.386	.130	-.012	-.024	12.3
	MID	A	.148	.351	.342	.167	.040	-.029	25.9
		B	.076	.391	.441	.087	0.000	.006	25.6
		C	.053	.423	.458	.092	-.007	-.019	22.6
F3	3/4	A	.062	.256	.353	.256	.084	-.011	13.3
		B	-.007	.283	.445	.267	.038	-.026	11.5
		C	-.087	.236	.507	.291	.037	.016	9.5
	MID	A	.061	.224	.407	.232	.085	-.011	27.6
		B	.017	.180	.583	.186	.045	-.011	26.1
		C	-.021	.210	.623	.185	.018	-.006	24.9

T A B L E B8 -- BRIDGE 4, M/ΣM AND ΣM VALUES (continued)

LOAD	SPAN	SER	GIRDER NUMBERS 1	2	3	4	5	6	SUM
F34	3/4	A	.023	.159	.317	.317	.159	.023	13.0
		B	-.011	.137	.375	.375	.137	-.011	13.3
		C	-.006	.152	.354	.354	.152	-.006	14.3
	MID	A	.011	.143	.346	.346	.143	.011	26.8
		B	-.017	.085	.432	.432	.085	-.017	25.9
		C	-.011	.090	.421	.421	.090	-.011	26.1
H4	3/4	A	.007	.021	.169	.622	.160	.021	20.7
		B	-.022	0.000	.149	.655	.197	.022	20.4
		C	-.008	0.000	.161	.667	.172	.008	19.8
	MID	A	-.040	.101	.253	.404	.211	.071	14.6
		B	-.012	.046	.231	.449	.217	.069	12.9
		C	.012	-.012	.265	.447	.227	.060	12.3
H6	3/4	A	-.015	-.015	.008	.059	.181	.785	20.0
		B	-.029	-.036	-.030	.006	.175	.911	20.5
		C	-.015	-.014	-.014	.016	.151	.875	20.6
	MID	A	-.012	-.025	0.000	.084	.313	.638	12.3
		B	0.000	-.047	0.000	-.024	.263	.799	12.3
		C	-.023	-.012	-.036	0.000	.260	.811	12.4
TA	3/4	A	.481	.378	.131	.024	-.012	-.002	42.4
		B	.527	.406	.101	-.003	-.019	-.011	41.6
		C	.514	.411	.099	-.002	-.011	-.011	41.8
	MID	A	.485	.341	.169	.043	-.012	-.026	53.6
		B	.504	.409	.104	.004	-.008	-.013	55.2
		C	.509	.410	.102	-.004	-.010	-.008	53.4
TB	3/4	A	.036	.114	.350	.350	.114	.036	43.6
		B	-.011	.103	.408	.408	.103	-.011	41.6
		C	-.009	.104	.404	.404	.104	-.009	43.1
	MID	A	.020	.164	.316	.316	.164	.020	51.2
		B	-.007	.111	.396	.396	.111	-.007	51.9
		C	-.003	.113	.390	.390	.113	-.003	54.6